

INFORMATION TO USERS

This manuscript has been reproduced from the microfilm master. UMI films the text directly from the original or copy submitted. Thus, some thesis and dissertation copies are in typewriter face, while others may be from any type of computer printer.

The quality of this reproduction is dependent upon the quality of the copy submitted. Broken or indistinct print, colored or poor quality illustrations and photographs, print bleedthrough, substandard margins, and improper alignment can adversely affect reproduction.

In the unlikely event that the author did not send UMI a complete manuscript and there are missing pages, these will be noted. Also, if unauthorized copyright material had to be removed, a note will indicate the deletion.

Oversize materials (e.g., maps, drawings, charts) are reproduced by sectioning the original, beginning at the upper left-hand corner and continuing from left to right in equal sections with small overlaps.

Photographs included in the original manuscript have been reproduced xerographically in this copy. Higher quality 6" x 9" black and white photographic prints are available for any photographs or illustrations appearing in this copy for an additional charge. Contact UMI directly to order.

**ProQuest Information and Learning
300 North Zeeb Road, Ann Arbor, MI 48106-1346 USA
800-521-0600**

UMI[®]



Université d'Ottawa • University of Ottawa

**Computation of Free Vibration Frequencies and Mode Shapes
of Cantilever Plates with Finite Discontinuities in Properties
Moving Outward from the Clamped Edge.**

Thesis Submitted to the School of Graduate Studies
as Partial Fulfilment of the Requirements for the
Degree of Master of Applied Science.

Wassim Labaki

Ottawa-Carleton Institute for Mechanical and Aerospace Engineering

University of Ottawa

Ottawa, Ontario, Canada, K1N5N6

June 2001



**National Library
of Canada**

**Acquisitions and
Bibliographic Services**

**395 Wellington Street
Ottawa ON K1A 0N4
Canada**

**Bibliothèque nationale
du Canada**

**Acquisitions et
services bibliographiques**

**395, rue Wellington
Ottawa ON K1A 0N4
Canada**

Your file Votre référence

Our file Notre référence

0-612-66067-2

The author has granted a non-exclusive licence allowing the National Library of Canada to reproduce, loan, distribute or sell copies of this thesis in microform, paper or electronic formats.

The author retains ownership of the copyright in this thesis. Neither the thesis nor substantial extracts from it may be printed or otherwise reproduced without the author's permission.

L'auteur a accordé une licence non exclusive permettant à la Bibliothèque nationale du Canada de reproduire, prêter, distribuer ou vendre des copies de cette thèse sous la forme de microfiche/film, de reproduction sur papier ou sur format électronique.

L'auteur conserve la propriété du droit d'auteur qui protège cette thèse. Ni la thèse ni des extraits substantiels de celle-ci ne doivent être imprimés ou autrement reproduits sans son autorisation.

Canada

ABSTRACT

The study of rectangular cantilever plates with step discontinuities in properties is of interest in many areas of industry. Cantilever plates are assigned different properties to represent change in stiffness and mass creating therefore the concept of step discontinuities in properties. The step discontinuity in properties is best represented by dividing the cantilever plate into separate segments called spans, with each span having its own stiffness and/or mass distribution as one moves outwards from the clamped edge.

This thesis presents the concept of dividing the cantilever plate into spans and provides accurate analytical solutions for free vibration frequencies and mode shapes. Chapter 1 introduces the reader to the theory of rectangular plates while chapter 2 concentrates on introducing the general solutions as applied to rectangular plates. Although there is no limit to the number of plate spans to be studied, three and four span cantilever plates were analysed in chapter 3. The computed eigenvalues are validated against previously published uniform rectangular cantilever plate free vibration results. They were found converging to the known values. Free vibration eigenvalues and mode shapes are then calculated for a variety of cantilever plates of different aspect ratios and with different span thicknesses creating a discontinuity in mass and flexural rigidity along the plate. The results are presented in chapter 4 and discussed in chapter 5.

ACKNOWLEDGEMENT

I would like to thank Dr. Gorman for his continuous support, valuable assistance and guidance. I have come to realize the importance of Dr. Gorman's achievement in the area of free vibration of plates throughout the past decades until today. For this, I would like to express my extreme appreciation and best wishes for a continuing success and my promise to deserve being his student in my future assignments.

I would also like to thank professors & staff of the mechanical engineering department at the University Of Ottawa. Thank you Solange Lamontagne for your encouragement.

I would also like to thank my parents for their encouragement and in particular my brother Walid for his valuable advice. I wish you all the best in your Phd, Brother.

This thesis is dedicated to my future family and to anyone who dares to dream of a better future. Dreams do come true.

Nomenclature

a	Building block edge dimension
a_i	Edge dimension of plate segment i
b	Plate dimension along clamped edge
D	Flexural rigidity of plate segment
D_i	Flexural rigidity of plate segment i
E	Modulus of elasticity of plate material
h	Plate thickness
h_i	Thickness of plate segment 'i'
w	Plate lateral displacement
W	Dimensionless plate lateral displacement
x,y	Distances along plate edges
ν	Poisson ratio of plate material
ν*	2-ν
ξ	x/a
η	y/b
ρ_i	Mass per unit area of span i of plate
ω	Circular frequency of vibration
λ_a², λ²	Dimensionless frequency = ω a_i² √(ρ_i/D_i) of span i
λ_b²	Eigenvalue = ω b² √(ρ_i/D_i)

Table Of Contents

Abstract.....	ii
Acknowledgements.....	iii
Nomenclature.....	iv
List of Figures and Charts.....	vii
List of Tables	ix
Chapter 1: Introduction.....	1
1.1 Rectangular Plates: The Continuing Interest	1
1.2 Historical Background.....	2
1.3 Alternative Techniques.....	4
1.4 The Governing Differential Equation.....	5
Chapter 2: The Rectangular Plate.....	8
2.1 Limitations.....	8
2.2 Classical Boundary Conditions.....	9
2.2.1 Mathematical Formulations.....	9
2.2.2 Clamped Edge.....	11
2.2.3 Simply Supported Edge.....	11
2.2.4 Slip Shear Edge.....	11
2.2.5 Free Edge.....	12
2.3 The Two Families of Problems.....	12

Chapter 3:	The Rectangular Cantilever Plate with Step Discontinuity in Properties.....	16
3.1	The Three Span Cantilever Plate.....	16
3.1.1	The Three Span Cantilever Plate Building Blocks.....	17
3.1.2	Building Block Solutions.....	26
3.1.2.a	Span 2 and 3 Building Block Solutions.....	26
3.1.2.b	Span 1 Building Block Solutions.....	41
3.1.3	Generation of the Eigenvalue Matrix	50
3.2	The Four Span Cantilever Plate.....	64
Chapter 4:	Presentation of Results.....	67
4.1	Results for the Three Span Cantilever Plate.....	68
4.2	Plotted Mode Shapes.....	74
4.3	Eigenvalues for Plates with Uniform Thickness Throughout.....	95
Chapter 5:	Discussion of Results.....	98
References:	100
Appendix 1:	The Four Span Cantilever Plate Results	101
Appendix 2:	List of Solved Integrals.....	106
Appendix 3:	Listing of the Fortran Program.....	109

List of Figures and Charts

Figure 1.1: Rectangular plate coordinate system.....	7
Figure 2.1: Distributed bending moments.....	10
Figure 2.2: Distributed vertical edge reactions shown in the positive direction.....	10
Figure 3.1: The three span cantilever plate.....	17
Figure 3.2: The three span cantilever plate building blocks.....	19
Figure 3.3: The superposition method building blocks.....	23
Figure 3.4: Analysis of building blocks “H”, “I”, “N”, “O” of spans 2 & 3.....	26
Figure 3.5: Analysis of building blocks “E”, “J”, “K”, “P”.....	32
Figure 3.6: Analysis of building blocks “G”, “L”, “M”.....	35
Figure 3.7: Analysis of span 1 building blocks “A”, “B”, “C”, “D”, “F”.....	41
Figure 3.8: Solution for block “A”.....	42
Figure 3.9: Solution for block “D”.....	44
Figure 3.10: Deriving the solution for block “F”.....	46
Figure 3.11: Summary of building block solutions.....	48
Figure 3.12: Eigenvalue matrix for the three span cantilever plate.....	51
Figure 3.13: Representation of the first row elements by their expressions.....	58
Figure 3.14: Flowchart for determining the eigenvalue for the three span cantilever plate.....	63
Figure 3.15a: First portion of the eigenvalue matrix for the four span cantilever plate...	65
Figure 3.15b: Final portion of matrix of figure 3.15a	66
Figure 4.1: First four mode shapes for Table 4.1.....	75
Figure 4.2: First four mode shapes for Table 4.2.....	76

Figure 4.3: First four mode shapes for Table 4.3.....77

Figure 4.4: First four mode shapes for Table 4.4.....78

Figure 4.5: First four mode shapes for Table 4.579

Figure 4.6: First four mode shapes for Table 4.680

Figure 4.7: First four mode shapes for Table 4.781

Figure 4.8: First four mode shapes for Table 4.882

Figure 4.9: First four mode shapes for Table 4.983

Figure 4.10: First four mode shapes for Table 4.1084

Figure 4.11: First four mode shapes for Table 4.1185

Figure 4.12: First four mode shapes for Table 4.1286

Figure 4.13: First four mode shapes for Table 4.1387

Figure 4.14: First four mode shapes for Table 4.1488

Figure 4.15: First four mode shapes for Table 4.1589

Figure 4.16: First four mode shapes for Table 4.1690

Figure 4.17: First four mode shapes for Table 4.1791

Figure 4.18: First four mode shapes for Table 4.1892

Figure 4.19: First four mode shapes for Table 4.1993

Figure 4.20: First four mode shapes for Table 4.2094

Chart 3.1: Flowchart providing a general overview of Chapter 315

Chart 3.2: Flowchart outlining solutions of spans 2 and 3 building blocks40

Chart 3.3: Flowchart outlining solutions for span 1 building blocks49

List of Tables

Table 2.1: Building block cases with Levy-type solutions for displacement	13
Table 2.2: Levy-type solutions for displacement for building block cases of Table 2.1 ...	14
Table 3.1: Summary of the remaining boundary conditions imposed by the eigenvalue matrix.....	52
Table 4.1: Eigenvalues for thickness ratios= $1, 3/4, 1/2$ & plate overall aspect ratio= 3	69
Table 4.2: Eigenvalues for thickness ratios= $1, 3/8, 1/4$ & plate overall aspect ratio= 3	69
Table 4.3: Eigenvalues for thickness ratios= $1, 3/4, 1/2$ & plate overall aspect ratio= 2	69
Table 4.4: Eigenvalues for thickness ratios= $1, 3/8, 1/4$ & plate overall aspect ratio= 2	69
Table 4.5: Eigenvalues for thickness ratios= $1, 3/4, 1/2$ & plate overall aspect ratio= 1.5 ...	70
Table 4.6: Eigenvalues for thickness ratios= $1, 3/8, 1/4$ & plate overall aspect ratio= 1.5 ...	70
Table 4.7: Eigenvalues for thickness ratios= $1, 3/4, 1/2$ & plate overall aspect ratio= 1	70
Table 4.8: Eigenvalues for thickness ratios= $1, 3/8, 1/4$ & plate overall aspect ratio= 1	70
Table 4.9: Eigenvalues for thickness ratios= $1, 3/4, 1/2$ & plate overall aspect ratio= $2/3$	71
Table 4.10: Eigenvalues for thickness ratios= $1, 3/8, 1/4$ & plate overall aspect ratio= $2/3$...	71
Table 4.11: Eigenvalues for thickness ratios= $1, 3/4, 1/2$ & plate overall aspect ratio= $1/2$...	71
Table 4.12: Eigenvalues for thickness ratios= $1, 3/8, 1/4$ & plate overall aspect ratio= $1/2$..	71
Table 4.13: Eigenvalues for thickness ratios= $1, 3/4, 1/2$ & plate overall aspect ratio= $1/3$..	72
Table 4.14: Eigenvalues for thickness ratios= $1, 3/8, 1/4$ & plate overall aspect ratio= $1/3$...	72
Table 4.15: Eigenvalues for thickness ratios= $1, 3/4, 1/2$ & plate overall aspect ratio= $2/9$..	72
Table 4.16: Eigenvalues for thickness ratios= $1, 3/8, 1/4$ & plate overall aspect ratio= $2/9$..	72
Table 4.17: Eigenvalues for thickness ratios= $1, 3/4, 1/2$ & plate overall aspect ratio= $1/6$..	73
Table 4.18: Eigenvalues for thickness ratios= $1, 3/8, 1/4$ & plate overall aspect ratio= $1/6$..	73

Table 4.19: Eigenvalues for thickness ratios=1,3/4,1/2 & plate overall aspect ratio=1/9...	73
Table 4.20: Eigenvalues for thickness ratios=1,3/8,1/4 & plate overall aspect ratio=1/9...	73
Table 4.21: Eigenvalues for thickness ratios=1,1,1 & plate overall aspect ratio=1/3.....	96
Table 4.22: Eigenvalues for thickness ratios=1,1,1 & plate overall aspect ratio=1.....	96
Table 4.23.a: Eigenvalues for thickness ratios=1,1,1 & plate overall aspect ratio=2.....	97
Table 4.23.b: Eigenvalues for thickness ratios=1,1,1 & plate overall aspect ratio=1.25...	97
Table 4.24: Eigenvalues for thickness ratios=1,1,1 & plate overall aspect ratio=1/1.25...	97
Table 4.25: Eigenvalues for thickness ratios=1,3/8,1/4,1/8 & plate overall aspect ratio=3.....	102
Table 4.26: Eigenvalues for thickness ratios=1,3/8,1/4,1/8 & plate overall aspect ratio=2.....	102
Table 4.27: Eigenvalues for thickness ratios=1,3/8,1/4,1/8 & plate overall aspect ratio=1.5.....	103
Table 4.28: Eigenvalues for thickness ratios=1,3/8,1/4,1/8 & plate overall aspect ratio=1.....	103
Table 4.29: Eigenvalues for thickness ratios=1,3/8,1/4,1/8 & plate overall aspect ratio=2/3.....	104
Table 4.30: Eigenvalues for thickness ratios=1,3/8,1/4,1/8 & plate overall aspect ratio=1/2.....	104
Table 4.31: Eigenvalues for and thickness ratios=1,3/8,1/4,1/8 & plate overall aspect ratio=1/3.....	105
Table 4.32: Eigenvalues for thickness ratios=1,1,1,1 & plate overall aspect ratio=1/3...	105
Table 4.33: Eigenvalues for thickness ratios=1,1,1,1 & plate overall aspect ratio=1.....	105

Chapter 1

INTRODUCTION

As one of the most commonly used lightweight structures in industry, rectangular plates have been extensively studied for many years. Before introducing the theory on which this thesis is based, the main reasons behind the continuing interest in this field of study are provided to the reader followed by a brief historical background of the theory. A comparison with some existing alternative techniques is provided before introducing the basic most important equation governing the free vibration of plates.

1.1 Rectangular Plates : The Continuing Interest

The study of rectangular plate free vibration even after several decades of research is still attracting the interest of researchers across the world. Although accurate analytical free vibration solutions for varieties of rectangular plates using the superposition method have been published, especially in the past two decades due to the work of Gorman[1], it is foreseen that new plate problems will emerge and will continue to motivate the interest of scientists being driven by several factors. One of the main driving factors is the continuous research requirement arising from the advance in composite materials and aerospace sciences and even computer hardware requirements where in some cases stringent vibration design tolerances necessitate the modelling of motherboards as rectangular plates with non conventional supporting media. Another major factor in advocating the use of the superposition method in the study of rectangular plates is the

extensive use of numerical methods like finite element methods in solving complicated engineering problems, and the necessity to validate those numerical results with the accurate analytical solutions provided by the superposition method. This is especially true in critical designs like Multi-Span bridges which are used world-wide. A brief historical background of the study of plate vibrations is presented next.

1.2 Historical Background

The study of the theory of plates started with Euler¹ in 1766 with the preliminary formulation of the membrane theory of plate free vibration using two systems of perpendicular strings to solve the problem of rectangular and circular membranes. This theory was extended by Bernoulli² to rectangular plates with little success in establishing a satisfactory correlation with the experimental results. Although Sophie Germain³ attempted to develop a differential equation governing the free vibration of plates, it was Lagrange⁴ who developed the correct form of the equation by adding missing terms to the equation developed by Germain. However, the complete derivation of the governing differential equation with flexural resistance included was attributed to Navier⁵ who used Fourier trigonometric double series to solve the problem of simply supported plates. Later Kirchoff⁶ extended the equation developed by Navier to include the effect of

¹ Euler L.(1707-1783) ,“De Motu Vibratorio Tympanorum”(1766).

² Bernoulli J.III-(1744-1807),“Essai Theorique sur les vibrations de plaques elastiques rectangulaires et libres”(1789).

³ Sophie Germain(1776-1831), famous for her work using the calculus of variations.(1811-1816)

⁴ Lagrange,J.L(1736-1813), believed to be the first to find the correct form of the equation in (1813).

⁵ Navier,C.L.M.H.(1785-1836), engineer who made important contributions to the theory of elasticity.

⁶ Kirchoff, G. R. (1824-1887).

⁷ Levy,M. “l’equilibre elastique d’une plaque rectangulaire”(1899).

combined bending moment and stretching. Levy⁷ proposed a single trigonometric series that provided a more accurate rapidly converging solution for rectangular plates with at least two opposite simply supported edges. This method was a more efficient and faster alternative to the slowly converging Navier double series which only handles plates with simple supports on all edges. In the early sixties and after the emergence of high speed computers, Timoshenko[2] introduced the western world to the successful work of Russian scientists in the domain of elasticity. Leissa[5] provided engineers and scientists in the late sixties with solutions and mode shapes to a whole variety of plate problems with different geometries. However, many of these solutions presented in Leissa's work do not satisfy exactly the governing differential equation, the boundary conditions or even both. Based on the work of Timoshenko and realizing the need for accurate plate solutions, and in the absence of an orderly presentation of these solutions in Leissa's work, Gorman[1] introduced the superposition method in the mid seventies and early eighties for the study of rectangular plate free vibration.

In his work, Gorman extended the use of the superposition method from the static plate applications to the dynamic plate problems in an orderly manner. This lead to accurate analytical solutions for rectangular plate problems with any combination of conventional¹ boundary conditions, and satisfied the governing differential equation exactly and the boundary conditions to any desired degree of accuracy. This method consists of superimposing a set of selected forced vibration problems for which exact series solutions exist and are known as Levy type solutions. These superposed solutions are called building blocks. They are usually driven by distributed harmonic moments or

¹ For a detailed description of conventional boundary conditions refer to explanations in chapter 2.

vertical edge reactions along the boundaries. Once the building blocks are superimposed, boundary conditions are imposed in order to obtain the solution for the unknown Fourier coefficients. In the late nineties, another book by Gorman[3] came into existence extending the vast capabilities of the superposition method to the solution of new families of plates such as orthotropic, parallelogram, triangular and laminated plates. This thesis takes origin in the work of Gorman and constitutes an extension of the powerful capabilities of the superposition method to permit solution of a new problem “the cantilever plate with varying discontinuities in properties moving out from the clamped edge”. The next section presents a brief comparison with the available alternative numerical solutions.

1.3 Alternative Techniques

According to Gorman[3] the superposition method can be compared to two other techniques in the solution of plate problems. These are the Rayleigh-Ritz and the finite element method. Both the superposition method and the Rayleigh-Ritz method are based on continuum mechanics. The Rayleigh-Ritz method consists of assuming a series of suitable functions for representing the plate lateral displacement that will satisfy as much as possible the boundary conditions. A solution is then obtained by an energy method. The finite element method (F.E) is a very powerful numerical method using high speed computers to obtain solution for complex structures where the application of analytical solutions becomes a formidable task.

Unlike the Rayleigh-Ritz and the F.E methods, the superposition method is the only one that generates solutions satisfying the governing differential equation throughout the whole domain of the plate. Moreover, it has been demonstrated that appropriate functions in the Rayleigh-Ritz method do not exist for representing plate displacements when free edges are involved.

1.4 The Governing Differential Equation

The governing differential equation of a plate in pure bending subjected to lateral loading was presented by Timoshenko[2] as follows :

$$\frac{\partial^4 W(x,y)}{\partial x^4} + 2 \frac{\partial^4 W(x,y)}{\partial x^2 \partial y^2} + \frac{\partial^4 W(x,y)}{\partial y^4} = \frac{q(x,y)}{D} \quad (1.1.a)$$

where $q(x,y)$ is the intensity of the applied static loading and D the plate flexural rigidity given by:

$$D = \frac{Eh^3}{12(1-\nu^2)}$$

where E is the modulus of elasticity, h the plate thickness and ν is Poisson ratio. However the previously stated differential equation for the static case should be modified in order to study the free vibration of plates. This is done by replacing the static loading $q(x,y)dA$ by the inertial load of magnitude

$$\rho dA \partial^2 W / \partial t^2$$

where t is time, W the lateral displacement, dA the plate differential surface area and ρ the mass of the plate per unit surface area. The governing differential equation for the free vibration of plates as stated by Gorman[2] is as follows :

$$\frac{\partial^4 W(x, y, t)}{\partial x^4} + 2 \frac{\partial^4 W(x, y, t)}{\partial x^2 \partial y^2} + \frac{\partial^4 W(x, y, t)}{\partial y^4} + \frac{\rho}{D} \frac{\partial^2 W(x, y, t)}{\partial t^2} = 0 \quad (1.1.b)$$

However, the current form of the differential equation is first altered by performing a separation of variables as $W(x, y, t) = W(x, y)T(t)$ where $T(t) = A \sin(\omega t + \alpha)$, is a sinusoidal time function with A and α constants to be determined. The time variable was successfully eliminated from the governing differential equation and two separate equal equations were obtained, one in function of time and the other in function of displacement. That could only mean that the two equations were equal to a constant. This constant was stated as ω^2 . ω will be known later as the circular frequency of vibration and will be the representation of the time factor in the plate equation obtained as:

$$\frac{\partial^4 W(x, y)}{\partial x^4} + 2 \frac{\partial^4 W(x, y)}{\partial x^2 \partial y^2} + \frac{\partial^4 W(x, y)}{\partial y^4} - \frac{\omega^2 \rho}{D} W(x, y) = 0 \quad (1.c)$$

It was found more convenient to express this equation in dimensionless form, thereby allowing a more general approach, it becomes,

$$\frac{\partial^4 W(\xi, \eta)}{\partial \xi^4} + 2 \frac{\partial^4 W(\xi, \eta)}{\phi^2 \partial \xi^2 \partial \eta^2} + \frac{\partial^4 W(\xi, \eta)}{\phi^4 \partial \eta^4} - \lambda^4 W(\xi, \eta) = 0 \quad (1.1.d)$$

or

$$\frac{\partial^4 W(\xi, \eta)}{\partial \eta^4} + 2\phi^2 \frac{\partial^4 W(\xi, \eta)}{\partial \eta^2 \partial \xi^2} + \phi^4 \frac{\partial^4 W(\xi, \eta)}{\partial \xi^4} - \phi^4 \lambda^4 W(\xi, \eta) = 0 \quad (1.2)$$

where $\xi = x/a$, $\eta = y/b$, $\phi = b/a$ the aspect ratio of the plate and a , b are the plate edge dimensions as represented in Figure 1.1. $\lambda^2 = \omega a^2 (\rho/D)^{1/2}$ will be known later as the dimensionless frequency, with D and ρ as previously stated.

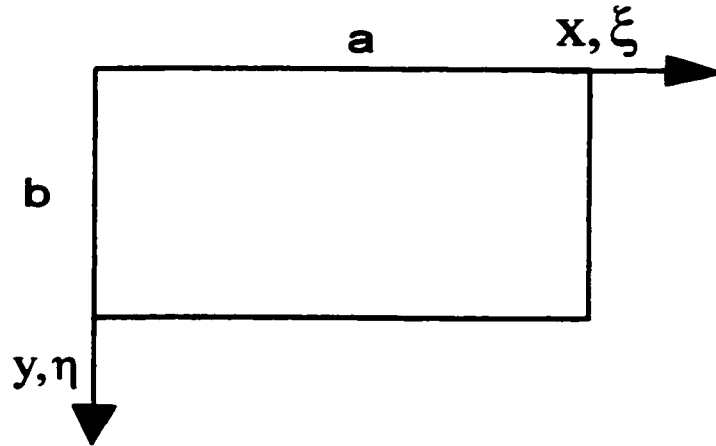


Figure 1.1 : Rectangular plate coordinate system.

Figure 1.1 represents the rectangular plate in dimensionless coordinates. Equation (1.2) is the governing differential equations that will be used for the free vibration problems. The general solutions for plate boundary conditions will now be examined in Chapter two.

Chapter 2

THE RECTANGULAR PLATE

In the previous chapter, the governing equation of plates was introduced to the reader. However, before exposing the analytical solutions for the multi-span cantilever plate problem in Chapter 3 it is necessary to introduce the underlying theory including general plate boundary conditions as per Gorman[1].

2.1 Limitations

The range of plate geometries for which the governing equations (1.1.d) and (1.2), presented in the previous chapter are applicable, is subject to limitations due to the assumptions made in setting up the governing equation for thin plates. The limitations as stated by Gorman[2] are repeated here for the sake of completeness.

- 1- The thickness of the plate is small compared to its lateral dimensions (theory of thin plates).
- 2- For higher vibration mode shapes, the plate thickness is small compared to distances between nodal lines (lines along which no vibratory displacement occurs).
- 3- The lateral displacement (W) of the plate is small compared to its thickness (h).
- 4- The effects of rotary inertia are negligible; that is, the plate never possesses significant energy due to rotation of its elements.
- 5- There are no significant net tensile or compressive forces in the plate.

6- The Levy type single series solution can only be applied to rectangular plates with at least two opposite simply supported or slip shear edges, or any combination of the two.

2.2 Classical Boundary Conditions

The three types of classical boundary conditions that have been studied extensively in the literature are clamped, simply supported and free edges. Each boundary condition implies specific constraints or continuity conditions regarding moment, vertical shear, displacement and slope.

2.2.1 Mathematical Formulations

The mathematical formulations were derived by Timoshenko[2] and were manipulated in dimensionless form by Gorman[1]. The slope can be expressed in terms of displacement $W(\xi, \eta)$ with respect to the ξ or η axis respectively as:

$$S_{\xi} = \frac{\partial W(\xi, \eta)}{\partial \xi} \quad \text{or} \quad S_{\eta} = \frac{\partial W(\xi, \eta)}{\partial \eta} \quad (2.1)$$

The bending moment with respect to the ξ or η axis is as follows and as shown in Figure 2.1:

$$M_{\xi} \frac{a}{D} = - \left[\frac{\partial^2 W(\xi, \eta)}{\partial \xi^2} + \frac{\nu}{\phi^2} \frac{\partial^2 W(\xi, \eta)}{\partial \eta^2} \right] \quad \text{or} \quad M_{\eta} \frac{\phi b}{D} = - \left[\frac{\partial^2 W(\xi, \eta)}{\partial \eta^2} + \nu \phi^2 \frac{\partial^2 W(\xi, \eta)}{\partial \xi^2} \right] \quad (2.2)$$

The vertical edge reaction with respect to the ξ or η axis is as follows and as shown in Figure 2.2:

$$V_{\xi} \frac{a^2}{D} = - \left[\frac{\partial^3 W(\xi, \eta)}{\partial \xi^3} + \frac{v^*}{\phi^2} \frac{\partial^3 W(\xi, \eta)}{\partial \xi \partial \eta^2} \right] \text{ or } V_{\eta} \frac{\phi b^2}{D} = - \left[\frac{\partial^3 W(\xi, \eta)}{\partial \eta^3} + v^* \phi^2 \frac{\partial^3 W(\xi, \eta)}{\partial \eta \partial \xi^2} \right] \quad (2.3)$$

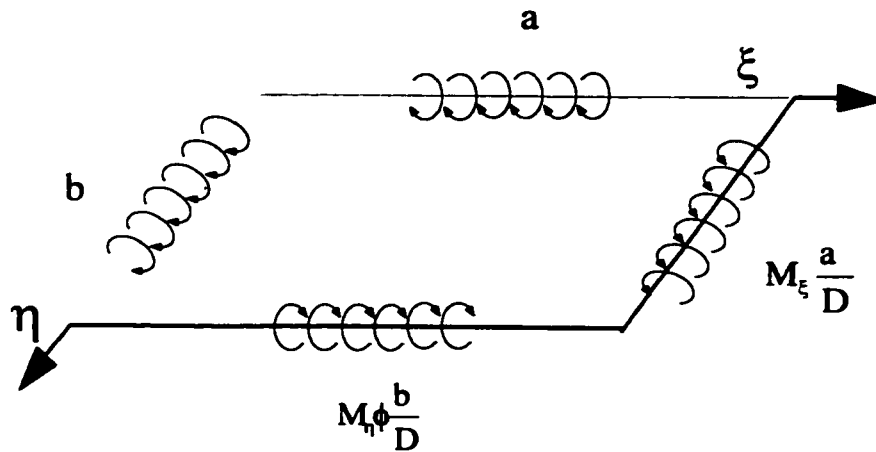


Figure 2.1: Distributed bending moments.

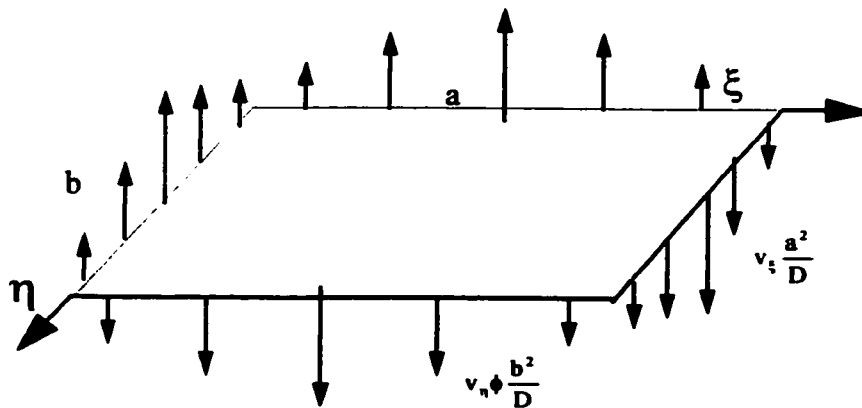


Figure 2.2 : Distributed vertical edge reactions shown in the positive direction.

2.2.2 Clamped Edge

A clamped edge is formulated by a zero displacement and zero slope along the edge as:

$$W(\xi, \eta) = 0 \quad (2.4)$$

$$\frac{\partial W(\xi, \eta)}{\partial \xi} = 0 \quad \text{or} \quad \frac{\partial W(\xi, \eta)}{\partial \eta} = 0 \quad (2.5)$$

2.2.3 Simply Supported Edge

A simply supported edge is formulated by a zero displacement and zero bending moment along the edge as follows:

$$W(\xi, \eta) = 0 \quad (2.6)$$

$$\frac{\partial^2 W(\xi, \eta)}{\partial \xi^2} = 0 \quad \text{or} \quad \frac{\partial^2 W(\xi, \eta)}{\partial \eta^2} = 0 \quad (2.7)$$

2.2.4 Slip Shear Edge

A slip shear edge is formulated by a zero shear force and zero slope along the edge as:

$$\frac{\partial^3 W(\xi, \eta)}{\partial \xi^3} = 0 \quad \text{or} \quad \frac{\partial^3 W(\xi, \eta)}{\partial \eta^3} = 0 \quad (2.8)$$

$$\frac{\partial W(\xi, \eta)}{\partial \xi} = 0 \quad \text{or} \quad \frac{\partial W(\xi, \eta)}{\partial \eta} = 0 \quad (2.9)$$

2.2.5 Free Edge

A free edge is formulated by a zero shear force & twisting moment and a zero bending moment along the edge as follows:

$$\frac{\partial^3 W(\xi, \eta)}{\partial \xi^3} + \frac{\nu}{\phi^2} \frac{\partial^3 W(\xi, \eta)}{\partial \xi \partial \eta^2} = 0 \quad \text{and} \quad \frac{\partial^2 W(\xi, \eta)}{\partial \xi^2} + \frac{\nu}{\phi^2} \frac{\partial^2 W(\xi, \eta)}{\partial \eta^2} = 0 \quad \text{or} \quad (2.10)$$

$$\frac{\partial^3 W(\xi, \eta)}{\partial \eta^3} + \nu \phi^2 \frac{\partial^3 W(\xi, \eta)}{\partial \xi^2 \partial \eta} = 0 \quad \text{and} \quad \frac{\partial^2 W(\xi, \eta)}{\partial \eta^2} + \nu \phi^2 \frac{\partial^2 W(\xi, \eta)}{\partial \xi^2} = 0 \quad (2.11)$$

2.3 The Two Families of Problems

Rectangular plate problems with classical boundary conditions fall into two distinct families. The first family is solved by Levy-type solutions for plates having at least two opposite simply supported edges or at least two opposite slip shear conditions, or an opposite pair consisting of one simply supported edge and the other with slip shear conditions. Levy-type solutions consist of a series solution involving Fourier sine or cosine series in one coordinate direction where the associated coefficients are functions of the other coordinate. Levy-type solutions are chosen to satisfy the boundary conditions of the two opposite simply supported or slip shear edges, or any combination of the two. The second family represents plates with any combination of classical boundary conditions that do not satisfy the first family. They can be solved by the superposition method that was introduced briefly in Chapter 1 and that will be implemented in detail in Chapter 3 for the solution of the cantilever plate problem. It is noted that the superposition method uses forced vibration solutions of the first family in different building blocks that are combined or superimposed to permit satisfaction of the given

plate boundary conditions. Table 2.1 presents a summary of building block representations for different available Levy-type solutions.

Table 2.1: Building block cases with Levy-type solutions for displacement. The double circles represent slip shear and the extended lines represent a simple support. The coordinate system of figure 1.1 applies.

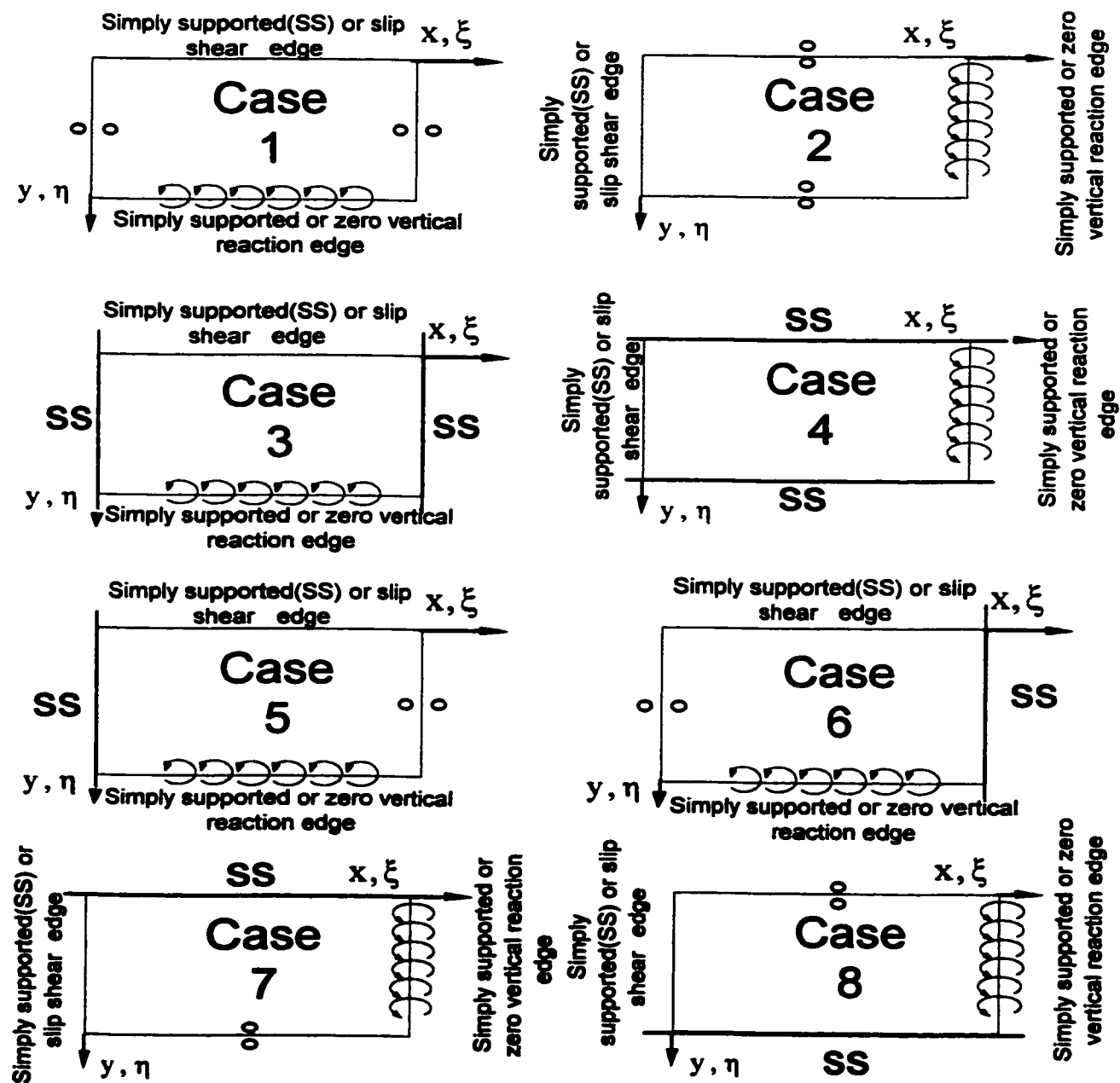


Table 2.2: Levy-type solutions for displacement for building block cases of Table 2.1.

$$\text{Case 1: } W(\xi, \eta) = \sum_{m=0,1,2}^{\infty} Y_m(\eta) \cos(m\pi\xi) \quad (2.12)$$

$$\text{Case 2: } W(\xi, \eta) = \sum_{n=0,1,2}^{\infty} Y_n(\xi) \cos(n\pi\eta) \quad (2.13)$$

$$\text{Case 3: } W(\xi, \eta) = \sum_{m=1,2,3}^{\infty} Y_m(\eta) \sin(m\pi\xi) \quad (2.14)$$

$$\text{Case 4: } W(\xi, \eta) = \sum_{n=1,2,3}^{\infty} Y_n(\xi) \sin(n\pi\eta) \quad (2.15)$$

$$\text{Case 5: } W(\xi, \eta) = \sum_{m=1,3,5}^{\infty} Y_m(\eta) \sin(m\pi\xi/2) \quad (2.16)$$

$$\text{Case 6: } W(\xi, \eta) = \sum_{m=1,3,5}^{\infty} Y_m(\eta) \cos(m\pi\xi/2) \quad (2.17)$$

$$\text{Case 7: } W(\xi, \eta) = \sum_{n=1,3,5}^{\infty} Y_n(\xi) \sin(n\pi\eta/2) \quad (2.18)$$

$$\text{Case 8: } W(\xi, \eta) = \sum_{n=1,3,5}^{\infty} Y_n(\xi) \cos(n\pi\eta/2) \quad (2.19)$$

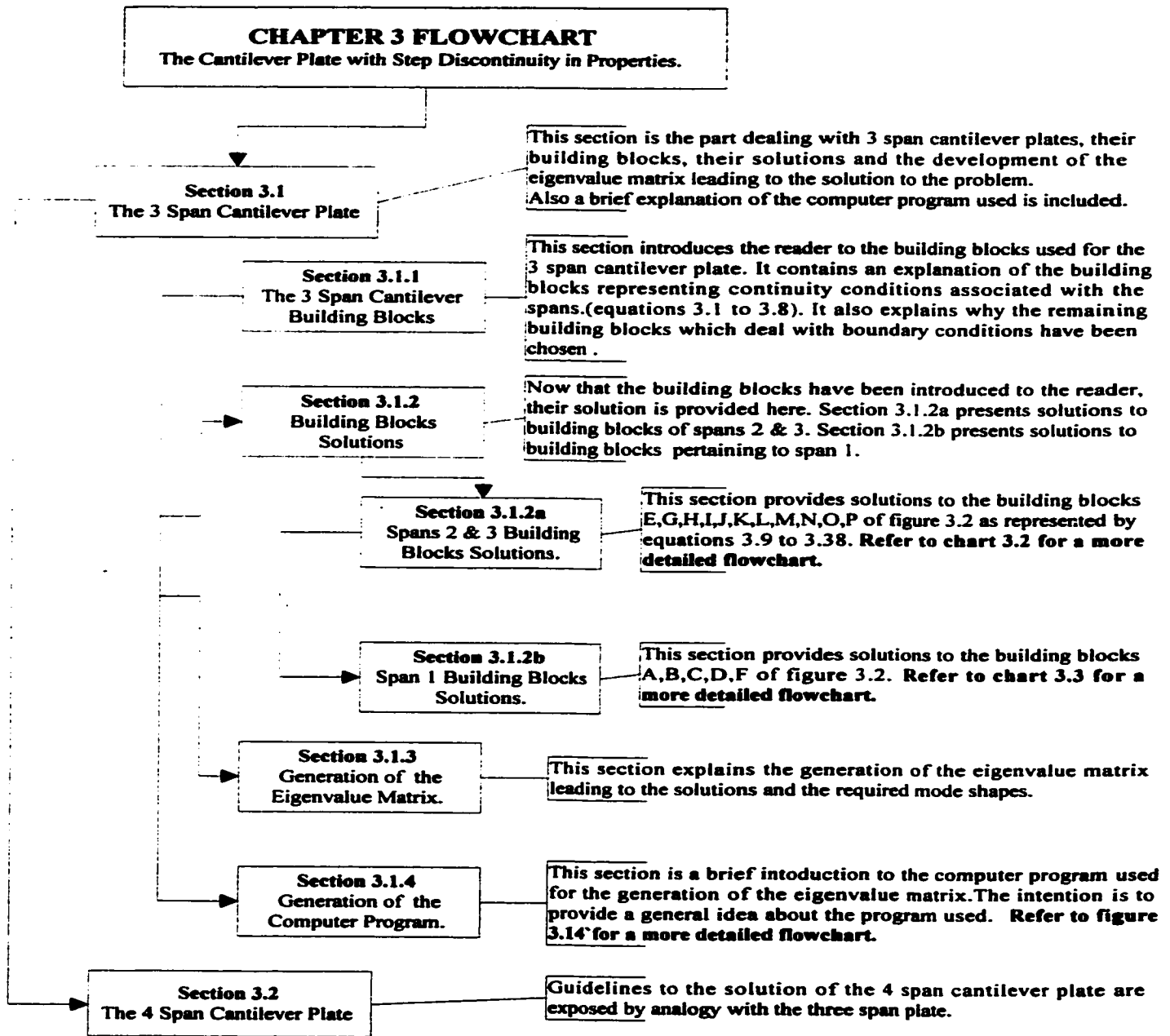


Chart 3.1 : Flowchart providing a general overview of Chapter 3.

Chapter 3

THE CANTILEVER PLATE WITH STEP DISCONTINUITIES IN PROPERTIES

The uniform cantilever plate problem has been solved three decades ago and solutions can be found in the work of Leissa[5] and more accurately in the work of Gorman[1] using the superposition method. In his work, Gorman realised that due to the cantilever plate geometry, asymmetry about the mid plate axis perpendicular to the clamped edge cannot be possible, simply because there are no preferred directions. Therefore all the analytical cantilever plate solutions were derived using symmetry or antisymmetry with respect to this axis choosing appropriate building blocks for each case. This thesis does not utilize the symmetry feature of the cantilever plate in developing the building blocks employed for deriving the analytical solutions. Solutions for all possible modes are thus obtained. The interested reader is referred to the mode shapes presented in Chapter 4 for an appreciation of the symmetry phenomenon. This chapter presents free vibration analytical solutions in detail for the three span cantilever plate and introduces the extension to the four span case. The reader is encouraged to consult Chart 3.1 for a quick overview of this chapter.

3.1 The Three Span Cantilever Plate

The plate coordinate system of Figure 3.1 applies to the three span cantilever plate. For the purpose of this thesis, the three span cantilever plate is composed of three segments of different structural properties. This fact creates two discontinuities parallel to

the clamped edge. The edge length b is constant throughout the plate and span lengths are a_1, a_2, a_3 . For demonstration purposes, the variation in structural properties from the clamped edge is represented by varying thicknesses per span h_1, h_2, h_3 creating a discontinuity in stiffness and mass. This is shown in Figure 3.1.

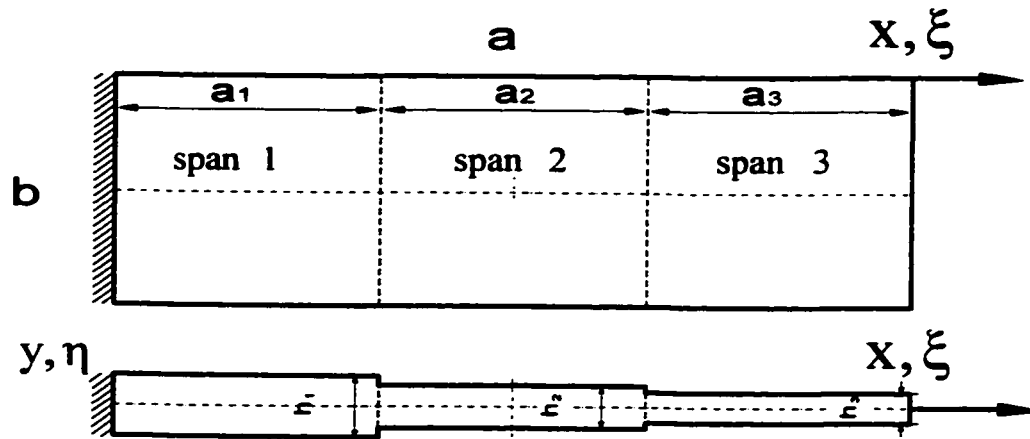


Figure 3.1 : The three span cantilever plate.

3.1.1 The Three Span Cantilever Plate Building Blocks

The cantilever plate is a CFFF rectangular plate (clamped, free, free, free) that does not belong to the first family of plate problems as discussed earlier in section 2.3. The use of the superposition method is therefore required to obtain accurate analytical solutions. For this purpose, the three span cantilever plate is divided into several superimposed building block sets for which Levy-type solutions are available. Each span represented in Figure 3.1 corresponds to a set of building blocks in Figure 3.2. The number inside each building block is relative to the span it represents. The building blocks are referenced by letters from "A" to "P". For an easier follow up of the coming

discussions, the reader may wish at this stage to produce a photocopy of Figure 3.2 in addition to tables 2.1 and 2.2.

Since the cantilever plate forms a continuous rectangular plate, continuity conditions are enforced between the plate spans. This is done by enforcing continuity of slope, vertical shear, moment and displacement. The enforcement of the continuity of moment and displacement will be discussed in section 3.1.3 while establishing the eigenvalue matrix. Blocks “D”+“E” and “F”+“G” of Figure 3.2.a form a coupled pair of building blocks. The continuity of slope between spans 1 and 2 is enforced by blocks “D”+“E”. Blocks “F”+“G” enforce the continuity conditions for vertical shear. Blocks “J”+“K” and “L”+“M” of Figure 3.2.b enforce the same conditions for spans 2 and 3. For the sake of completeness the continuity conditions of slope and vertical shear are formulated next.

Considering block “D” of Figure 3.2.a, the reader will realise that this building block is a case2 Levy-type solution with a response $W(\xi,\eta)$ as per equation 2.13 in Table 2.2. In this building block, a forced rotation is imposed at edge $x = a_1$ of the plate. In dimensionless form, this edge corresponds to $\xi=1$. The unknown spatial distribution of the imposed edge rotation is expressed in the same cosine series form as equation 2.13. By using equation 2.1 for the expression of the slope, the following relation could be obtained at edge $\xi=1$ as:

$$\frac{\partial W(\xi, \eta)}{\partial \xi} \Big|_{\xi=1} = \sum_{n=0,1,2}^{\infty} E_n \cos(n\pi\eta) \quad (3.1)$$

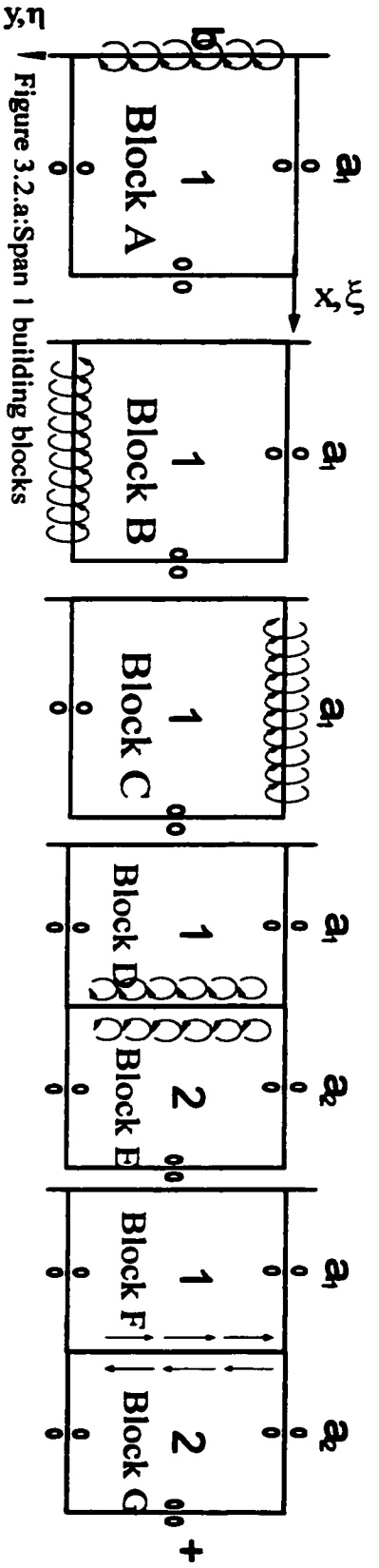


Figure 3.2.a: Span 1 building blocks

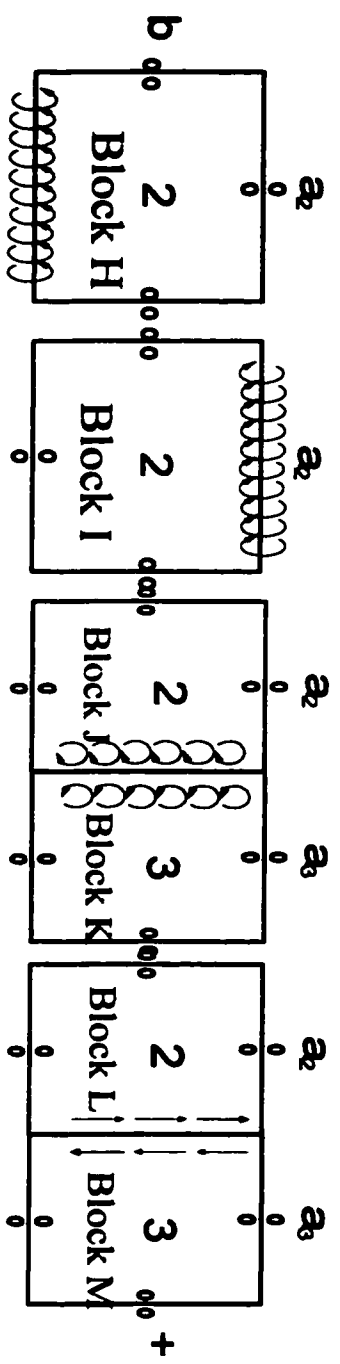


Figure 3.2.b: Span 2 building blocks

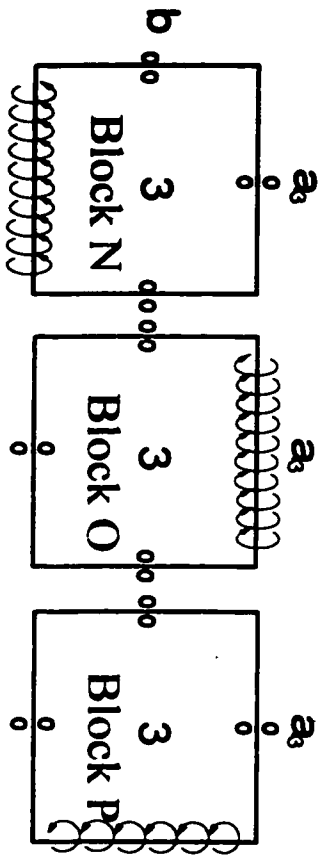


Figure 3.2.c: Span 3 building blocks.

Figure 3.2: The three span cantilever plate building blocks .

where E_n is the driving coefficient for span 1 and where $W(\xi,\eta)$ is the lateral displacement divided by segment width 'b'. The subscript "n" has been utilised to indicate the driving coefficients. Now, considering block "E" of span 2, the forced rotations are imposed at edge $x = 0$, or in dimensionless form at edge $\xi=0$. Following the same principles discussed above, the imposed edge rotation at edge $\xi=0$ is expressed in series form as:

$$\frac{\partial W(\xi,\eta)}{\partial \xi} \Big|_{\xi=0} = - \sum_{n=0,1,2}^{\infty} E_n^* \cos(n\pi\eta) \quad (3.2)$$

where E_n^* is the driving coefficient for span 2, $W(\xi,\eta)$ is non-dimensionalised through division by edge length 'b' and the negative sign reflects the orientation change of the rotations. It is recognised that the condition of continuity of slope at the inter-span boundary is enforced by relating the driving coefficients pertaining to spans 1 and 2. In fact, the imposed driving coefficients at each span must generate the same actual slope since the two building blocks in the coupled pair under consideration are the only ones that can contribute toward slope at the inter-span location between spans 1 and 2. Equation 2.1 presented earlier in section 2.2.1 is an expression of the slope S_ξ where $\xi=0$ and $W(\xi,\eta)$ is the lateral displacement divided by segment width 'a'. Since the Displacement for blocks "D"+"E" is non dimensionalised through division by edge length 'b' as was the case for equations 3.1 and 3.2, the contribution towards slope of this building block must be multiplied by the plate segment aspect ratio as follows:

$$\frac{\partial W(\xi, \eta)}{\partial \xi} \Big|_{\xi=1} b/a_i = \sum_{n=0,1,2}^{\infty} E_n b/a_i \cos(n\pi\eta) \quad (3.3)$$

and

$$\frac{\partial W(\xi, \eta)}{\partial \xi} \Big|_{\xi=0} b/a_j = - \sum_{n=0,1,2}^{\infty} E_n^* b/a_j \cos(n\pi\eta) \quad (3.4)$$

where i and j are a general denotation of the successive building blocks in each coupled pair. Equating 3.3 and 3.4 the following relationship can be written at the interface:

$$E_n^* = E_n \left\{ -\phi_i/\phi_j \right\} \quad (3.5)$$

where all the driving coefficients pertaining to the second building block of the coupled pair are multiplied by the factor $-\phi_i/\phi_j$ and where ϕ is the aspect ratio. The same applies for spans 2 & 3.

The coupled pair “F”+“G” enforces the condition of continuity of vertical shear at the inter-span boundary by relating the driving coefficients pertaining to spans 1 and 2. Each span must generate the same actual vertical shear since the actual transverse shear forces must be continuous across the interface of the pair. It is noticed that for this coupled pair with analytical solutions running in the ξ direction, it is necessary to multiply the right hand side of equations 2.3 by the quantity b/a . Block “F” of the coupled pair will have the following non-dimensionalized vertical edge reaction:

$$V_{\xi} \frac{a_i^3}{bD_i} \Big|_{\xi=1} = \left[\frac{\partial^3 W(\xi, \eta)}{\partial \xi^3} + \frac{v^*}{\phi^2} \frac{\partial^3 W(\xi, \eta)}{\partial \xi \partial \eta^2} \right] \Big|_{\xi=1} = \sum_{n=0,1,2}^{\infty} E_n \psi(\eta) \quad (3.6)$$

where $\psi(\eta)$ is a trigonometric function of η . Now, considering block “G” relative of span 2, the vertical shear at the inter-span edge $\xi=0$ is expressed as:

$$V_{\xi} \frac{a_j^3}{bD_j} \Big|_{\xi=0} = - \left[\frac{\partial^3 W(\xi, \eta)}{\partial \xi^3} + \frac{v^*}{\phi^2} \frac{\partial^3 W(\xi, \eta)}{\partial \xi \partial \eta^2} \right] \Big|_{\xi=0} = \sum_{n=0,1,2}^{\infty} -E_n^* \psi(\eta) \quad (3.7)$$

where the negative sign of E_n^* is necessary so that the shear forces between the building blocks are opposite. Relating equations 3.6 and 3.7 for the same vertical shear V_{ξ} the following driving coefficients relation is obtained:

$$E_n^* = E_n \left\{ (D_i/D_j) [\phi_i/\phi_j]^3 \right\} \quad (3.8)$$

where the right hand term is the multiplying factor for the driving coefficients of block “G” throughout. D_i and D_j are the flexural rigidities of the respective plate segments i & j .

As a summary to the above discussions, the bracketed term of equation 3.5 is a multiplication factor used to derive the solutions of blocks “E & K” from blocks “D” & “J”. The bracketed term of equation 3.8 is used to derive the same for blocks “G” & “M” from blocks “F” & “L”.

The reader will realise that the remaining building blocks of Figure 3.2 enforce the boundary conditions of the plate. In fact, looking at span 1 of Figure 3.3, the edge along $\xi=0$ is clamped and edges $\eta=0$ ($y=0$) and $\eta=1$ ($y=b$) are free. The three building blocks taking care of this condition of span 1 are blocks “A”, “B” and “C”. It is noticed that those building blocks are from the first family of plates for which Levy-type solutions as per Table 2.2 exist. The boundary conditions imposed along their edges are simple support, slip shear, and forced analytical solutions (rotations). Again, a simply supported edge is

represented by an extended line whereas a slip shear edge is represented by two adjacent circles. Block "A" shows a forced rotation along edge $\xi=0$ that is simply supported for reasons that will be discussed next.

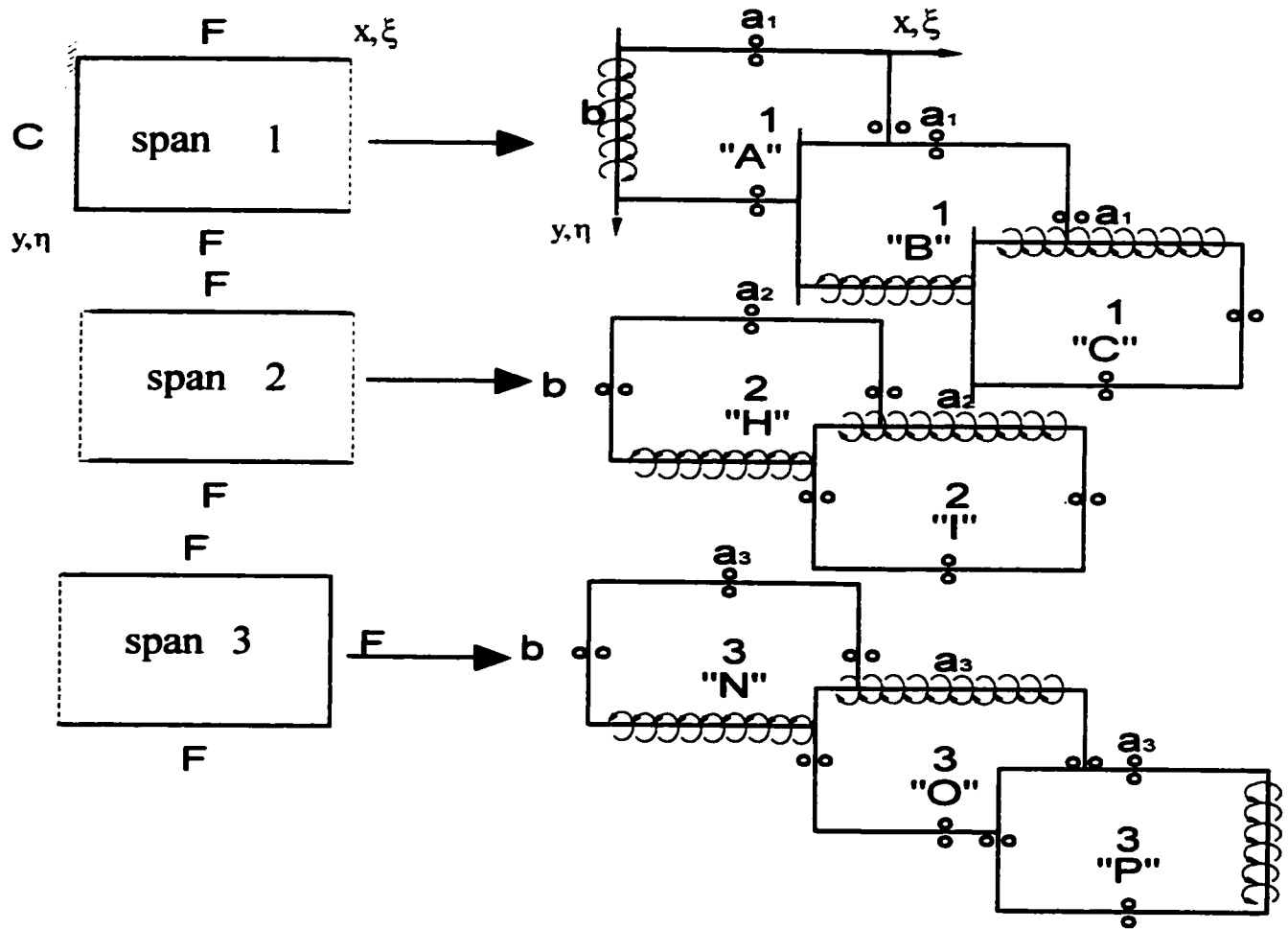


Figure 3.3 : The superposition method building blocks

Slip shear conditions are enforced along the other edges. Block "B" has simple support along edge $\xi=0$ and slip shear condition along $\eta=0$. A forced rotation is imposed at edge $\eta=1$. Block "C" shows simple support along edge $\xi=0$, slip shear condition along $\eta=1$ and a forced rotation along $\eta=0$. The superposition of the three building blocks "A", "B"

and “C” along with the enforcement of the boundary conditions in the generation of the eigenvalue matrix in section 3.1.3 will generate the first span contribution in the cantilever plate problem. The reasons for the choice of the building block boundary conditions are obvious and are discussed in the three cases below.

a) Simply supported edge $\xi=0$:

Considering blocks “A”, “B”, “C”. Since the cantilever plate edge $\xi=0$ is clamped, all the building blocks of span1 contribute towards enforcing clamped edge conditions along this edge. These conditions are zero displacement and zero slope as per equations 2.4 & 2.5. In order to satisfy the zero displacement condition, a simple support is imposed along edge $\xi=0$ of each of these building blocks (as per equation 2.6). The zero slope condition along this edge will be enforced in the first row of the eigenvalue matrix generated in section 3.1.3. By enforcing these boundary conditions, the driving coefficients (E_n or E_m) of the forcing functions are constrained.

b) Slip shear along edges

Considering span1, the edges along $\eta=0$ and $\eta=1$ are free. Therefore blocks “A”, “B”, “C”, participate in enforcing free edge conditions along these two edges. Free edge conditions are satisfied by adjusting the applied bending moments of building blocks “B” and “C”. The condition of zero bending moment is satisfied in the second and third row of the generated eigenvalue matrix of section 3.1.3. The same applies along edges $\eta=0$ and $\eta=1$ for blocks “H”, “I” of span 2 and blocks “N”, “O”, “P” of span 3. The condition of zero bending moment along the free edge of span 2 is satisfied in the sixth and seventh rows of the generated eigenvalue matrix of section 3.1.3. For span 3, this condition is satisfied in rows ten, eleven and twelve of the same matrix. Spans 2 and 3 differ from

span 1 since a slip shear condition is imposed along edge $\xi=0$ for each span instead of simple support. This is obvious since the inter-spans 1,2 & 2,3 are not clamped but in fact continuity conditions have been enforced.

c) Forced rotations or vertical reactions on edges

Considering blocks “A”, “B”, “C”, the forced rotations imposed at edges $\xi=0$, $\eta=0$ and $\eta=1$ respectively, are utilised to satisfy the boundary conditions for free vibration related to span 1. For block “A”, in addition to the imposed rotation at edge $\xi=0$, a condition of zero displacement representing a simple support is also imposed. For blocks “B” & “C”, in addition to the imposed rotation at edges $\eta=0$ and $\eta=1$, a condition of zero vertical shear is also imposed. This is in conformance with the cases shown in Table 2.1. The superposition method uses these building blocks to generate a solution satisfying the boundary conditions of the first span. In each block, the forcing function coefficients are expressed in the solution as will be explained in section 3.1.2. Blocks “A”, “B”, “C” are then superimposed and are forced to satisfy the constraints imposed in rows one, two, three and four of the eigenvalue matrix of section 3.1.3. It is noted that block “D” of span 1 in Figure 3.2a also employs a forcing function at edge $\xi=1$ resulting in equation 3.1. These forced building blocks contribute towards obtaining the eigenvalues of the plate. A condition of zero vertical shear is imposed along the same driven edges of the blocks that follow next. Considering blocks “H” & “I” of span 2, forcing functions are imposed on edges $\eta=0$ and $\eta=1$. Block “J” of Figure 3.2b enforces the same condition along edge $\xi=1$. The superposition of these building blocks, through satisfying the constraints imposed in rows four to nine of the eigenvalue matrix contribute towards satisfying boundary conditions for span 2. Blocks “N”, “O”, “P” of span 3 are forced along edges

$\eta=0, \eta=1$ and $\xi=1$. Block “K” pertaining to span 3 of Figure 3.2c is driven as well along edge $\xi=0$. The superposition of these building blocks, and satisfying the constraints imposed in rows eight to twelve of the eigenvalue matrix, contribute towards satisfying required conditions related to span 3.

3.1.2 Building Block Solutions

3.1.2.a Span 2 and 3 Building Blocks Solutions

It is now appropriate to derive the analytical solutions provided for each building block before generating the eigenvalue matrix in section 3.1.3 for the whole cantilever plate. The intention of this section is to present the analytical solutions to the multiple blocks of spans 2 and 3 (blocks “H” to “P”) presented in Figure 3.2b and 3.2c. The reader is referred to the work of Gorman[1],[3] for a detailed derivation of the solutions and to Chart 3.2 at the end of this section for a brief outline of the derivations.

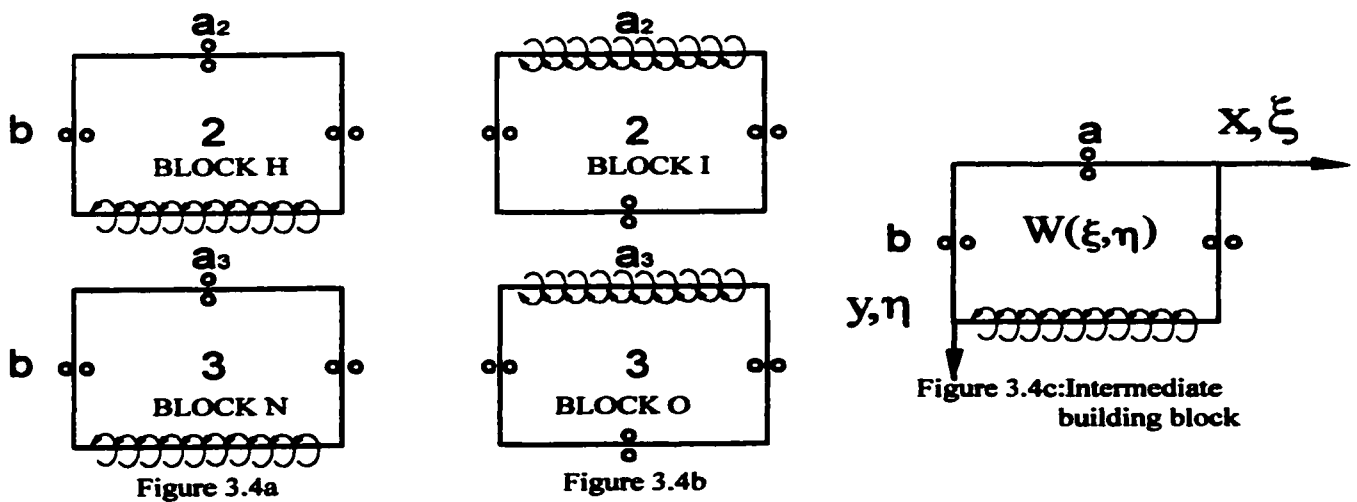


Figure 3.4 : Analysis of building blocks “H”, “I”, “N”, “O” of spans 2 & 3.

We examine Figure 3.2b, building blocks “H”&“I” of span 2 and blocks “N”& “O” of span 3 reproduced in figures 3.4a and 3.4b. A solution for those four building blocks could be obtained by analysing the building block of Figure 3.4c. This building block is of the type shown in case 1 of Table 2.1. Equation 2.12 is a Levy-type solution for the spatial response of this specific building block and is written as:

$$W(\xi, \eta) = \sum_{m=0,1,2}^{\infty} Y_m(\eta) \cos(m\pi\xi) \quad (2.12)$$

where $W(\xi, \eta)$ is the lateral dimensionless displacement with respect to length “a”, (equals w/a). Substituting equation 2.12 into the governing differential equation 1.2 and rearranging, one can write the following equation:

$$\frac{d^4 Y_m(\eta)}{d\eta^4} - 2\phi^2 (m\pi)^2 \frac{d^2 Y_m(\eta)}{d\eta^2} + \phi^4 \{(m\pi)^4 - \lambda^4\} Y_m(\eta) = 0$$

The solution of the above equation is well known and it depends on whether $\lambda^2 - (m\pi)^2$ is positive or negative.

$$\text{For } \lambda^2 > (m\pi)^2, Y_m(\eta) = A_m \cosh \beta_m \eta + B_m \sinh \beta_m \eta + C_m \cos \gamma_m \eta + D_m \sin \gamma_m \eta \quad (3.9)$$

$$\text{For } \lambda^2 < (m\pi)^2, Y_m(\eta) = A_m \cosh \beta_m \eta + B_m \sinh \beta_m \eta + C_m \cosh \gamma_m \eta + D_m \sinh \gamma_m \eta \quad (3.10)$$

where, $\beta_m^2 = \phi^2 \{\lambda^2 + (m\pi)^2\}$, $\gamma_m^2 = \phi^2 \{\lambda^2 - (m\pi)^2\}$, or $= \phi^2 \{(m\pi)^2 - \lambda^2\}$, whichever is positive.

λ^2 (equals $\omega a^2(\rho/D)^{1/2}$) is the dimensionless frequency as stated in section 1.4. It is now necessary to determine the constants A_m , B_m , C_m and D_m by imposing the boundary

conditions along the building block edges. Since a slip shear condition is imposed at edge $\eta=0$, all anti-symmetric terms in equations 3.9 and 3.10 must vanish, eliminating therefore the B_m , and D_m coefficients. The previous equations can now be written as:

$$\text{For } \lambda^2 > (m\pi)^2, \quad Y_m(\eta) = A_m \cosh \beta_m \eta + C_m \cos \gamma_m \eta \quad (3.9a)$$

$$\text{For } \lambda^2 < (m\pi)^2, \quad Y_m(\eta) = A_m \cosh \beta_m \eta + C_m \cosh \gamma_m \eta \quad (3.10a)$$

Considering k^* equal upper limit of “m” for $\lambda^2 - (m\pi)^2$ positive, and replacing the above values for Y_m in equation 2.12, the following equation can be obtained:

$$W(\xi, \eta) = \sum_{m=0,1}^{k^*} (A_m \cosh \beta_m \eta + C_m \cos \gamma_m \eta) \cos(m\pi\xi) + \sum_{m=k^*+1}^{\infty} (A_m \cosh \beta_m \eta + C_m \cosh \gamma_m \eta) \cos(m\pi\xi) \quad (3.11)$$

Equation 3.11, with the anti-symmetric terms removed, satisfies the boundary condition at edge $\eta=0$. Furthermore this equation satisfies exactly the prescribed boundary conditions at $\xi=0$ and $\xi=1$ as required for Levy solutions. The two boundary conditions along $\eta=1$ remain to be satisfied. The first is a condition of zero vertical shear and the second is an imposed edge rotation along the same edge.

We begin by enforcing a zero vertical edge reaction along the driven edge $\eta=1$, as expressed by equation 3.12. The second step is to substitute equation 2.12 into this equation to obtain a differential equation in terms of $Y_m(\eta)$ (equation 3.13).

$$\left\{ \frac{\partial^3 W(\xi, \eta)}{\partial \eta^3} + v^* \phi^2 \frac{\partial^3 W(\xi, \eta)}{\partial \eta \partial \xi^2} \right\} \Big|_{\eta=1} = 0 \quad (3.12)$$

$$\text{or } Y''(\eta) - v^* \phi^2(m\pi)^2 Y'_m(\eta) \Big|_{\eta=1} = 0 \quad (3.13)$$

The third step is to substitute the values for $Y_m(\eta)$, given as expressed by the bracketed terms of equation 3.11, into equation 3.13 to obtain an expression relating coefficients A_m and C_m as follows:

$$\text{For } \lambda^2 > (m\pi)^2, \quad A_m \left\{ \beta_m \left[\beta_m^2 - v^* \phi^2(m\pi)^2 \right] \sinh \beta_m + C_m \left[\gamma_m \left[\gamma_m^2 + v^* \phi^2(m\pi)^2 \right] \sin \gamma_m \right\} = 0 \quad (3.14)$$

$$\text{For } \lambda^2 < (m\pi)^2, \quad A_m \left\{ \beta_m \left[\beta_m^2 - v^* \phi^2(m\pi)^2 \right] \sinh \beta_m + C_m \left[\gamma_m \left[\gamma_m^2 + v^* \phi^2(m\pi)^2 \right] \sinh \gamma_m \right\} = 0 \quad (3.15)$$

A rearrangement of the previous equations by expressing C_m in function of A_m readily shows that the bracketed quantities of the summations in equation 3.11 may be written for each term m as per equations 3.16 and 3.17, as follows:

$$\text{For } \lambda^2 > (m\pi)^2, \quad Y_m(\eta) = A_m \{ \cosh \beta_m \eta + \theta_{1m} \cos \gamma_m \eta \} \quad (3.16)$$

$$\text{For } \lambda^2 < (m\pi)^2, \quad Y_m(\eta) = A_m \{ \cosh \beta_m \eta + \theta_{2m} \cosh \gamma_m \eta \} \quad (3.17)$$

$$\text{where } \theta_{1m} = -\frac{\beta_m (\beta_m^2 - v^* \phi^2(m\pi)^2) \sinh \beta_m}{\gamma_m (\gamma_m^2 + v^* \phi^2(m\pi)^2) \sin \gamma_m}; \theta_{2m} = -\frac{\beta_m (\beta_m^2 - v^* \phi^2(m\pi)^2) \sinh \beta_m}{\gamma_m (\gamma_m^2 - v^* \phi^2(m\pi)^2) \sinh \gamma_m}$$

and the solution 3.11 will be expressed as :

$$W(\xi, \eta) = \sum_{m=0,1,2}^{k^*} [A_m \{ \cosh \beta_m \eta + \theta_{1m} \cos \gamma_m \eta \}] \cos(m\pi \xi) + \sum_{m=k^*+1}^{\infty} [A_m \{ \cosh \beta_m \eta + \theta_{2m} \cosh \gamma_m \eta \}] \cos(m\pi \xi) \quad (3.18a)$$

Next, in order to satisfy the last prescribed boundary condition along edge $\eta=1$, the imposed edge rotation is now expanded in the same series form as the building block response (equation 2.12) and is expressed as:

$$\left. \frac{\partial W(\xi, \eta)}{\partial \eta} \right|_{\eta=1} = \sum_{m=0}^{\infty} E_m \cos m\pi\xi \quad (3.18b)$$

The intention is to express the building block response in equation 3.18a in terms of the above Fourier driving coefficients E_m of equation 3.18b. This is done by substituting equation 3.18a into the left hand side of equation 3.18b to get equation 3.18c for each term m :

$$\begin{aligned} \text{For } \lambda^2 > (m\pi)^2, \quad \left. \frac{\partial W(\xi, \eta)}{\partial \eta} \right|_{\eta=1} &= A_m \{ \beta_m \sinh \beta_m - \gamma_m \theta_{1m} \sin \gamma_m \} \cos m\pi\xi \\ \text{For } \lambda^2 < (m\pi)^2, \quad \left. \frac{\partial W(\xi, \eta)}{\partial \eta} \right|_{\eta=1} &= A_m \{ \beta_m \sinh \beta_m + \gamma_m \theta_{2m} \sinh \gamma_m \} \cos m\pi\xi \end{aligned} \quad (3.18c)$$

expressing A_m in terms of E_m by equating the right hand sides of equations 3.18b and 3.18c, the following relations are obtained for each term m :

$$\text{For } \lambda^2 > (m\pi)^2, \quad Y_m(\eta) = E_m \theta_{11m} \{ \cosh \beta_m \eta + \theta_{1m} \cos \gamma_m \eta \} \quad (3.19)$$

$$\text{For } \lambda^2 < (m\pi)^2, \quad Y_m(\eta) = E_m \theta_{22m} \{ \cosh \beta_m \eta + \theta_{2m} \cosh \gamma_m \eta \} \quad (3.20)$$

$$\text{where } \theta_{11m} = \frac{1}{\beta_m \sinh \beta_m - \theta_{1m} \gamma_m \sin \gamma_m}; \theta_{22m} = \frac{1}{\beta_m \sinh \beta_m + \theta_{2m} \gamma_m \sinh \gamma_m} \quad (3.21)$$

The response for building blocks “H” & “N” is therefore expressed as:

$$W(\xi, \eta) = \sum_{m=0,1,2}^{k^*} [E_m \theta_{11m} \{ \cosh \beta_m \eta + \theta_{1m} \cos \gamma_m \eta \}] \cos(m\pi\xi) + \sum_{m=k^*+1}^{\infty} [E_m \theta_{22m} \{ \cosh \beta_m \eta + \theta_{2m} \cosh \gamma_m \eta \}] \cos(m\pi\xi) \quad (3.22)$$

The solution for building blocks “I” & “O” in figure 3.4b is derived by replacing the quantity η in the previous solutions by $1-\eta$. This covers all the equations from 3.11 till 3.22. The procedure won't be repeated here. However in view of sign convention, the slope will change sign and the solution of this building block is preceded by a minus sign as represented by equation 3.23:

$$W(\xi, \eta) = - \sum_{m=0,1,2}^{k^*} [E_m \theta_{11m} \{ \cosh \beta_m (1-\eta) + \theta_{1m} \cos \gamma_m (1-\eta) \}] \cos m\pi\xi - \sum_{m=k^*+1}^{\infty} [E_m \theta_{22m} \{ \cosh \beta_m (1-\eta) + \theta_{2m} \cosh \gamma_m (1-\eta) \}] \cos m\pi\xi \quad (3.23)$$

and the rotation along edge $\eta=0$ is represented as:

$$\left. \frac{\partial W(\xi, \eta)}{\partial \eta} \right|_{\eta=0} = - \sum_{m=0}^{\infty} E_m \cos m\pi(\xi)$$

$$\text{where } \theta_{11m} = \frac{1}{\beta_m \sinh \beta_m - \theta_{1m} \gamma_m \sin \gamma_m}, \theta_{22m} = \frac{1}{\beta_m \sinh \beta_m - \theta_{2m} \gamma_m \sinh \gamma_m}$$

$$\theta_{1m} = - \frac{\beta_m (\beta_m^2 - v^* \phi^2 (m\pi)^2) \sinh \beta_m}{\gamma_m (\gamma_m^2 + v^* \phi^2 (m\pi)^2) \sin \gamma_m}, \theta_{2m} = - \frac{\beta_m (\beta_m^2 - v^* \phi^2 (m\pi)^2) \sinh \beta_m}{\gamma_m (\gamma_m^2 - v^* \phi^2 (m\pi)^2) \sinh \gamma_m} \quad (3.24)$$

Blocks “E”, “J”, “K”, “P” of spans 2 & 3 in Figure 3.2b and 3.2.c, are represented in Figure 3.5a and their solution is provided by analysing the intermediate building block in Figure 3.5b.

The solution for the building block in Figure 3.5b is easily extracted from the one in figure 3.4c through a proper interchange of axis.

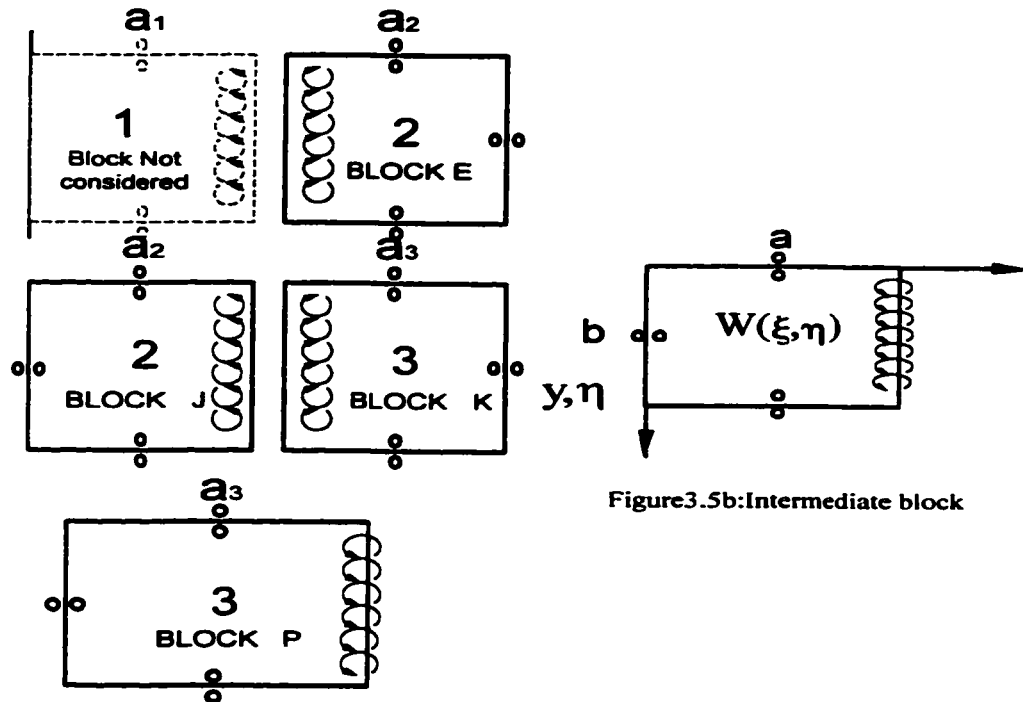


Figure 3.5a

Figure3.5b:Intermediate block

Figure 3.5 : Analysis of blocks “E”, “J”, “K”, “P”.

This implies that ξ and η must be interchanged. This interchange of axis induces the following changes in the new formulation as follows:

a) In Figure 3.4c the aspect ratio is $\phi=b/a$ and since the building block of Figure 3.5b is extracted by an interchange of axis the corresponding new aspect ratio is the inverse $\phi=a/b$. Therefore ϕ is replaced by $1/\phi$.

b) The parameter $\lambda^2=\omega a^2(\rho/D)^{1/2}$ relative to building block of Figure 3.4c is based on edge length “a”. It must now be replaced by the parameter $\lambda_b^2=\omega b^2(\rho/D)^{1/2}$ which is equal to $\lambda^2\phi^2$, so that it is based on the edge length “b” in the new formulation.

c) The lateral displacement $W(\xi, \eta) = w/a$, is the dimensionless displacement with respect to length “a”. The change of axis requires that $W(\xi, \eta) = w/b$ which is non-dimensionalised by edge length”b”.

d) The forcing function coefficients of the imposed rotations are expressed by E_n instead of E_m .

The solutions for building block 3.5b and blocks “J” & “P” are obtained by performing the above changes on equations 3.11 till 3.22. The procedure won’t be repeated here and the solution is as follows:

$$W(\xi, \eta) = \sum_{n=0,1}^{\infty} Y_n(\xi) \cos n\pi\eta \quad (3.25)$$

$$\text{For } \lambda^2\phi^2 > (n\pi)^2, \quad Y_n(\xi) = E_n\theta_{11n} \{ \cosh \beta_n \xi + \theta_{1n} \cos \gamma_n \xi \} \quad (3.26)$$

$$\text{For } \lambda^2\phi^2 < (n\pi)^2, \quad Y_n(\xi) = E_n\theta_{22n} \{ \cosh \beta_n \xi + \theta_{2n} \cosh \gamma_n \xi \} \quad (3.27)$$

where, $\beta_n^2 = \{\lambda^2\phi^2 + (n\pi)^2\}/\phi^2, \gamma_n^2 = \{\lambda^2\phi^2 - (n\pi)^2\}/\phi^2$, or $= \{(n\pi)^2 - \lambda^2\phi^2\}$, whichever

is positive or in other terms :

$$W(\xi, \eta) = \sum_{n=0,1,2}^{k^*} [E_n\theta_{11n} \{ \cosh \beta_n \xi + \theta_{1n} \cos \gamma_n \xi \}] \cos(n\pi\eta) + \sum_{n=k^*+1}^{\infty} [E_n\theta_{22n} \{ \cosh \beta_n \xi + \theta_{2n} \cosh \gamma_n \xi \}] \cos(n\pi\eta) \quad (3.27a)$$

The subscript n is used here for all solutions where the analytical functions runs in the ξ direction.

$$\theta_{1n} = -\frac{\beta_n (\beta_n^2 - v^* (n\pi)^2 / \phi^2) \sinh \beta_n}{\gamma_n (\gamma_n^2 + v^* (n\pi)^2 / \phi^2) \sin \gamma_n}, \theta_{2n} = -\frac{\beta_n (\beta_n^2 - v^* (n\pi)^2 / \phi^2) \sinh \beta_n}{\gamma_n (\gamma_n^2 - v^* (n\pi)^2 / \phi^2) \sinh \gamma_n}$$

and $\theta_{11n} = \frac{1}{\beta_n \sinh \beta_n - \theta_{1n} \gamma_n \sin \gamma_n}, \theta_{22n} = \frac{1}{\beta_n \sinh \beta_n + \theta_{2n} \gamma_n \sinh \gamma_n}$ (3.28)

The rotations imposed at edge $\xi=1$ are expressed in series form as follows:

$$\left. \frac{\partial W(\xi, \eta)}{\partial \xi} \right|_{\xi=1} = \sum_{n=0}^{\infty} E_n \cos n\pi(\eta)$$

The solutions for blocks “E” & “K” in Figure 3.5a are extracted by replacing ξ by $1-\xi$ in equations 3.25 to 3.28. Since the imposed rotation will change sign it is necessary to introduce a minus sign to the solution in keeping with the sign convention. The solution for these building blocks is then expressed as:

$$W(\xi, \eta) = - \sum_{n=0,1}^{\infty} Y_n (1-\xi) \cos n\pi(\eta) \quad (3.29)$$

$$\text{For } \lambda^2 \phi^2 < (n\pi)^2, \quad Y_n(\xi) = E_n \theta_{22n} \{ \cosh \beta_n (1-\xi) + \theta_{2n} \cosh \gamma_n (1-\xi) \} \quad (3.31)$$

$$\text{For } \lambda^2 \phi^2 > (n\pi)^2, \quad Y_n(\xi) = E_n \theta_{11n} \{ \cosh \beta_n (1-\xi) + \theta_{1n} \cos \gamma_n (1-\xi) \} \quad (3.30)$$

$$\text{where } \theta_{1n} = -\frac{\beta_n (\beta_n^2 - v^* (n\pi)^2 / \phi^2) \sinh \beta_n}{\gamma_n (\gamma_n^2 + v^* (n\pi)^2 / \phi^2) \sin \gamma_n}, \theta_{2n} = -\frac{\beta_n (\beta_n^2 - v^* (n\pi)^2 / \phi^2) \sinh \beta_n}{\gamma_n (\gamma_n^2 - v^* (n\pi)^2 / \phi^2) \sinh \gamma_n}$$

$$\text{and } \theta_{11n} = \frac{1}{\beta_n \sinh \beta_n - \theta_{1n} \gamma_n \sin \gamma_n}, \theta_{22n} = \frac{1}{\beta_n \sinh \beta_n + \theta_{2n} \gamma_n \sinh \gamma_n} \quad (3.32)$$

The rotation imposed at edge $\xi=0$ is expressed as:

$$\left. \frac{\partial W(\xi, \eta)}{\partial \xi} \right|_{\xi=0} = - \sum_{n=0}^{\infty} E_n \cos(n\pi\eta)$$

The final solution is expressed as:

$$W(\xi, \eta) = - \sum_{n=0,1,2}^{k'} [E_n \theta_{1n} \{ \cosh \beta_n (1-\xi) + \theta_{1n} \cos \gamma_n (1-\xi) \}] \cos(n\pi\eta) - \sum_{n=k'+1}^{\infty} [E_n \theta_{2n} \{ \cosh \beta_n (1-\xi) + \theta_{2n} \cosh \gamma_n (1-\xi) \}] \cos(n\pi\eta) \quad (3.32a)$$

The remaining building blocks of spans 2 and 3, are those enforcing the continuity of vertical shear in blocks "G", "L", "M".

The intention is to obtain the response for the building block in Figure 3.6b by

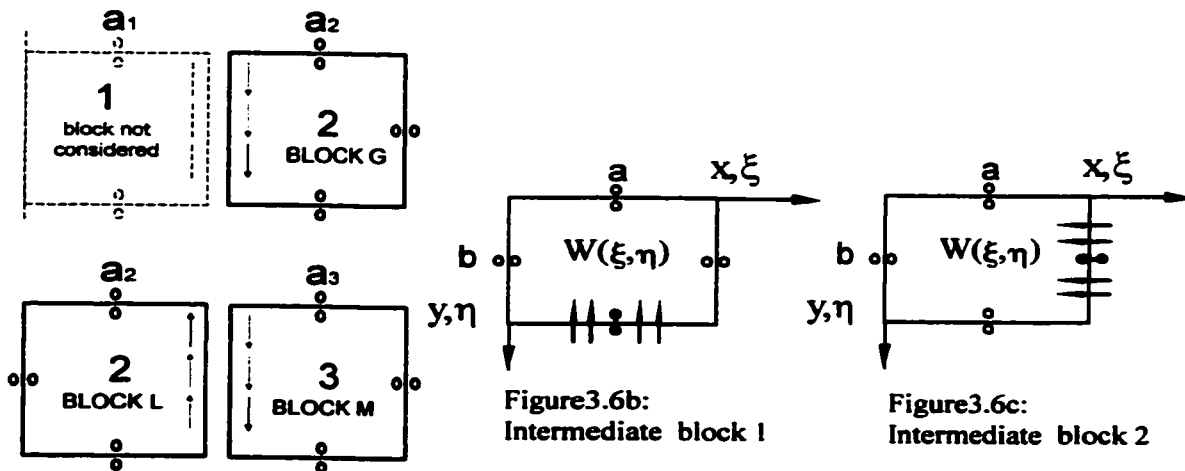


Figure 3.6 a

Figure 3.6 : Analysis of building blocks "G", "L", "M".

performing a change of axis where ξ is replaced by η etc., solutions for the block of Figure 3.6c as well as block “L” are obtained. By substituting ξ for $1-\xi$ in the previous solutions, solutions for blocks “G” and “M” are obtained.

The building block of Figure 3.6b has a condition of zero slope imposed along edge $\eta=1$ (represented by two black dots connected by a line), along with a distributed forced harmonic vertical shear at the same edge. The solution is extracted from the one of the block in Figure 3.4c and can be rewritten as follows:

$$W(\xi, \eta) = \sum_{m=0,1,2}^{\infty} Y_m(\eta) \cos(m\pi\xi) \quad (3.33)$$

Since only symmetric functions with respect to the axis, $\eta=0$ can be retained here for the same reasons discussed earlier and with reference to equations 3.9a and 3.10a the following applies:

$$\text{For } \lambda^2 > (m\pi)^2, \quad Y_m(\eta) = A_m \cosh \beta_m \eta + C_m \cos \gamma_m \eta \quad (3.34)$$

$$\text{For } \lambda^2 < (m\pi)^2, \quad Y_m(\eta) = A_m \cosh \beta_m \eta + C_m \cosh \gamma_m \eta \quad (3.35)$$

where, $\beta_m^2 = \phi^2 \{\lambda^2 + (m\pi)^2\}$, $\gamma_m^2 = \phi^2 \{\lambda^2 - (m\pi)^2\}$, or $= \phi^2 \{(m\pi)^2 - \lambda^2\}$, whichever is positive.

Imposing the zero slope boundary condition at edge $\eta=1$ the following equation is written as:

$$\left. \frac{\partial W(\xi, \eta)}{\partial \eta} \right|_{\eta=1} = 0 \quad (3.36)$$

The procedures applied for obtaining the solutions for building blocks “H” and “N” (equations 3.11 to 3.21) are applied here but won't be repeated. It is noted that equation 3.12 is replaced by equation 3.36. Equation 3.18b representing the imposed harmonic rotation is replaced by equation 3.37 representing instead a distributed vertical shear as follows:

$$V_{\eta} \frac{b^3}{a_i D_i} \Big|_{\eta=1} = - \left[\frac{\partial^3 W(\xi, \eta)}{\partial \eta^3} + v \cdot \phi^2 \frac{\partial^3 W(\xi, \eta)}{\partial \xi^2 \partial \eta} \right] \Big|_{\eta=1} = \sum_{m=0,1,2}^{\infty} E_m \cos m\pi\xi \quad (3.37)$$

Imposing the zero slope condition (equation 3.36) and the edge condition represented by equation 3.37 the expressions for $Y_m(\eta)$ become:

$$\text{For } \lambda^2 > (m\pi)^2 \quad Y_m(\eta) = [E_m \theta_{11m} \{ \cosh \beta_m \eta + \theta_{1m} \cos \gamma_m \eta \}]$$

$$\text{For } \lambda^2 < (m\pi)^2 \quad Y_m(\eta) = E_m \theta_{22m} \{ \cosh \beta_m \eta + \theta_{2m} \cosh \gamma_m \eta \} \quad (3.38)$$

for which the response is expressed by equation 3.39:

$$W(\xi, \eta) = \sum_{m=0,1,2}^{k^*} [E_m \theta_{11m} \{ \cosh \beta_m \eta + \theta_{1m} \cos \gamma_m \eta \}] \cos(m\pi\xi) + \sum_{m=k^*+1}^{\infty} [E_m \theta_{22m} \{ \cosh \beta_m \eta + \theta_{2m} \cosh \gamma_m \eta \}] \cos(m\pi\xi) \quad (3.39)$$

$$\begin{aligned}
\text{where } \theta_{11m} &= -\frac{1}{\left[\beta_m \sinh \beta_m (\beta_m^2 - v^* (m\pi)^2 \phi^2) \right] + \theta_{1m} \gamma_m (\gamma_m^2 + v^* (m\pi)^2 \phi^2) \sin \gamma_m}, \\
\theta_{22m} &= -\frac{1}{\left[\beta_m \sinh \beta_m (\beta_m^2 - v^* (m\pi)^2 \phi^2) \right] + \theta_{2m} \gamma_m (\gamma_m^2 - v^* (m\pi)^2 \phi^2) \sin \gamma_m} \\
\theta_{1m} &= \frac{\beta_m \sinh \beta_m}{\gamma_m \sin \gamma_m}, \quad \theta_{2m} = \frac{-\beta_m \sinh \beta_m}{\gamma_m \sinh \gamma_m} \quad (3.40)
\end{aligned}$$

The solution for the building block of Figure 3.6c can be extracted from the one in Figure 3.6b through a transformation of axis by interchanging ξ and η and following the rules of transformation as outlined previously in steps a) to d). The response can then be written as:

$$\begin{aligned}
W(\xi, \eta) &= \sum_{n=0,1,2}^{k^*} \left[E_n \theta_{11n} \{ \cosh \beta_n \xi + \theta_{1n} \cos \gamma_n \xi \} \right] \cos(n\pi\eta) + \\
&\quad \sum_{n=k^*+1}^{\infty} \left[E_n \theta_{22n} \{ \cosh \beta_n \xi + \theta_{2n} \cosh \gamma_n \xi \} \right] \cos(n\pi\eta) \quad (3.41) \\
&:
\end{aligned}$$

$$\begin{aligned}
\text{where } \theta_{11n} &= -\frac{1}{\left[\beta_n \sinh \beta_n (\beta_n^2 - v^* (n\pi)^2 / \phi^2) \right] + \theta_{1n} \gamma_n (\gamma_n^2 + v^* (n\pi)^2 / \phi^2) \sin \gamma_n}, \\
\theta_{22n} &= -\frac{1}{\left[\beta_n \sinh \beta_n (\beta_n^2 - v^* (n\pi)^2 / \phi^2) \right] + \theta_{2n} \gamma_n (\gamma_n^2 - v^* (n\pi)^2 / \phi^2) \sin \gamma_n} \\
\theta_{1n} &= \frac{\beta_n \sinh \beta_n}{\gamma_n \sin \gamma_n}, \quad \theta_{2n} = \frac{-\beta_n \sinh \beta_n}{\gamma_n \sinh \gamma_n} \quad (3.42)
\end{aligned}$$

The solution for block "L" is represented by the equations 3.41 and 3.42 above. The solution for blocks "G" and "M" can be derived from the above solutions by replacing ξ by $1-\xi$. One further change must be made. In view of the sign convention for vertical

edge reactions, the previous solutions must be preceded with a minus sign. The solutions are expressed in equations 3.43 and 3.44 as follows:

$$W(\xi, \eta) = - \sum_{n=0,1,2}^{k'} [E_n \theta_{11n} (\cosh \beta_n \xi + \theta_{1n} \cos \gamma_n \xi)] \cos(n\pi\eta) - \sum_{n=k'+1}^{\infty} [E_n \theta_{22n} (\cosh \beta_n \xi + \theta_{2n} \cosh \gamma_n \xi)] \cos(n\pi\eta) \quad (3.43)$$

$$\text{where } \theta_{11n} = - \frac{1}{[\beta_n \sinh \beta_n (\beta_n^2 - v^* (n\pi)^2 / \phi^2)] + \theta_{1n} \gamma_n (\gamma_n^2 + v^* (n\pi)^2 / \phi^2) \sin \gamma_n},$$

$$\theta_{22n} = - \frac{1}{[\beta_n \sinh \beta_n (\beta_n^2 - v^* (n\pi)^2 / \phi^2)] + \theta_{2n} \gamma_n (\gamma_n^2 - v^* (n\pi)^2 / \phi^2) \sin \gamma_n}$$

$$\theta_{1n} = \frac{\beta_n \sinh \beta_n}{\gamma_n \sin \gamma_n}, \quad \theta_{2n} = \frac{-\beta_n \sinh \beta_n}{\gamma_n \sinh \gamma_n} \quad (3.44)$$

The solutions for span 2 & 3 building blocks of figures 3.2.b and 3.2.c have now been described. The next section presents solutions for the remaining building blocks of Figure 3.2.a pertaining to span 1.

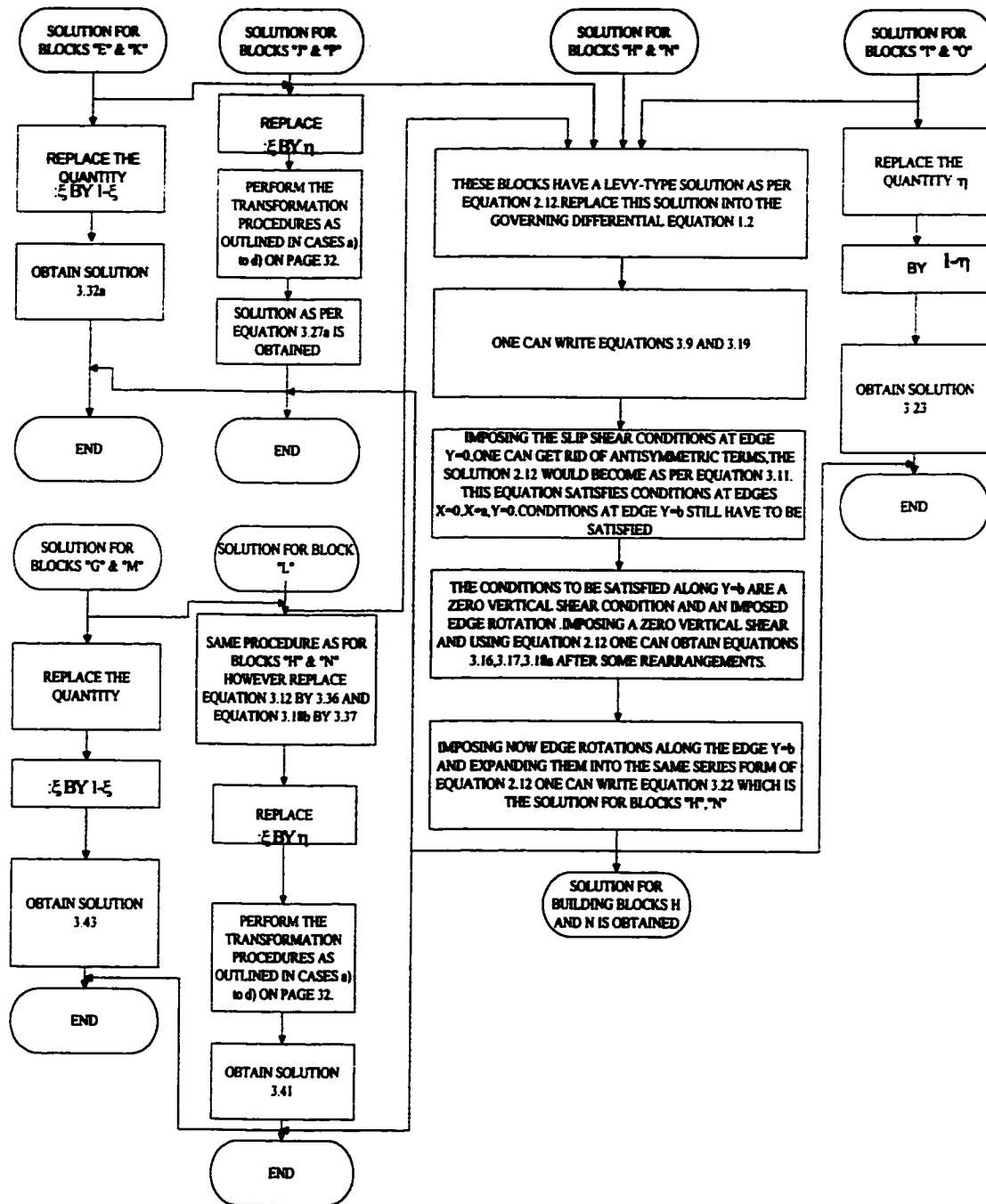


Chart 3.2 Flowchart outlining solutions of spans 2 and 3 building blocks.

3.1.2.b Span 1 Building Block Solutions

The remaining building blocks to be analysed are of span 1 and are shown in Figure 3.7.

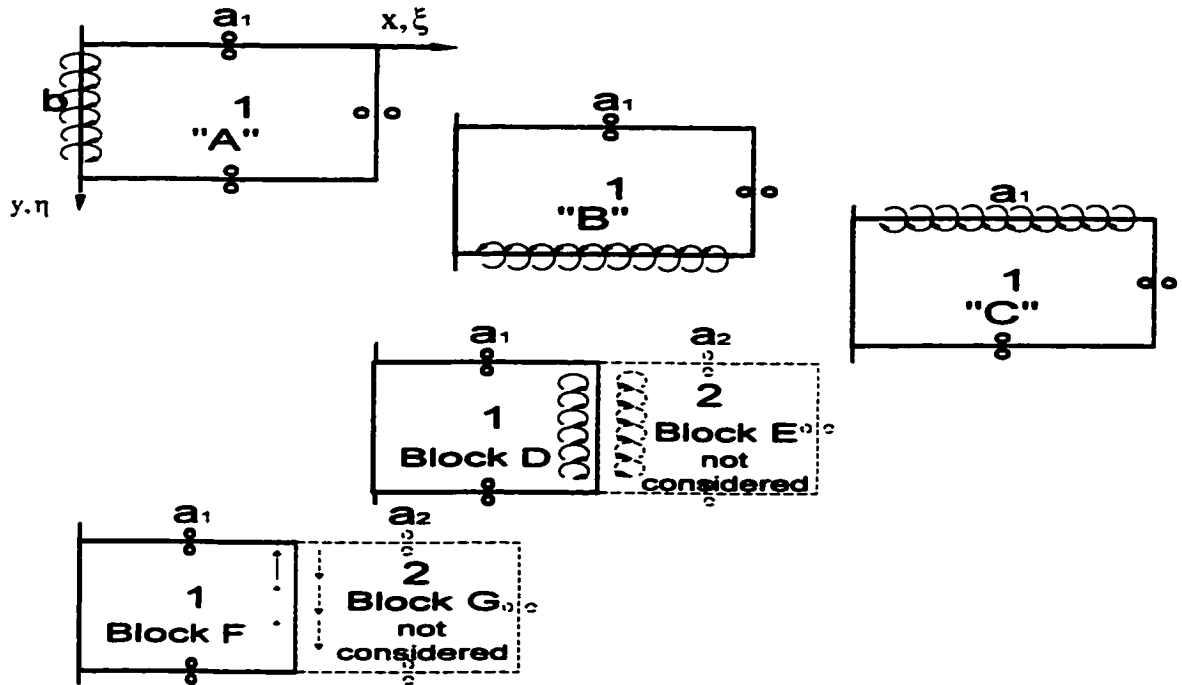


Figure 3.7 : Analysis of span 1 building blocks "A", "B", "C", "D", "F".

The building blocks of span 1 are denoted by "A", "B", "C", "D", "F". These blocks, when combined, satisfy the clamped edge condition at edge $\xi=0$. Extended lines along this edge, indicate a simple support. Focusing first on block "A", the solution for this block is extracted from the blocks shown in Figure 3.8.

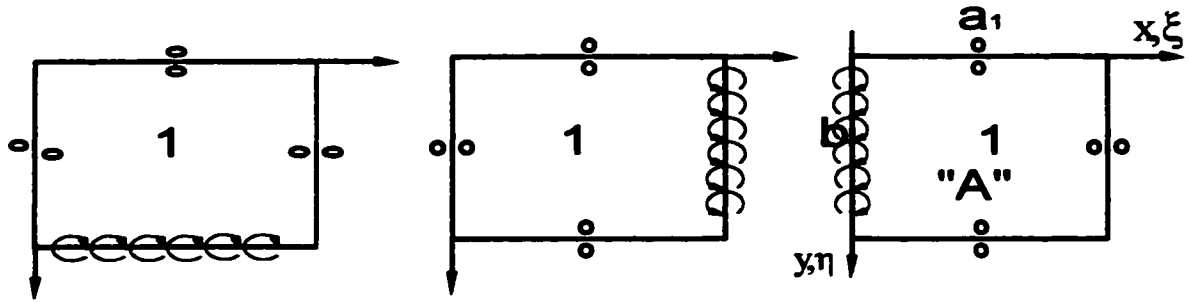


Figure 3.8a:Intermediate block Figure 3.8b:Intermediate block Figure 3.8c: Block "A"

Figure 3.8 : Solution for block "A".

The solution for the response of the intermediate block in Figure 3.8a is first sought. This block differs from block "H" shown in Figure 3.4a only in that a condition of zero lateral displacement, rather than zero vertical edge reaction is enforced along the driven edge. The solution will be identical to that given by equations 2.12 and 3.9 to 3.11. However the boundary condition of equation 3.12 is replaced by equation 3.45:

$$W(\xi, \eta) \Big|_{\eta=1} = 0 \quad (3.45)$$

The solution for this problem won't be repeated here since it is easily generated by following the steps outlined in the case of block "H". However in this case only the quantities θ_{1m} and θ_{2m} are different. The solution is as follows:

$$W(\xi, \eta) = \sum_{m=0,1,2}^{k'} [E_m \theta_{11m} \{ \cosh \beta_m \eta + \theta_{1m} \cos \gamma_m \eta \}] \cos(m\pi\xi) + \sum_{m=k'+1}^{\infty} [E_m \theta_{22m} \{ \cosh \beta_m \eta + \theta_{2m} \cosh \gamma_m \eta \}] \cos(m\pi\xi) \quad (3.46)$$

$$\text{where } \theta_{11m} = \frac{1}{\beta_m \sinh \beta_m - \theta_{1m} \gamma_m \sin \gamma_m} ; \theta_{22m} = \frac{1}{\beta_m \sinh \beta_m + \theta_{2m} \gamma_m \sinh \gamma_m}$$

$$\theta_{1m} = \frac{-\cosh \beta_m}{\cos \gamma_m} ; \theta_{2m} = -\frac{\cosh \beta_m}{\cosh \gamma_m} \quad (3.47)$$

The transformation rules discussed earlier are applied to the above solution to generate the solution for the intermediate building block of Figure 3.8b. The solution of block “A” is then derived from the one of Figure 3.8b by replacing the quantity ξ by $1-\xi$ and preceding this solution with a negative sign as follows:

$$W(\xi, \eta) = - \sum_{n=0,1,2}^{k^*} [E_n \theta_{11n} \{ \cosh \beta_n (1-\xi) + \theta_{1n} \cos \gamma_n (1-\xi) \}] \cos(n\pi\eta) - \sum_{n=k^*+1}^{\infty} [E_n \theta_{22n} \{ \cosh \beta_n (1-\xi) + \theta_{2n} \cosh \gamma_n (1-\xi) \}] \cos(n\pi\eta) \quad (3.48)$$

$$\text{where } \theta_{11n} = \frac{1}{\beta_n \sinh \beta_n - \theta_{1n} \gamma_n \sin \gamma_n} ; \theta_{22n} = \frac{1}{\beta_n \sinh \beta_n + \theta_{2n} \gamma_n \sinh \gamma_n}$$

$$\theta_{1n} = \frac{-\cosh \beta_n}{\cos \gamma_n} ; \theta_{2n} = -\frac{\cosh \beta_n}{\cosh \gamma_n} \quad (3.49)$$

The solution for building block “B” is sought next. This block has a simple support condition at edge $\xi=0$ and a slip shear condition at edge $\xi=1$. The Levy-type solution for this block is as per equation 2.16 of case 5 as follows :

$$\text{Case 5: } W(\xi, \eta) = \sum_{m=1,3,5}^{\infty} Y_m(\eta) \sin(m\pi\xi/2) \quad (2.16)$$

where m is an odd integer. This same equation can be rewritten with a proper change of integer as:

$$W(\xi, \eta) = \sum_{m=1,2,3}^{\infty} Y_m(\eta) \sin[(2m-1)\pi\xi/2] \quad (3.50)$$

The solution for this building block is immediately extracted from the one for building block "H" simply by replacing the term $m\pi$ by the term $(2m-1)\pi/2$ as follows:

$$W(\xi, \eta) = \sum_{m=1,2,3}^{k^*} [E_m \theta_{11m} \{ \cosh \beta_m \eta + \theta_{1m} \cos \gamma_m \eta \}] \sin[(2m-1)\pi/2]\xi + \sum_{m=k^*+1}^{\infty} [E_m \theta_{22m} \{ \cosh \beta_m \eta + \theta_{2m} \cosh \gamma_m \eta \}] \sin[(2m-1)\pi/2]\xi \quad (3.51)$$

with the θ terms unchanged as per block "H" equations 3.16, 3.17 and 3.21. The solution for block "C" is derived from the previous solution by replacing the quantity η with $1-\eta$ and preceding it by a minus sign as follows:

$$W(\xi, \eta) = - \sum_{m=1,2,3}^{k^*} [E_m \theta_{11m} \{ \cosh \beta_m (1-\eta) + \theta_{1m} \cos \gamma_m (1-\eta) \}] \sin[(2m-1)\pi/2]\xi - \sum_{m=k^*+1}^{\infty} [E_m \theta_{22m} \{ \cosh \beta_m (1-\eta) + \theta_{2m} \cosh \gamma_m (1-\eta) \}] \sin[(2m-1)\pi/2]\xi \quad (3.52)$$

with the θ terms unchanged as per block "H" equations 3.16, 3.17 and 3.21 and k^* equals m , for $\lambda^2 - [(2m-1)\pi/2]^2$ positive. The next building block to be analysed is block "D". It is wise to analyse first the intermediate block shown in figure 3.9a.

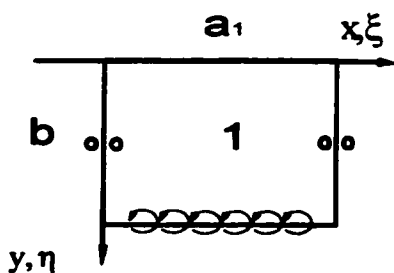


Figure 3.9a : Intermediate Block

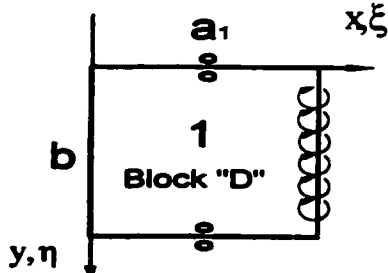


Figure 3.9b : Block "D"

Figure 3.9 : Solution for block "D".

This block differs from block “H” only in that a simple support, rather than a slip-shear condition, is imposed at edge $\eta=0$. The solution takes the form of equation 2.12 however in equations 3.9 and 3.10, the symmetric terms must be deleted rather than the anti-symmetric terms, that is the cosine and hyperbolic cosine terms are replaced by sine and sine hyperbolic sine. Following the same steps as for block “H”, the quantities $Y_m(\eta)$ now become,

$$\text{For } \lambda^2 > (m\pi)^2, \quad Y_m(\eta) = E_m \theta_{11m} \{ \sinh \beta_m \eta + \theta_{1m} \sin \gamma_m \eta \} \quad (3.53)$$

$$\text{For } \lambda^2 < (m\pi)^2, \quad Y_m(\eta) = E_m \theta_{22m} \{ \sinh \beta_m \eta + \theta_{2m} \sinh \gamma_m \eta \} \quad (3.54)$$

$$\text{where } \theta_{11m} = \frac{1}{\beta_m \cosh \beta_m - \theta_{1m} \gamma_m \cos \gamma_m}, \quad \theta_{22m} = \frac{1}{\beta_m \cosh \beta_m + \theta_{2m} \gamma_m \cosh \gamma_m}$$

$$\theta_{1m} = -\frac{\beta_m (\beta_m^2 - v^* \phi^2 (m\pi)^2) \cosh \beta_m}{\gamma_m (\gamma_m^2 + v^* \phi^2 (m\pi)^2) \cos \gamma_m}, \quad \theta_{2m} = -\frac{\beta_m (\beta_m^2 - v^* \phi^2 (m\pi)^2) \cosh \beta_m}{\gamma_m (\gamma_m^2 - v^* \phi^2 (m\pi)^2) \cosh \gamma_m} \quad (3.55)$$

where the values for β_m and γ_m remain unchanged.

The solution for block “D” is extracted from the previous solution through a transformation of axis as outlined earlier:

$$W(\xi, \eta) = \sum_{n=0,1,2}^{k^*} [E_n \theta_{11n} \{ \sinh \beta_n \xi + \theta_{1n} \sin \gamma_n \xi \}] \cos(n\pi\eta) +$$

$$\sum_{n=k^*+1}^{\infty} [E_n \theta_{22n} \{ \sinh \beta_n \xi + \theta_{2n} \sinh \gamma_n \xi \}] \cos(n\pi\eta) \quad (3.56)$$

$$\text{where } \theta_{11n} = \frac{1}{\beta_n \cosh \beta_n - \theta_{1n} \gamma_n \cos \gamma_n}, \quad \theta_{22n} = \frac{1}{\beta_n \cosh \beta_n + \theta_{2n} \gamma_n \cosh \gamma_n}$$

$$\theta_{1n} = -\frac{\beta_n (\beta_n^2 - v^* (n\pi)^2 / \phi^2) \cosh \beta_n}{\gamma_n (\gamma_n^2 + v^* (n\pi)^2 / \phi^2) \cos \gamma_n}, \quad \theta_{2n} = -\frac{\beta_n (\beta_n^2 - v^* (n\pi)^2 / \phi^2) \cosh \beta_n}{\gamma_n (\gamma_n^2 - v^* (n\pi)^2 / \phi^2) \cosh \gamma_n} \quad (3.57)$$

The last block to be analysed in this thesis is block "F". A solution for this block is obtained by first analysing the intermediate block in Figure 3.10a.

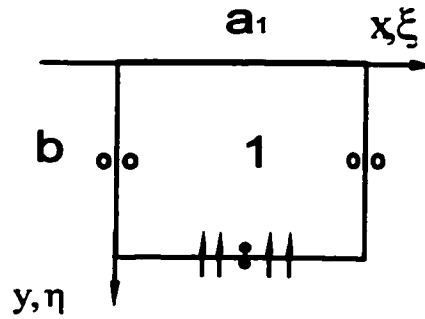


Figure 3.10a: Intermediate Block
Figure 3.10 : Deriving the solution for block "F".

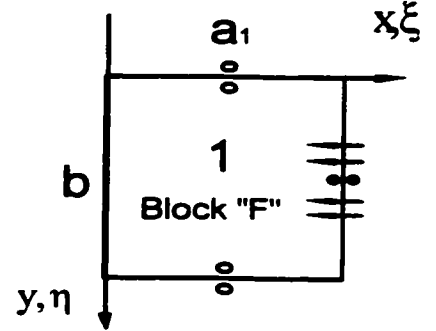


Figure 3.10b: Block "F"

The solution for the intermediate block in Figure 3.10a differs from the one in Figure 3.6b, only in that simple support instead of slip-shear condition is imposed at edge $\eta=0$. Again the solution is identical to the one described by equations 3.38 to 3.40 except that the symmetric terms for $Y_m(\eta)$ will be replaced by anti-symmetric terms as follows:

$$\begin{aligned} \text{For } \lambda^2 > (m\pi)^2 \quad Y_m(\eta) &= [E_m \theta_{11m} \{ \sinh \beta_m \eta + \theta_{1m} \sin \gamma_m \eta \}] \\ \text{For } \lambda^2 < (m\pi)^2 \quad Y_m(\eta) &= E_m \theta_{22m} \{ \sinh \beta_m \eta + \theta_{2m} \sinh \gamma_m \eta \} \end{aligned} \quad (3.58)$$

$$\text{where } \theta_{11m} = \frac{-1}{[\beta_m \cosh \beta_m (\beta_m^2 - \nu^* (m\pi)^2 \phi^2)] + \theta_{1m} \gamma_m (\gamma_m^2 + \nu^* (m\pi)^2 \phi^2) \cos \gamma_m},$$

$$\theta_{22m} = \frac{-1}{[\beta_m \cosh \beta_m (\beta_m^2 - \nu^* (m\pi)^2 \phi^2)] + \theta_{2m} \gamma_m (\gamma_m^2 - \nu^* (m\pi)^2 \phi^2) \cos \gamma_m}$$

$$\theta_{1m} = \frac{\beta_m \cosh \beta_m}{\gamma_m \cos \gamma_m}, \quad \theta_{2m} = \frac{-\beta_m \cosh \beta_m}{\gamma_m \cosh \gamma_m} \quad (3.59)$$

The final solution for block “F” is derived by a transformation of axis as:

$$W(\xi, \eta) = \sum_{n=0,1,2}^{k^*} [E_n \theta_{11n} \{ \sinh \beta_n \xi + \theta_{1n} \sin \gamma_n \xi \}] \cos(n\pi\eta) + \sum_{n=k^*+1}^{\infty} [E_n \theta_{22n} \{ \sinh \beta_n \xi + \theta_{2n} \sinh \gamma_n \xi \}] \cos(n\pi\eta) \quad (3.60)$$

$$\text{where } \theta_{11n} = -\frac{1}{[\beta_n \cosh \beta_n (\beta_n^2 - v^* (n\pi)^2 / \phi^2)] + \theta_{1n} \gamma_n (\gamma_n^2 + v^* (n\pi)^2 / \phi^2) \cos \gamma_n},$$

$$\theta_{22n} = -\frac{1}{[\beta_n \cosh \beta_n (\beta_n^2 - v^* (n\pi)^2 / \phi^2)] + \theta_{2n} \gamma_n (\gamma_n^2 - v^* (n\pi)^2 / \phi^2) \cos \gamma_n}$$

$$\theta_{1n} = \frac{\beta_n \cosh \beta_n}{\gamma_n \cos \gamma_n}, \quad \theta_{2n} = \frac{-\beta_n \cosh \beta_n}{\gamma_n \cosh \gamma_n} \quad (3.61)$$

It is noted that solution for block “F” could also have been derived by direct comparison to the block in Figure 3.6c through replacing the symmetric terms by antisymmetric terms in equation 3.41. The solutions for each building block constituting the three span cantilever plate have now been presented. A summary of the building blocks solutions is shown in Figure 3.11. Section 3.1.3 describes the generation of the eigenvalue matrix for the purpose of calculating the free vibration frequencies, using the solutions mentioned above.

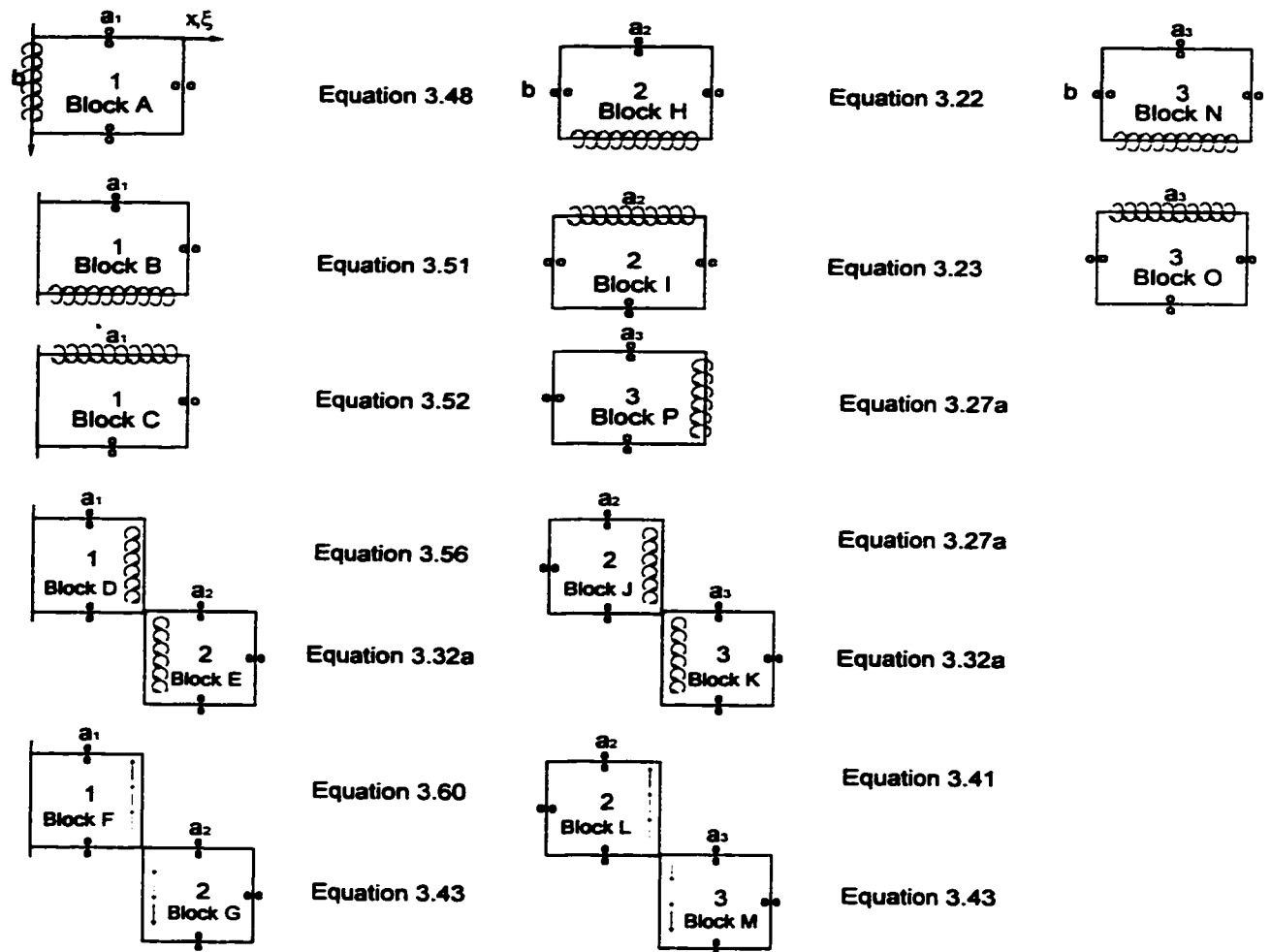


Figure 3.11 : Summary of building blocks solutions.

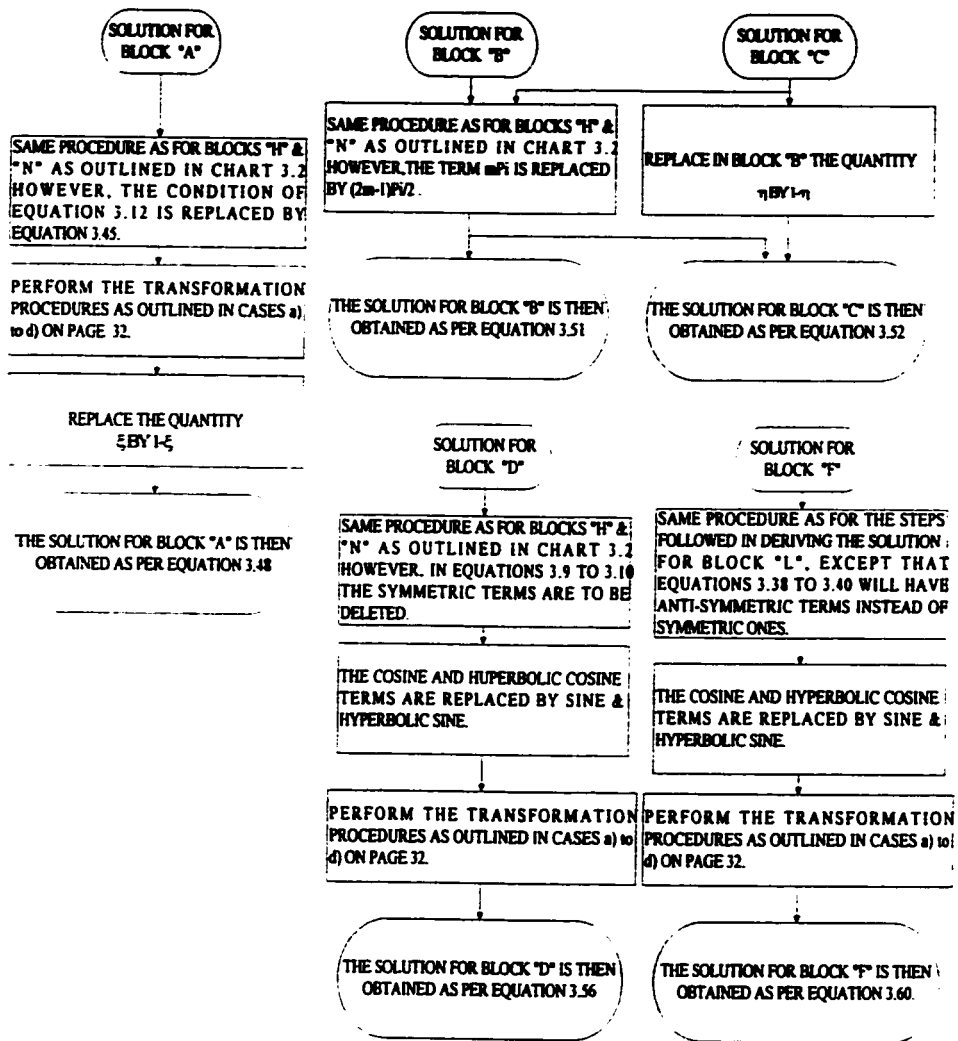


Chart 3.3 : Flowchart outlining solutions for span 1 building blocks.

3.1.3 Generation of the Eigenvalue Matrix

This section describes the generation of the eigenvalue matrix leading to determining the eigenvalues and therefore the free vibration frequencies and mode shapes of the three span cantilever plate. To achieve this end, the building blocks for each of the three plate spans are superimposed one upon the other. The solution for the three span cantilever plate is obtained by means of the building blocks solutions as derived in the previous section. Since the governing differential equation is linear, and since each of the building block solutions satisfies it exactly, the sum of these solutions also satisfies it exactly. The eigenvalue matrix is shown schematically in Figure 3.12 based on three term building block solutions. The building blocks of the three span cantilever plate are shown on the top of the matrix. As stated previously, the numbers inside the blocks correspond to the span they represent.

Since the summation of the superimposed block solutions satisfies the governing differential equation, it is only necessary to constrain the Fourier coefficients in the expressions of the solutions so as to satisfy the boundary conditions of the plate. Turning to those boundary conditions for the superimposed set, it is noted that twelve boundary conditions remain to be satisfied. They are listed to the right of the matrix of Figure 3.12. These conditions were stated in section 3.1.1 and are summarised for the various rows of matrix segments in Table 3.1.

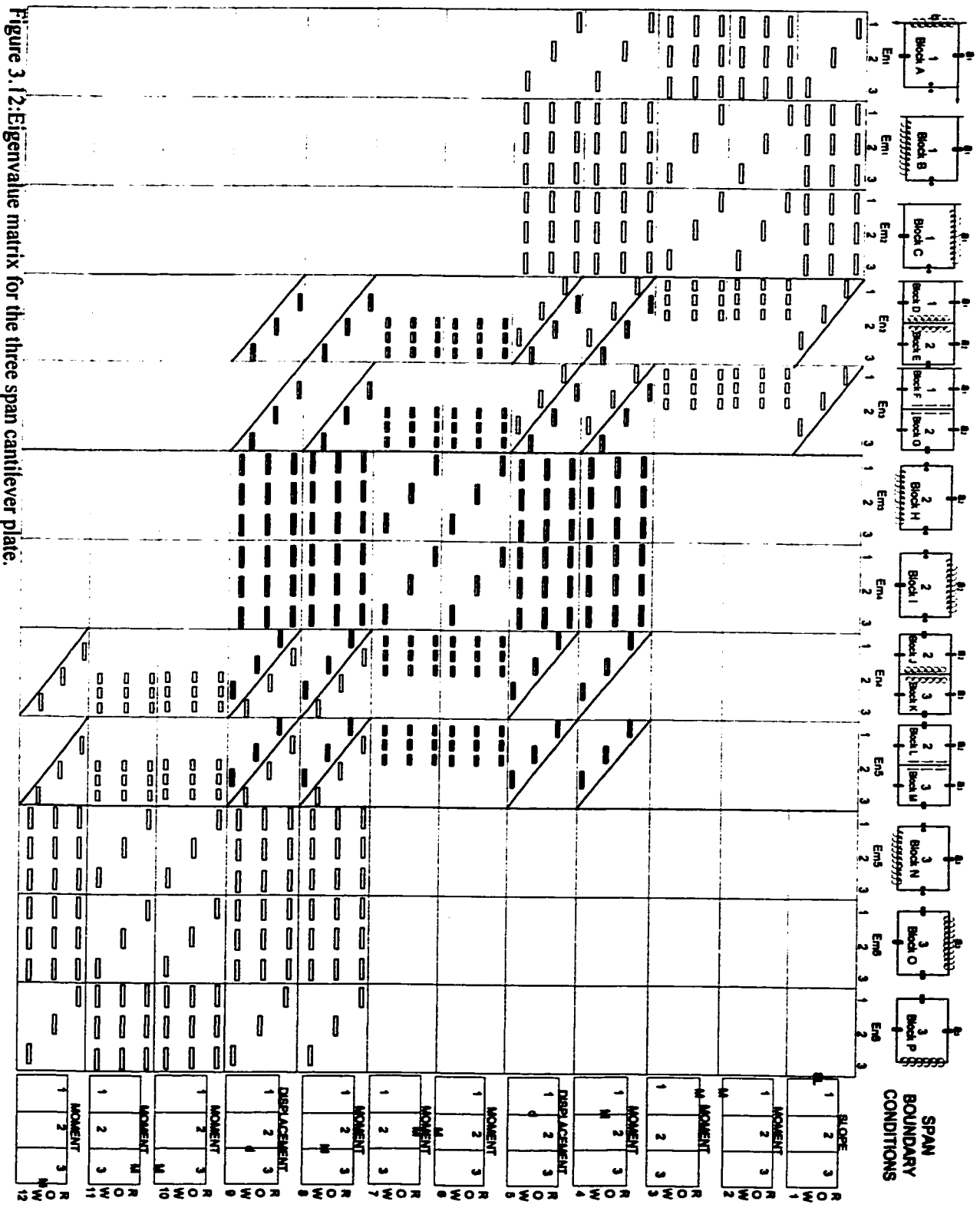


Figure 3.12: Eigenvalue matrix for the three span cantilever plate.

Table 3.1 : Summary of the remaining boundary conditions imposed by the eigenvalue matrix.

Row 1	Zero slope condition at edge $x=0$ of span 1.	Row 7	Zero moment condition at edge $y=0$ of span 2.
Row 2	Zero moment condition at edge $y=b$ of span 1.	Row 8	Continuity of moment condition at interspan 2 & 3.
Row 3	Zero moment condition at edge $y=0$ of span 1.	Row 9	Continuity of displacement condition at interspan 2 & 3.
Row 4	Continuity of moment condition at interspan 1 & 2.	Row 10	Zero moment condition at edge $y=b$ of span 3.
Row 5	Continuity of displacement condition at interspan 1 & 2.	Row 11	Zero moment condition at edge $y=0$ of span 3.
Row 6	Zero moment condition at edge $y=b$ of span 2.	Row 12	Zero moment condition at edge $x=a_3$ of span 3.

The value of K has been arbitrarily set equal to three. K is a symbol representing the number of terms utilised in the series solution of each building block. Although the computations are performed using $K=15$ terms, it is more convenient to represent the matrix for $K=3$. The unknown driving coefficients associated with the various building blocks are listed immediately beneath the building blocks of the figure. For example, the coefficients for the first block of span 1 are $E_{n1}(i)$ where $i=1,2,3$ (for a max value of $K=3$). The coefficients of the second block of span 1 are $E_{m1}(i)$ where $i=1,2,3$. It is noted that for the three span cantilever plate there are 12 sets of driving coefficients. There are 12 sets of boundary conditions constraining those coefficients. These conditions were previously summarised in Table 3.1. The numbers inside these inserts indicate the plate segment to which reference is made. For example, the first insert indicates that a condition of zero slope along the clamped edge of the first plate segment (or span) must be satisfied. The second and third inserts indicate edges along which a condition of zero bending moment must be enforced. The fourth insert enforces a condition of continuity of moment at the interface of span 1 & 2 etc.

Matrix elements generated in this process are represented by bars. Heavier bars are used to designate terms of the central plate segment (span 2). This is done for the convenience of the reader. Matrix elements pertaining to each block of the coupled pairs are separated by diagonals. These elements are not independent. In fact, they differ by a fixed multiplying factor as per equations 3.5 and 3.8 respectively. For example, matrix elements pertaining to coupled blocks “D” & “F” in the first row lie immediately beneath those blocks to the left of a diagonal line drawn through the matrix segment. The reader should conclude that these elements pertain to the left building block of the coupled pair. In row three, when elements pertain to the right building block of the coupled pair, they will appear to the right of the diagonal line. The matrix elements are generated using well established procedures employed by the superposition method as will be shown next. For the three span cantilever plate 12K unknown driving coefficients are present. This necessitates the development of 12K homogeneous algebraic equations relating those unknown driving coefficients. The eigenvalue matrix consists of the coefficient matrix for this set of equations. Almost all of the elements of the matrix will be functions of the eigenvalue λ^2 . By employing eigenvalue techniques, the unknown coefficients are obtained and the plate responses are determined. These techniques consist of a computational procedure that involves searching for those values of λ^2 which cause the determinant of the matrix to vanish. The 12K equations are reduced to triangular form by using the Gauss elimination method through pivotal reduction. The determinant of the triangular matrix is then easily obtained. The process permits the mode shapes to be plotted. This will be described later. A detailed description of the superposition method procedures employed in deriving the matrix elements is explained next.

Focusing first on the first row, the reader will realise that only building blocks pertaining to span 1 contribute to the condition of zero slope along the clamped edge $\xi=0$. Therefore elements are shown only under building blocks pertaining to span 1. These blocks are “A”, “B”, “C”, “D”, “F”. Referring to Figure 3.11, solutions for these blocks are depicted by equations 3.48, 3.51, 3.52, 3.56, 3.60, respectively. Denoting those solutions by $W_A(\xi,\eta), W_B(\xi,\eta), W_C(\xi,\eta), W_D(\xi,\eta), W_F(\xi,\eta)$, it is now important to superimpose those solutions. However for row 1, it is necessary to constrain the Fourier coefficients in the above respective solutions expressions so that the net effect is to satisfy the boundary condition of zero net slope normal to edge $\xi=0$. Using equation 2.1 for the expression of the slope, the contribution to slope along edge $\xi=0$ of each term of the solutions stated above, is expanded in the same trigonometric series $\cos(n\pi\eta)$ representing the contribution of the first building block in row1. The net coefficient of each term in the new series is set equal to zero. This gives rise to a set of K homogeneous algebraic equations relating the driving coefficients $E_{a1}, E_{m1}, E_{m2}, E_{a2}, E_{a3}$ based on the following equation:

$$\left. \frac{\partial W_A(\xi, \eta)}{\partial \xi} \right|_{\xi=0} + \left. \frac{\partial W_B(\xi, \eta)}{\partial \xi} \right|_{\xi=0} + \left. \frac{\partial W_C(\xi, \eta)}{\partial \xi} \right|_{\xi=0} + \left. \frac{\partial W_D(\xi, \eta)}{\partial \xi} \right|_{\xi=0} + \left. \frac{\partial W_F(\xi, \eta)}{\partial \xi} \right|_{\xi=0} = 0 \quad (3.62)$$

As stated earlier, in the case of span 1 the response $W(\xi,\eta)$ is non-dimensionalised through division by span edge length a_1 . Since displacements for blocks “A”, “D”, “F” are non-dimensionalised through division by edge length “b”, each contribution towards slope of these blocks must be multiplied by the plate segment aspect ratio ϕ_1 in order to preserve consistency. Equation 3.62 then becomes as follows:

$$\begin{aligned} & \phi_1 \frac{\partial W_A(\xi, \eta)}{\partial \xi} \Big|_{\xi=0} + \frac{\partial W_B(\xi, \eta)}{\partial \xi} \Big|_{\xi=0} + \frac{\partial W_C(\xi, \eta)}{\partial \xi} \Big|_{\xi=0} + \\ & \phi_1 \frac{\partial W_D(\xi, \eta)}{\partial \xi} \Big|_{\xi=0} + \phi_1 \frac{\partial W_F(\xi, \eta)}{\partial \xi} \Big|_{\xi=0} = 0 \end{aligned} \quad (3.63)$$

This equation is solved for each term “m” of the respective series creating therefore K homogeneous equations. From equation 3.63, it is seen that the first, fourth and fifth terms of the left hand side of this equation are already expanded in a cosine series. Therefore it is found advantageous to expand the contributions towards slope of blocks “B” & “C” in terms of the same series so that the sum in equation 3.63 relating the Fourier coefficients can be imposed and set equal zero. Looking at the first row of elements in the matrix, it is noticed that blocks “A”, “D”, “F”, have diagonal elements, while blocks “B” & “C” have full matrix elements. This is because slope contributions for blocks “B” & “C” are expanded in the same series as of those for blocks “A”, “D”, “F”. The expansion procedure is explained next. For this purpose, the slope contributions for blocks “A” and “B” are expressed as:

$$\begin{aligned} \text{For each term } n: \quad & \phi_1 \frac{\partial W_A(\xi, \eta)}{\partial \xi} \Big|_{\xi=0} = \phi_1 E_n \theta_{11n} \cos(n\pi\eta) [\beta_n \sinh \beta_n - \theta_{1n} \gamma_n \sin \gamma_n] \\ \text{or} \quad & = \phi_1 E_n \theta_{22n} \cos(n\pi\eta) [\beta_n \sinh \beta_n + \theta_{2n} \gamma_n \sinh \gamma_n] \end{aligned}$$

with the θ terms as given by equation 3.49 . (3.64)

$$\begin{aligned} \text{For each term } m: \quad & \frac{\partial W_B(\xi, \eta)}{\partial \xi} \Big|_{\xi=0} = (2m-1) \frac{\pi}{2} E_m \theta_{11m} [\cosh \beta_m \eta + \theta_{1m} \cos \gamma_m \eta] \\ \text{or} \quad & = (2m-1) \frac{\pi}{2} E_m \theta_{22m} [\cosh \beta_m \eta + \theta_{2m} \cosh \gamma_m \eta] \end{aligned}$$

with the θ terms as given by equations 3.16, 3.17 and 3.21 (3.65)

where m and n are the terms for the appropriate series.

From equation 3.64, it is seen that the first, fourth and fifth terms on the left-hand side of equation 3.63 are in the form of a Fourier series involving the trigonometric functions $\cos(n\pi\eta)$. The coefficients of this series involve the quantity E_n . It is obvious that we must expand the second and the third terms on the left-hand side of equation 3.63 in the same series. We must then impose the constraint that the sum of the coefficients before each of the Fourier trigonometric functions in the expansion of the above contributions must equal zero. The expansion process will be shown next for the second term only. As per Gorman[1], the coefficients A_n for a function $f(\eta)$ expanded in a series of the type $\cos(n\pi\eta)$ over the interval from 0 to 1 are known to be given by:

$$2 \int_0^1 f(\eta) \cos n\pi\eta d\eta$$

It is seen on examining equation 3.65 that integrals are required of the type:

$$2 \int_0^1 \cosh \beta_m \eta \cos n\pi\eta d\eta$$

and

$$2 \int_0^1 \cos \gamma_m \eta \cos n\pi\eta d\eta$$

for which solutions are available in appendix 2.

The expanded terms of equation 3.63 can be represented as a truncated series of analytical functions of the coordinate η :

$$\text{For } K = 3 \text{ therefore three terms } m : \left. \frac{\partial W_B(\xi, \eta)}{\partial \xi} \right|_{\xi=0} = E_1' f_1^B(\eta) + E_2' f_2^B(\eta) + E_3' f_3^B(\eta)$$

$$\text{For } K = 3 \text{ therefore three terms } m : \left. \frac{\partial W_C(\xi, \eta)}{\partial \xi} \right|_{\xi=0} = E_1' f_1^C(\eta) + E_2' f_2^C(\eta) + E_3' f_3^C(\eta)$$

where the primes indicate that the coefficients E are related to the subscript “m” and where the letters “f^B” & “f^C” indicate functions for blocks “B” & “C”.

Considering any term “n” of equation 3.64, the following is written for blocks “A”, “D”, “F”:

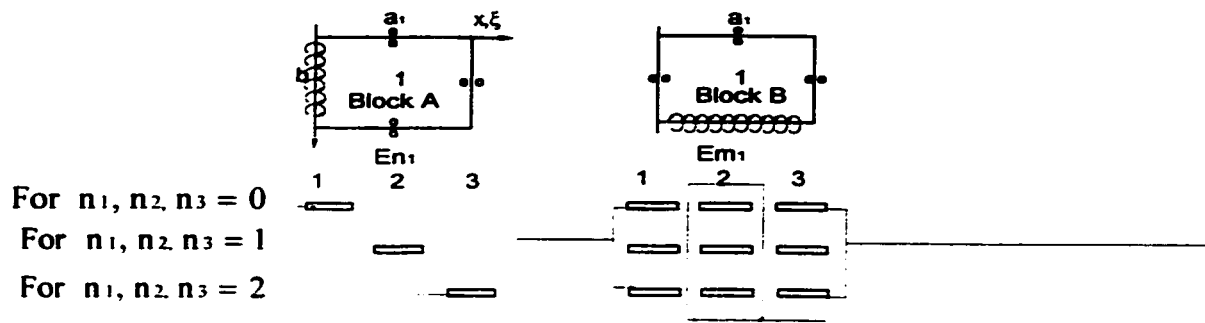
$$\text{For each term n: } \left. \frac{\partial W_A(\xi, \eta)}{\partial \xi} \right|_{\xi=0} = E_n \alpha_n^A \cos(n\pi\eta) ; \left. \frac{\partial W_D(\xi, \eta)}{\partial \xi} \right|_{\xi=0} = E_n \alpha_n^D \cos(n\pi\eta)$$

$$\left. \frac{\partial W_F(\xi, \eta)}{\partial \xi} \right|_{\xi=0} = E_n \alpha_n^F \cos(n\pi\eta)$$

where the α terms are functions of β and γ . In keeping with the boundary condition of zero slope as formulated in equation 3.63, the following can be written for each term n:

$$\begin{aligned} & \phi_1 E_n \alpha_n^A + 2E_1 \int_0^1 f_1^B(\eta) \cos(n\pi\eta) d\eta + 2E_2 \int_0^1 f_2^B(\eta) \cos(n\pi\eta) d\eta + 2E_3 \int_0^1 f_3^B(\eta) \cos(n\pi\eta) d\eta + \\ & 2E_1 \int_0^1 f_1^C(\eta) \cos(n\pi\eta) d\eta + 2E_2 \int_0^1 f_2^C(\eta) \cos(n\pi\eta) d\eta + 2E_3 \int_0^1 f_3^C(\eta) \cos(n\pi\eta) d\eta + \\ & \phi_1 E_n \alpha_n^D + \phi_1 E_n \alpha_n^F = 0 \end{aligned} \quad (3.66)$$

Figure 3.13 shows each term of equation 3.66 as represented in the matrix. Equation 3.66 is a homogeneous algebraic equation relating the unknown coefficients E_n and E_m . For K coefficients E_n and E_m employed in the expression of the slope, equation 3.66, would allow writing K linear homogeneous algebraic equations relating these 12K unknowns. The remaining eleven boundary conditions allow writing another 11K linear



$$\phi_1 E_1 \alpha_1^A + 2 E_1 \int_0^1 f_1^A(\eta) \cos(n\pi\eta) d\eta + 2 E_2 \int_0^1 f_2^B(\eta) \cos(n\pi\eta) d\eta + 2 E_3 \int_0^1 f_3^B(\eta) \cos(n\pi\eta) d\eta +$$

$$2 E_1 \int_0^1 f_1^C(\eta) \cos(n\pi\eta) d\eta + 2 E_2 \int_0^1 f_2^C(\eta) \cos(n\pi\eta) d\eta + 2 E_3 \int_0^1 f_3^C(\eta) \cos(n\pi\eta) d\eta +$$

$$\phi_1 E_1 \alpha_1^D + \phi_1 E_1 \alpha_1^F = 0$$

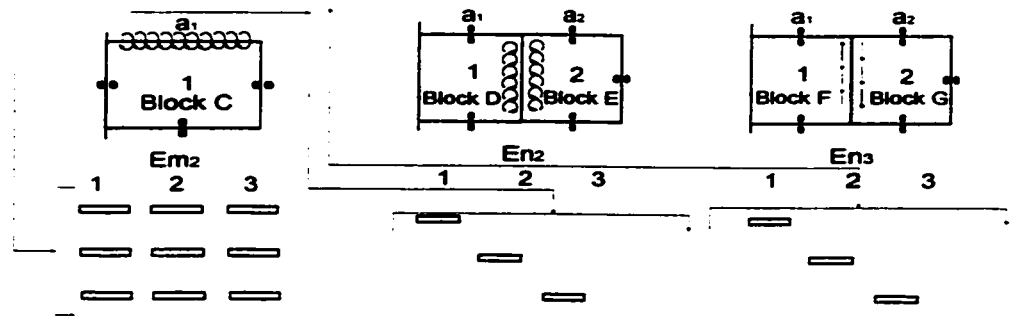


Figure 3.13 : Representation of the first row elements by their expressions.

homogeneous algebraic equations. The set of equations can best be handled by matrix techniques. Before explaining the procedure of calculating the eigenvalue, the reader is briefed about the derivation of the expressions for the other remaining rows.

In the second row of matrix segments of Figure 3.12, it is necessary to expand the contributions of building blocks toward bending moment along the edge $\eta=1$ of span 1 in an appropriate series. Here it is advantageous to utilise the sine series of equation 3.50 as contributions of two of the building blocks are available in the form of this series. The

required bending moment M_η is obtained from equation 2.2. When applying this equation to building block solutions with lateral displacement $W(\xi,\eta)$ non-dimensionalised through edge length “b”, the results must be multiplied by the aspect ratio of the plate segment involved. An identical procedure permits generation of matrix elements of the third row for edge $\eta=0$.

The fourth row of segments is generated by an enforcement of the condition of continuity of bending moment at the interface of the first and second plate segments. This is one of the continuity conditions to be satisfied as stated earlier in section 3.1.1. All building blocks of the first and second plate segments contribute toward moment at the interface. The practice here is to enter moment contributions toward the left side of the interface as positive and those contributing to the right side as negative, thus keeping the constraining equations in regular homogeneous form. The driving coefficients of the coupled pairs are multiplied by the factors of equations 3.5 and 3.8 as appropriate. In this row it is found appropriate to expand all building block contributions toward bending moment at the interface of the first and second spans in a cosine series. Bending moments M_ξ are obtained for each building block according to equation 2.2. Again all expansions developed for building blocks with analytical functions running in the ξ direction must be multiplied by the aspect ratio of the plate segment involved. Denoting the plate segments to the left hand side and right hand side of the interface as “i” and “j” respectively, it is seen that for the left hand side of the interface equation 2.2 provides the quantity $M_\xi a_i/D_i$. For the right hand side the same equation provides the quantity $M_\xi a_j/D_j$. Since

enforcement of continuity of actual moment M_{ξ} is required, matrix elements to the right hand side must be multiplied by the quantity $\phi_i D_j / \phi_i D_i$.

The fifth row of segments is generated by an enforcement of the condition of continuity of displacement at the interface of the first and second plate segments. This is the last of the continuity conditions to be satisfied as stated earlier in section 3.1.1. All building blocks of the first and second plate segments contribute toward displacement at the interface. All lateral displacements must be non-dimensionalised throughout the row of segments by the same length. Here it is found advantageous to non-dimensionalise all displacements through division by edge length “b”. Since displacements for solutions with analytical solutions running in the ξ direction are already non-dimensionalised in this manner, no multiplication factor is required. However for displacements with analytical functions running in the η direction and for any segment “i”, the solutions must be multiplied by the factor $1/\phi_i$.

The remainder of the matrix is easily generated following the same procedures described above. For the last row, a condition of zero bending moment along the plate outer edge must be enforced. For illustration purposes, the first quadrant of the first row of the eigenvalue matrix is represented next. Expressions for any quadrant can be derived using the guidelines above.

Quadrant (1,1): for $\lambda^2 > n_1 \pi^2$ and $n_1 = 1, 2, 3, \dots$

$$\phi_1 E_{n_1} \theta_{11n_1} \cos(n_1 \pi \eta) [\beta_{n_1} \sinh \beta_{n_1} - \theta_{1n_1} \gamma_{n_1} \sin \gamma_{n_1}]$$

for $\lambda^2 < n_1 \pi^2$ and $n_1 = 1, 2, 3, \dots$

$$\phi_1 E_{n_1} \theta_{22n_1} \cos(n_1 \pi \eta) [\beta_{n_1} \sinh \beta_{n_1} + \theta_{2n_1} \gamma_{n_1} \sinh \gamma_{n_1}]$$

The steps followed using matrix techniques for solving the problem of the three span cantilever plate are as follows:

- 1- The number of terms, K , is first selected to be used in the series. In this thesis $K=15$ was found suitable. Of course, more accuracy is obtained by using more terms. A trial value for the eigenvalue λ^2 is first selected. It is important to start at a very low value so that no eigenvalues are missed. For this selected eigenvalue, the coefficient matrix of Figure 3.12 is generated.
- 2- The determinant of the matrix is next evaluated and stored.
- 3- The trial eigenvalue is incremented upward progressively, first by larger increments then by smaller ones, repeating steps 1 and 2 in order to establish that value of λ^2 which causes the determinant of the matrix to vanish while passing continuously from positive to negative or from negative to positive. A vanishing determinant indicates that a nontrivial solution exists for the quantities E_n and E_m and hence the associated λ^2 is an eigenvalue.
- 4- The next step is to determine the mode shapes for this specific eigenvalue. This is done first by solving for the coefficients E_n and E_m . This may be achieved by arbitrarily setting one of the now-zero coefficients equal to unity, say E_m where $m=1$. The eigenvalue matrix, thus modified, represents a set of non-homogeneous algebraic equations relating the $12K-1$ driving coefficients E_n and E_m . Any set of the $12K-1$ equations may be selected from the set of $12K$. For example the first $12K-1$ equations are solved thereby assigning values to the remaining driving coefficients. With the entire set of driving coefficients calculated, the mode shapes represented by the superimposed building blocks are generated. A computer program shown in

Appendix 3 was prepared to carry out those operations. The flowchart of Figure 3.14 is a brief description of those operations.

- 5- The dimension “a” of the individual plate segments can take any desired value while edge length “b” remains constant i.e., the ratio b/a is arbitrarily selected. It is convenient to express the value for the dimensionless frequency as λ_b^2 , where the frequency is non-dimensionalised through use of edge length “b”. While length “a” may change from span to span, the length “b” is constant. It is also accepted in this thesis that each segment may take different values for effective mass per unit area and plate flexural rigidity. The practice is to base the eigenvalue λ_b^2 on the mass and flexural rigidity of the first span, i.e the plate segment bounded by the clamped edge. For an eigenvalue λ_b^2 equal $\omega b^2 \sqrt{\rho_1/D_1}$, it follows therefore, that for any segment “i”, the associated quantity λ_a^2 becomes:

$\lambda_a^2 = \{\lambda_b^2/\phi^2\}R_i$ where, $R_i = \sqrt{\frac{e_i/D_i}{e_1/D_1}}$. Subscript “1” refers to span1 and e_i & D_i are mass per unit area and flexural rigidity respectively, of the plate span to which subscript “i” refers.

This completes the detailed description of the computations required to solve the problem of the three span cantilever plate. Solutions for cases analysed are presented in Chapter 4.

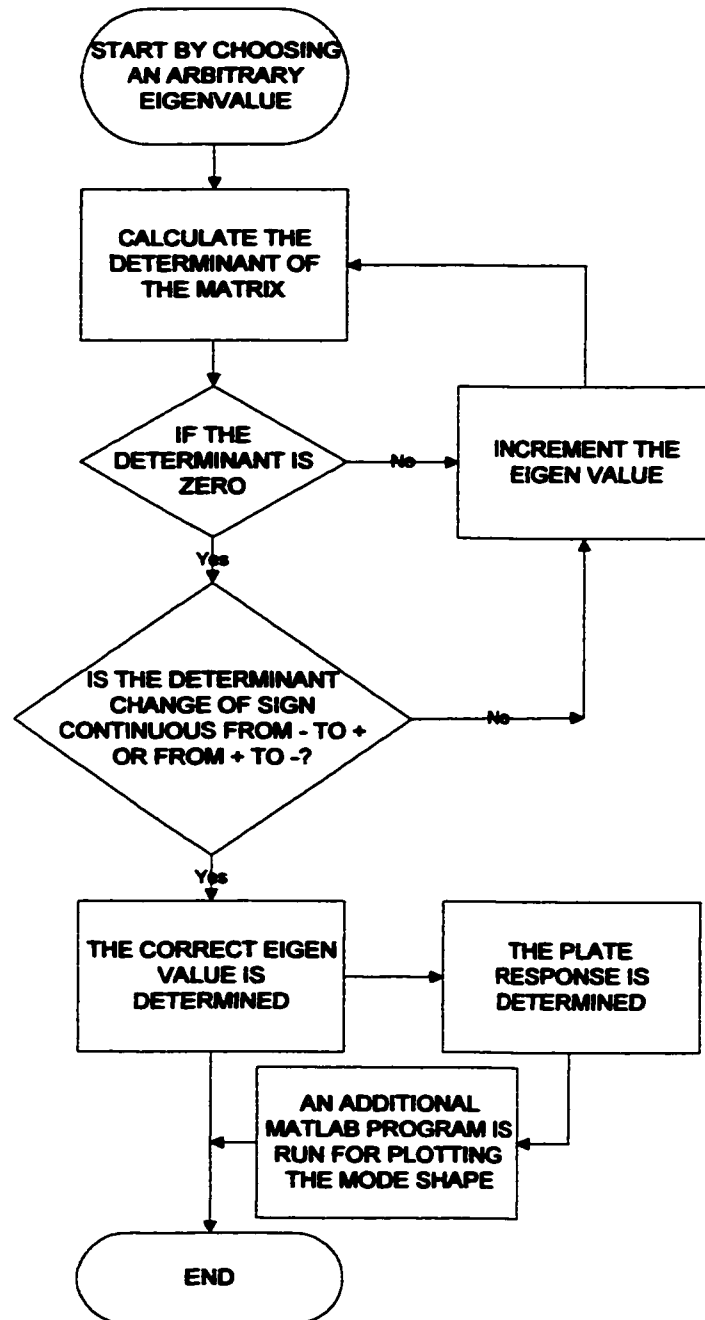


Figure 3.14 : Flowchart for computing the eigenvalue for the 3 span cantilever plate.

3.2 The Four Span Cantilever Plate

The computer routine for solving the problem of the three span cantilever plate can be applied to any number of plate spans. For the case of the four span plate, the matrix will comprise an array of 16 x 16 segments instead of the 12 x 12 array associated with the three span plate. The matrix for the four span cantilever plate is derived from the one in figure 3.12. This is done by focusing on the central portion of the matrix associated with the second plate segment (or span) and augmenting it with a similar section, downward to the right. The final portion of the new segment is then associated with the fourth and final plate segment. Figure 3.15 is a representation of the eigenvalue matrix as applied to the four span cantilever plate. Chapter 4 presents the results obtained for eigenvalues and modes shapes of different three span and four span cantilever plates.

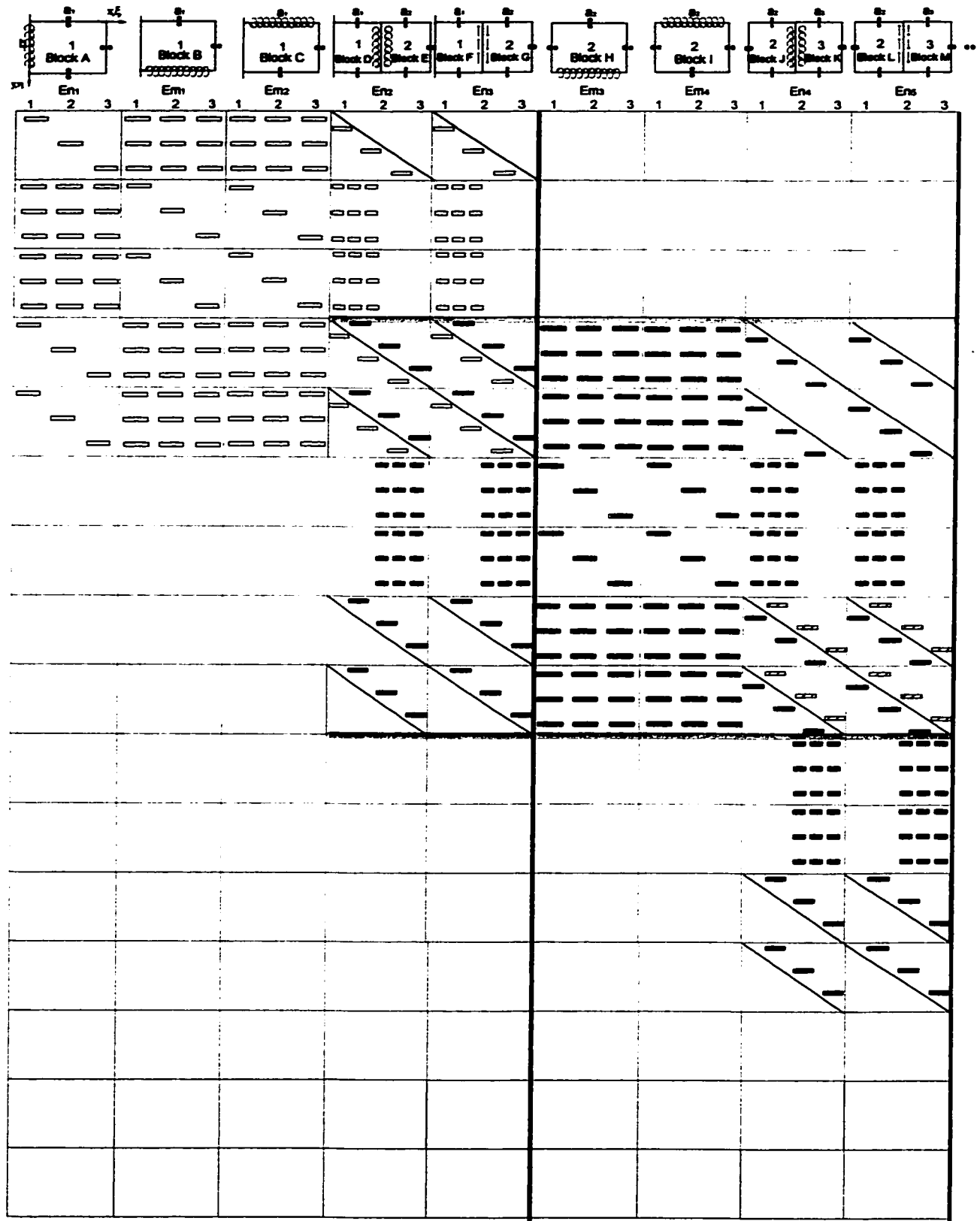


Figure 3.15a : First portion of the eigenvalue matrix for the four span cantilever plate.

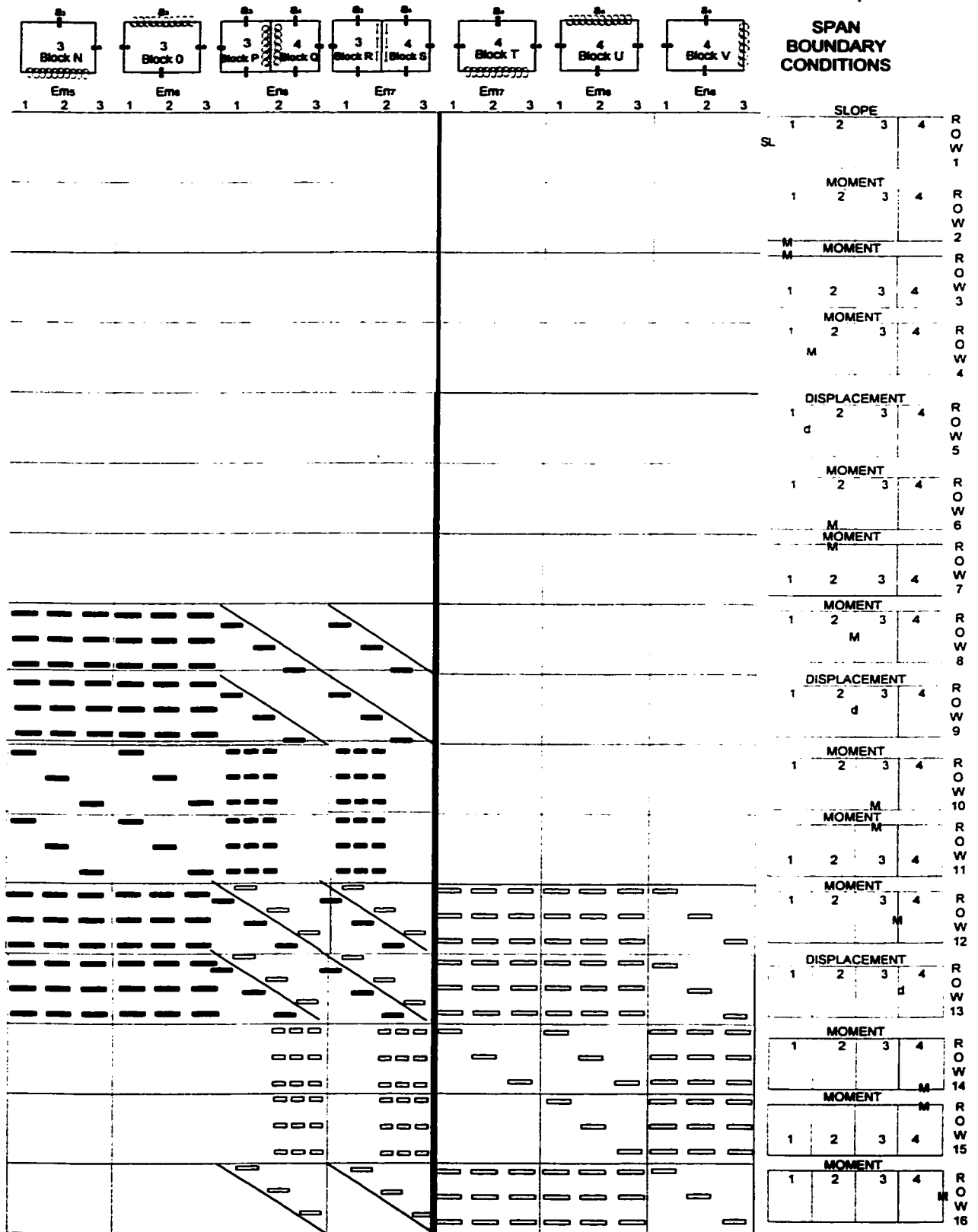


Figure 3.15b : Final portion of matrix of Figure 3.15a.

Chapter 4

PRESENTATION OF RESULTS

It is appreciated that no comprehensive set of eigenvalues could be prepared to cover the range of any plate geometries and property discontinuities which might be encountered. For this reason this chapter presents results of limited scope of plate geometries. It will provide researchers and designers with data against which their computed results can be compared. Towards this end this thesis presents the mode shapes and eigenvalues of a cantilever plate with finite discontinuities in thickness moving outward from the clamped edge as stated earlier in the beginning of Chapter 3. The superposition method with a value of $K=15$, is employed. These results constitute an analytical computation of free vibration frequencies and mode shapes of such plates. A three span cantilever plate of equal span widths is first considered with a discontinuity in thickness represented by varying ratios from the clamped edge. Only the ratio of plate span thicknesses is required. The thickness ratio h_i/h_1 represents the ratio of the i 'th span thickness to that of the first span. In section 4.1, for the case of the 3 span plate, three thickness ratios are therefore generated. The results presented in this thesis correspond to h_i/h_1 equal 1, 3/4, 1/2, for $i=1,2,3$ respectively. Another reduced set of thickness ratios 1,3/8,1/4 is also considered for spans 1,2 & 3 for comparison purposes. The plate overall aspect ratios $b/(a_1+a_2+a_3)$ considered are 3, 2, 1.5, 1, 1/1.5, 1/2, 1/3, 2/9, 1/6, 1/9. The eigenvalues generated correspond to the first 10 vibration modes. Mode shapes for the first 4 modes are plotted for all the aspect ratios in section 4.2. The results for the four span cantilever plate are presented in Appendix 1. A comprehensive set of

overall aspect ratios $\phi=b/(a_1+a_2+a_3+a_4)$ ranging from 3 to 1/3 is considered for this plate. Thickness ratios of 1, 3/8, 1/4, 1/8, are considered throughout.

It will be recalled that mass per unit area of each segment is proportional to segment thickness "h_i". Moreover, flexural rigidity of each segment is proportional to h³. All the cases considered for the three span and four span plates have equal span aspect ratios. $a_1 = a_2 = a_3 = a_4$, for four span plates and therefore $\phi_1, \phi_2, \phi_3, \phi_4$ are equal. Finally, it is of interest to carry out verification tests. This is done in section 4.3. Three span cantilever plates with uniform thicknesses throughout the spans have been considered. Known results for uniform cantilever plates are compared to the results generated using the present analytical approach. The results are then compared and discussed in Chapter 5.

4.1 Results for the Three Span Cantilever Plate with Varying Thicknesses Per Span and Equal Spans Aspect Ratios.

The tables below present computed eigenvalues for the first 10 modes of the three span cantilever plate of overall aspect ratio equal three. Using 15 terms in the series solutions is believed to give four significant digit accuracy in most cases. For each span the aspect ratio is therefore 9. Tables 4.1 and 4.2 differ in the thickness ratios assigned to their individual spans. The plate of Table 4.1 is a much thicker plate compared to the one of Table 4.2. These tables show the effect of thickness ratios on the eigenvalues, for different plate geometries.

Table 4.1. Eigenvalues for thickness ratios 1,3/4,1/2 & plate overall aspect ratio $\phi=3$

Span1 Aspect Ratio $\phi_1=9$	Span2 Aspect Ratio $\phi_2=9$	Span3 Aspect Ratio $\phi_3=9$
Thickness Ratio		
$h_1/h_1 = 1$	$h_2/h_1 = 3/4$	$h_3/h_1 = 1/2$
Mode	Eigenvalue λ_b^2	
1	37.65	
2	41.43	
3	53.64	
4	74.55	
5	105.1	
6	144.5	
7	154.3	
8	160.9	
9	176.3	
10	198.9	

Table 4.2. Eigenvalues for thickness ratios 1,3/8,1/4 & plate overall aspect ratio $\phi=3$

Span1 Aspect Ratio $\phi_1=9$	Span2 Aspect Ratio $\phi_2=9$	Span3 Aspect Ratio $\phi_3=9$
Thickness Ratio		
$h_1/h_1 = 1$	$h_2/h_1 = 3/8$	$h_3/h_1 = 1/4$
Mode	Eigenvalue λ_b^2	
1	27.91	
2	29.62	
3	35.42	
4	45.36	
5	78.90	
6	102.8	
7	111.8	
8	114.1	
9	124.7	
10	132.2	

Table 4.3. Eigenvalues for thickness ratios 1,3/4,1/2 & plate overall aspect ratio $\phi=2$

Span1 Aspect Ratio $\phi_1=6$	Span2 Aspect Ratio $\phi_2=6$	Span3 Aspect Ratio $\phi_3=6$
Thickness Ratio		
$h_1/h_1 = 1$	$h_2/h_1 = 3/4$	$h_3/h_1 = 1/2$
Mode	Eigenvalue λ_b^2	
1	16.68	
2	20.59	
3	32.39	
4	52.78	
5	68.21	
6	73.93	
7	82.80	
8	92.31	
9	117.2	
10	126.8	

Table 4.4. Eigenvalues for thickness ratios 1,3/8,1/4 & plate overall aspect ratio $\phi=2$

Span1 Aspect Ratio $\phi_1=6$	Span2 Aspect Ratio $\phi_2=6$	Span3 Aspect Ratio $\phi_3=6$
Thickness Ratio		
$h_1/h_1 = 1$	$h_2/h_1 = 3/8$	$h_3/h_1 = 1/4$
Mode	Eigenvalue λ_b^2	
1	12.38	
2	14.20	
3	19.93	
4	29.70	
5	43.99	
6	49.63	
7	52.33	
8	62.26	
9	63.81	
10	77.69	

Table 4.5. Eigenvalues for thickness ratios 1,3/4,1/2 & plate overall aspect ratio $\phi=1.5$

Span1 Aspect Ratio $\phi_1=4.5$	Span2 Aspect Ratio $\phi_2=4.5$	Span3 Aspect Ratio $\phi_3=4.5$
Thickness Ratio		
$h_1/h_1 = 1$	$h_2/h_1 = 3/4$	$h_3/h_1 = 1/2$
Mode	Eigenvalue λ_b^2	
1	9.354	
2	13.20	
3	24.42	
4	38.49	
5	41.91	
6	46.81	
7	59.65	
8	75.99	
9	87.11	
10	94.77	

Table 4.6. Eigenvalues for thickness ratios 1,3/8,1/4 & plate overall aspect ratio $\phi=1.5$

Span1 Aspect Ratio $\phi_1=4.5$	Span2 Aspect Ratio $\phi_2=4.5$	Span3 Aspect Ratio $\phi_3=4.5$
Thickness Ratio		
$h_1/h_1 = 1$	$h_2/h_1 = 3/8$	$h_3/h_1 = 1/4$
Mode	Eigenvalue λ_b^2	
1	6.946	
2	8.792	
3	14.29	
4	23.85	
5	27.73	
6	30.98	
7	37.87	
8	40.84	
9	53.85	
10	58.53	

Table 4.7. Eigenvalues for thickness ratios 1,3/4,1/2 & plate overall aspect ratio $\phi=1$

Span1 Aspect Ratio $\phi_1=3$	Span2 Aspect Ratio $\phi_2=3$	Span3 Aspect Ratio $\phi_3=3$
Thickness Ratio		
$h_1/h_1 = 1$	$h_2/h_1 = 3/4$	$h_3/h_1 = 1/2$
Mode	Eigenvalue λ_b^2	
1	4.132	
2	7.597	
3	16.51	
4	18.76	
5	21.92	
6	36.97	
7	38.52	
8	42.04	
9	48.21	
10	63.91	

Table 4.8. Eigenvalues for thickness ratios 1,3/8,1/4 & plate overall aspect ratio $\phi=1$

Span1 Aspect Ratio $\phi_1=3$	Span2 Aspect Ratio $\phi_2=3$	Span3 Aspect Ratio $\phi_3=3$
Thickness Ratio		
$h_1/h_1 = 1$	$h_2/h_1 = 3/8$	$h_3/h_1 = 1/4$
Mode	Eigenvalue λ_b^2	
1	3.072	
2	4.820	
3	9.875	
4	12.37	
5	19.74	
6	23.40	
7	26.34	
8	31.19	
9	34.32	
10	36.41	

Table 4.9. Eigenvalues for thickness ratios 1,3/4,1/2 & plate overall aspect ratio $\phi=2/3$

Span1 Aspect Ratio $\phi_1=2$	Span2 Aspect Ratio $\phi_2=2$	Span3 Aspect Ratio $\phi_3=2$
Thickness Ratio		
$h_1/h_1 = 1$	$h_2/h_1 = 3/4$	$h_3/h_1 = 1/2$
Mode	Eigenvalue λ_b^2	
1	1.823	
2	4.658	
3	12.02	
4	15.00	
5	18.61	
6	24.41	
7	25.98	
8	34.73	
9	38.50	
10	41.58	

Table 4.10. Eigenvalues for thickness ratios 1,3/8,1/4 & plate overall aspect ratio $\phi=2/3$

Span1 Aspect Ratio $\phi_1=2$	Span2 Aspect Ratio $\phi_2=2$	Span3 Aspect Ratio $\phi_3=2$
Thickness Ratio		
$h_1/h_1 = 1$	$h_2/h_1 = 3/8$	$h_3/h_1 = 1/4$
Mode	Eigenvalue λ_b^2	
1	1.356	
2	2.852	
3	5.394	
4	7.782	
5	8.129	
6	11.69	
7	15.23	
8	21.67	
9	24.71	
10	26.72	

Table 4.11. Eigenvalues for thickness ratios 1,3/4,1/2 & plate overall aspect ratio $\phi=1/2$

Span1 Aspect Ratio $\phi_1=1.5$	Span2 Aspect Ratio $\phi_2=1.5$	Span3 Aspect Ratio $\phi_3=1.5$
Thickness Ratio		
$h_1/h_1 = 1$	$h_2/h_1 = 3/4$	$h_3/h_1 = 1/2$
Mode	Eigenvalue λ_b^2	
1	1.020	
2	3.367	
3	4.190	
4	8.184	
5	10.33	
6	13.69	
7	15.85	
8	21.15	
9	22.22	
10	26.43	

Table 4.12. Eigenvalues for thickness ratios 1,3/8,1/4 & plate overall aspect ratio $\phi=1/2$

Span1 Aspect Ratio $\phi_1=1.5$	Span2 Aspect Ratio $\phi_2=1.5$	Span3 Aspect Ratio $\phi_3=1.5$
Thickness Ratio		
$h_1/h_1 = 1$	$h_2/h_1 = 3/8$	$h_3/h_1 = 1/4$
Mode	Eigenvalue λ_b^2	
1	0.759	
2	2.026	
3	3.030	
4	5.439	
5	7.015	
6	10.56	
7	11.70	
8	15.13	
9	16.69	
10	19.34	

Table 4.13. Eigenvalues for thickness ratios 1,3/4,1/2 & plate overall aspect ratio $\phi=1/3$

Span1 Aspect Ratio $\phi_1=1$	Span2 Aspect Ratio $\phi_2=1$	Span3 Aspect Ratio $\phi_3=1$
Thickness Ratio		
$h_1/h_1 = 1$	$h_2/h_1 = 3/4$	$h_3/h_1 = 1/2$
Mode	Eigenvalue λ_b^2	
1	0.450	
2	1.853	
3	4.578	
4	4.974	
5	9.160	
6	9.473	
7	12.37	
8	14.06	
9	15.30	
10	18.32	

Table 4.14. Eigenvalues for thickness ratios 1,3/8,1/4 & plate overall aspect ratio $\phi=1/3$

Span1 Aspect Ratio $\phi_1=1$	Span2 Aspect Ratio $\phi_2=1$	Span3 Aspect Ratio $\phi_3=1$
Thickness Ratio		
$h_1/h_1 = 1$	$h_2/h_1 = 3/8$	$h_3/h_1 = 1/4$
Mode	Eigenvalue λ_b^2	
1	0.335	
2	1.339	
3	2.883	
4	3.227	
5	5.290	
6	6.111	
7	6.255	
8	8.250	
9	9.095	
10	9.485	

Table 4.15. Eigenvalues for thickness ratios 1,3/4,1/2 & plate overall aspect ratio $\phi=2/9$

Span1 Aspect Ratio $\phi_1=1/1$	Span2 Aspect Ratio $\phi_2=1/1.5$	Span3 Aspect Ratio $\phi_3=1/1.5$
Thickness Ratio		
$h_1/h_1 = 1$	$h_2/h_1 = 3/4$	$h_3/h_1 = 1/2$
Mode	Eigenvalue λ_b^2	
1	0.199	
2	0.819	
3	1.411	
4	2.021	
5	3.124	
6	4.197	
7	5.587	
8	8.068	
9	9.999	
10	11.43	

Table 4.16. Eigenvalues for thickness ratios 1,3/8,1/4 & plate overall aspect ratio $\phi=2/9$

Span1 Aspect Ratio $\phi_1=1/1.5$	Span2 Aspect Ratio $\phi_2=1/1.5$	Span3 Aspect Ratio $\phi_3=1/1.5$
Thickness Ratio		
$h_1/h_1 = 1$	$h_2/h_1 = 3/8$	$h_3/h_1 = 1/4$
Mode	Eigenvalue λ_b^2	
1	0.148	
2	0.592	
3	0.824	
4	1.272	
5	1.984	
6	3.684	
7	3.974	
8	4.816	
9	5.815	
10	6.579	

Table 4.17. Eigenvalues for thickness ratios 1,3/4,1/2 & plate overall aspect ratio $\phi=1/6$

Span1 Aspect Ratio $\phi_1=1/2$	Span2 Aspect Ratio $\phi_2=1/2$	Span3 Aspect Ratio $\phi_3=1/2$
Thickness Ratio		
$h_1/h_1 = 1$	$h_2/h_1 = 3/4$	$h_3/h_1 = 1/2$
Mode	Eigenvalue λ_b^2	
1	0.112	
2	0.459	
3	1.045	
4	2.276	
5	2.350	
6	4.020	
7	7.863	
8	7.960	
9	10.29	
10	10.52	

Table 4.18. Eigenvalues for thickness ratios 1,3/8,1/4 & plate overall aspect ratio $\phi=1/6$

Span1 Aspect Ratio $\phi_1=1/2$	Span2 Aspect Ratio $\phi_2=1/2$	Span3 Aspect Ratio $\phi_3=1/2$
Thickness Ratio		
$h_1/h_1 = 1$	$h_2/h_1 = 3/8$	$h_3/h_1 = 1/4$
Mode	Eigenvalue λ_b^2	
1	0.083	
2	0.331	
3	0.606	
4	0.711	
5	1.321	
6	2.232	
7	2.624	
8	3.395	
9	3.562	
10	4.381	

Table 4.19. Eigenvalues for thickness ratios 1,3/4,1/2 & plate overall aspect ratio $\phi=1/9$

Span1 Aspect Ratio $\phi_1=1/3$	Span2 Aspect Ratio $\phi_2=1/3$	Span3 Aspect Ratio $\phi_3=1/3$
Thickness Ratio		
$h_1/h_1 = 1$	$h_2/h_1 = 3/4$	$h_3/h_1 = 1/2$
Mode	Eigenvalue λ_b^2	
1	0.049	
2	0.203	
3	0.501	
4	0.687	
5	1.039	
6	1.477	
7	1.654	
8	2.486	
9	2.582	
10	3.517	

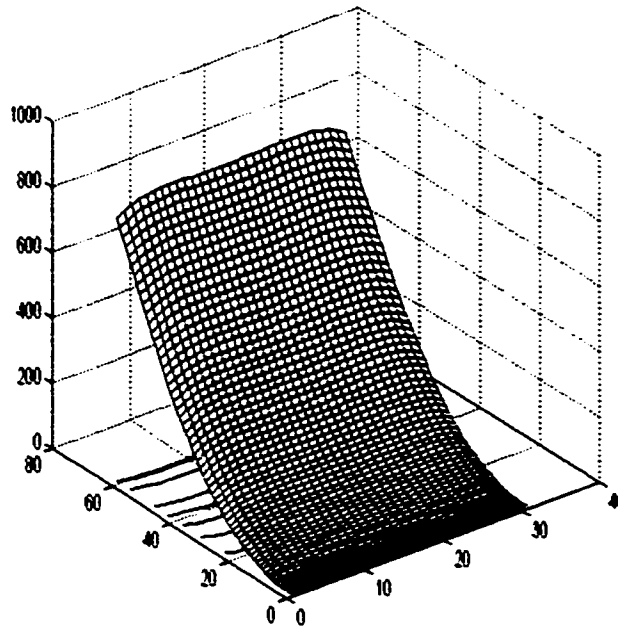
Table 4.20. Eigenvalues for thickness ratios 1,3/8,1/4 & plate overall aspect ratio $\phi=1/9$

Span1 Aspect Ratio $\phi_1=1/3$	Span2 Aspect Ratio $\phi_2=1/3$	Span3 Aspect Ratio $\phi_3=1/3$
Thickness Ratio		
$h_1/h_1 = 1$	$h_2/h_1 = 3/8$	$h_3/h_1 = 1/4$
Mode	Eigenvalue λ_b^2	
1	0.037	
2	0.147	
3	0.314	
4	0.396	
5	0.583	
6	0.917	
7	0.986	
8	1.575	
9	1.662	
10	2.083	

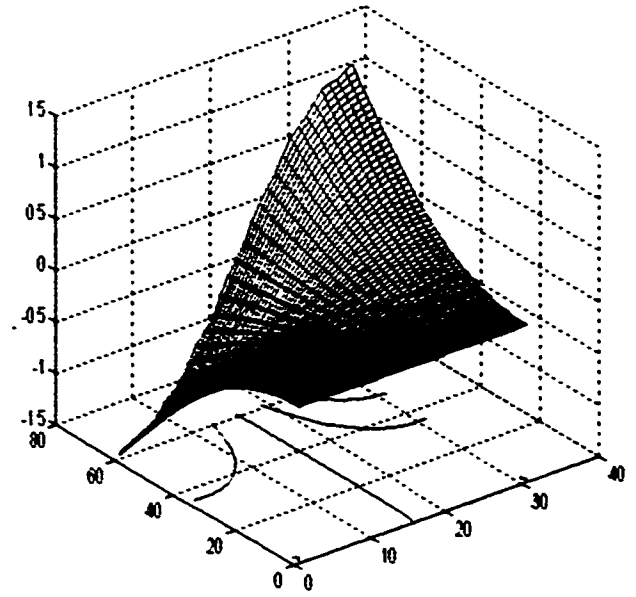
The above results are discussed in Chapter 5. The next section presents mode shapes for the first four modes of tables 4.1 to 4.20.

4.1 Plotted Mode Shapes

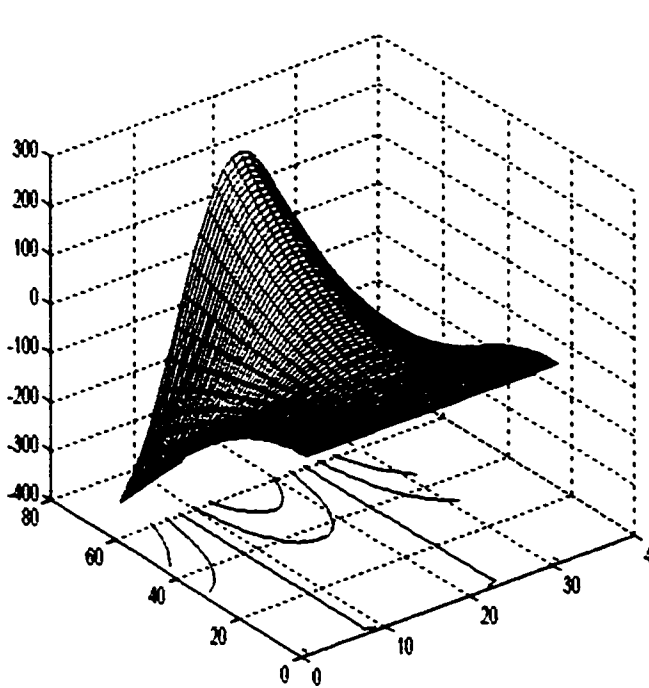
The first four mode shapes are plotted for each plate considered above. The reader will notice there are symmetric and anti-symmetric mode responses. The lines projected on the horizontal plane represent contour lines and nodal lines. Location of clamped edges will be obvious.



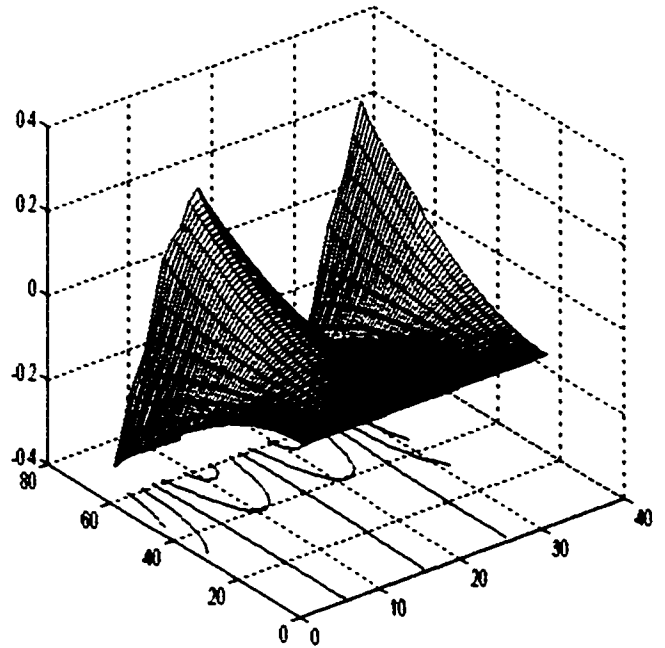
MODE 1



MODE 2

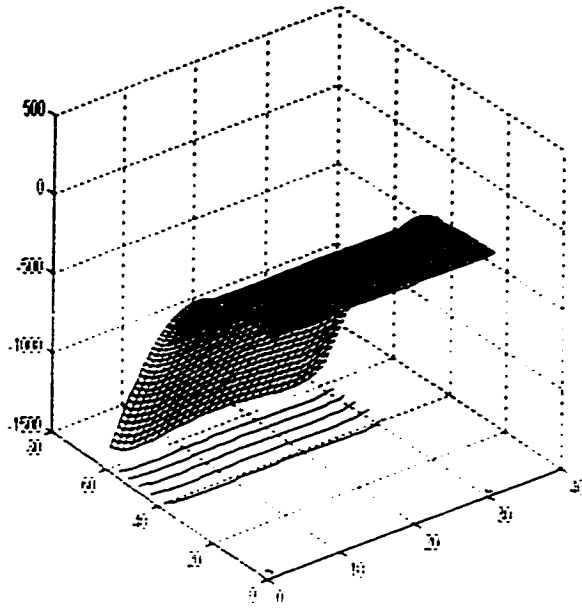


MODE 3

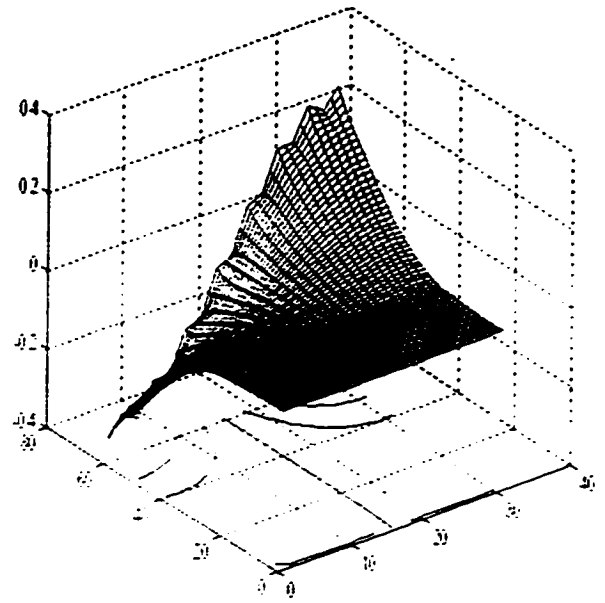


MODE 4

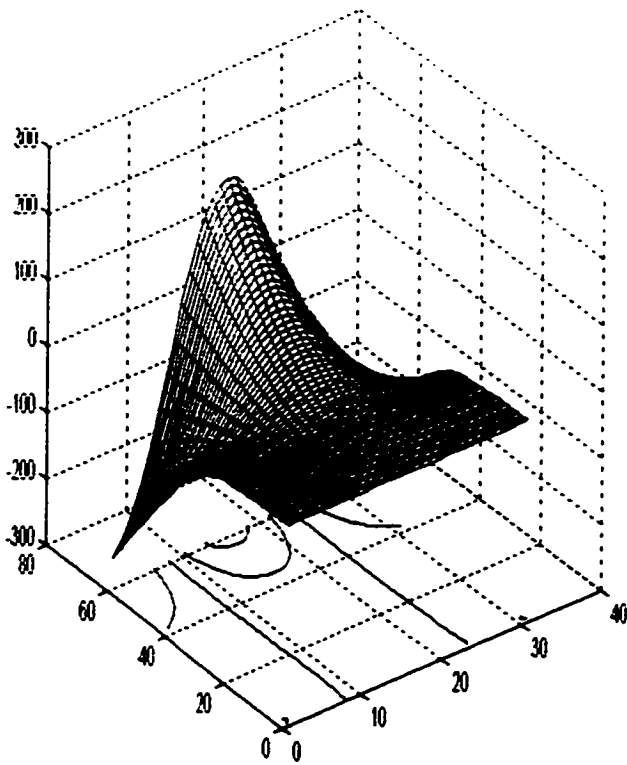
Figure 4.1 : First four mode shapes for Table 4.1.



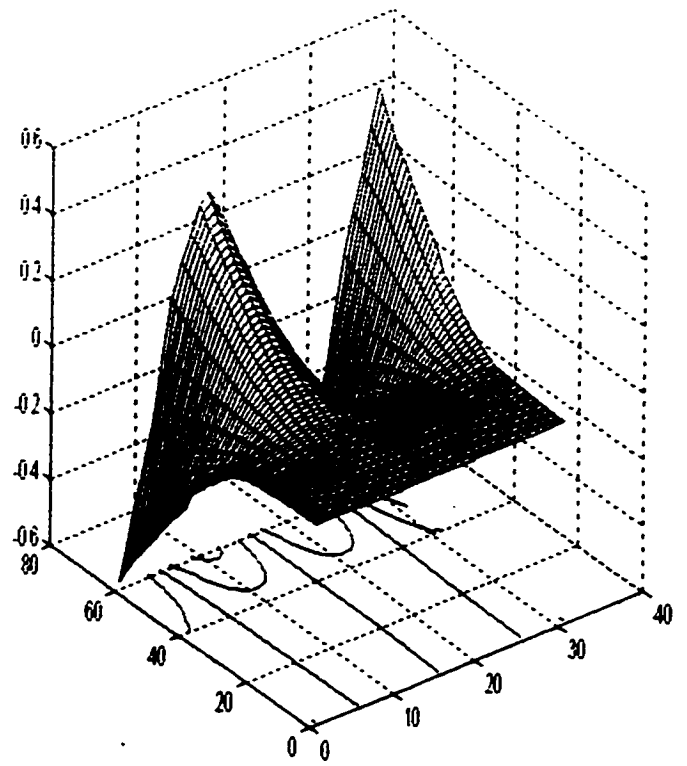
MODE 1



MODE 2

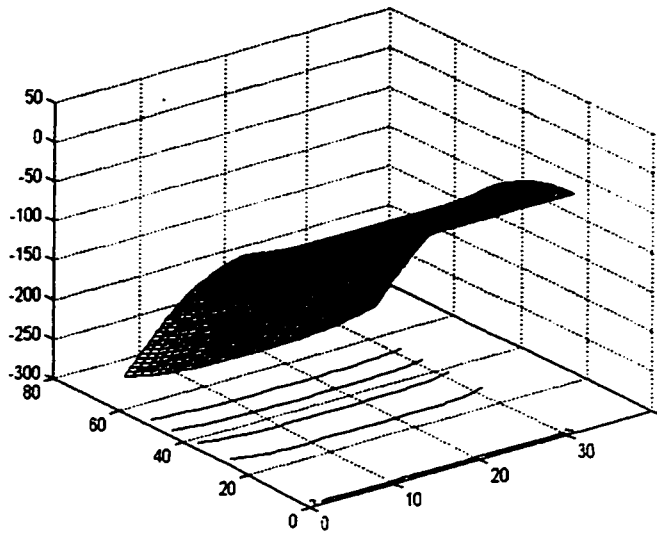


MODE 3

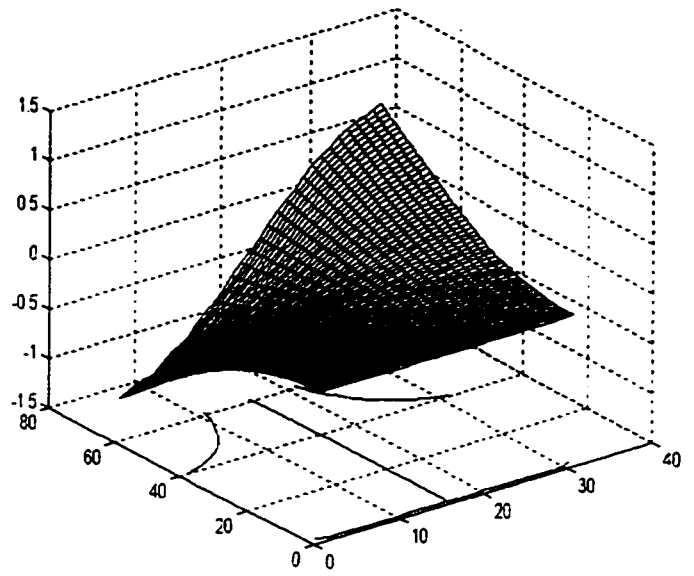


MODE 4

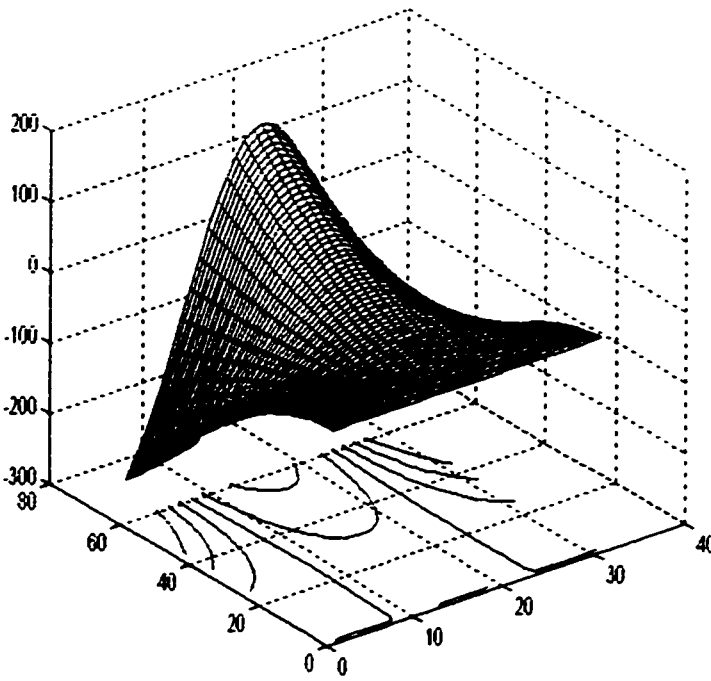
Figure 4.2 : First four mode shapes for Table 4.2.



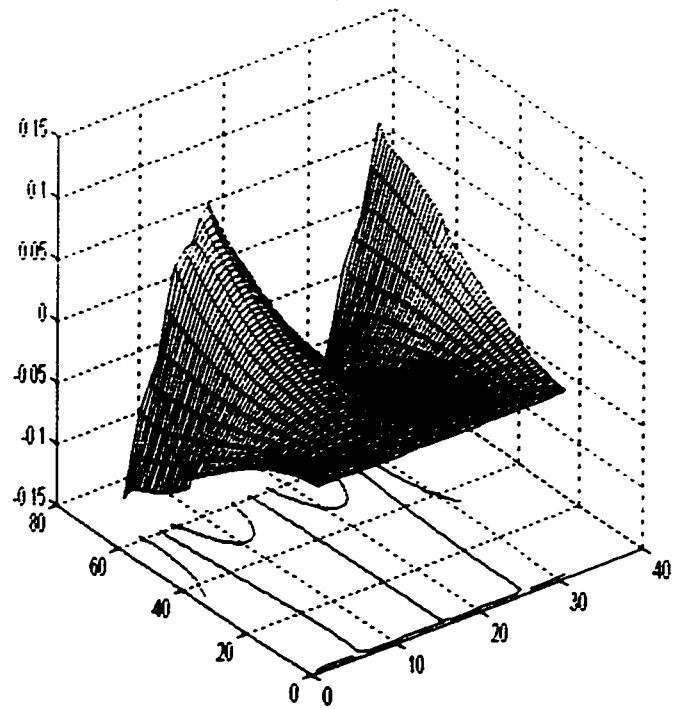
MODE 1



MODE 2

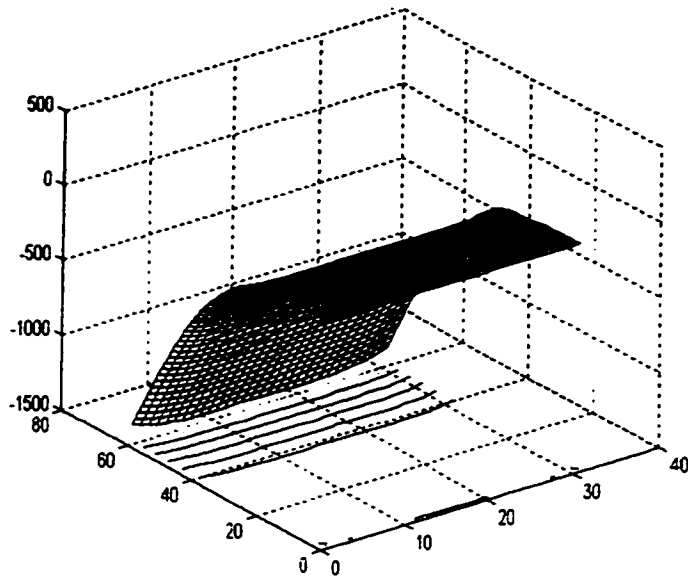


MODE 3

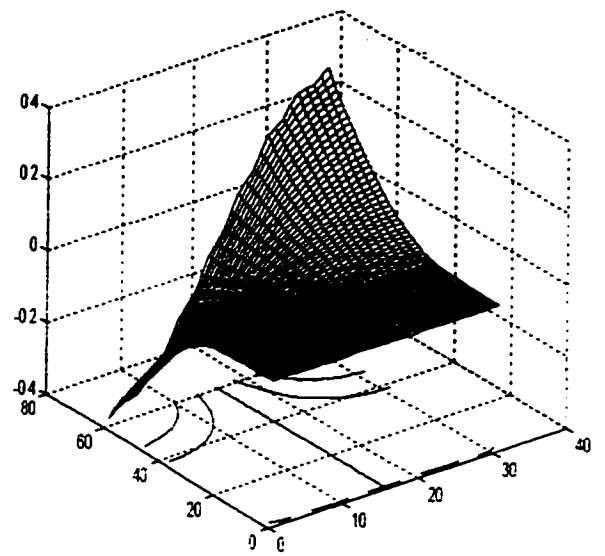


MODE 4

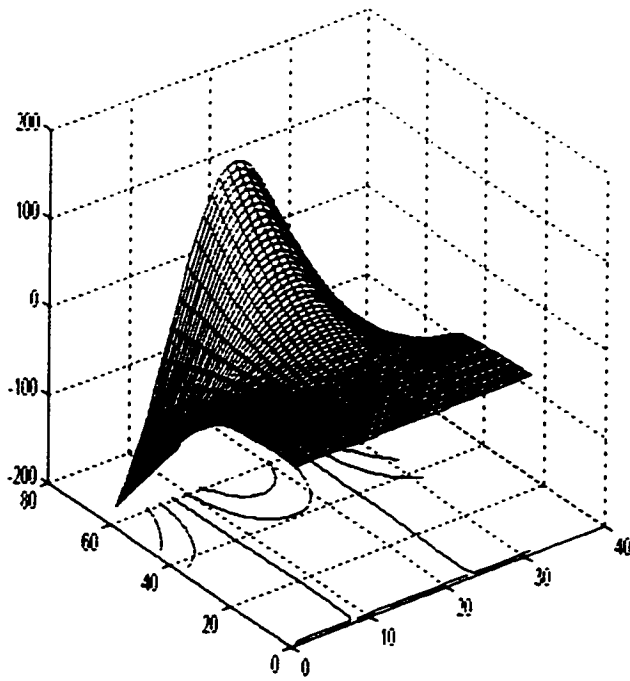
Figure 4.3 : First four mode shapes for Table 4.3.



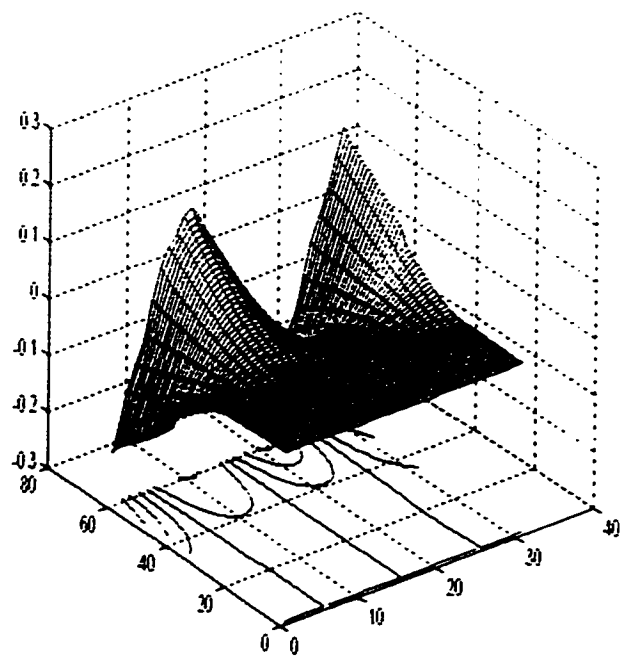
MODE 1



MODE 2

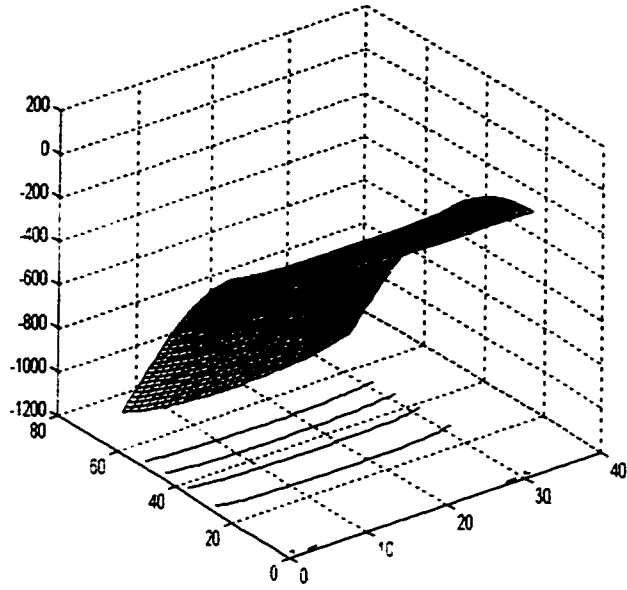


MODE 3

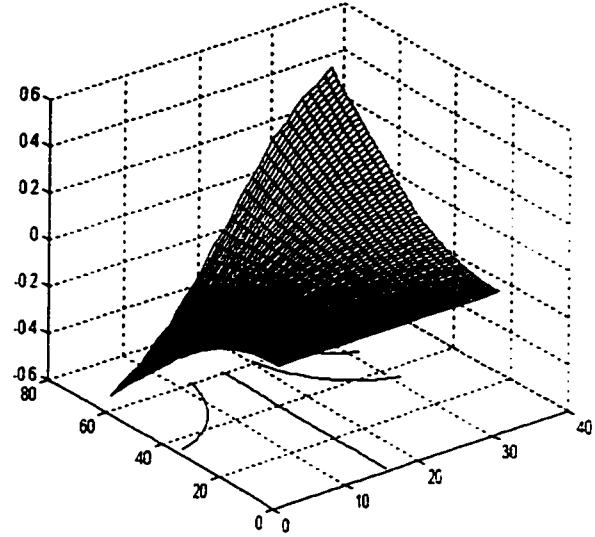


MODE 4

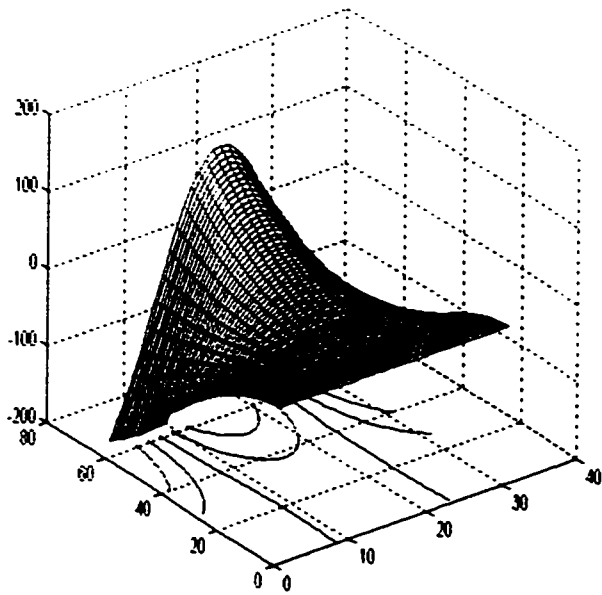
Figure 4.4 : First four mode shapes for Table 4.4.



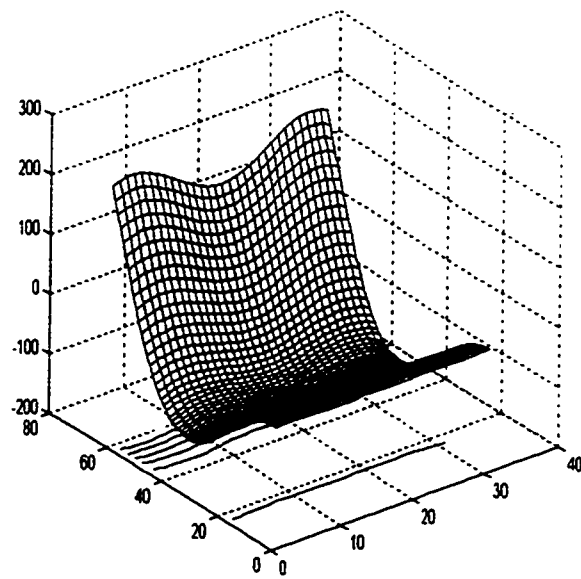
MODE 1



MODE 2

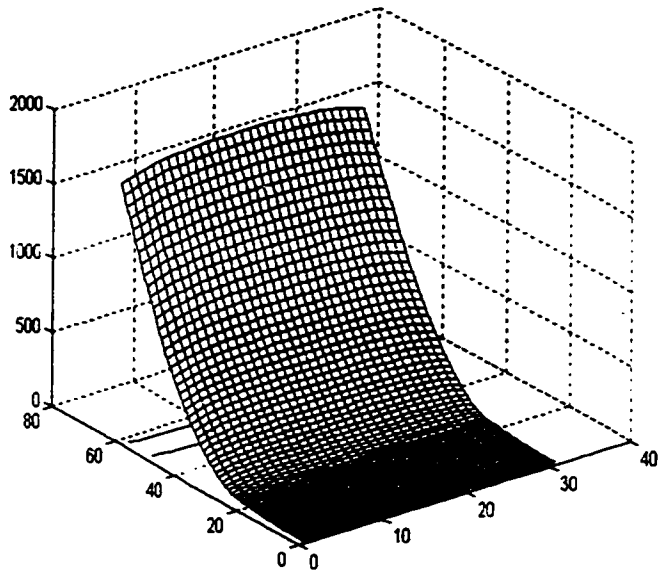


MODE 3

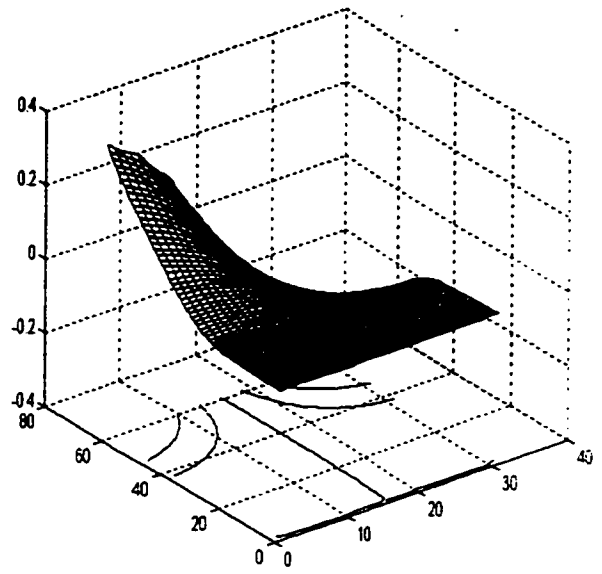


MODE 4

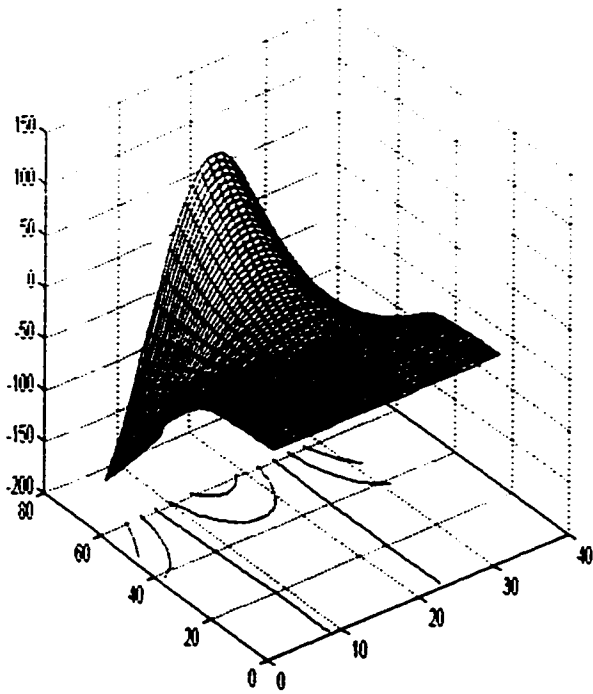
Figure 4.5 : First four mode shapes for Table 4.5.



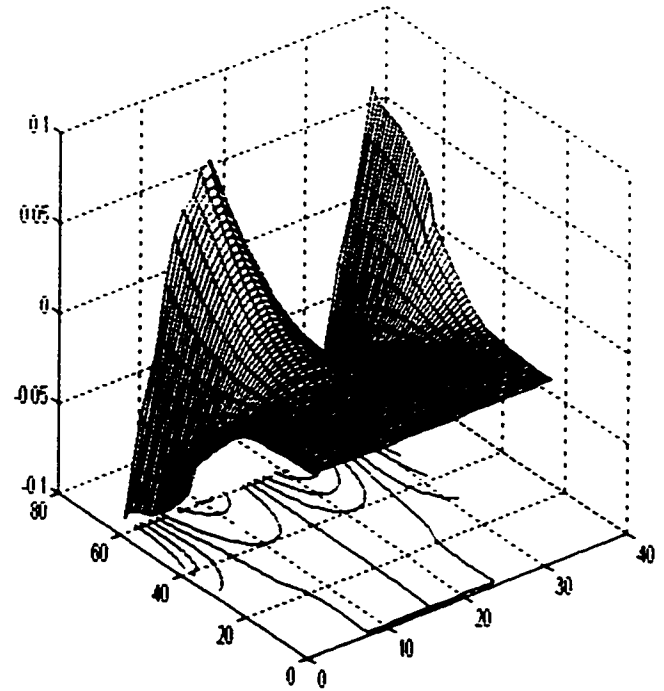
MODE 1



MODE 2

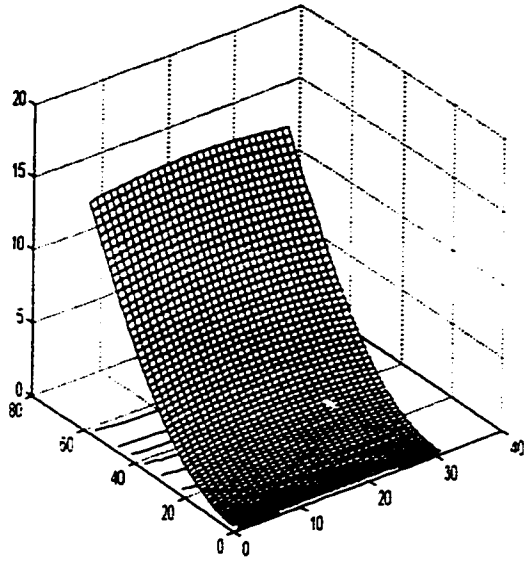


MODE 3

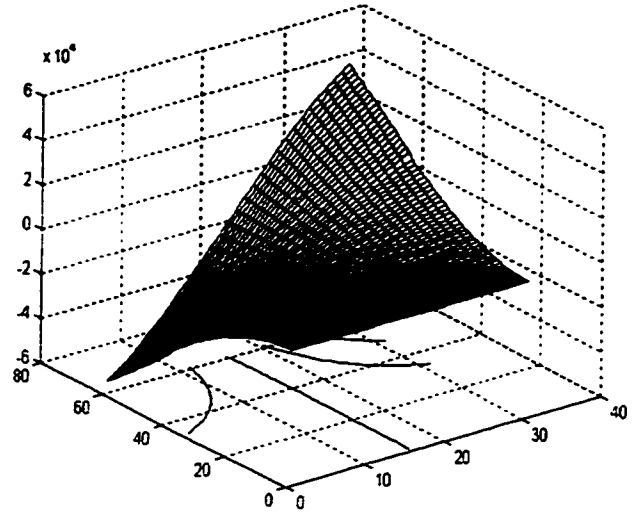


MODE 4

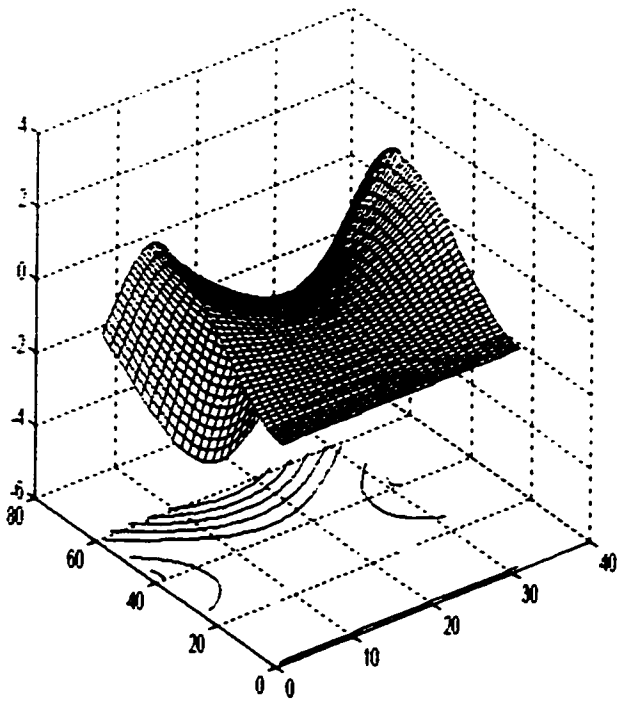
Figure 4.6 : First four mode shapes for Table 4.6.



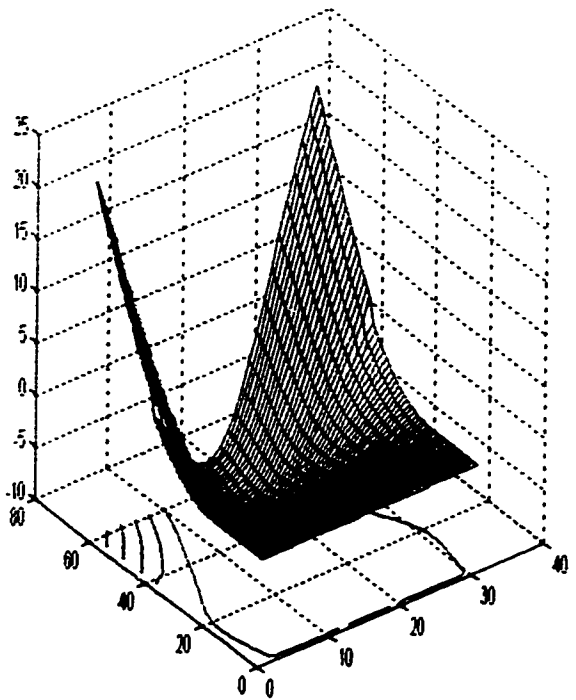
MODE 1



MODE 2

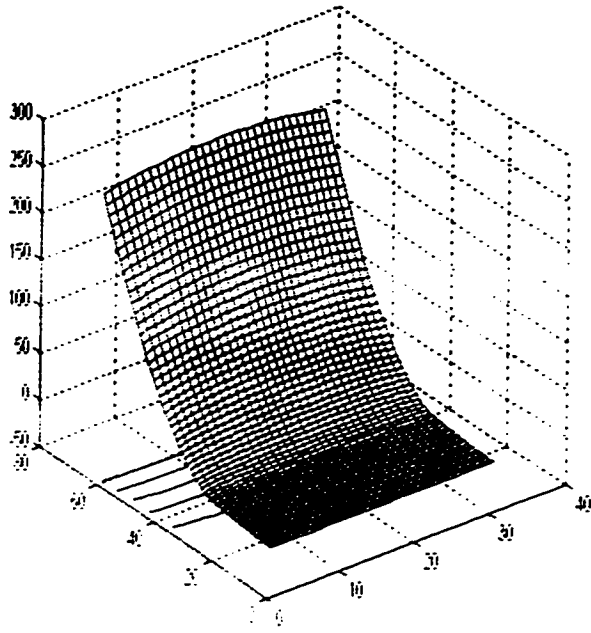


MODE 3

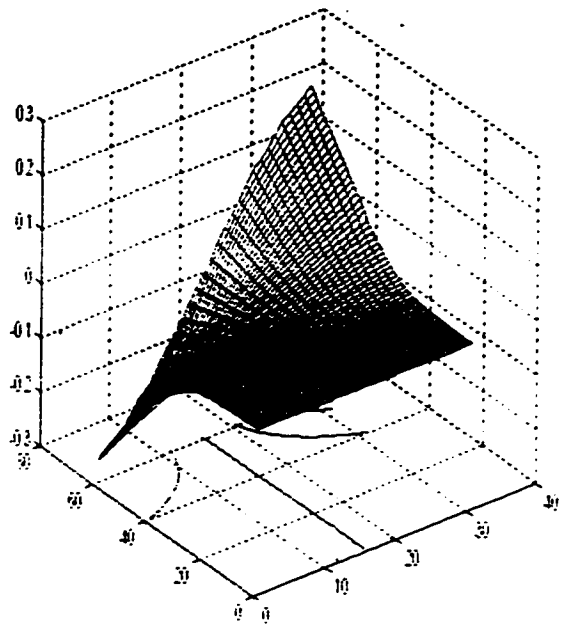


MODE 4

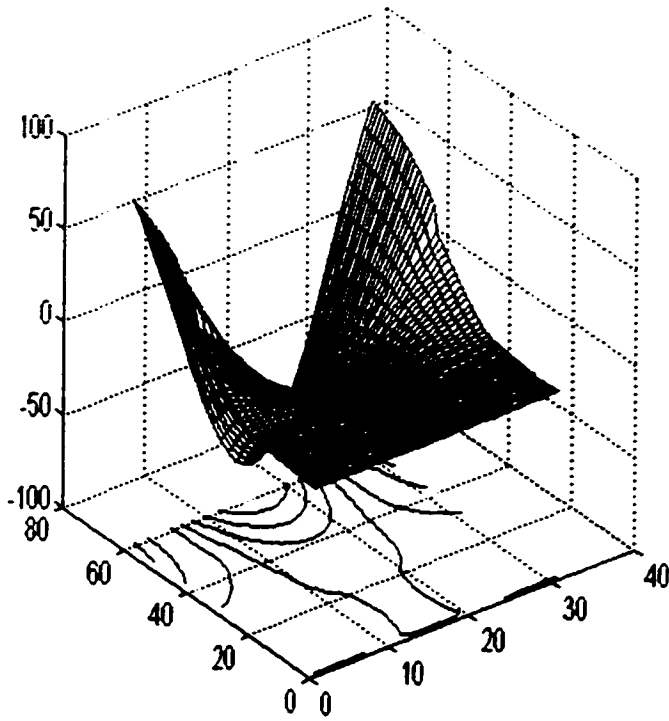
Figure 4.7 : First four mode shapes for Table 4.7.



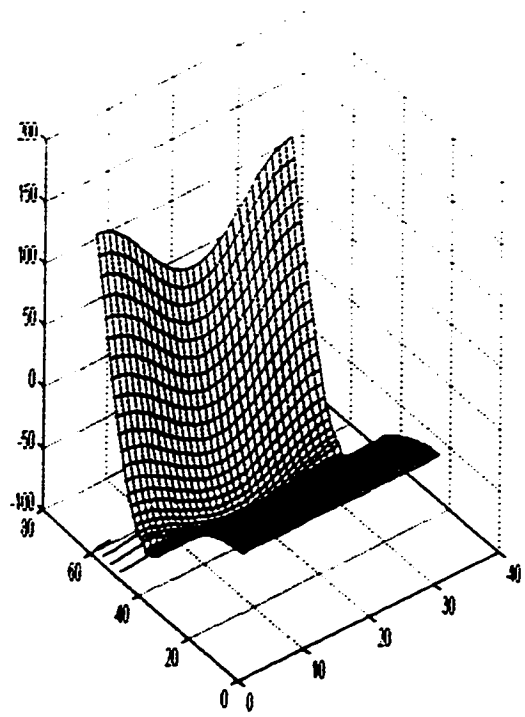
MODE 1



MODE 2

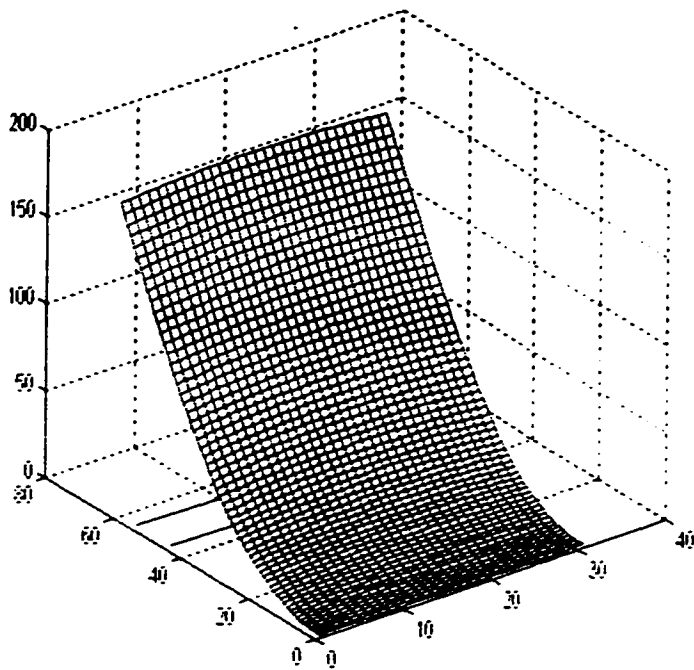


MODE 3

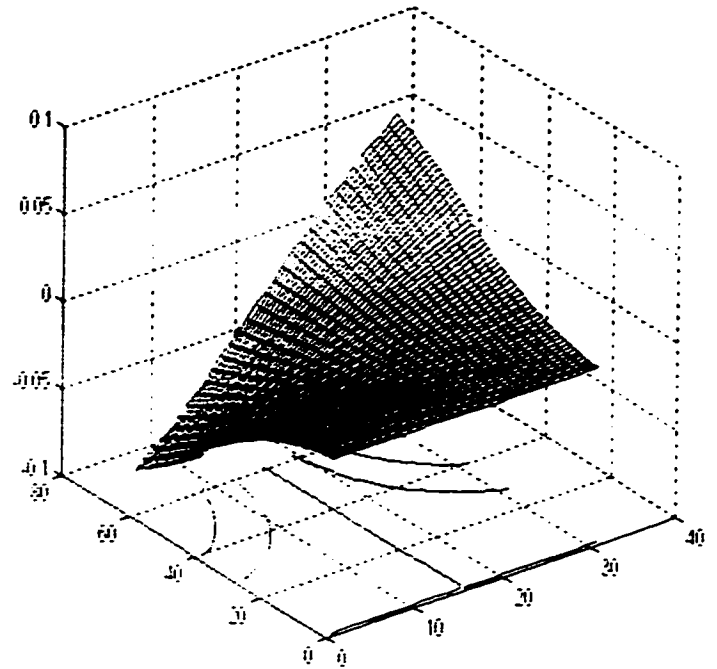


MODE 4

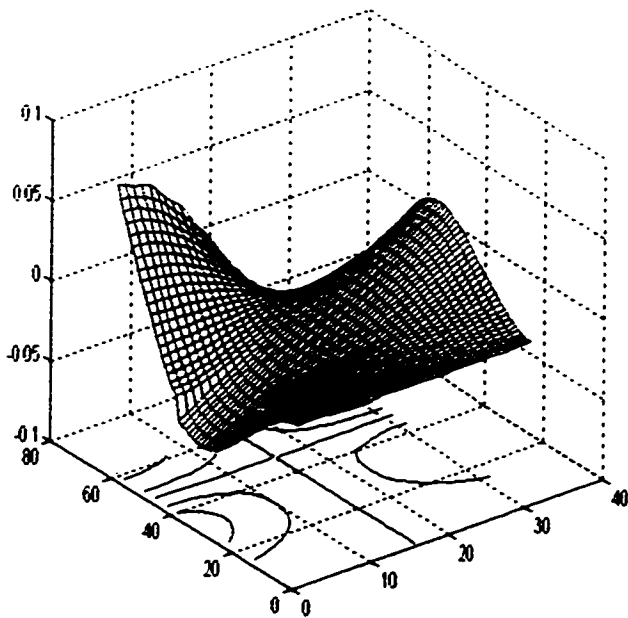
Figure 4.8 : First four mode shapes for Table 4.8.



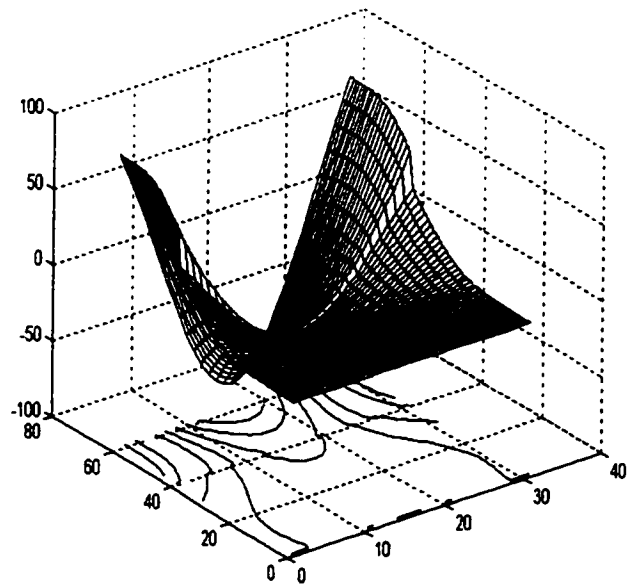
MODE 1



MODE 2

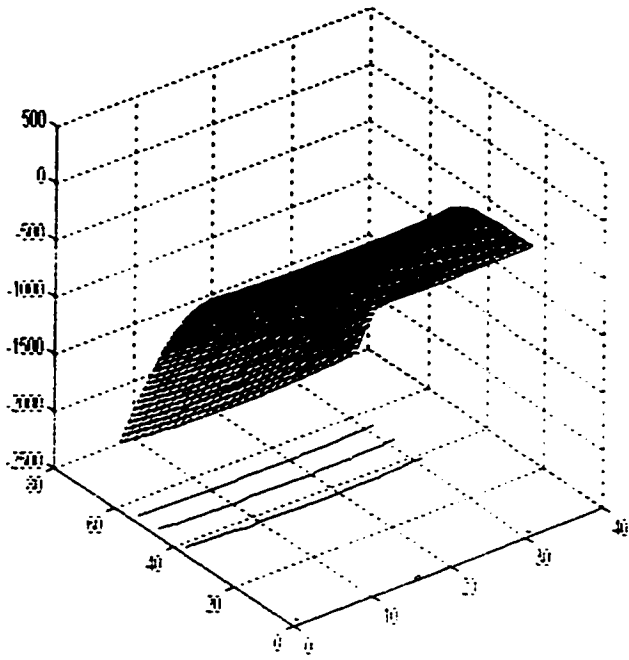


MODE 3

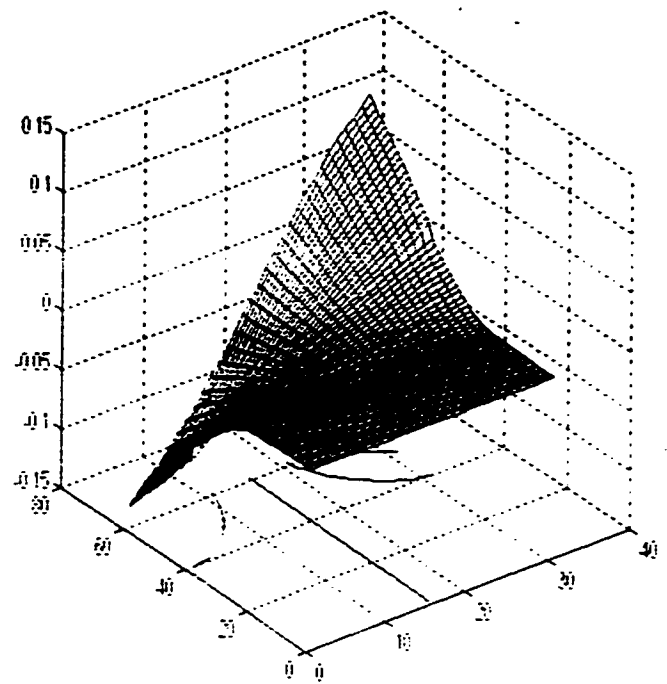


MODE 4

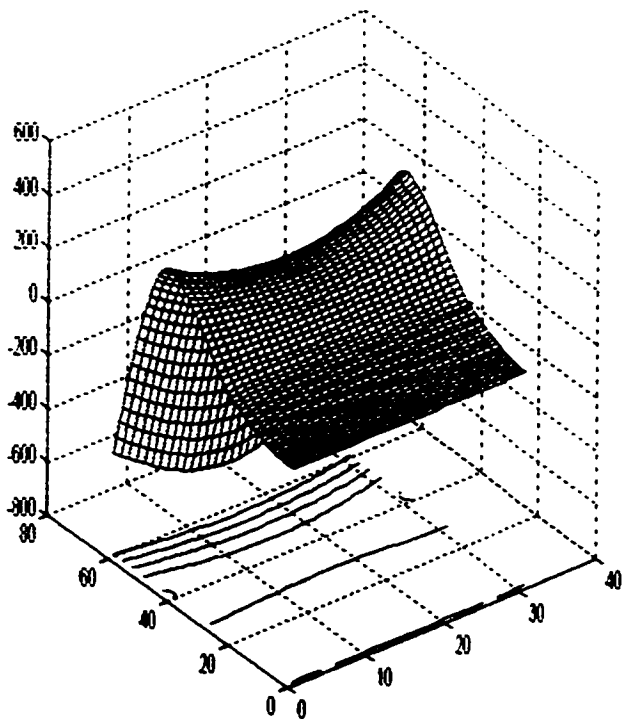
Figure 4.9 : First four mode shapes for Table 4.9.



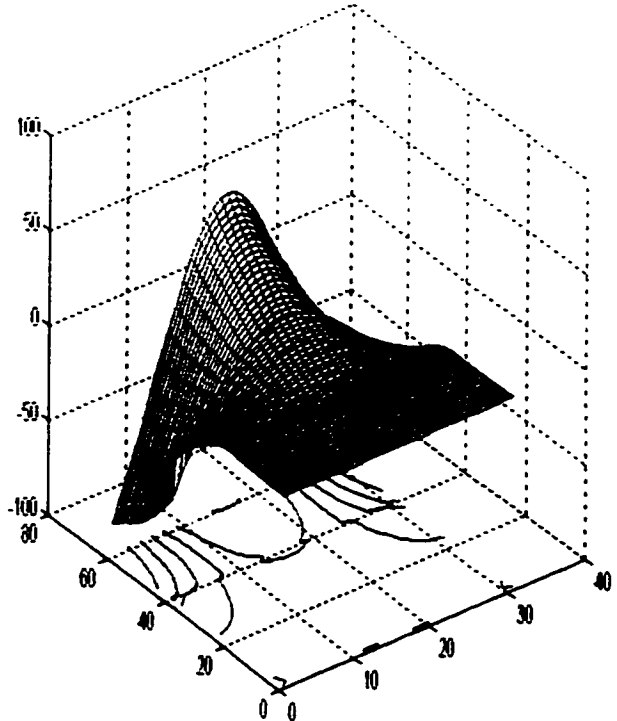
MODE 1



MODE 2

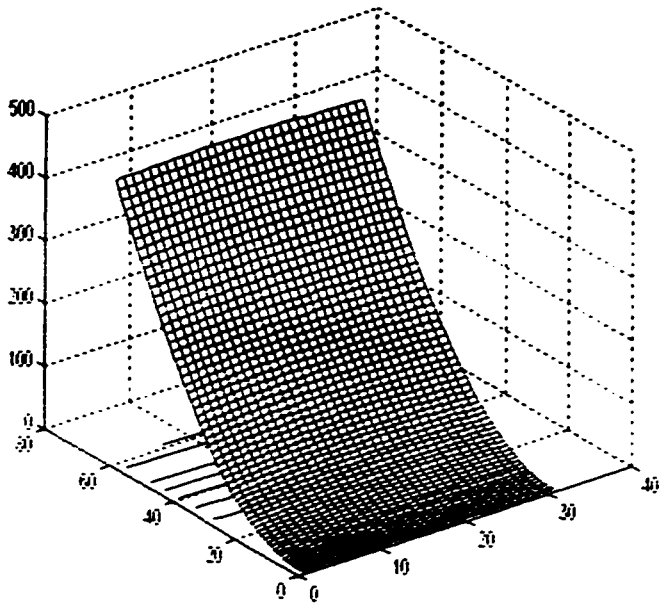


MODE 3

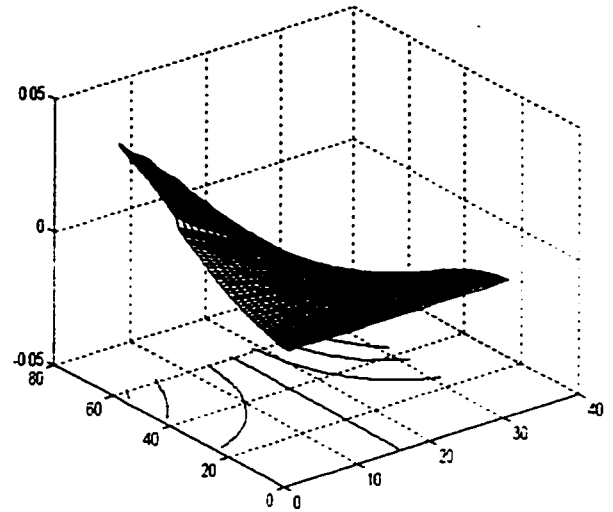


MODE 4

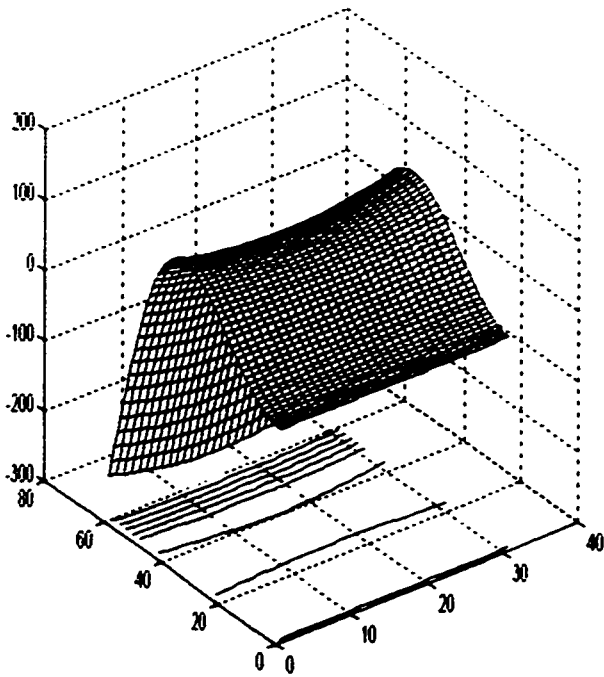
Figure 4.10 : First four mode shapes for Table 4.10.



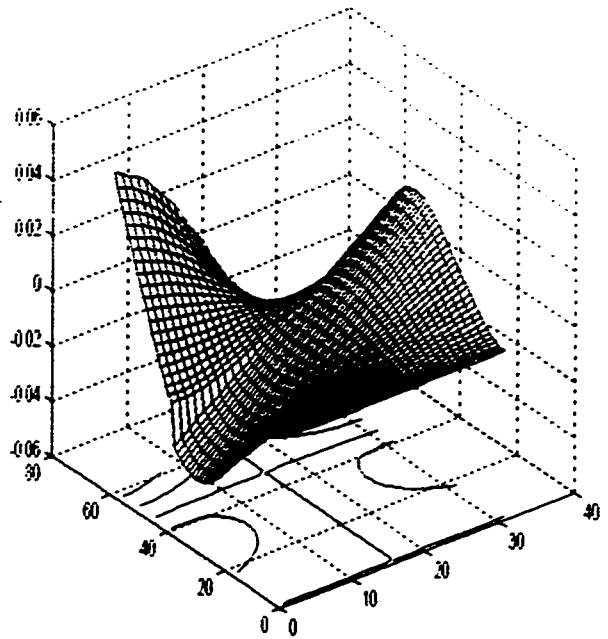
MODE 1



MODE 2

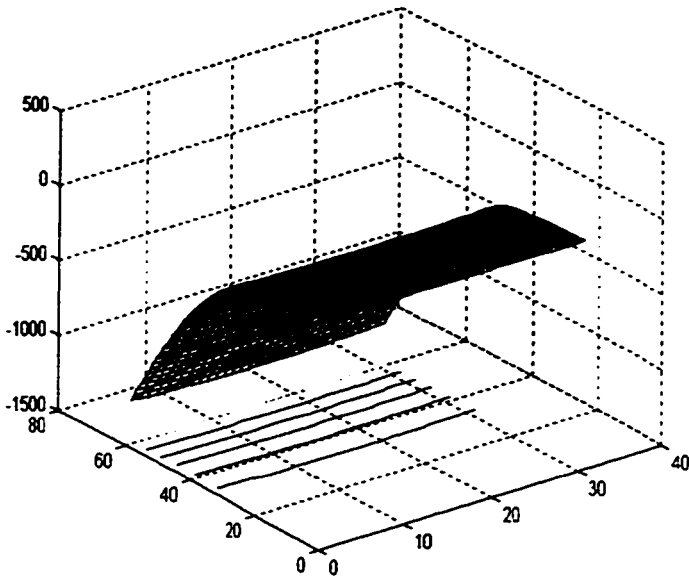


MODE 3

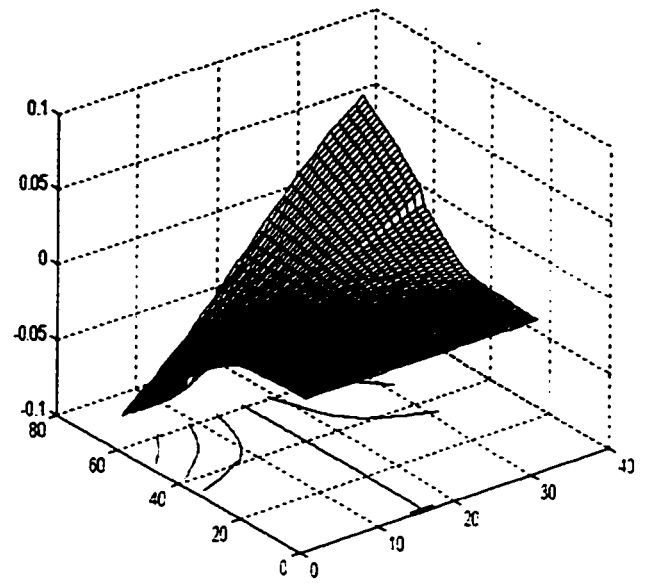


MODE 4

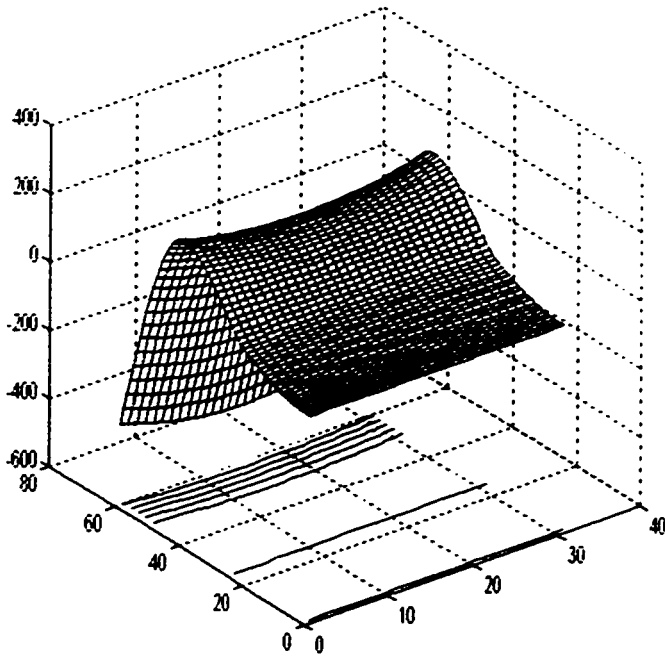
Figure 4.11 : First four mode shapes for Table 4.11.



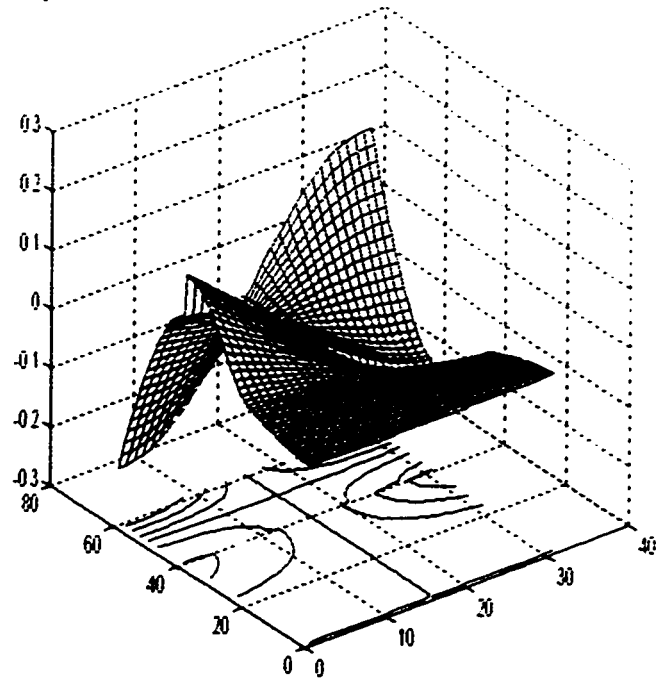
MODE 1



MODE 2

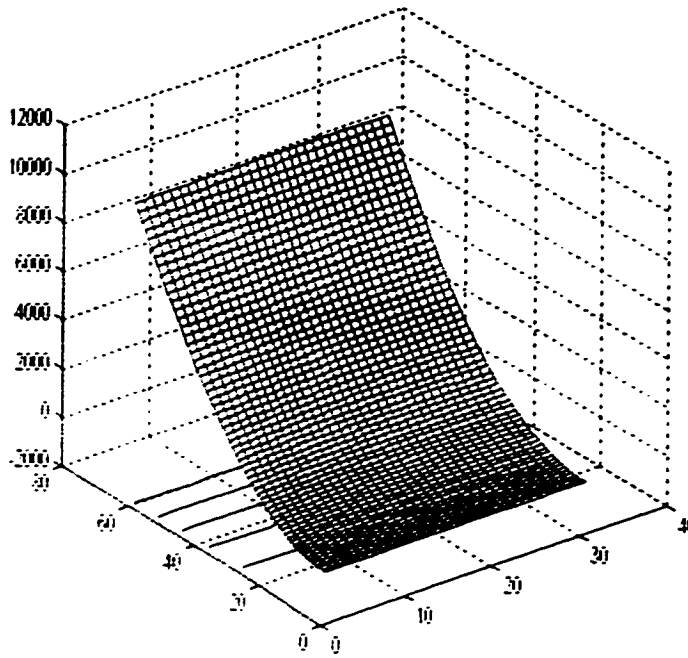


MODE 3

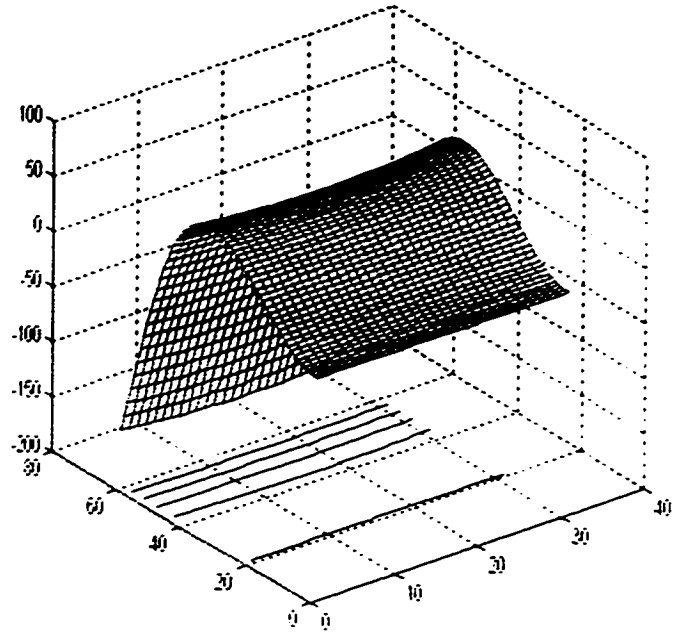


MODE 4

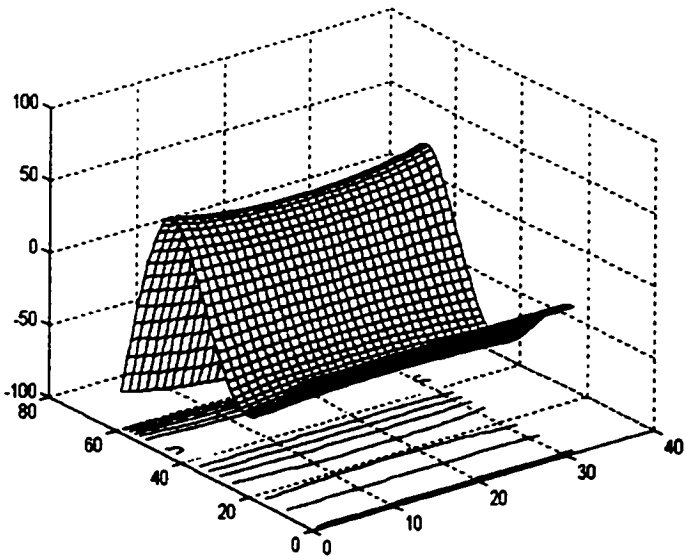
Figure 4.12 : First four mode shapes for Table 4.12.



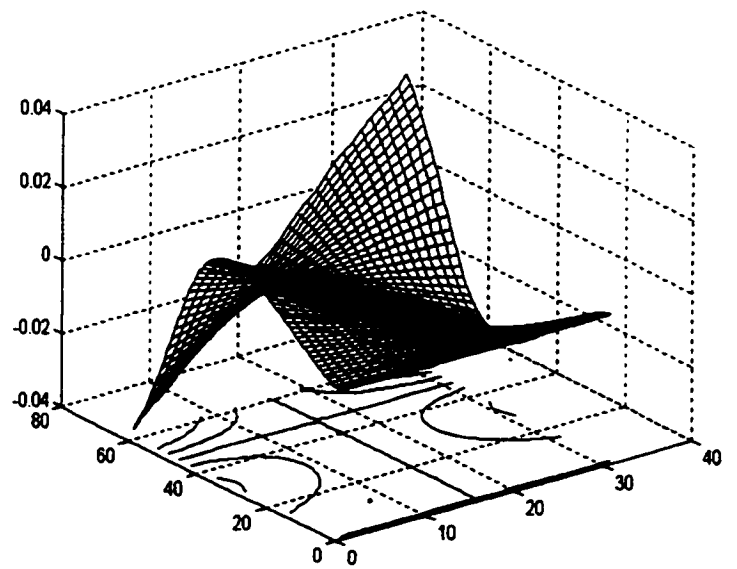
MODE 1



MODE 2

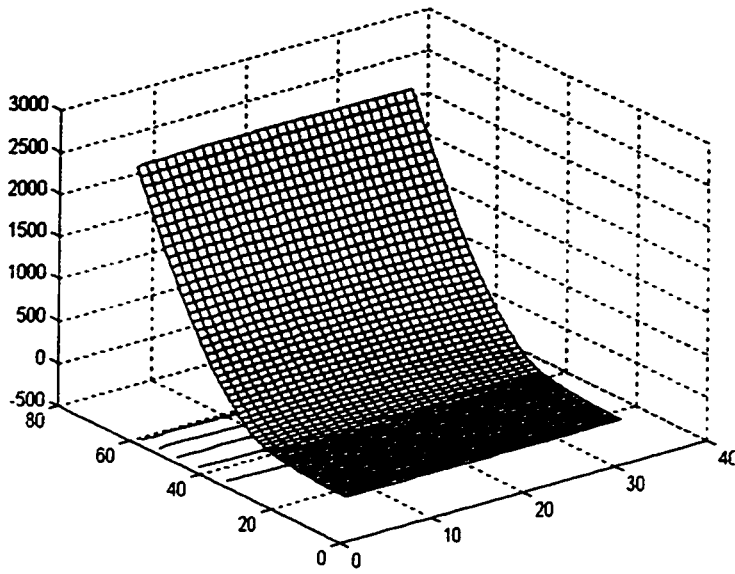


MODE 3

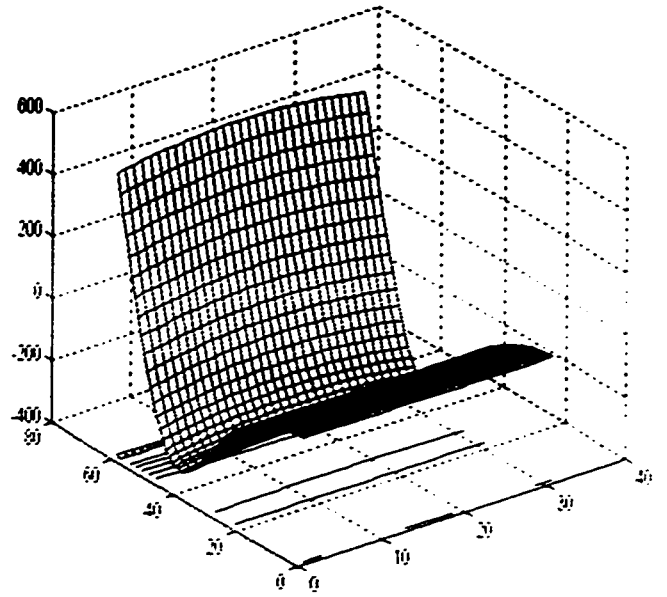


MODE 4

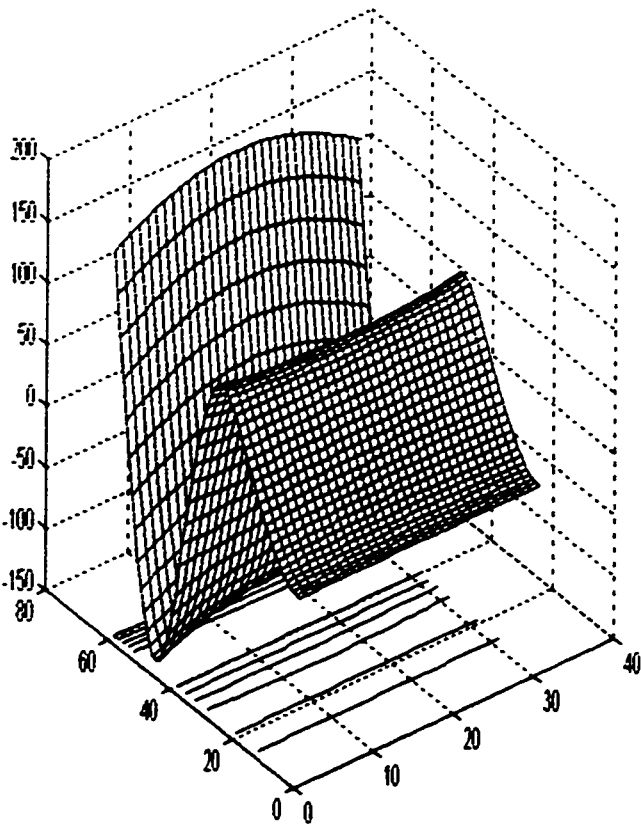
Figure 4.13 : First four mode shapes for Table 4.13.



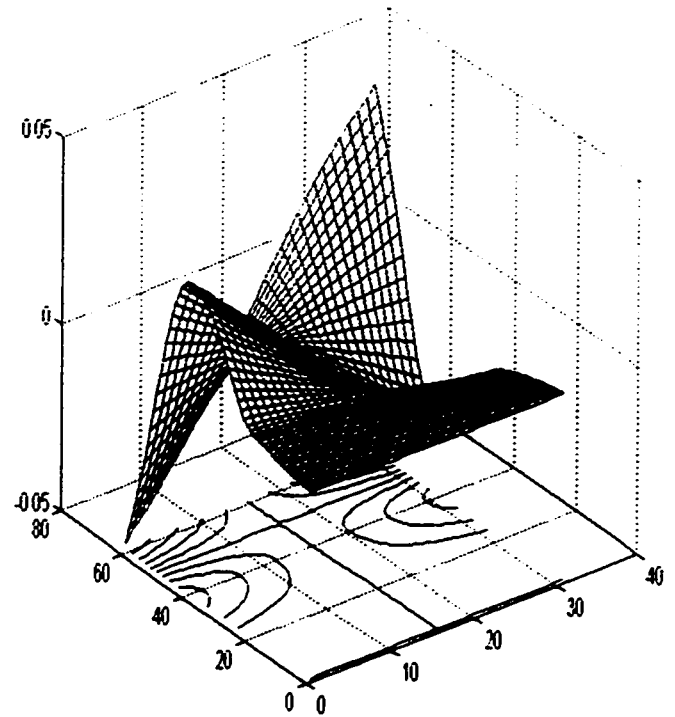
MODE 1



MODE 2

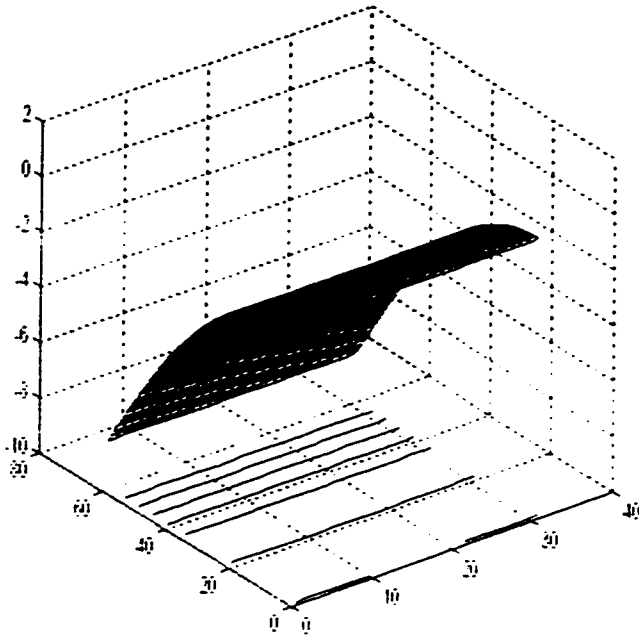


MODE 3

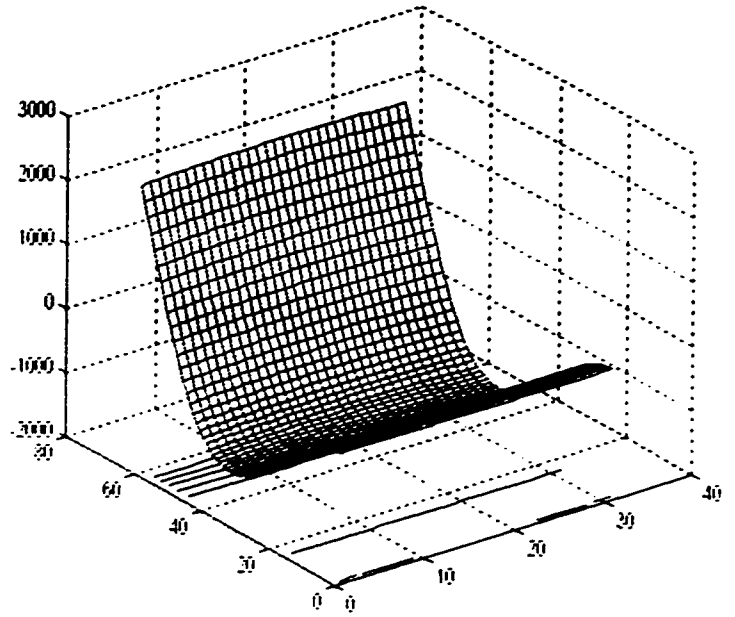


MODE 4

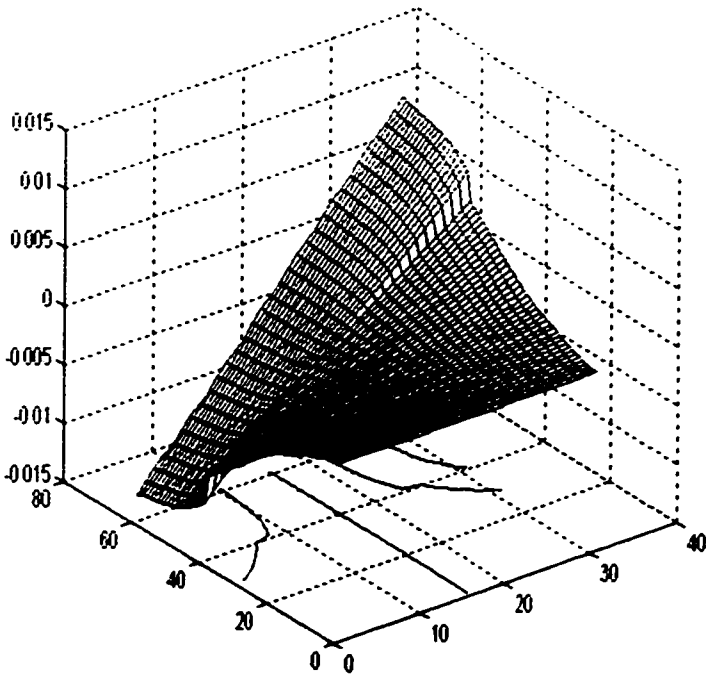
Figure 4.14 : First four mode shapes for Table 4.14.



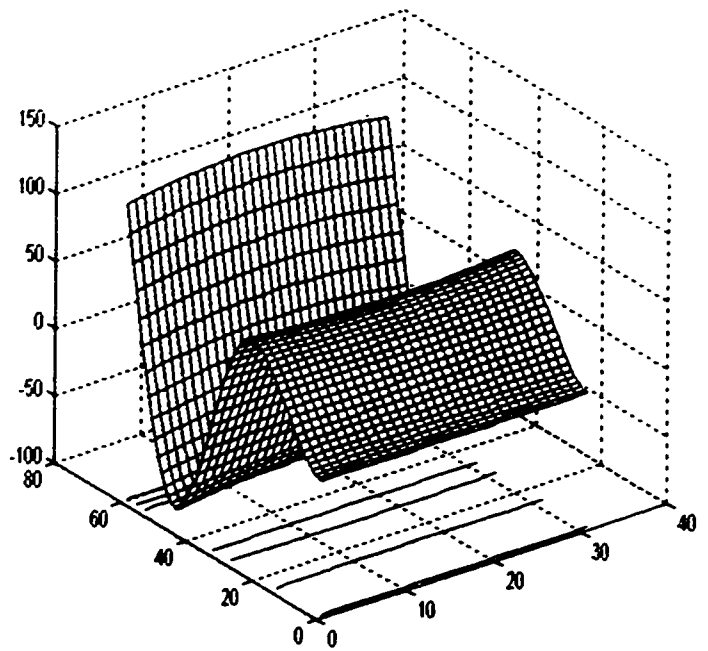
MODE 1



MODE 2

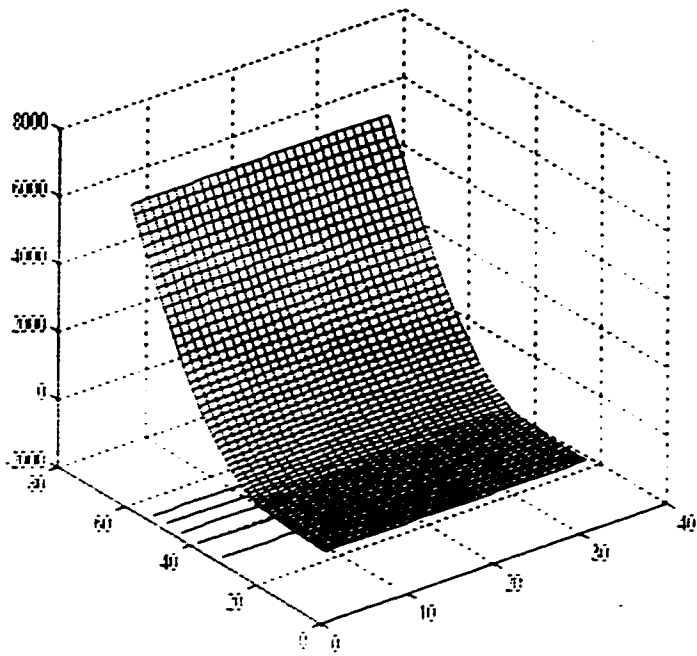


MODE 3

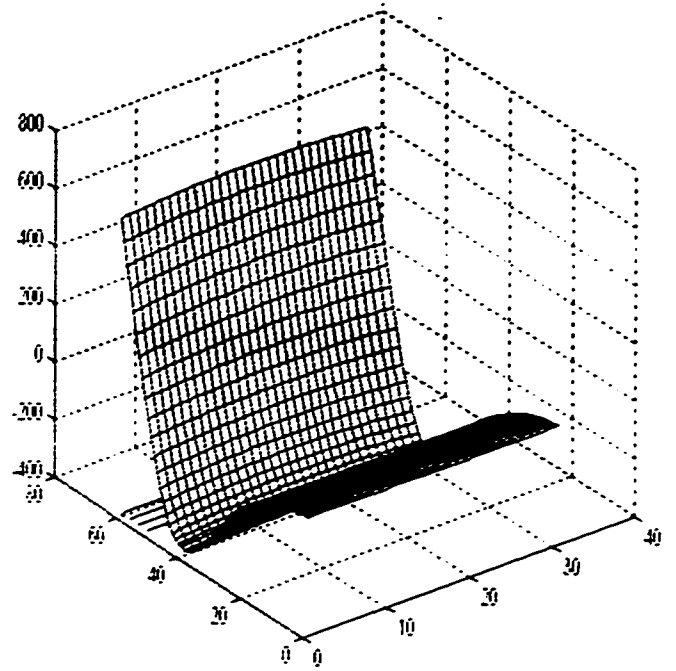


MODE 4

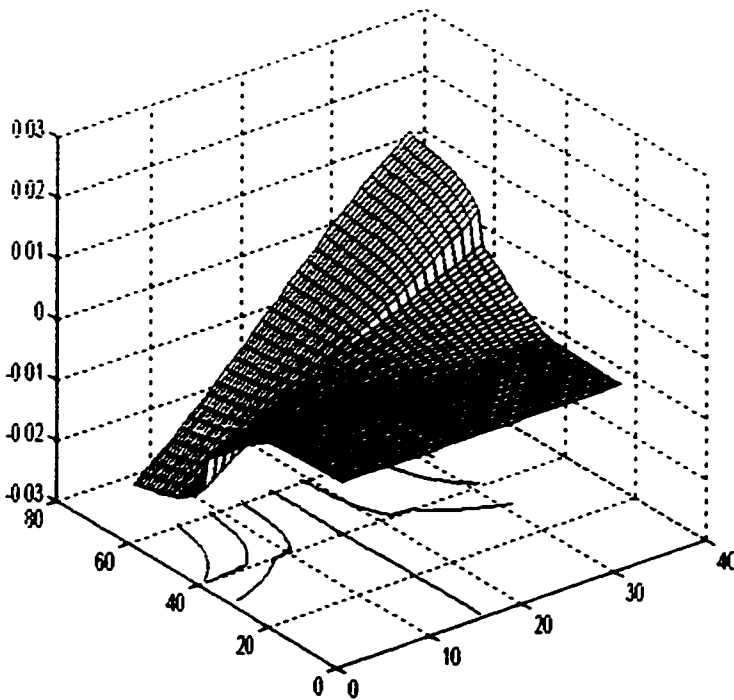
Figure 4.15 : First four mode shapes for Table 4.15.



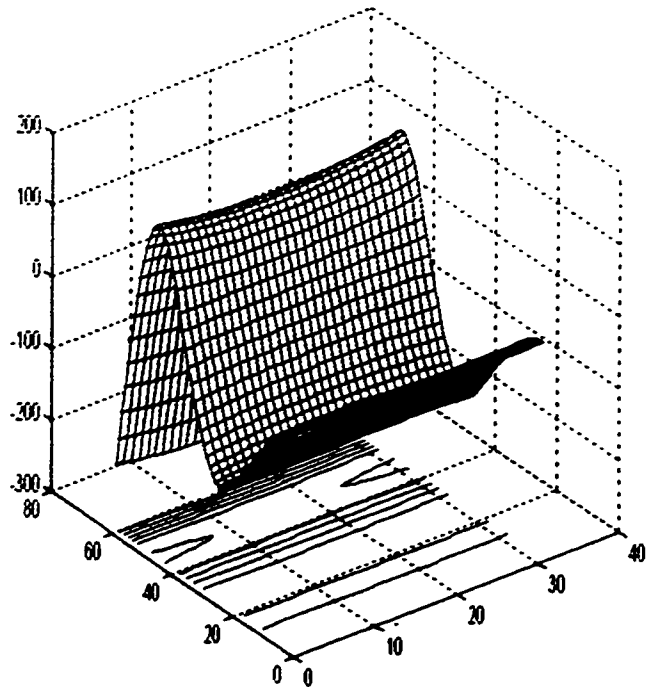
MODE 1



MODE 2

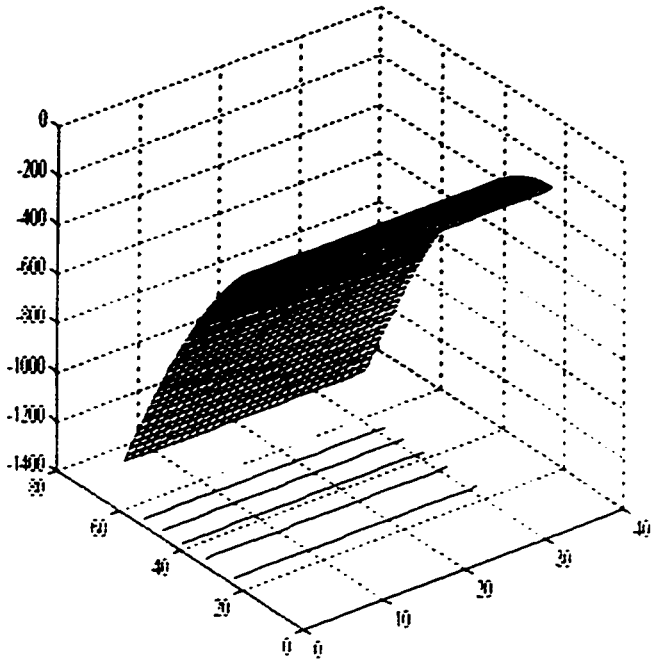


MODE 3

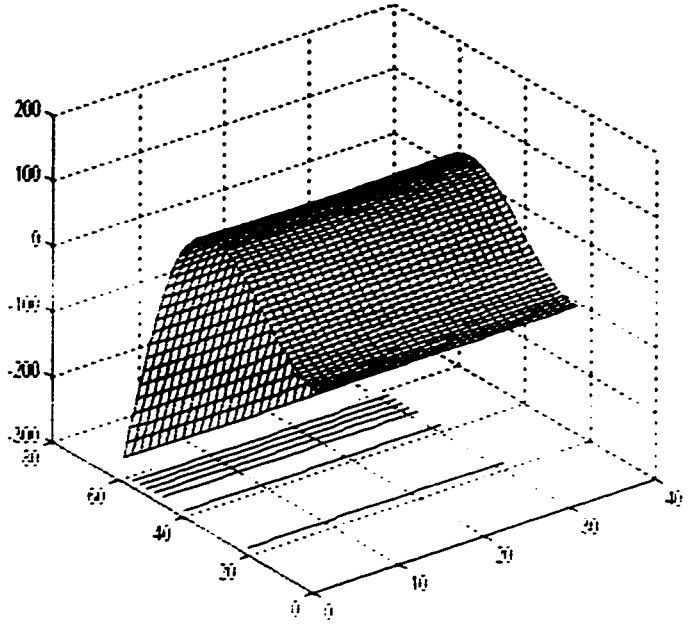


MODE 4

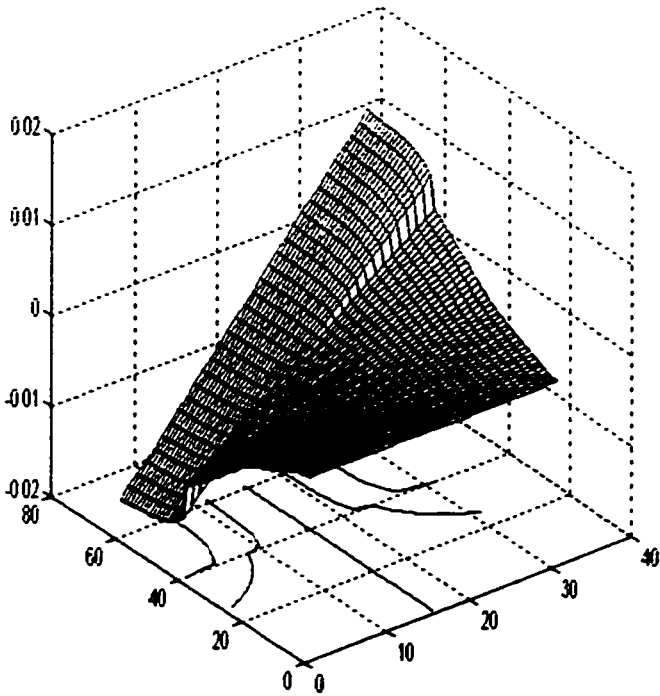
Figure 4.16 : First four mode shapes for Table 4.16.



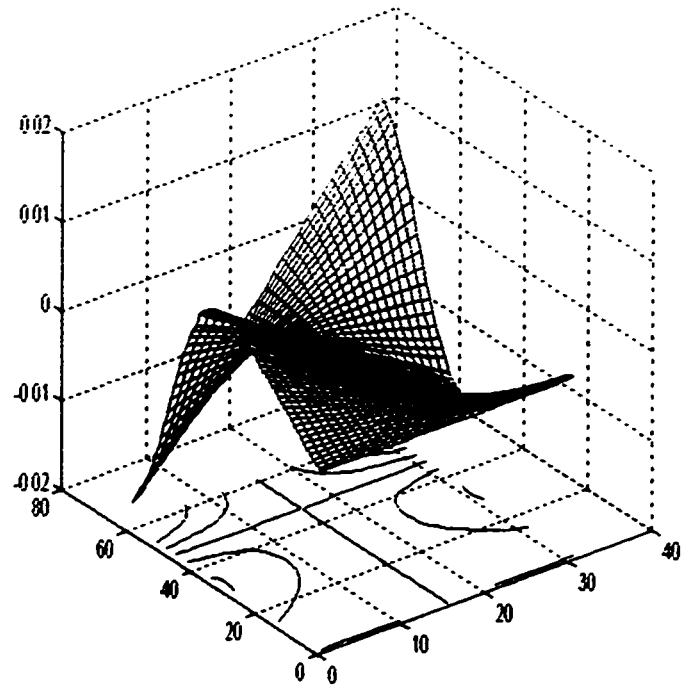
MODE 1



MODE 2

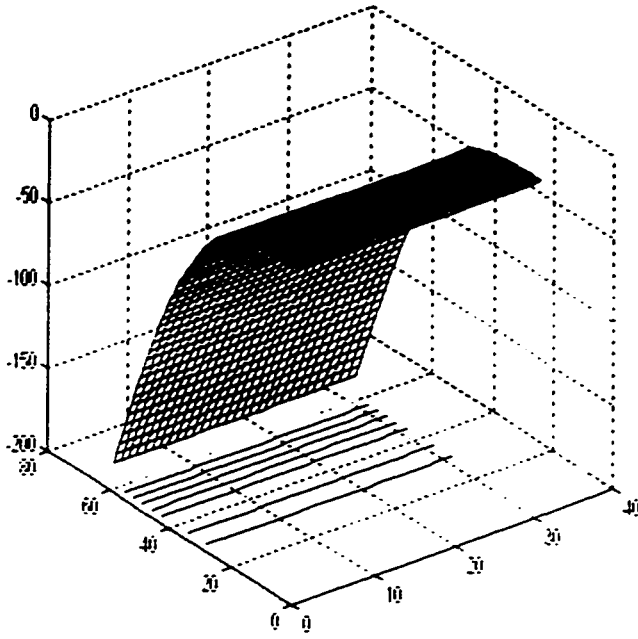


MODE 3

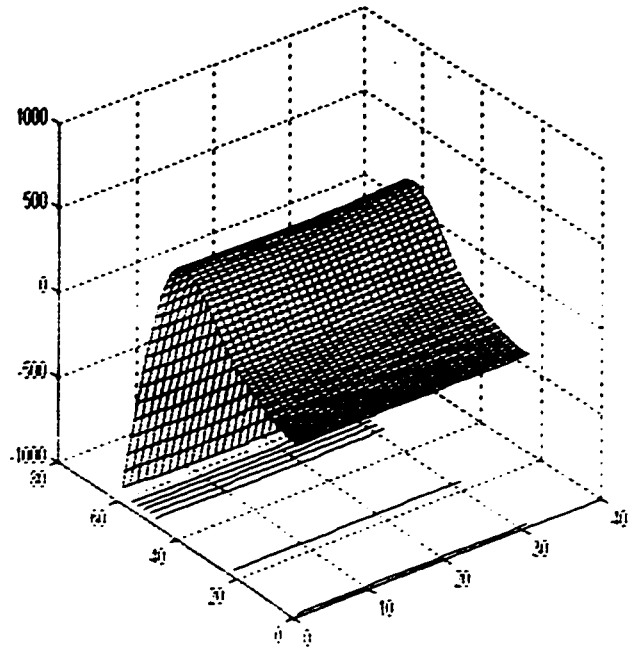


MODE 4

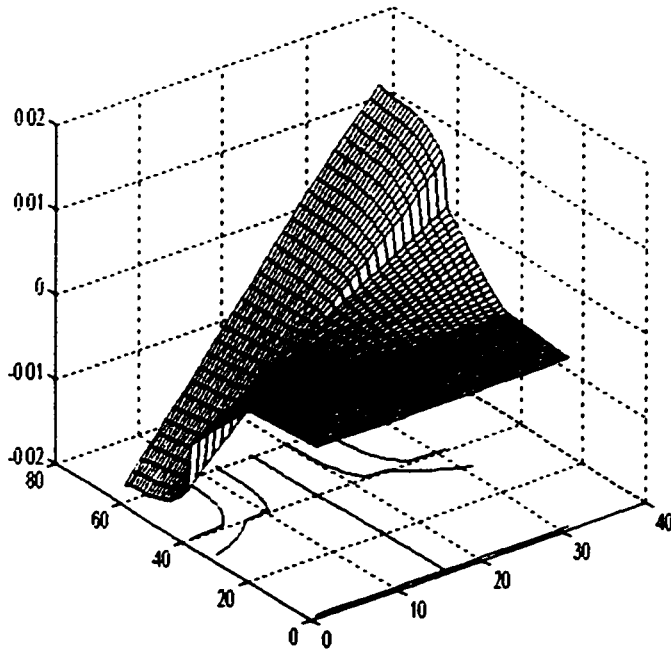
Figure 4.17 : First four mode shapes for Table 4.17.



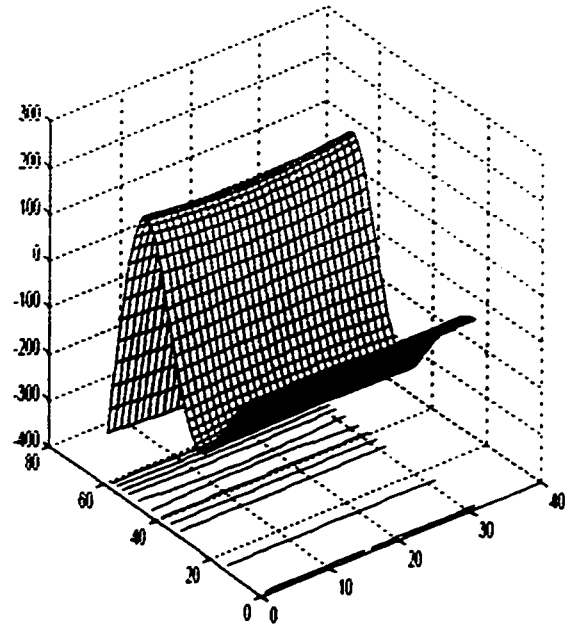
MODE 1



MODE 2

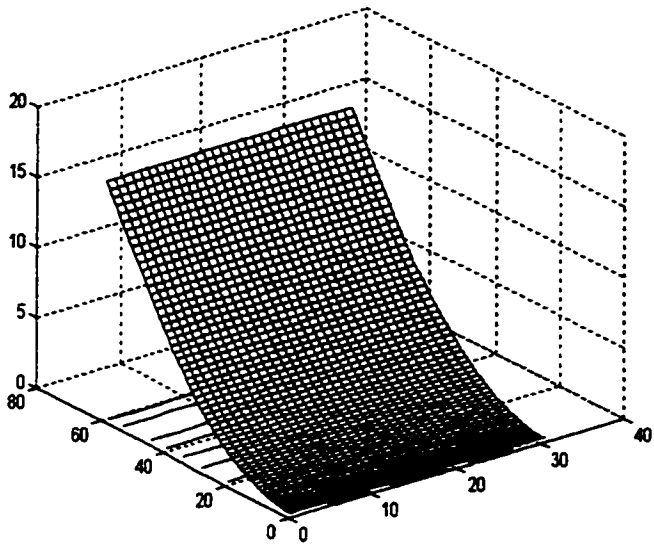


MODE 3

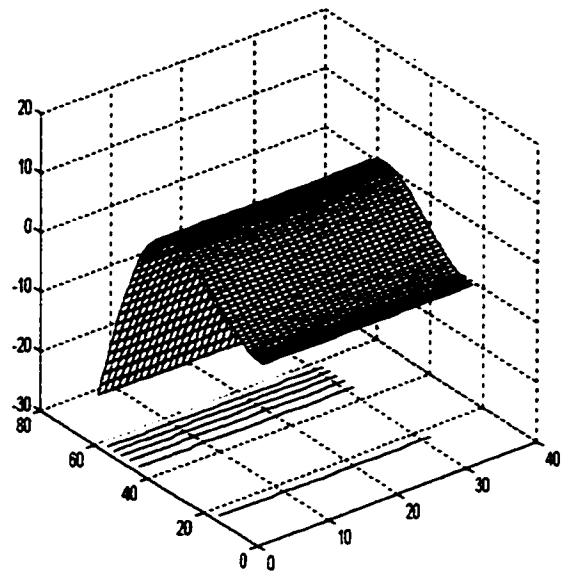


MODE 4

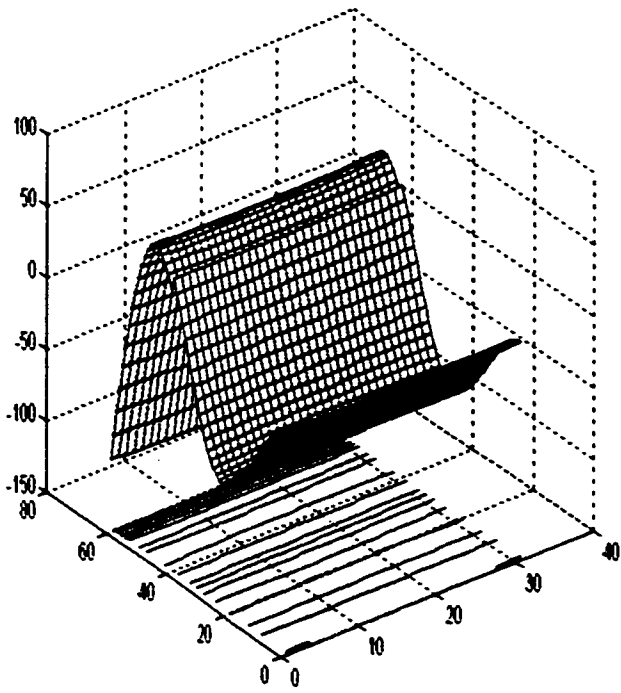
Figure 4.18 : First four mode shapes for Table 4.18.



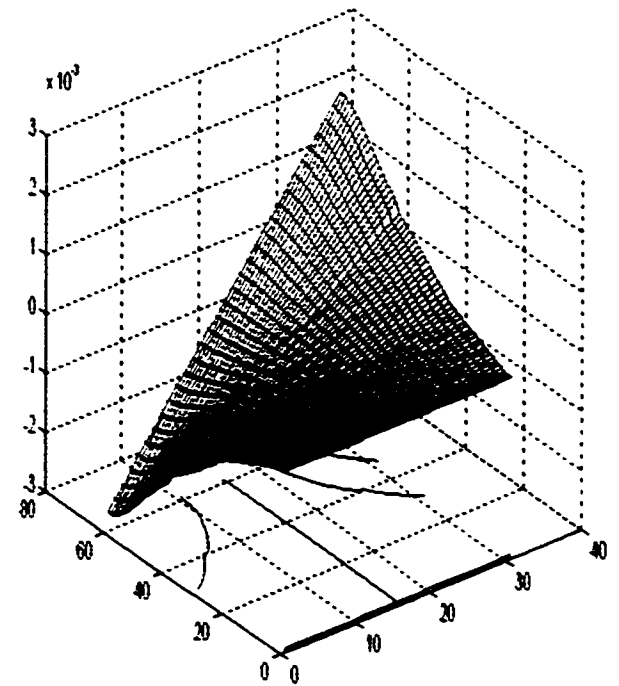
MODE 1



MODE 2

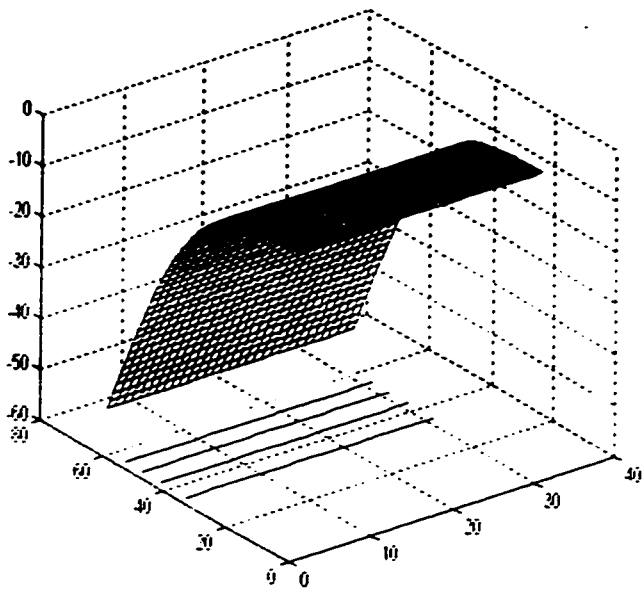


MODE 3

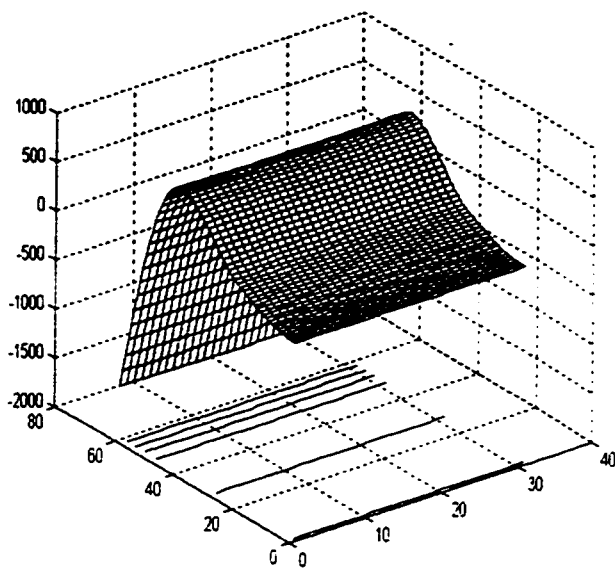


MODE 4

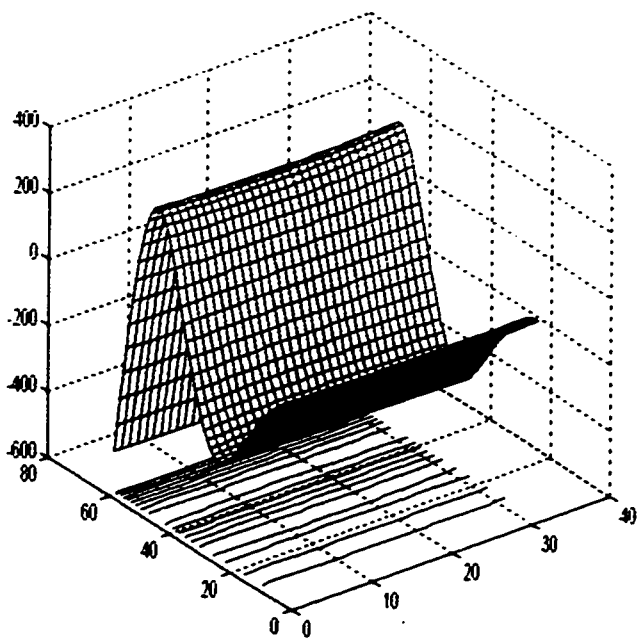
Figure 4.19 : First four mode shapes for Table 4.19.



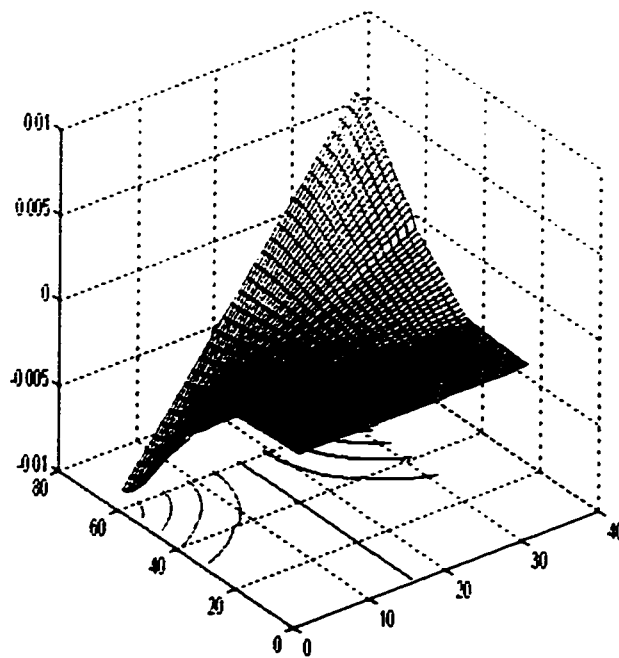
MODE 1



MODE 2



MODE 3



MODE 4

Figure 4.20 : First four mode shapes for Table 4.20.

4.3 Eigenvalues for Plates with Uniform Thickness Throughout

As stated in Chapter 4, the purpose of this section is to provide a partial validation of the analytical approach used in this thesis. For this purpose eigenvalues for uniform thickness plates with aspect ratios equal 2, 1, 1/1.25, 1/3 are compared with previously published uniform plate data. These results are shown in tables 4.21 to 4.24 and are discussed in Chapter 5. In this validation process, each span is assigned a thickness ratio of 1. The model therefore represents a uniform cantilever plate. The results of this approach are then compared to the already published values by Gorman[1]. This process allows the reader to compare results computed here with the previously known values in order to determine the accuracy of the analytical approach used in this thesis. It is noted that the values published by Gorman[1] correspond to eigenvalues λ^2_a with respect to edge length "a". Since the eigenvalues published in this thesis λ^2_b correspond to edge length "b" it is necessary to multiply those values by $1/\phi^2$ for comparison purposes.

Table 4.21. Eigenvalues for thickness ratios 1,1,1 & plate overall aspect ratio $\phi=1/3$.

Span1 Aspect Ratio $\phi_1=1$	Span2 Aspect Ratio $\phi_2=1$	Span3 Aspect Ratio $\phi_3=1$	Eigenvalues with respect to Edge Length "a"		Previously Published Eigenvalues- Gorman[1]
Mode	Computed Eigenvalue λ_b^2		Mode	Computed Eigenvalues λ_a^2	Gorman[1] Eigenvalues
1	0.377		1	3.393	3.395
2	2.296		2	20.66	20.68
3	2.355		3	21.19	21.24
4	6.621		4	59.59	59.60
5	7.224		5	65.02	65.07
6	13.03		6	117.3	117.3
7	13.10		7	117.9	118.0
8	20.39		8	183.5	183.7
9	21.32		9	191.9	191.9
10	22.99		10	206.9	NA
11	26.36		11	237.2	NA
12	29.45		12	265.1	265.2

Table 4.22. Eigenvalues for thickness ratios 1,1,1 & plate overall aspect ratio $\phi=1$.

Span1 Aspect Ratio $\phi_1=3$	Span2 Aspect Ratio $\phi_2=3$	Span3 Aspect Ratio $\phi_3=3$	Eigenvalues with respect to Edge Length "a"		Previously Published Eigenvalues- Gorman[1]
Mode	Computed Eigenvalue λ_b^2		Mode	Computed Eigenvalues λ_a^2	Gorman[1] Eigenvalues
1	3.459		1	3.459	3.459
2	8.339		2	8.339	8.356
3	21.08		3	21.08	21.09
4	27.04		4	27.04	27.06
5	30.53		5	30.53	30.55
6	53.44		6	53.44	53.53
7	61.11		7	61.11	61.12
8	63.57		8	63.57	63.62
9	70.63		9	70.63	70.64
10	92.03		10	92.03	92.21

Table 4.23.a. Eigenvalues for thickness ratios 1,1,1 & plate overall aspect ratio $\phi=2$.

Span1 Aspect Ratio $\phi_1=6$	Span2 Aspect Ratio $\phi_2=6$	Span3 Aspect Ratio $\phi_3=6$	Eigenvalues with respect to Edge Length "a"	Previously Published Eigenvalues- Gorman[1]
Mode	Computed Eigenvalue λ_b^2		Mode	Computed Eigenvalues λ_a^2 Gorman[1] Eigenvalues
1	13.94		1	3.486 3.487
2	21.07		2	5.268 5.278
3	39.98		3	9.996 10.03
4	75.11		4	18.78 18.84

Table 4.23.b. Eigenvalues for thickness ratios 1,1,1 & plate overall aspect ratio $\phi=1.25$

Span1 Aspect Ratio $\phi_1=15/4$	Span2 Aspect Ratio $\phi_2=15/4$	Span3 Aspect Ratio $\phi_3=15/4$	Eigenvalues with respect to Edge Length "a"	Previously Published Eigenvalues- Gorman[1]
Mode	Computed Eigenvalue λ_b^2		Mode	Computed Eigenvalues λ_a^2 Gorman[1] Eigenvalues
1	5.421		1	3.469 3.470
2	11.09		2	7.101 7.115
3	28.35		3	18.14 18.18
4	34.69		4	22.20 22.21

Table 4.24. Eigenvalues for thickness ratios 1,1,1 & plate overall aspect ratio $\phi=1/1.25$

Span1 Aspect Ratio $\phi_1=12/5$	Span2 Aspect Ratio $\phi_2=12/5$	Span3 Aspect Ratio $\phi_3=12/5$	Eigenvalues with respect to Edge Length "a"	Previously Published Eigenvalues- Gorman[1]
Mode	Computed Eigenvalue λ_b^2		Mode	Computed Eigenvalues λ_a^2 Gorman[1] Eigenvalues
1	2.206		1	3.447 3.448
2	6.322		2	9.878 9.897
3	13.63		3	21.30 21.31
4	22.08		4	34.50 34.53

Chapter 5

DISCUSSION OF RESULTS

Considering the values tabulated in section 4.1, the eigenvalues decreased with decreasing overall plate aspect ratio. These eigenvalues are more concentrated for lower aspect ratios (meaning that the values for different modes are much closer together) and are more spread out for higher plate aspect ratios. This is a feature of the multi span cantilever plate. Symmetric and Anti-symmetric modes are established on studying mode shape figures. For example, the first, third and fourth mode shapes represented in figure 4.8 are symmetric modes. The second mode in the same figure represents an anti-symmetric mode. Mode shapes for the first four modes represented in tables 4.1 to 4.20 were shown in figures 4.1 to 4.20.

Section 4.1 presented the effect of a varying thickness ratio decreasing as one moves along the plate. From these results, it was concluded that the eigenvalues for a 3 span cantilever plate decrease significantly with a decrease in span thickness ratios. Section 4.3 presented other computed eigenvalues for plates with uniform thickness throughout. Results of tables 4.21,4.22,4.23,4.24 pertain to rectangular cantilever plates with equal thicknesses and equal aspect ratios per span. This creates uniform rectangular plates for which free vibration frequencies were tabulated by Gorman[1]. The computed values obtained using the analytical approach of this thesis converged to the previously published values provided by Gorman.

It is known that convergence to more accurate eigenvalues can be obtained if desired. A convergence test was performed for mode 2 of the square plate (Table 4.22)

and mode 4 for the plate of aspect ratio=2 (Table 4.23) by increasing the number of K terms used. Test results were as follows:

Mode 2, Plate overall aspect ratio =1	Correct Eigenvalue = 8.356			
K terms used	K=15	K=17	K=19	K=20
Computed Eigenvalue	8.339	8.343	8.347	8.348
Mode 4, Plate overall aspect ratio =2	Correct Eigenvalue = 18.84			
K terms used	K=15	K=17	K=19	K=20
Computed Eigenvalue	18.77	18.79	18.80	18.81

The calculated eigenvalues shown above for the plate of aspect ratio 2 have been multiplied by the factor $1/\phi^2$ as previously stated.

The superposition method provides an analytical type solution that satisfies the governing differential equation exactly. It also satisfies the boundary conditions of the plate with accuracy as required by selecting a sufficiently high value for K, the number of terms utilized in the building block solutions. It provides accurate analytical results that can be used for validation purposes when employing numerical methods such as the finite element method.

Finally, this thesis provides the basis for deriving solutions for cantilever plates with any number of spans and varying properties per span.

REFERENCES

- [1] Gorman, D.J., *Free Vibration Analysis Of Rectangular Plates*, Elsevier North Holland, Inc., New York, 1982.
- [2] Timoshenko, S. and Woinowsky- Krieger , *Theory Of Plates and Shells*, McGraw-Hill, Toronto, 1959.
- [3] Gorman, D.J., *Vibration Analysis Of Plates By the Superposition Method*, World Scientific Publishing Co. Pte. Ltd., 1999.
- [4] *Dictionary Of Scientific Biography*, New York, 1990
- [5] Leissa, A.W., *Vibration Of Plates*, National Aeronautics And Space Administration, 1969.
- [6] Page, R and Didday, R, *Fortran 77 for Humans*, West Publishing Co., 1980.
- [7] Marchand, P., *Graphics and GUIs with Matlab*, CRC Press, New York, 1996.
- [8] Kreyszig, E., *Advanced Engineering Mathematics*, John Wiley & Sons, 1988.
- [9] Chopra, A.K., *Dynamics Of Structures – Theory and Applications to Earthquake Engineering*, Prentice Hall, 1993.

APPENDIX 1
Eigenvalue Results for the Four Span
Cantilever Plate

Table 4.25. Eigenvalues for Thickness Ratios 1, 3/8, 1/4, 1/8 & Plate Overall Aspect Ratio $\phi=3$

Span1 Aspect Ratio $\phi_1=12$	Span2 Aspect Ratio $\phi_2=12$	Span3 Aspect Ratio $\phi_3=12$	Span4 Aspect Ratio $\phi_4=12$
Thickness Ratio			
$h_1/h_1 = 1$	$h_2/h_1 = 3/8$	$h_3/h_1 = 1/4$	$h_3/h_1 = 1/8$
		Mode	Eigenvalue λ_b^2
		1	22.21
		2	25.89
		3	30.32
		4	36.26
		5	44.74
		6	55.55
		7	68.84
		8	79.27
		9	79.73
		10	84.68

Table 4.26. Eigenvalues for Thickness Ratios 1, 3/8, 1/4, 1/8 & Plate Overall Aspect Ratio $\phi=2$

Span1 Aspect Ratio $\phi_1=8$	Span2 Aspect Ratio $\phi_2=8$	Span3 Aspect Ratio $\phi_3=8$	Span4 Aspect Ratio $\phi_4=8$
Thickness Ratio			
$h_1/h_1 = 1$	$h_2/h_1 = 3/8$	$h_3/h_1 = 1/4$	$h_3/h_1 = 1/8$
		Mode	Eigenvalue λ_b^2
		1	11.49
		2	12.55
		3	16.07
		4	21.96
		5	25.46
		6	27.83
		7	34.99
		8	36.23
		9	37.32
		10	41.94

Table 4.27. Eigenvalues for Thickness Ratios 1, 3/8, 1/4, 1/8 & Plate Overall Aspect Ratio $\phi=1.5$

Span1 Aspect Ratio $\phi_1=6$	Span2 Aspect Ratio $\phi_2=6$	Span3 Aspect Ratio $\phi_3=6$	Span4 Aspect Ratio $\phi_4=6$
Thickness Ratio			
$h_1/h_1 = 1$	$h_2/h_1 = 3/8$	$h_3/h_1 = 1/4$	$h_3/h_1 = 1/8$
		Mode	Eigenvalue λ_b^2
		1	6.440
		2	7.553
		3	11.00
		4	14.80
		5	19.74
		6	21.34
		7	24.40
		8	26.72
		9	33.99
		10	35.95

Table 4.28. Eigenvalues for Thickness Ratios 1, 3/8, 1/4, 1/8 & Plate Overall Aspect Ratio $\phi=1$

Span1 Aspect Ratio $\phi_1=4$	Span2 Aspect Ratio $\phi_2=4$	Span3 Aspect Ratio $\phi_3=4$	Span4 Aspect Ratio $\phi_4=4$
Thickness Ratio			
$h_1/h_1 = 1$	$h_2/h_1 = 3/8$	$h_3/h_1 = 1/4$	$h_3/h_1 = 1/8$
		Mode	Eigenvalue λ_b^2
		1	2.852
		2	3.975
		3	7.137
		4	8.787
		5	10.21
		6	12.55
		7	14.80
		8	19.89
		9	20.60
		10	22.57

Table 4.29. Eigenvalues for Thickness Ratios 1, 3/8, 1/4, 1/8 & Plate Overall Aspect Ratio $\phi=2/3$

Span1 Aspect Ratio $\phi_1=8/3$	Span2 Aspect Ratio $\phi_2=8/3$	Span3 Aspect Ratio $\phi_3=8/3$	Span4 Aspect Ratio $\phi_4=8/3$
Thickness Ratio			
$h_1/h_1 = 1$	$h_2/h_1 = 3/8$	$h_3/h_1 = 1/4$	$h_3/h_1 = 1/8$
Mode		Eigenvalue λ_b^2	
1		1.259	
2		2.285	
3		5.166	
4		5.327	
5		9.800	
6		9.938	
7		17.49	
8		17.86	
9		20.10	
10		24.18	

Table 4.30. Eigenvalues for Thickness Ratios 1, 3/8, 1/4, 1/8 & Plate Overall Aspect Ratio $\phi=1/2$

Span1 Aspect Ratio $\phi_1=2$	Span2 Aspect Ratio $\phi_2=2$	Span3 Aspect Ratio $\phi_3=2$	Span4 Aspect Ratio $\phi_4=2$
Thickness Ratio			
$h_1/h_1 = 1$	$h_2/h_1 = 3/8$	$h_3/h_1 = 1/4$	$h_3/h_1 = 1/8$
Mode		Eigenvalue λ_b^2	
1		0.704	
2		1.608	
3		2.167	
4		3.516	
5		4.275	
6		5.087	
7		7.205	
8		7.905	
9		9.071	
10		9.753	

Table 4.31. Eigenvalues for Thickness Ratios 1, 3/8, 1/4, 1/8 & Plate Overall Aspect Ratio $\phi=1/3$

Span1 Aspect Ratio $\phi_1=4/3$	Span2 Aspect Ratio $\phi_2=4/3$	Span3 Aspect Ratio $\phi_3=4/3$	Span4 Aspect Ratio $\phi_4=4/3$
Thickness Ratio			
$h_1/h_1 = 1$	$h_2/h_1 = 3/8$	$h_3/h_1 = 1/4$	$h_3/h_1 = 1/8$
Mode		Eigenvalue λ_b^2	
1		0.310	
2		0.957	
3		1.010	
4		2.074	
5		3.500	
6		4.072	
7		4.800	
8		6.003	
9		6.316	
10		8.847	

Table 4.32. Eigenvalues for Thickness Ratios 1, 1, 1, 1 & Plate Overall Aspect Ratio $\phi=1/3$

Span1 Aspect Ratio $\phi_1=4/3$	Span2 Aspect Ratio $\phi_2=4/3$	Span3 Aspect Ratio $\phi_3=4/3$	Span4 Aspect Ratio $\phi_4=4/3$
Thickness Ratio			
$h_1/h_1 = 1$	$h_2/h_1 = 1$	$h_3/h_1 = 1$	$h_3/h_1 = 1$
Mode		Eigenvalue λ_b^2	
1		0.377	
2		2.295	
3		2.355	
4		6.626	

Table 4.33. Eigenvalues for Thickness Ratios 1, 1, 1, 1 & Plate Overall Aspect Ratio $\phi=1$

Span1 Aspect Ratio $\phi_1=4$	Span2 Aspect Ratio $\phi_2=4$	Span3 Aspect Ratio $\phi_3=4$	Span4 Aspect Ratio $\phi_4=4$
Thickness Ratio			
$h_1/h_1 = 1$	$h_2/h_1 = 1$	$h_3/h_1 = 1$	$h_3/h_1 = 1$
Mode		Eigenvalue λ_b^2	
1		3.459	
2		8.334	
3		21.08	
10		27.03	

Comparing tables 4.32 and 4.33 to tables 4.21 and 4.22, the reader will deduce that results for the four span plate are less accurate than the ones obtained for the three span case using the same $K=15$. Again, the accuracy of the results could be increased using higher K terms as explained previously .

APPENDIX 2

Listing of Integrals

$$\int_0^1 \cosh \beta \xi \cos m \pi \xi d\xi = \frac{\beta \cos m \pi \sinh \beta}{\beta^2 + (m \pi)^2} \quad (\text{A2.1})$$

$$\int_0^1 \sinh \beta \xi \cos m \pi \xi d\xi = \frac{\beta}{\beta^2 + (m \pi)^2} (\cosh \beta \cos m \pi - 1) \quad (\text{A2.2})$$

$$\int_0^1 \cos \beta \xi \cos m \pi \xi d\xi = \frac{\beta \sin \beta \cos m \pi}{\beta^2 - (m \pi)^2} \quad (\text{A2.3})$$

$$\int_0^1 \sin \beta \xi \cos m \pi \xi d\xi = \frac{\beta}{\beta^2 - (m \pi)^2} (1 - \cos \beta \cos m \pi) \quad (\text{A2.4})$$

$$\int_0^1 \cosh \beta \xi \sin \frac{m \pi \xi}{2} d\xi = \frac{m \pi / 2 + \beta \sinh \beta \sin m \pi / 2}{\beta^2 + (m \pi / 2)^2} \quad (\text{A2.5})$$

$$\int_0^1 \sinh \beta \xi \sin \frac{m \pi \xi}{2} d\xi = \frac{\beta \cosh \beta \sin m \pi / 2}{\beta^2 + (m \pi / 2)^2} \quad (\text{A2.6})$$

$$\int_0^1 \cos \beta \xi \sin \frac{m \pi \xi}{2} d\xi = \frac{m \pi / 2 - \beta \sin(m \pi / 2) \sin \beta}{(m \pi / 2)^2 - \beta^2} \quad (\text{A2.7})$$

$$\int_0^1 \sin \beta \xi \sin \frac{m \pi \xi}{2} d\xi = \frac{-\beta \cos \beta \sin m \pi / 2}{\beta^2 - (m \pi / 2)^2} \quad (\text{A2.8})$$

Equation (A2.6) is valid for $m = 1, 3, 5, \dots$ only.

$$\int_0^1 \cosh[\beta(1-\xi)] \sin \frac{m \pi \xi}{2} d\xi = \frac{(m \pi / 2) \cosh \beta}{\beta^2 + (m \pi / 2)^2} \quad (\text{A2.9})$$

$$\int_0^1 \sinh[\beta(1-\xi)] \sin \frac{m \pi \xi}{2} d\xi = \frac{(m \pi / 2) \sinh \beta - \beta \sin(m \pi / 2)}{\beta^2 + (m \pi / 2)^2} \quad (\text{A2.10})$$

$$\int_0^1 \cos[\beta(1-\xi)] \sin \frac{m \pi \xi}{2} d\xi = \frac{-(m \pi / 2) \cos \beta}{\beta^2 - (m \pi / 2)^2} \quad (\text{A2.11})$$

$$\int_0^1 \sin[\beta(1-\xi)] \sin \frac{m \pi \xi}{2} d\xi = \frac{\beta \sin(m \pi / 2) - (m \pi / 2) \sin \beta}{\beta^2 - (m \pi / 2)^2} \quad (\text{A2.12})$$

Equations (A2.9) and (A2.11) are valid for $m = 1, 3, 5, \dots$ only.

$$\int_0^1 \sinh \beta \xi \sin m \pi \xi d\xi = \frac{-m \pi \cos m \pi \sinh \beta}{\beta^2 + (m \pi)^2} \quad (\text{A2.13})$$

$$\int_0^1 \cosh \beta \xi \sin m \pi \xi d\xi = \frac{m \pi (1 - \cos m \pi \cosh \beta)}{\beta^2 + (m \pi)^2} \quad (\text{A2.14})$$

$$\int_0^1 \sin \beta \xi \sin m \pi \xi d\xi = \frac{m \pi \cos m \pi \sin \beta}{\beta^2 - (m \pi)^2} \quad (\text{A2.15})$$

$$\int_0^1 \cos \beta \xi \sin m \pi \xi d\xi = \frac{m \pi (1 - \cos m \pi \cos \beta)}{(m \pi)^2 - \beta^2} \quad (\text{A2.16})$$

$$\int_0^1 \sinh[\beta(1-\xi)] \sin m \pi \xi d\xi = \frac{m \pi \sinh \beta}{(m \pi)^2 + \beta^2} \quad (\text{A2.17})$$

$$\int_0^1 \cosh[\beta(1-\xi)] \sin m \pi \xi d\xi = \frac{m \pi (\cosh \beta - \cos m \pi)}{\beta^2 + (m \pi)^2} \quad (\text{A2.18})$$

$$\int_0^1 \sin[\beta(1-\xi)] \sin m \pi \xi d\xi = \frac{m \pi \sin \beta}{(m \pi)^2 - \beta^2} \quad (\text{A2.19})$$

$$\int_0^1 \cos[\beta(1-\xi)] \sin m\pi\xi d\xi = \frac{m\pi(\cos\beta - \cos m\pi)}{(m\pi)^2 - \beta^2} \quad (\text{A2.20})$$

$$\int_0^1 \cosh[\beta(1-\xi)] \cos m\pi\xi d\xi = \frac{\beta \sinh \beta}{\beta^2 + (m\pi)^2} \quad (\text{A2.21})$$

$$\int_0^1 \sinh[\beta(1-\xi)] \cos m\pi\xi d\xi = \frac{\beta(\cosh \beta - \cos m\pi)}{\beta^2 + (m\pi)^2} \quad (\text{A2.22})$$

$$\int_0^1 \cos[\beta(1-\xi)] \cos m\pi\xi d\xi = \frac{\beta \sin \beta}{\beta^2 - (m\pi)^2} \quad (\text{A2.23})$$

$$\int_0^1 \sin[\beta(1-\xi)] \cos m\pi\xi d\xi = \frac{\beta(\cos m\pi - \cos \beta)}{\beta^2 - (m\pi)^2} \quad (\text{A2.24})$$

APPENDIX 3
Listing of the Computer Program

```

ZZ200010
CCCCCCCCCCCCCCCCCCCCCCCCCCCCCCCCCCCCCCCCCCCCCCCCCCCCCCCCCCCC
C
C THIS IS A PGM SOLVING THE MULTI-SPAN CANTILEVER PLATE PROBLEM C
C -TO BE USED WITH SUBROUTINE PGM. 'SUBSPAN'. C
C C
CCCCCCCCCCCCCCCCCCCCCCCCCCCCCCCCCCCCCCCCCCCCCCCCCCCCCCCCCCCC ZZ200020
IMPLICIT DOUBLE PRECISION (A-H,O-Z) ZZ200030
C DIMENSION ARRAYS: NOTE- LARGER MATRIX ARRAYS MAY BE REQUIRED C
C IF NUMBER OF SPANS EXCEEDS 4 . C
C DIMENSION A(250,250),ANS(251),AMMS(150),ANNS(150),ANNSS(150),
C PHIST(25),EM(30,30),EN(30,30),W(4,61,61),WS(4,61,61),WW(61,61)
C ,WPK(4,61,61),WPKY(4,61,61),RATIO(25),ROW(25),DE(25),WV(4,61,61)
C
C SET UP COMMON STATEMENTS
COMMON POI,POIS,PI,K,K2,K3,K4,NST,DE,
C K5,K6,K7,K8,K9,K10,K11,K12,ALMDS,ALMDS1,ALMDS2,WV,
C ALMDS3,PHIST,AMMS,ANNS,ANNSS,EM,EN,ALMDS,W,WS,WPK,WPKY,RATIO
C
C SET PRINTING FORMAT AND EVALUATE PI
1 FORMAT (7(E13.6,3X)) ZZ200040
C=1. ZZ200030
PI=4.*DATAN(C) ZZ2000370
C XXX=65.7*2.572*16.*16./(3.470*144.)
C
C R=.0975 *0.5/386.
C X=10 000 000. *.125/(12.*(1.-.333*.333)*R)
C X=DSQRT(X)
C FREQ=3.470*X/(2.*PI*16.*16.)
C WRITE (6,1) XXX,XXX
C IF(PI.GT.0.) GO TO 118
C
C ENTER INPUT HERE. MAY ENTER DIRECTLY IF DESIRED EG., XXI=
C SEE BELOW.
open(9,file='input.inp')
read(9,*) xx1
read(9,*) xx2
read(9,*) xx3
read(9,*) l11
CC read(9,*) l12
CCC OPEN (8, FILE='C:\DATA\DATA.OUT')
C
C XX2=0.
C
C INPUT DATA:
C
C XXI=18.74
C l11=9
C
C NST BELOW = NUMBER OF SPANS (TOTAL). PHIST(1)=ASPECT RATIO
C OF FIRST SPAN, ETC.
NST=3
EPSL=.0
PHIST(1)=12./(4.-EPSL)
PHIST(2)=12./(4.+EPSL)
C PHIST(1)=4.*12./16.
C PHIST(2)=PHIST(1)
C PHIST(3)=PHIST(1)
C PHIST(4)=PHIST(1)
ROW(1)=1.
ROW(2)=3./4.
ROW(3)=1./2.
C ROW(4)=1./4.
C ROW(2)=1.
C ROW(3)=1.
C ROW(4)=1.
DE(1)=1.
DE(2)=27./64.
DE(3)=1./8.

```

```

C   DE(4)=1./64.
C   DE(2)=1.
C   DE(3)=1.
C   DE(4)=1.

RATIO(1)=ROW(1)/DE(1)
RATIO(2)=ROW(2)/DE(2)
RATIO(3)=ROW(3)/DE(3)
C   RATIO(4)=ROW(4)/DE(4)

C   NOTE : MAY READ IN DATA OR ENTER IT HERE. TEST DATA
C   HERE. EG. FOR 3 SPAN DECK
C   XK1=10.03
C   XK2=0.01
C   XK3=1.1
C   L11=7

C   ABOVE INPUT DEMANDS EIGENVALUE SEARCH. ALMDS BEGINS AT XK1. IS
C   INCREMENTED BY XK2, AND PHIST(2) IS SET EQUAL TO XK3.
C   TO RUN FIRST MODE SHAPE SET XK1=10.076, XK2=0.

C   K= NO TERMS IN BUILDING BLOCK SOLUTIONS.

K=LL1
AKK=K
C   WRITE (6,1) AKK
K2=2*K
K3=3*K
K4=4*K
K5=5*K
K6=6*K
K7=7*K
K8=8*K
K9=9*K
K10=10*K
K11=K*11
K12=K*12
K13=K*13
K14=K*14
K15=K*15
K16=K*16

C   POI=POISON RATIO.

POI=0.333
POIS=2.-POI
ALMDS=XK1
DEL=XK2
DLIM=ALMDS +10.*DEL

C   MATRIX INITIALIZING OPERATION

C   Z1 AND Z2 SET EQUAL TO ZERO FOR USE IN CALLING INTEGRALS FROM
C   OUR SUBROUTINES. MUST SET MATRIX ELEMENTS EQUAL ZERO.
Z1=0.
Z2=0.

NRN=K*(3*NST-1)
KKK=(4*NST)*K
9 DO 17 M=1,KKK
DO 17 N=1,KKK
17 A(M,N)=0.

C   AUGMENT TRIAL EIGENVALUE ALMDS, AND STORE AS ALMDS.
C   ALMDS IS THE DIMENSIONLESS FREQUENCY.

ALMDS=ALMDS+DEL
ALMDS=ALMDS

C   CONDENSE GENERATION OF EIGENVALUE MATRIX.

DO 54 M=1,K
DO 54 N=1,K

C   SET UP DIVISOR DIV REQUIRED FOR COSINE EXPANSION TERMS AND
C   CONTINUE WITH COMPUTATIONS.

DIV=2.
IF(N.LT.2) GO TO 600
DIV=1.

600 CONTINUE

C   COMPUTE MATRIX ELEMENTS ASSOCIATED WITH FIRST SPAN BUILDING BLOCKS.
C   UP TO LABEL 54 WE HANDLE BLOCKS WITH ANALYTICAL FUNCTIONS RUNNING
C   IN THE ETA DIRECTION ONLY

```

ZZ200380

ZZ200780

ZZ200830

ZZ200850

ZZ201390

ZZ201410

ZZ201710

ZZ201720

ZZ201730

ZZ201740

ZZ201780

ZZ201790

ZZ201800

ZZ201810

```

PHI=PHIST(1)
PHIS=PHI*PHI
ALMDS=ALMDS/PHIS
EMP=(2*M-1)*PI/2.
EMPS=EMP*EMP
ENP=(N-1)*PI
EM=PHI*DSORT(ALMDS+EMPS)
EMS=EM*EM
ZZ=ALMDS-EMPS

```

ZZ

ZZ201830
ZZ201840
ZZ201860

C DECIDE WHAT FORM OF SOLUTION IS APPLICABLE.

```

IF(ZZ.LT.0.) GO TO 100
GM=PHI*DSORT(ZZ)
GMS=GM*GM
TD1M=-EM*(EMS-POIS*PHIS*EMPS)*DSINH(EM)/(GM*(GMS+POIS*PHIS*EMPS)
1 *DSINH(GM))
TD1M=1./(EM*DSINH(EM)-TD1M*GM*DSINH(GM))
IF(N.GT.1) GO TO 150
A(K+M,K+M)=-TD1M*((EMS-POI*PHIS*EMPS)*DCOSH(EM)-TD1M*(GMS+POI*
1 PHIS*EMPS)*DCOS(GM))
A(M+K2,M+K)=-TD1M*((EMS-POI*PHIS*EMPS)-TD1M*(GMS+POI*PHIS*EMPS
1 ))
A(M+K,M+K2)=A(M+K2,M+K)
A(M+K2,M+K2)=A(M+K,M+K)
150 CALL SCC11(EM,Z1,Z2,ENP,X1,X2)
CALL SCC2(GM,Z1,Z2,ENP,Y1,Y2)
A(N+K4,M+K)=2.*TD1M*(X2+TD1M*Y2)*DSIN(EMP)/(DIV*PHIST(1))
A(N+K4,M+K2)=A(N+K4,M+K)*DCOS(ENP)
A(N,M+K)=2.*EMP*TD1M*(X2+TD1M*Y2)/DIV
A(N,M+K2)=A(N,M+K)*DCOS(ENP)

A(N+K3,M+K)=-2.*(TD1M*((-EMPS+POI*EMS/PHIS)*X2+TD1M*(-EMPS-
1 POI*GMS/PHIS)*Y2))*DSIN(EMP)/DIV
A(N+K3,M+K2)=A(N+K3,M+K)*DCOS(ENP)

```

```

GO TO 160
100 ZZ=-ZZ
GM=PHI*DSORT(ZZ)
GMS=GM*GM
TD2M=-EM*(EMS-POIS*PHIS*EMPS)*DSINH(EM)/(GM*(GMS-POIS*PHIS*EMPS)
1 *DSINH(GM))
TD2M=1./(EM*DSINH(EM)+TD2M*GM*DSINH(GM))
IF(N.GT.1) GO TO 151
A(M+K,M+K)=-TD2M*((EMS-POI*PHIS*EMPS)*DCOSH(EM)+TD2M*(GMS-POI*
1 PHIS*EMPS)*DCOS(GM))
A(M+K2,M+K)=-TD2M*((EMS-POI*PHIS*EMPS)+TD2M*(GMS-POI*PHIS*EMPS))
A(M+K,M+K2)=A(M+K2,M+K)
A(M+K2,M+K2)=A(M+K,M+K)
151 CALL SCC11(EM,Z1,Z2,ENP,X1,X2)
CALL SCC11(GM,Z1,Z2,ENP,Y1,Y2)
A(N+K4,M+K)=2.*TD2M*(X2+TD2M*Y2)*DSIN(EMP)/(DIV*PHIST(1))
A(N+K4,M+K2)=A(N+K4,M+K)*DCOS(ENP)
A(N,M+K)=2.*EMP*TD2M*(X2+TD2M*Y2)/DIV
A(N,M+K2)=A(N,M+K)*DCOS(ENP)

A(N+K3,M+K)=-2.*(TD2M*((-EMPS+POI*EMS/PHIS)*X2+TD2M*(-EMPS+
1 POI*GMS/PHIS)*Y2))*DSIN(EMP)/DIV
A(N+K3,M+K2)=A(N+K3,M+K)*DCOS(ENP)

```

160 CONTINUE

C NOW COMPUTE MATRIX ELEMENTS ASSOCIATED WITH SECOND SPAN BUILDING
C BLOCKS

```

DO 1600 J=2,NST-1
RATE=PHIST(J)/PHIST(J-1)
PHI=PHIST(J)
PHIS=PHI*PHI
ALMDS=ALMDS/PHIS
X=RATIO(J)
ALMDS=ALMDS*DSORT(X)
C
II=(J-2)*K3
II=(J-2)*K4
M=M+II
N=N+II
EMP=(M-1)*PI
EMPS=EMP*EMP
ENP=(N-1)*PI
EM=PHI*DSORT(ALMDS+EMPS)
EMS=EM*EM
ZZ=ALMDS-EMPS
IF(ZZ.LT.0.) GO TO 300
GM=PHI*DSORT(ZZ)
GMS=GM*GM

```

ZZ

ZZ

Z

ZZ

```

      TD1M=EM*(EMS-POIS*PHIS*EMPS)*DSINH(EM)/(GM*(GMS+POIS*PHIS*EMPS)
1  *DSIN(GM)
      TD1M=1./(EM*DSINH(EM)-TD1M*GM*DSIN(GM))
      IF(N.GT.1) GO TO 350

      A(MM+K5,MM+K5)=-TD1M*((EMS-POI*PHIS*EMPS)*DCOSH(EM)-TD1M*(GMS+POI
1  *PHIS*EMPS)*DCOS(GM))
      A(MM+K6,MM+K5)=-TD1M*((EMS-POI*PHIS*EMPS)-TD1M*(GMS+POI*PHIS
1  *EMPS))
      A(MM+K5,MM+K6)=A(MM+K6,MM+K5)
      A(MM+K6,MM+K6)=A(MM+K5,MM+K5)

350 CALL SCC11(EM,Z1,Z2,ENP,X1,X2)
      CALL SCC2(GM,Z1,Z2,ENP,Y1,Y2)

      A(NN+K4,MM+K5)=-2.*TD1M*(X2+TD1M*Y2)/(DIV*PHIST(J))
      A(NN+K4,MM+K6)=A(NN+K4,MM+K5)*DCOS(ENP)

      A(NN+K8,MM+K5)=2.*TD1M*(X2+TD1M*Y2)*DCOS(ENP)/(DIV*PHIST(J))
      A(NN+K8,MM+K6)=A(NN+K8,MM+K5)*DCOS(ENP)

      A(NN+K3,MM+K5)=2.*(TD1M*((-EMPS+POI*EMS/PHIS)*X2+TD1M*(-EMPS-
1  POI*GMS/PHIS)*Y2))*PHIST(J)*DE(J)/(PHIST(J-1)*DE(J-1)*DIV)

      A(NN+K3,MM+K6)=A(NN+K3,MM+K5)*DCOS(ENP)

      A(NN+K7,MM+K5)=-2.*(TD1M*((-EMPS+POI*EMS/PHIS)*X2+TD1M*(-EMPS-
1  POI*GMS/PHIS)*Y2))*DCOS(ENP)/DIV
      A(NN+K7,MM+K6)=A(NN+K7,MM+K5)*DCOS(ENP)

      GO TO 360
300 ZZ=-ZZ
      GM=PHI*DSQRT(ZZ)
      GMS=GM*GM
      TD2M=-EM*(EMS-POIS*PHIS*EMPS)*DSINH(EM)/(GM*(GMS-POIS*PHIS*EMPS)
1  *DSINH(GM))
      TD2M=1./(EM*DSINH(EM)+TD2M*GM*DSIN(GM))
      IF(N.GT.1) GO TO 351
      A(MM+K5,MM+K5)=-TD2M*((EMS-POI*PHIS*EMPS)*DCOSH(EM)+TD2M*(GMS-
1  POI*PHIS*EMPS)*DCOS(GM))
      A(MM+K6,MM+K5)=-TD2M*((EMS-POI*PHIS*EMPS)+TD2M*(GMS-POI*PHIS*
1  EMPS))
      A(MM+K5,MM+K6)=A(MM+K6,MM+K5)
      A(MM+K6,MM+K6)=A(MM+K5,MM+K5)

351 CALL SCC11(EM,Z1,Z2,ENP,X1,X2)
      CALL SCC11(GM,Z1,Z2,ENP,Y1,Y2)
      A(NN+K4,MM+K5)=-2.*TD2M*(X2+TD2M*Y2)/(DIV*PHIST(J))
      A(NN+K4,MM+K6)=A(NN+K4,MM+K5)*DCOS(ENP)
      A(NN+K8,MM+K5)=2.*TD2M*(X2+TD2M*Y2)*DCOS(ENP)/(DIV*PHIST(J))
      A(NN+K8,MM+K6)=A(NN+K8,MM+K5)*DCOS(ENP)

      A(NN+K3,MM+K5)=2.*(TD2M*((-EMPS+POI*EMS/PHIS)*X2+TD2M*(-EMPS+
1  POI*GMS/PHIS)*Y2))*PHIST(J)*DE(J)/(PHIST(J-1)*DE(J-1)*DIV)

      A(NN+K3,MM+K6)=A(NN+K3,MM+K5)*DCOS(ENP)

      A(NN+K7,MM+K5)=-2.*(TD2M*((-EMPS+POI*EMS/PHIS)*X2+TD2M*(-EMPS+
1  POI*GMS/PHIS)*Y2))*DCOS(ENP)/DIV
      A(NN+K7,MM+K6)=A(NN+K7,MM+K5)*DCOS(ENP)

360 CONTINUE
1600 CONTINUE

C      NOW COMPUTE MATRIX ELEMENTS ASSOCIATED WITH LAST SPAN BUILDING
C      BLOCK

      PHI=PHIST(NST)
      PHIS=PHI*PHI
      ALMS=ALMS/PHIS
      X=RATIO(NST)
      ALMS=ALMS*DSQRT(X)
C      II=(NST-3)*K3
      II=(NST-3)*K4
      MM=MM+II
      NN=NN+II

      ENP=(N-1)*PI
      ENP3=ENP*ENP
      ENP=(N-1)*PI
      EM=PHI*DSQRT(ALMS+ENP3)
      EMS=EM*EM
      ZZ=ALMS-ENP3
      IF(ZZ.LT.0.) GO TO 640
      GM=PHI*DSQRT(ZZ)
      GMS=GM*GM

```

```

      TD1M=-EM*(EMS-POIS*PHIS*EMPS)*DSINE(EM)/(GM*(GMS+POIS*PHIS*EMPS)
1  *DSINE(GM))
      TD1M=1./(EM*DSINE(EM)-TD1M*GM*DSINE(GM))
      IF(N.GT.1) GO TO 650
      A(MM+K9,MM+K9)=-TD1M*((EMS-POI*PHIS*EMPS)*DCOSH(EM)-TD1M*(GMS+POI
1  *PHIS*EMPS)*DCOS(GM))
      A(MM+K10,MM+K9)=-TD1M*((EMS-POI*PHIS*EMPS)-TD1M*(GMS+POI*PHIS*
1  EMPS))
      A(MM+K9,MM+K10)=A(MM+K10,MM+K9)
      A(MM+K10,MM+K10)=A(MM+K9,MM+K9)
650 CALL SCC11(EM,Z1,Z2,ENP,X1,X2)
      CALL SCC2(GM,Z1,Z2,ENP,Y1,Y2)
      A(NN+K8,MM+K9)=-2.*TD1M*(X2+TD1M*Y2)/(DIV*PHIST(NST))
      A(NN+K8,MM+K10)=A(NN+K8,MM+K9)*DCOS(ENP)
      A(NN+K11,MM+K9)=-2.*(TD1M*((-EMPS+POI*EMS/PHIS)*X2+TD1M*(-EMPS-
1  POI*GMS/PHIS)*Y2))*DCOS(ENP)/DIV
      A(NN+K11,MM+K10)=A(NN+K11,MM+K9)*DCOS(ENP)

      A(NN+K7,MM+K9)=2.*(TD1M*((-EMPS+POI*EMS/PHIS)*X2+TD1M*(-EMPS-
1  POI*GMS/PHIS)*Y2))*PHIST(NST)*DE(NST)/(PHIST(NST-1)*DE(NST-1)*DIV)
      A(NN+K7,MM+K10)=A(NN+K7,MM+K9)*DCOS(ENP)

      GO TO 369
640 ZZ=-ZZ
      GM=PHI*DSQRT(ZZ)
      GMS=GM*GM
      TD2M=-EM*(EMS-POIS*PHIS*EMPS)*DSINE(EM)/(GM*(GMS-POIS*PHIS*EMPS)
1  *DSINE(GM))
      TD2M=1./(EM*DSINE(EM)+TD2M*GM*DSINE(GM))
      IF(N.GT.1) GO TO 651
      A(MM+K9,MM+K9)=-TD2M*((EMS-POI*PHIS*EMPS)*DCOSH(EM)+TD2M*(GMS-
1  POI*PHIS*EMPS)*DCOSH(GM))
      A(MM+K10,MM+K9)=-TD2M*((EMS-POI*PHIS*EMPS)+TD2M*(GMS-POI*PHIS*
1  EMPS))
      A(MM+K9,MM+K10)=A(MM+K10,MM+K9)
      A(MM+K10,MM+K10)=A(MM+K9,MM+K9)
651 CALL SCC11(EM,Z1,Z2,ENP,X1,X2)
      CALL SCC11(GM,Z1,Z2,ENP,Y1,Y2)
      A(NN+K8,MM+K9)=-2.*TD2M*(X2+TD2M*Y2)/(DIV*PHIST(NST))
      A(NN+K8,MM+K10)=A(NN+K8,MM+K9)*DCOS(ENP)
      A(NN+K11,MM+K9)=-2.*(TD2M*((-EMPS+POI*EMS/PHIS)*X2+TD2M*(-EMPS+
1  POI*GMS/PHIS)*Y2))*DCOS(ENP)/DIV
      A(NN+K11,MM+K10)=A(NN+K11,MM+K9)*DCOS(ENP)

      A(NN+K7,MM+K9)=2.*(TD2M*((-EMPS+POI*EMS/PHIS)*X2+TD2M*(-EMPS+
1  POI*GMS/PHIS)*Y2))*PHIST(J)*DE(NST)/(PHIST(J-1)*DE(NST-1)*DIV)
      A(NN+K7,MM+K10)=A(NN+K7,MM+K9)*DCOS(ENP)

369 CONTINUE
54 CONTINUE
ZZ203330

C      NOW COMPUTE MATRIX ELEMENTS ASSOCIATED WITH BUILDING BLOCKS WITH
C      ANALYTICAL FUNCTIONS RUNNING IN THE PSI DIRECTION.

      DO 74 N=1,K
ZZ203390
      DO 74 M=1,K
ZZ203430

C      SET UP DIVISOR DIV REQUIRED FOR COSINE TERM EXPANSION.

      DIV=2.
ZZ203440
      IF(M.LT.2) GO TO 601
ZZ203450
      DIV=1.
ZZ203460

601 CONTINUE

C      COMPUTE ELEMENTS ASSOCIATED WITH FIRST SPAN.

      ENP=(2*M-1)*PI/2.
      ENP=(N-1)*PI
ZZ203480
      ENPS=ENP*ENP
ZZ203490
      ALMDS=ALMDS
      PHI=1./PHIST(1)
      PHIS=PHI*PHI
      EN=PHI*DSQRT(ALMDS+ENPS)
      EMS=EN*EM
      EZ=ALMDS-ENPS
      IF(EZ.LT.0.) GO TO 200
      GM=PHI*DSQRT(EZ)
      GMS=GM*GM
      TD1M=-DCOSH(EM)/DCOS(GM)
      TD1M=1./(EM*DSINE(EM)-TD1M*GM*DSINE(GM))

      TD1MP=-EM*(EMS-POIS*PHIS*EMPS)*DCOSH(EM)/(GM*(GMS+POIS*PHIS*EMPS)
1  *DCOS(GM))
      TD1MP=1./(EM*DCOSH(EM)+TD1MP*GM*DCOS(GM))

      TD1MV=-EM*DCOSH(EM)/(GM*DCOS(GM))

```

```

      TD11NV=-1./ (BN*(BNS-POIS*PHIS*ENPS)*DCOSH(BN)-TD1NV*GN*(GNS+POIS*
1 PHIS*ENPS)*DCOS(GN)
      IF(M.GT.1) GO TO 250
      A(N,N)=TD11N*(-BN*DSINH(BN)+TD1N*GN*DSIN(GN))*PHIST(1)
      A(N+K4,N)=TD11N*(1.+TD1N)
      A(N,N+K3)=TD11N*(BN+GN*TD1N)*PHIST(1)
      A(N,N+K4)=TD11NV*(BN+GN*TD1NV)*PHIST(1)

      A(N+K4,N+K3)=TD11N*(DSINH(BN)+TD1N*DSIN(GN))
      A(N+K3,N+K4)=TD11NV*(BN*DCOSH(BN)+TD1NV*GN*DCOS(GN))*PHIST(1)
      A(N+K4,N+K4)=TD11NV*(DSINH(BN)+TD1NV*DSIN(GN))

      A(N+K3,N)=-TD11N*((BNS-POI*PHIS*ENPS)-TD1N*(GNS+POI*PHIS*
1 ENPS))*PHIST(1)
      A(N+K3,N+K3)=-TD11N*((BNS-POI*PHIS*ENPS)*DSINH(BN)-TD1N*(GNS+
1 POI*PHIS*ENPS)*DSIN(GN))*PHIST(1)
      A(N+K3,N+K4)=-TD11NV*((BNS-POI*PHIS*ENPS)*DSINH(BN)-TD1NV*(GNS+
1 POI*PHIS*ENPS)*DSIN(GN))*PHIST(1)

250 CONTINUE
      Z1=1.
      CALL SCS11(BN,Z1,Z2,EMP,X2,X1)
      CALL SCS2(GN,Z1,Z2,EMP,Y2,Y1)
      Z1=0.
      XXX=-2.*TD11N*((-ENPS+POI*BNS/PHIS)*X1+TD1N*(-ENPS-POI*
1 GNS/PHIS)*Y1)*DCOS(EMP)

      A(M+K,N)=XXX*PHIST(1)

      YYY=-2.*TD11N*((-ENPS+POI*BNS/PHIS)*X1+TD1N*(-ENPS-POI*
1 GNS/PHIS)*Y1)

      A(M+K2,N)=YYY*PHIST(1)

      CALL SCS11(BN,Z1,Z2,EMP,X1,X2)
      .....
      CALL SCS2(GN,Z1,Z2,EMP,Y1,Y2)
      A(M+K,N+K3)=-2.*TD11N*((-ENPS+POI*BNS/PHIS)*X1+TD1N*(-ENPS-POI*
1 GNS/PHIS)*Y1)*DCOS(EMP)*PHIST(1)
      A(M+K2,N+K3)=-2.*TD11N*((-ENPS+POI*BNS/PHIS)*X1+TD1N*(-ENPS-POI*
1 GNS/PHIS)*Y1)*PHIST(1)

      A(M+K,N+K4)=-2.*TD11NV*((-ENPS+POI*BNS/PHIS)*X1+TD1NV*(-ENPS-POI*
1 GNS/PHIS)*Y1)*DCOS(EMP)*PHIST(1)
      A(M+K2,N+K4)=-2.*TD11NV*((-ENPS+POI*BNS/PHIS)*X1+TD1NV*(-ENPS-POI*
1 GNS/PHIS)*Y1)*PHIST(1)
      GO TO 260
200 ZZ=-ZZ
      GN=PHI*DSQRT(ZZ)
      GNS=GN*GN
      TD2N=-DCOSH(BN)/DCOSH(GN)
      TD22N=1./ (BN*DSINH(BN)+TD2N*GN*DSINH(GN))

      TD2NP=-BN*(BNS-POIS*PHIS*ENPS)*DCOSH(BN)/(GN*(GNS-POIS*PHIS*ENPS)
1 *DCOSH(GN))
      TD22NP=1./ (BN*DCOSH(BN)+TD2NP*GN*DCOSH(GN))

      TD2NV=-BN*DCOSH(BN)/(GN*DCOSH(GN))
      TD22NV=-1./ (BN*(BNS-POIS*PHIS*ENPS)*DCOSH(BN)+TD2NV*GN*(GNS-POIS*
1 PHIS*ENPS)*DCOSH(GN))
      IF(M.GT.1) GO TO 251
      A(N,N)=TD22N*(-BN*DSINH(BN)-TD2N*GN*DSINH(GN))*PHIST(1)
      A(N+K4,N)=TD22N*(1.+TD2N)
      A(N,N+K3)=TD22NP*(BN+GN*TD2NP)*PHIST(1)
      A(N,N+K4)=TD22NV*(BN+GN*TD2NV)*PHIST(1)

      A(N+K4,N+K3)=TD22NP*(DSINH(BN)+TD2NP*DSINH(GN))
      A(N+K4,N+K4)=TD22NV*(DSINH(BN)+TD2NV*DSINH(GN))

      A(N+K3,N)=-TD22N*((BNS-POI*PHIS*ENPS)+TD2N*(GNS-POI*PHIS*
1 ENPS))*PHIST(1)
      A(N+K3,N+K3)=-TD22NP*((BNS-POI*PHIS*ENPS)*DSINH(BN)+TD2NP*(GNS-
1 POI*PHIS*ENPS)*DSINH(GN))*PHIST(1)
      A(N+K3,N+K4)=-TD22NV*((BNS-POI*PHIS*ENPS)*DSINH(BN)+TD2NV*(GNS-
1 POI*PHIS*ENPS)*DSINH(GN))*PHIST(1)

251 CONTINUE
      Z1=1.
      CALL SCS11(BN,Z1,Z2,EMP,X2,X1)
      CALL SCS11(GN,Z1,Z2,EMP,Y2,Y1)
      Z1=0.
      XXX=-2.*TD22N*((-ENPS+POI*BNS/PHIS)*X1+TD2N*(-ENPS+POI*
1 GNS/PHIS)*Y1)*DCOS(EMP)

      A(M+K,N)=XXX*PHIST(1)

```

```

    YYY=-2.*TD22N*((-ENPS+POI*BNS/PHIS)*X1+TD2N*(-ENPS+POI*
1 GNS/PHIS)*Y1)
    A(M+K2,N)=YYY*PHIST(1)
    CALL SCS11(BN,Z1,Z2,EMP,X1,X2)
    CALL SCS11(GN,Z1,Z2,EMP,Y1,Y2)
    A(M+K,N+K3)=-2.*TD22NP*((-ENPS+POI*BNS/PHIS)*X1+TD2NP*(-ENPS+POI*
1 GNS/PHIS)*Y1)*DCOS(EMP)*PHIST(1)
    A(M+K2,N+K3)=-2.*TD22NP*((-ENPS+POI*BNS/PHIS)*X1+TD2NP*(-ENPS+POI*
1 GNS/PHIS)*Y1)*PHIST(1)
    A(M+K,N+K4)=-2.*TD22NV*((-ENPS+POI*BNS/PHIS)*X1+TD2NV*(-ENPS+POI*
1 GNS/PHIS)*Y1)*DCOS(EMP)*PHIST(1)
    A(M+K2,N+K4)=-2.*TD22NV*((-ENPS+POI*BNS/PHIS)*X1+TD2NV*(-ENPS+POI*
1 GNS/PHIS)*Y1)*PHIST(1)

```

260 CONTINUE

C NOW COMPUTE ELEMENTS ASSOCIATED WITH SECOND SPAN

```

    EMP=(M-1)*PI
    DO 2610 J=2,NST-1
    X=RATIO(J)
    ALMS=ALMDBS*DSQRT(X)
    RATE=PHIST(J)/PHIST(J-1)
C    II=(J-2)*K3
    II=(J-2)*K4
    RAT12S=-PHIST(J-1)*PHIST(J-1)/(PHIST(J)*PHIST(J))
    RAT12C=RAT12S*PHIST(J-1)/PHIST(J)
    RAT12C=RAT12C*DE(J-1)/DE(J)
    RAT12S=-PHIST(J-1)/PHIST(J)
    MM=M+II
    NN=N+II
    PHI=1./PHIST(J)
    PHIS=PHI*PHI
    BN=PHI*DSQRT(ALMS+ENPS)
    BNS=BN*BN
    ZZ=ALMS-ENPS
    IF(ZZ.LT.0.) GO TO 400
    GN=PHI*DSQRT(ZZ)
    GNS=GN*GN
    TD1NV=BN*DSINE(BN)/(GN*DSIN(GN))
    TD11NV=-1./(BN*(BNS-POIS*PHIS*ENPS)*DSINE(BN)+TD1NV*GN*(GNS+POIS*
1 PHIS*ENPS)*DSIN(GN))
    TD1NP=-BN*(BNS-POIS*PHIS*ENPS)*DSINE(BN)/(GN*(GNS+POIS*PHIS*ENPS)*
1 DSIN(GN))
    TD11NP=1./(BN*DSINE(BN)-TD1NP*GN*DSIN(GN))
    IF(M.GT.1) GO TO 450
    XXX=TD11NP*((BNS-POI*PHIS*ENPS)*DCOSH(BN)-TD1NP*(GNS+POI*PHIS*ENPS
1)*DCOS(GN))*PHIST(J)*RAT12S*DE(J)/DE(J-1)
    YYY=TD11NV*((BNS-POI*PHIS*ENPS)*DCOSH(BN)-TD1NV*(GNS+POI*PHIS*ENPS
1)*DCOS(GN))*PHIST(J)*RAT12C*DE(J)/DE(J-1)
    A(NN+K3,NN+K3)=A(NN+K3,NN+K3)+XXX*PHIST(J)/PHIST(J-1)
    A(NN+K3,NN+K4)=A(NN+K3,NN+K4)+YYY*PHIST(J)/PHIST(J-1)
    A(NN+K3,NN+K7)=TD11NP*((BNS-POI*PHIS*ENPS)-TD1NP*(GNS+POI*PHIS*
1 ENPS))*PHIST(J)*PHIST(J)*DE(J)/(PHIST(J-1)*DE(J-1))
    A(NN+K3,NN+K8)=TD11NV*((BNS-POI*PHIS*ENPS)-TD1NV*(GNS+POI*PHIS*
1 ENPS))*PHIST(J)*PHIST(J)*DE(J)/(PHIST(J-1)*DE(J-1))
    XXXX=-TD11NP*(DCOSH(BN)+TD1NP*DCOS(GN))*RAT12S
    A(NN+K4,NN+K3)=A(NN+K4,NN+K3)+XXXX
    A(NN+K4,NN+K4)=A(NN+K4,NN+K4)-TD11NV*(DCOSH(BN)+TD1NV*DCOS(GN))*
1 RAT12C
    A(NN+K4,NN+K7)=-TD11NP*(1.+TD1NP)
    A(NN+K4,NN+K8)=-TD11NV*(1.+TD1NV)
    A(NN+K7,NN+K3)=-TD11NP*((BNS-POI*PHIS*ENPS)-TD1NP*(GNS+POI*PHIS*
1 ENPS))*PHIST(J)*RAT12S
    A(NN+K7,NN+K4)=-TD11NV*((BNS-POI*PHIS*ENPS)-TD1NV*(GNS+POI*PHIS*
1 ENPS))*PHIST(J)*RAT12C
    A(NN+K7,NN+K7)=-TD11NP*((BNS-POI*PHIS*ENPS)*DCOSH(BN)-TD1NP*(GNS
1 +POI*PHIS*ENPS)*DCOS(GN))*PHIST(J)
    A(NN+K7,NN+K8)=-TD11NV*((BNS-POI*PHIS*ENPS)*DCOSH(BN)-TD1NV*(GNS
1 +POI*PHIS*ENPS)*DCOS(GN))*PHIST(J)
    A(NN+K8,NN+K7)=TD11NP*(DCOSH(BN)+TD1NP*DCOS(GN))
    A(NN+K8,NN+K8)=TD11NV*(DCOSH(BN)+TD1NV*DCOS(GN))
    A(NN+K8,NN+K3)=TD11NP*(1.+TD1NP)*RAT12S
    A(NN+K8,NN+K4)=TD11NV*(1.+TD1NV)*RAT12C

```

450 CONTINUE

```
CALL SCC11(BN,Z1,Z2,EMP,X2,X1)
CALL SCC2(GN,Z1,Z2,EMP,Y2,Y1)
XXX=-2.*TD11NP*((-ENPS+POI*BNS/PHIS)*X1+TD1NP*(-ENPS-POI*
1 GNS/PHIS)*Y1)*DCOS(EMP)/DIV
XXV=-2.*TD11NV*((-ENPS+POI*BNS/PHIS)*X1+TD1NV*(-ENPS-POI*
1 GNS/PHIS)*Y1)*DCOS(EMP)/DIV

A(MN+K5,NN+K3)=XXX*DCOS((M-1)*PI)*PHIST(J)*RAT12S
A(MN+K5,NN+K4)=XXV*DCOS((M-1)*PI)*PHIST(J)*RAT12C
A(MN+K5,NN+K7)=XXX*PHIST(J)
A(MN+K5,NN+K8)=XXV*PHIST(J)

YYY=-2.*TD11NP*((-ENPS+POI*BNS/PHIS)*X1+TD1NP*(-ENPS-POI*
1 GNS/PHIS)*Y1)/DIV
YYV=-2.*TD11NV*((-ENPS+POI*BNS/PHIS)*X1+TD1NV*(-ENPS-POI*
1 GNS/PHIS)*Y1)/DIV

A(MN+K6,NN+K3)=YYY*DCOS((M-1)*PI)*PHIST(J)*RAT12S
A(MN+K6,NN+K4)=YYV*DCOS((M-1)*PI)*PHIST(J)*RAT12C
A(MN+K6,NN+K7)=YYY*PHIST(J)
A(MN+K6,NN+K8)=YYV*PHIST(J)

GO TO 460
400 ZZ=ZZ
GN=PHI*DSQRT(ZZ)
GNS=GN*GN
TD2NV=-BN*DSINE(BN)/(GN*DSINE(GN))
TD22NV=-1./(BN*(BNS-POIS*PHIS*ENPS)*DSINE(BN)+TD2NV*GN*(GNS-POIS*
1 PHIS*ENPS)*DSINE(GN))

TD2NP=-BN*(BNS-POIS*PHIS*ENPS)*DSINE(BN)/(GN*(GNS-POIS*PHIS*ENPS)*
1 DSINE(GN))
TD22NP=1./(BN*DSINE(BN)+TD2NP*GN*DSINE(GN))

IF(M.GT.1) GO TO 455
XXX=TD22NP*((BNS-POI*PHIS*ENPS)*DCOSH(BN)+TD2NP*(GNS-POI*PHIS*
1 ENPS)*DCOSH(GN))*PHIST(J)*RAT12S*DE(J)/DE(J-1)
YYY=TD22NV*((BNS-POI*PHIS*ENPS)*DCOSH(BN)+TD2NV*(GNS-POI*PHIS*
1 ENPS)*DCOSH(GN))*PHIST(J)*RAT12C*DE(J)/DE(J-1)
A(MN+K3,NN+K4)=A(MN+K3,NN+K4)+YYY*PHIST(J)/PHIST(J-1)
A(MN+K3,NN+K3)=A(MN+K3,NN+K3)+XXX*PHIST(J)/PHIST(J-1)

A(MN+K3,NN+K7)=TD22NP*((BNS-POI*PHIS*ENPS)+TD2NP*(GNS-POI*PHIS*
1 ENPS))*PHIST(J)*PHIST(J)*DE(J)/(PHIST(J-1)*DE(J-1))
A(MN+K3,NN+K8)=TD22NV*((BNS-POI*PHIS*ENPS)+TD2NV*(GNS-POI*PHIS*
1 ENPS))*PHIST(J)*PHIST(J)*DE(J)/(PHIST(J-1)*DE(J-1))

XXXX=-TD22NP*(DCOSH(BN)+TD2NP*DCOSH(GN))*RAT12S
A(MN+K4,NN+K3)=A(MN+K4,NN+K3)+XXXX
A(MN+K4,NN+K4)=A(MN+K4,NN+K4)-TD22NV*(DCOSH(BN)+TD2NV*DCOSH(GN))*
1 RAT12C
A(MN+K4,NN+K7)=-TD22NP*(1.+TD2NP)
A(MN+K4,NN+K8)=-TD22NV*(1.+TD2NV)
A(MN+K7,NN+K3)=-TD22NP*((BNS-POI*PHIS*ENPS)+TD2NP*(GNS-POI*PHIS*
1 ENPS))*PHIST(J)*RAT12S
A(MN+K7,NN+K4)=-TD22NV*((BNS-POI*PHIS*ENPS)+TD2NV*(GNS-POI*PHIS*
1 ENPS))*PHIST(J)*RAT12C
A(MN+K7,NN+K7)=-TD22NP*((BNS-POI*PHIS*ENPS)*DCOSH(BN)+TD2NP*(GNS
1 -POI*PHIS*ENPS)*DCOSH(GN))*PHIST(J)
A(MN+K7,NN+K8)=-TD22NV*((BNS-POI*PHIS*ENPS)*DCOSH(BN)+TD2NV*(GNS
1 -POI*PHIS*ENPS)*DCOSH(GN))*PHIST(J)

A(MN+K8,NN+K7)=TD22NP*(DCOSH(BN)+TD2NP*DCOSH(GN))
A(MN+K8,NN+K8)=TD22NV*(DCOSH(BN)+TD2NV*DCOSH(GN))

A(MN+K8,NN+K3)=TD22NP*(1.+TD2NP)*RAT12S
A(MN+K8,NN+K4)=TD22NV*(1.+TD2NV)*RAT12C
```

455 CONTINUE

```
CALL SCC11(BN,Z1,Z2,EMP,X2,X1)
CALL SCC11(GN,Z1,Z2,EMP,Y2,Y1)
XXX=-2.*TD22NP*((-ENPS+POI*BNS/PHIS)*X1+TD2NP*(-ENPS+POI*
1 GNS/PHIS)*Y1)*DCOS(EMP)/DIV
XXV=-2.*TD22NV*((-ENPS+POI*BNS/PHIS)*X1+TD2NV*(-ENPS+POI*
1 GNS/PHIS)*Y1)*DCOS(EMP)/DIV

A(MN+K5,NN+K3)=XXX*DCOS((M-1)*PI)*PHIST(J)*RAT12S
A(MN+K5,NN+K4)=XXV*DCOS((M-1)*PI)*PHIST(J)*RAT12C
A(MN+K5,NN+K7)=XXX*PHIST(J)
A(MN+K5,NN+K8)=XXV*PHIST(J)

YYY=-2.*TD22NP*((-ENPS+POI*BNS/PHIS)*X1+TD2NP*(-ENPS+POI*
```

```

1 GNS/PHIS)*Y1)/DIV
YV=-2.*TD22NV*((-ENPS+POI*ENS/PHIS)*X1+TD2NV*(-ENPS+POI*
1 GNS/PHIS)*Y1)/DIV

A(04+K6,NN+K3)=YYY*DCOS((M-1)*PI)*PHIST(J)*RAT12S
A(04+K6,NN+K4)=YV*DCOS((M-1)*PI)*PHIST(J)*RAT12C
A(04+K6,NN+K7)=YYY*PHIST(J)
A(04+K6,NN+K8)=YV*PHIST(J)

460 CONTINUE
2610 CONTINUE
C   NOW COMPUTE ELEMENTS ASSOCIATED WITH THIRD SPAN.

C   II=(NST-3)*K3
   II=(NST-3)*K4
   NN=M+II
   NN=N+II
   J=NST-1
   RATE=PHIST(J)/PHIST(J-1)
   RAT12S=-PHIST(NST-1)*PHIST(NST-1)/(PHIST(NST)*PHIST(NST))
   RAT12C=RAT12S*PHIST(NST-1)/PHIST(NST)
   RAT12C=RAT12C*DE(NST-1)/DE(NST)
   RAT12S=-PHIST(NST-1)/PHIST(NST)

   PHI=1./PHIST(NST)
   PHIS=PHI*PHI
   X=RATIO(NST)
   ALMS=ALMDS*DSQRT(X)
   EN=PHI*DSQRT(ALMS+ENPS)
   ENS=EN*EN
   ZZ=ALMS-ENPS
   IF(ZZ.LT.0.) GO TO 800
   GN=PHI*DSQRT(ZZ)
   GNS=GN*GN

   TD1NV=EN*DSINH(EN)/(GN*DSIN(GN))
   TD11NV=-1./(EN*(ENS-POIS*PHIS*ENPS)*DSINH(EN)+TD1NV*GN*(GNS+POIS*
1 PHIS*ENPS)*DSIN(GN))

   TD1NP=-EN*(ENS-POIS*PHIS*ENPS)*DSINH(EN)/(GN*(GNS+POIS*PHIS*ENPS)*
1 DSIN(GN))
   TD11NP=1./(EN*DSINH(EN)-TD1NP*GN*DSIN(GN))

   TD11NPP=-1./((ENS-POI*PHIS*ENPS)*DCOSH(EN)-TD1NP*(GNS+POI*PHIS*
1 ENPS)*DCOS(GN))

   IF(M.GT.1) GO TO 850

   XXX=-TD11NP*((ENS-POI*PHIS*ENPS)*DCOSH(EN)-TD1NP*(GNS+POI*PHIS*
1 ENPS)*DCOS(GN))*PHIST(NST)*RAT12S*DE(NST)/DE(NST-1)
   YYY=-TD11NV*((ENS-POI*PHIS*ENPS)*DCOSH(EN)-TD1NV*(GNS+POI*PHIS*
1 ENPS)*DCOS(GN))*PHIST(NST)*RAT12C*DE(NST)/DE(NST-1)
   A(NN+K7,NN+K7)=A(NN+K7,NN+K7)-XXX*PHIST(NST)/PHIST(NST-1)
   A(NN+K7,NN+K8)=A(NN+K7,NN+K8)-YYY*PHIST(NST)/PHIST(NST-1)

   A(NN+K7,NN+K11)=TD11NPP*((ENS-POI*PHIS*ENPS)-TD1NP*(GNS+POI*PHIS*
1 ENPS))*PHIST(NST)*PHIST(NST)*DE(NST)/(PHIST(NST-1)*DE(NST-1))

   XXX=TD11NP*(DCOSH(EN)+TD1NP*DCOS(GN))
   YYY=TD11NV*(DCOSH(EN)+TD1NV*DCOS(GN))
   A(NN+K8,NN+K7)=A(NN+K8,NN+K7)-XXX*RAT12S

   A(NN+K8,NN+K8)=A(NN+K8,NN+K8)-YYY*RAT12C

   XXX=TD11NPP*(1.+TD1NP)
   A(NN+K8,NN+K11)=-XXX
   A(NN+K11,NN+K11)=PHIST(NST)
   A(NN+K11,NN+K7)=-TD11NP*((ENS-POI*PHIS*ENPS)-TD1NP*(GNS+POI*PHIS*
1 ENPS))*PHIST(NST)*RAT12S
   A(NN+K11,NN+K8)=-TD11NV*((ENS-POI*PHIS*ENPS)-TD1NV*(GNS+POI*PHIS*
1 ENPS))*RAT12C*PHIST(NST)

850 CONTINUE

   CALL SCC11(BN,Z1,Z2,EMP,X2,X1)
   CALL SCC2(GN,Z1,Z2,EMP,Y2,Y1)
   XXX=-2.*TD11NPP*((-ENPS+POI*ENS/PHIS)*X1+TD1NP*(-ENPS-POI*
1 GNS/PHIS)*Y1)*DCOS(EMP)/DIV

   A(04+K9,NN+K11)=XXX*PHIST(NST)
   YYY=-2.*TD11NPP*((-ENPS+POI*ENS/PHIS)*X1+TD1NP*(-ENPS-POI*
1 GNS/PHIS)*Y1)/DIV

   A(04+K10,NN+K11)=YYY*PHIST(NST)

```

```

CALL SCC11 (BN,Z1,Z2,EMP,X2,X1)
CALL SCC2 (GN,Z1,Z2,EMP,Y2,Y1)
XCK=-2.*TD11MP*((-ENPS+POI*BNS/PHIS)*X1+TD1MP*(-ENPS-POI*
1 GNS/PHIS)*Y1)*DCOS(EMP)/DIV
XKV=-2.*TD11NV*((-ENPS+POI*BNS/PHIS)*X1+TD1NV*(-ENPS-POI*
1 GNS/PHIS)*Y1)*DCOS(EMP)/DIV

A (NN+K9,NN+K7)=-XCK*DCOS(EMP)*PHIST(NST)*RAT12S
A (NN+K9,NN+K8)=-XKV*DCOS(EMP)*PHIST(NST)*RAT12C

YYY=-2.*TD11MP*((-ENPS+POI*BNS/PHIS)*X1+TD1MP*(-ENPS-POI*
1 GNS/PHIS)*Y1)/DIV
YYV=-2.*TD11NV*((-ENPS+POI*BNS/PHIS)*X1+TD1NV*(-ENPS-POI*
1 GNS/PHIS)*Y1)/DIV

A (NN+K10,NN+K7)=-YYY*DCOS(EMP)*PHIST(NST)*RAT12S
A (NN+K10,NN+K8)=-YYV*DCOS(EMP)*PHIST(NST)*RAT12C

GO TO 560
800 ZZ=-ZZ
GN=PHI*DSQRT(ZZ)
GNS=GN*GN

TD2NV=-BN*DSINH(BN)/(GN*DSINH(GN))
TD22NV=-1./(BN*(BNS-POIS*PHIS*ENPS)*DSINH(BN)+TD2NV*GN*(GNS-POIS*
1 PHIS*ENPS)*DSINH(GN))

TD2NP=-BN*(BNS-POIS*PHIS*ENPS)*DSINH(BN)/(GN*(GNS-POIS*PHIS*ENPS)*
1 DSINH(GN))
TD22NP=-1./(BN*DSINH(BN)+TD2NP*GN*DSINH(GN))

TD22NPP=-1./((BNS-POI*PHIS*ENPS)*DCOSH(BN)+TD2NP*(GNS-POI*PHIS*
1 ENPS)*DCOSH(GN))
IF(M.GT.1) GO TO 451

XCK=-TD22NP*((BNS-POI*PHIS*ENPS)*DCOSH(BN)+TD2NP*(GNS-POI*PHIS*
1 ENPS)*DCOSH(GN))*PHIST(NST)*RAT12S*DE(NST)/DE(NST-1)
YYY=-TD22NV*((BNS-POI*PHIS*ENPS)*DCOSH(BN)+TD2NV*(GNS-POI*PHIS*
1 ENPS)*DCOSH(GN))*PHIST(NST)*RAT12C*DE(NST)/DE(NST-1)
A (NN+K7,NN+K7)=A (NN+K7,NN+K7)-XCK*PHIST(NST)/PHIST(NST-1)
A (NN+K7,NN+K8)=A (NN+K7,NN+K8)-YYY*PHIST(NST)/PHIST(NST-1)

A (NN+K7,NN+K11)=-TD22NPP*((BNS-POI*PHIS*ENPS)+TD2NP*(GNS-POI*PHIS*
1 ENPS))*PHIST(NST)*PHIST(NST)*DE(NST)/(PHIST(NST-1)*DE(NST-1))
XCK=TD22NP*(DCOSH(BN)+TD2NP*DCOSH(GN))
YYY=TD22NV*(DCOSH(BN)+TD2NV*DCOSH(GN))
A (NN+K8,NN+K7)=A (NN+K8,NN+K7)-XCK*RAT12S
A (NN+K8,NN+K8)=A (NN+K8,NN+K8)-YYY*RAT12C

XCK=TD22NPP*(1.+TD2NP)
A (NN+K8,NN+K11)=-XCK
A (NN+K11,NN+K11)=PHIST(NST)
A (NN+K11,NN+K7)=-TD22NP*((BNS-POI*PHIS*ENPS)+TD2NP*(GNS-POI*PHIS*
1 ENPS))*PHIST(NST)*RAT12S
A (NN+K11,NN+K8)=-TD22NV*((BNS-POI*PHIS*ENPS)+TD2NV*(GNS-POI*PHIS*
1 ENPS))*RAT12C*PHIST(NST)

451 CONTINUE

CALL SCC11 (BN,Z1,Z2,EMP,X2,X1)
CALL SCC11 (GN,Z1,Z2,EMP,Y2,Y1)
XCK=-2.*TD22NPP*((-ENPS+POI*BNS/PHIS)*X1+TD2NP*(-ENPS+POI*
1 GNS/PHIS)*Y1)*DCOS(EMP)/DIV

A (NN+K9,NN+K11)=-XCK*PHIST(NST)
YYY=-2.*TD22NPP*((-ENPS+POI*BNS/PHIS)*X1+TD2NP*(-ENPS+POI*
1 GNS/PHIS)*Y1)/DIV

A (NN+K10,NN+K11)=-YYY*PHIST(NST)

CALL SCC11 (BN,Z1,Z2,EMP,X2,X1)
CALL SCC11 (GN,Z1,Z2,EMP,Y2,Y1)
XCK=-2.*TD22NP*((-ENPS+POI*BNS/PHIS)*X1+TD2NP*(-ENPS+POI*
1 GNS/PHIS)*Y1)*DCOS(EMP)/DIV
XKV=-2.*TD22NV*((-ENPS+POI*BNS/PHIS)*X1+TD2NV*(-ENPS+POI*
1 GNS/PHIS)*Y1)*DCOS(EMP)/DIV

A (NN+K9,NN+K7)=-XCK*DCOS(EMP)*PHIST(NST)*RAT12S
A (NN+K9,NN+K8)=-XKV*DCOS(EMP)*PHIST(NST)*RAT12C

YYY=-2.*TD22NP*((-ENPS+POI*BNS/PHIS)*X1+TD2NP*(-ENPS+POI*
1 GNS/PHIS)*Y1)/DIV
YYV=-2.*TD22NV*((-ENPS+POI*BNS/PHIS)*X1+TD2NV*(-ENPS+POI*
1 GNS/PHIS)*Y1)/DIV

A (NN+K10,NN+K7)=-YYY*DCOS(EMP)*PHIST(NST)*RAT12S

```

A (M+K10, M+K8) = YV * DCOS (M) * PHIST (MST) * RAT12C
560 CONTINUE

74 CONTINUE
ALMDS-ALMDS

ZZ204850

C DO 2200 I=1, K
C DO 2200 J=1, K8
C A(I+K, J) = A(I+K3, J)
C A(I+K2, J) = A(I+K4, J)
C2200 A(I+K3, J) = A(I+K7, J)
C DO 2201 I=1, K4
C DO 2201 J=1, K
C A(I, J+K) = A(I, J+K3)
C A(I, J+K2) = A(I, J+K4)
C2201 A(I, J+K3) = A(I, J+K7)

KK = (NST*4) * K
IF (DEL.EQ.0.) GO TO 93

C DO 2205 I=1, KK
C AII = I
C WRITE (6,1) PI, AII
C PAUSE
C DO 2206 J=1, KK
C AJJ = J
C IF (J.NE.16) GO TO 2206
C PAUSE
C2206 WRITE (6,1) AII, AJJ, A(I, J)
C PAUSE
C2205 CONTINUE
C IF (PI.GT.0.) GO TO 118
C DO 2149 I=1, KK
C DO 2149 J=1, KK
2149 A(I, J) = A(I, J) / 10.

2117 CALL DETERM1(A, KK, Y)

ZZ204990

WRITE (6,1) ALMDS, Y

ZZ205010

6699 IF (ALMDS.LT.DLIM) GO TO 9

ZZ205020

GO TO 118

ZZ205030

93 CONTINUE

ZZ205100

DO 811 I=1, KK
811 ANS(I) = 0.

ZZ205140

C EVALUATE DRIVING COEFFICIENTS SO THAT MODE SHAPE CAN BE GENERATED
C LAST COEFFICIENT IS SET=-1.

C DO 5000 I=1, K
C AII = I
C DO 5001 J=1, K2
C XK = A(I+K4, J+K5) - A(I+K8, J+K9)
C AJJ = J
C5001 WRITE (6,1) AII, AJJ, XK
C PAUSE
C5000 CONTINUE
C WRITE (6,1) A(K8+1, K8+1), PI

CALL DETR(A, KK, ANS)

ZZ205170

C NOW PUT COEFFICIENTS, ANS, IN ORDER AND STORE IN ARRAYS EM AND EN.

XX = 1.
DO 8110 I=1, K
EM(1, I) = ANS(I+K) * XX
EM(2, I) = ANS(I+K2) * XX
EM(3, I) = ANS(I+K5) * XX
EM(4, I) = ANS(I+K6) * XX
EM(5, I) = ANS(I+K9) * XX
EM(6, I) = ANS(I+K10) * XX
IF (NST.EQ.3) GO TO 8110
EM(7, I) = ANS(I+K13) * XX
EM(8, I) = ANS(I+K14) * XX
8110 CONTINUE

DO 8111 I=1, K
EN(1, I) = ANS(I) * XX
EN(2, I) = ANS(I+K3) * XX
EN(3, I) = ANS(I+K4) * XX
EN(4, I) = ANS(I+K7) * XX
EN(5, I) = ANS(I+K8) * XX
EN(6, I) = ANS(I+K11) * XX
IF (NST.EQ.3) GO TO 8111
EN(6, I) = ANS(I+K11)

```

EN(7,I)=ANS(I+K12)
EN(8,I)=ANS(I+K15)

8111 CONTINUE
C EN(5,1)=1.

C DO 8120 I=1,K
C WRITE (6,1) EN(1,I),EN(2,I),EN(3,I),EN(4,I),EN(5,I)
C WRITE (6,1) EN(1,I),EN(2,I),EN(3,I),EN(4,I),EN(5,I)
C WRITE (6,1) EN(6,I),EN(6,I)
C8120 CONTINUE
C IF(PI.GT.0) GO TO 118

CALL SHAPERC
ZZ205620

IF(PI.GT.0.) GO TO 8200
SUM=0.
DO 8121 I=1,61
XX= (I-1)*PI/60.
SUM=SUM+WMY(3,61,I)
8121 CONTINUE
SUM= SUM/61.
WRITE (6,1) SUM,SUM,SUM
IF(PI.GT.0.) GO TO 118

C PRINT OUT SPAN DISPLACEMENTS ON GRID FORMAT AS DESIRED.
C NOTE: IF NST=3 , W(4,I,J) WILL =0.

8200 CONTINUE
DO 5000 I=1,61,1
DO 5001 J=1,20
JJ=1+(J-1)*3
5001 WW(I,J)=W(1,I,JJ)
DO 5002 J=21,40
JJ=1+(J-21)*3
5002 WW(I,J)=W(2,I,JJ)
DO 5003 J=41,61
JJ=1+(J-41)*3
5003 WW(I,J)=W(3,I,JJ)
5000 CONTINUE

CC DO 1241 I= 1,61,2
CC AII=I
C WRITE (6,1) PI
ZZ205940
CC DO 1240 J= 1,61,1
CC AJJ=J
C WRITE (6,1) AII,AJJ,WW(I,J)
ZZ205970
CC WRITE (8,1) WW(I,J)
ZZ205990
C1240 CONTINUE
C PAUSE
C1241 CONTINUE
C1240 WRITE (6,1) W(1,I,J),W(2,I,J),W(3,I,J)
C PAUSE
C XX= WS (1,I,61)-WS (2,I,1)
C YY= WS (2,I,61)-WS (3,I,1)
C ZZ= WV (1,I,61)-WV (2,I,1)
C ZZZ= WV (2,I,61)-WV (3,I,1)
C1241 CONTINUE

C DO 1340 I=1,61,3
C AII=I
C YY=W(2,I,61)-W(3,I,1)
C XX=W(1,I,61)-W(2,I,1)
C1340 WRITE (6,1) AII,XX,YY

C PAUSE
118 CONTINUE
STOP
END
ZZ206960
ZZ206970

```

□

SUBROUTINE PROGRAM "SUBSPAN" STARTS HERE

SUBROUTINE SEAPERC

IMPLICIT DOUBLE PRECISION (A-H,O-Z)

DIMENSION PHIST(25),AMMS(150),ANMS(150),ANNSS(150),EM(30,30),
C EN(30,30),W(4,61,61),WS(4,61,61),WGX(4,61,61),WGY(4,61,61),
C RATIO(25),WV(4,61,61),DE(25)

COMMON POI,POIS,PI,K,K2,K3,K4,NST,DE,
C K5,K6,K7,K8,K9,K10,K11,K12,ALMDS,ALMD1S,ALMD2S,WV,
C ALMD3S,PHIST,AMMS,ANMS,ANNSS,EM,EN,ALMDBS,W,WS,WGX,WGY,RATIO

1 FORMAT(7(E13.6,3X))

NCK=61
DO 47 L= 1,61,1
ETA=(L-1)/ FLOAT(NCK-1)
ET1=1.-ETA
DO 47 J= 1,61,3
PSI=(J-1)/ FLOAT(NCK-1)
PS1=1.-PSI

DO 540 M=1,K ZZ20

PHI=PHIST(1) ZZ

PHIS=PHI*PHI

ALMDS=ALMDBS/PHIS

EMP=(2*M-1)*PI/2.

EMPS=EMP*EMP ZZ20

EM=PHI*DSQRT(ALMDS+EMPS) ZZ20

EMS=EM*EM

ZZ=ALMDS-EMPS

IF(ZZ.LT.0.) GO TO 1000

GM=PHI*DSQRT(ZZ)

GMS=GM*GM

TD1M=-EM*(EMS-POIS*PHIS*EMPS)*DSINH(EM)/(GM*(GMS+POIS*PHIS*EMPS)

1 *DSIN(GM)

TD11M=1./(EM*DSINH(EM)-TD1M*GM*DSIN(GM))

W(1,L,J)=W(1,L,J)+EM(1,M)*TD11M*(DCOSH(EM*ETA)+TD1M*DCOS(GM*ETA))*

1 DSIN(EMP*PSI)/PHIST(1)

W(1,L,J)=W(1,L,J)+EM(2,M)*TD11M*(DCOSH(EM*ET1)+TD1M*DCOS(GM*ET1))*

1 DSIN(EMP*PSI)/PHIST(1)

WS(1,L,J)=WS(1,L,J)+EM(1,M)*EMP*TD11M*(DCOSH(EM*ETA)+TD1M*DCOS(GM

1 *ETA))*DCOS(EMP*PSI)

WS(1,L,J)=WS(1,L,J)+EM(2,M)*EMP*TD11M*(DCOSH(EM*ET1)+TD1M*DCOS(GM

1 *ET1))*DCOS(EMP*PSI)

WGY(1,L,J)=WGY(1,L,J)-EM(1,M)*TD11M*((EMS-POI*PHIS*EMPS)*DCOSH(EM

1 *ETA)-TD1M*(GMS+POI*PHIS*EMPS)*DCOS(GM*ETA))*DSIN(EMP*PSI)

WGY(1,L,J)=WGY(1,L,J)-EM(2,M)*TD11M*((EMS-POI*PHIS*EMPS)*DCOSH(EM

1 *ET1)-TD1M*(GMS+POI*PHIS*EMPS)*DCOS(GM*ET1))*DSIN(EMP*PSI)

WGX(1,L,J)=WGX(1,L,J)-EM(1,M)*TD11M*((-EMPS+POI*EMS/PHIS)*DCOSH(

1 EM*ETA)+TD1M*(-EMPS-POI*GMS/PHIS)*DCOS(GM*ETA))*DSIN(EMP*PSI)

WGX(1,L,J)=WGX(1,L,J)-EM(2,M)*TD11M*((-EMPS+POI*EMS/PHIS)*DCOSH(

1 EM*ET1)+TD1M*(-EMPS-POI*GMS/PHIS)*DCOS(GM*ET1))*DSIN(EMP*PSI)

GO TO 1610

1000 ZZ=-ZZ

GM=PHI*DSQRT(ZZ)

GMS=GM*GM

TD2M=-EM*(EMS-POIS*PHIS*EMPS)*DSINE(EM)/(GM*(GMS-POIS*PHIS*EMPS)

1 *DSINE(GM)

TD22M=1./(EM*DSINE(EM)+TD2M*GM*DSINE(GM))

W(1,L,J)=W(1,L,J)+EM(1,M)*TD22M*(DCOSH(EM*ETA)+TD2M*DCOSH(GM*ETA))*

1 *DSIN(EMP*PSI)/PHIST(1)

W(1,L,J)=W(1,L,J)+EM(2,M)*TD22M*(DCOSH(EM*ET1)+TD2M*DCOSH(GM*ET1))*

1 *DSIN(EMP*PSI)/PHIST(1)

WS(1,L,J)=WS(1,L,J)+EM(1,M)*EMP*TD22M*(DCOSH(EM*ETA)+TD2M*DCOSH(GM

1 *ETA))*DCOS(EMP*PSI)

WS(1,L,J)=WS(1,L,J)+EM(2,M)*EMP*TD22M*(DCOSH(EM*ET1)+TD2M*DCOSH(GM

1 *ET1))*DCOS(EMP*PSI)

WGY(1,L,J)=WGY(1,L,J)-EM(1,M)*TD22M*((EMS-POI*PHIS*EMPS)*DCOSH(EM

1 *ETA)+TD2M*(GMS-POI*PHIS*EMPS)*DCOS(GM*ETA))*DSIN(EMP*PSI)

WGY(1,L,J)=WGY(1,L,J)-EM(2,M)*TD22M*((EMS-POI*PHIS*EMPS)*DCOSH(EM

1 *ET1)+TD2M*(GMS-POI*PHIS*EMPS)*DCOS(GM*ET1))*DSIN(EMP*PSI)

WGX(1,L,J)=WGX(1,L,J)-EM(1,M)*TD22M*((-EMPS+POI*EMS/PHIS)*DCOSH(

1 EM*ETA)+TD2M*(-EMPS+POI*GMS/PHIS)*DCOS(GM*ETA))*DSIN(EMP*PSI)

WGX(1,L,J)=WGX(1,L,J)-EM(2,M)*TD22M*((-EMPS+POI*EMS/PHIS)*DCOSH(

```

1 (EM*ET1)+TD2M*(-EMPS+POI*GMS/PHIS)*DCOSH(GM*ET1)*DSIN(EMP*PSI)
1610 CONTINUE
DO 2620 I=2,NST-1
II=(I-1)*2+1
PHI=PHIST(I) ZZ
PHIS=PHI*PHI
ALMS=ALMS/PHIS
X=RATIO(I)
ALMS=ALMS*DSQRT(X)
EMP=(M-1)*PI ZZ
EMPS=EMP*EMP ZZ
EM=PHI*DSQRT(ALMS+EMPS) ZZ
EMS=EM*EM
ZZ=ALMS-EMPS
IF(ZZ.LT.0.) GO TO 3000
GM=PHI*DSQRT(ZZ)
GMS=GM*GM
TD1M=-EM*(EMS-POIS*PHIS*EMPS)*DSINH(EM)/(GM*(GMS+POIS*PHIS*EMPS)
1 *DSIN(GM))
TD1M=1./(EM*DSINH(EM)-TD1M*GM*DSIN(GM))

W(I,L,J)=W(I,L,J)+EM(II,M)*TD1M*(DCOSH(EM*ETA)+TD1M*DCOS(GM*ETA
1 ))*DCOS(EMP*PSI)/PHIST(I)
W(I,L,J)=W(I,L,J)+EM(II+1,M)*TD1M*(DCOSH(EM*ET1)+TD1M*DCOS(GM*ET1
1 ))*DCOS(EMP*PSI)/PHIST(I)

WS(I,L,J)=WS(I,L,J)-EM(II,M)*EMP*TD1M*(DCOSH(EM*ETA)+TD1M*DCOS(GM
1 *ETA))*DSIN(EMP*PSI)
WS(I,L,J)=WS(I,L,J)-EM(II+1,M)*EMP*TD1M*(DCOSH(EM*ET1)+TD1M*DCOS(
1 GM*ET1))*DSIN(EMP*PSI)

WMY(2,L,J)=WMY(2,L,J)-EM(3,M)*TD1M*((EMS-POI*PHIS*EMPS)*DCOSH(EM
1 *ETA)-TD1M*(GMS+POI*PHIS*EMPS)*DCOS(GM*ETA))*DCOS(EMP*PSI)
WMY(2,L,J)=WMY(2,L,J)-EM(4,M)*TD1M*((EMS-POI*PHIS*EMPS)*DCOSH(EM
1 *ET1)-TD1M*(GMS+POI*PHIS*EMPS)*DCOS(GM*ET1))*DCOS(EMP*PSI)

WMX(I,L,J)=WMX(I,L,J)-EM(II,M)*TD1M*((-EMPS+POI*EMS/PHIS)*DCOSH(
1 EM*ETA)+TD1M*(-EMPS-POI*GMS/PHIS)*DCOS(GM*ETA))*DCOS(EMP*PSI)

WMX(I,L,J)=WMX(I,L,J)-EM(II+1,M)*TD1M*((-EMPS+POI*EMS/PHIS)*DCOSH(
1 (EM*ET1)+TD1M*(-EMPS-POI*GMS/PHIS)*DCOS(GM*ET1))*DCOS(EMP*PSI)

GO TO 3600
3000 ZZ=-ZZ
GM=PHI*DSQRT(ZZ)
GMS=GM*GM
TD2M=-EM*(EMS-POIS*PHIS*EMPS)*DSINH(EM)/(GM*(GMS-POIS*PHIS*EMPS)
1 *DSIN(GM))
TD2M=1./(EM*DSINH(EM)+TD2M*GM*DSIN(GM))

W(I,L,J)=W(I,L,J)+EM(II,M)*TD2M*(DCOSH(EM*ETA)+TD2M*DCOSH(GM*
1 ETA))*DCOS(EMP*PSI)/PHIST(I)
W(I,L,J)=W(I,L,J)+EM(II+1,M)*TD2M*(DCOSH(EM*ET1)+TD2M*DCOSH(GM*
1 ET1))*DCOS(EMP*PSI)/PHIST(I)

WS(I,L,J)=WS(I,L,J)-EM(II,M)*EMP*TD2M*(DCOSH(EM*ETA)+TD2M*DCOSH(
1 GM*ETA))*DSIN(EMP*PSI)
WS(I,L,J)=WS(I,L,J)-EM(II+1,M)*EMP*TD2M*(DCOSH(EM*ET1)+TD2M*
1 DCOSH(GM*ET1))*DSIN(EMP*PSI)

WMY(2,L,J)=WMY(2,L,J)-EM(3,M)*TD2M*((EMS-POI*PHIS*EMPS)*DCOSH(EM
1 *ETA)+TD2M*(GMS-POI*PHIS*EMPS)*DCOSH(GM*ETA))*DCOS(EMP*PSI)
WMY(2,L,J)=WMY(2,L,J)-EM(4,M)*TD2M*((EMS-POI*PHIS*EMPS)*DCOSH(EM
1 *ET1)+TD2M*(GMS-POI*PHIS*EMPS)*DCOSH(GM*ET1))*DCOS(EMP*PSI)

WMX(I,L,J)=WMX(I,L,J)-EM(II,M)*TD2M*((-EMPS+POI*EMS/PHIS)*DCOSH(
1 EM*ETA)+TD2M*(-EMPS+POI*GMS/PHIS)*DCOSH(GM*ETA))*DCOS(EMP*PSI)

WMX(I,L,J)=WMX(I,L,J)-EM(II+1,M)*TD2M*((-EMPS+POI*EMS/PHIS)*DCOSH(
1 (EM*ET1)+TD2M*(-EMPS+POI*GMS/PHIS)*DCOSH(GM*ET1))*DCOS(EMP*PSI)

3600 CONTINUE
2620 CONTINUE

I=NST
II=2*NST-1
PHI=PHIST(NST) ZZ
PHIS=PHI*PHI
ALMS=ALMS/PHIS
X=RATIO(NST)
ALMS=ALMS*DSQRT(X)
EMP=(M-1)*PI ZZ
EMPS=EMP*EMP ZZ
EM=PHI*DSQRT(ALMS+EMPS) ZZ
EMS=EM*EM
ZZ=ALMS-EMPS
IF(ZZ.LT.0.) GO TO 6400

```

```

GM=PHI*DSQRT(ZZ)
GMS=GM*GM
TD1M=-EM*(BMS-POIS*PHIS*EMPS)*DSINH(EM)/(GM*(GMS+POIS*PHIS*EMPS)
1 *DSIN(GM)
TD1M=1./(EM*DSINH(EM)-TD1M*GM*DSIN(GM))

W(I,L,J)=W(I,L,J)+EM(II,M)*TD1M*(DCOSH(EM*ETA)+TD1M*DCOS(GM*ETA
1 ))*DCOS(EMP*PSI)/PHIST(I)
W(I,L,J)=W(I,L,J)+EM(II+1,M)*TD1M*(DCOSH(EM*ET1)+TD1M*DCOS(GM*ET1
1 ))*DCOS(EMP*PSI)/PHIST(I)

WS(I,L,J)=WS(I,L,J)-EM(II,M)*EMP*TD1M*(DCOSH(EM*ETA)+TD1M*DCOS(
1 GM*ETA))*DSIN(EMP*PSI)
WS(I,L,J)=WS(I,L,J)-EM(II+1,M)*EMP*TD1M*(DCOSH(EM*ET1)+TD1M*DCOS(
1 GM*ET1))*DSIN(EMP*PSI)

WIK(I,L,J)=WIK(I,L,J)-EM(II,M)*TD1M*((-EMPS+POI*BMS/PHIS)*DCOSH(
1 EM*ETA)+TD1M*(-EMPS-POI*GMS/PHIS)*DCOS(GM*ETA))*DCOS(EMP*PSI)

WIK(I,L,J)=WIK(I,L,J)-EM(II+1,M)*TD1M*((-EMPS+POI*BMS/PHIS)*DCOSH
1 (EM*ET1)+TD1M*(-EMPS-POI*GMS/PHIS)*DCOS(GM*ET1))*DCOS(EMP*PSI)

WXY(I,L,J)=WXY(I,L,J)-EM(II,M)*TD1M*((BMS-POI*PHIS*EMPS)*DCOSH(EM
1 *ETA)-TD1M*(GMS+POI*PHIS*EMPS)*DCOS(GM*ETA))*DCOS(EMP*PSI)
WXY(I,L,J)=WXY(I,L,J)-EM(II+1,M)*TD1M*((BMS-POI*PHIS*EMPS)*DCOSH(
1 EM*ET1)-TD1M*(GMS+POI*PHIS*EMPS)*DCOS(GM*ET1))*DCOS(EMP*PSI)

GO TO 3690
6400 ZZ=-ZZ
GM=PHI*DSQRT(ZZ)
GMS=GM*GM
TD2M=-EM*(BMS-POIS*PHIS*EMPS)*DSINH(EM)/(GM*(GMS-POIS*PHIS*EMPS)
1 *DSINH(GM)
TD2M=1./(EM*DSINH(EM)+TD2M*GM*DSINH(GM))

WS(I,L,J)=WS(I,L,J)-EM(II,M)*EMP*TD2M*(DCOSH(EM*ETA)+TD2M*DCOSH(
1 GM*ETA))*DSIN(EMP*PSI)
WS(I,L,J)=WS(I,L,J)-EM(II+1,M)*EMP*TD2M*(DCOSH(EM*ET1)+TD2M*
1 DCOSH(GM*ET1))*DSIN(EMP*PSI)

WIK(I,L,J)=WIK(I,L,J)-EM(II,M)*TD2M*((-EMPS+POI*BMS/PHIS)*DCOSH(
1 EM*ETA)+TD2M*(-EMPS+POI*GMS/PHIS)*DCOSH(GM*ETA))*DCOS(EMP*PSI)

WIK(I,L,J)=WIK(I,L,J)-EM(II+1,M)*TD2M*((-EMPS+POI*BMS/PHIS)*DCOSH
1 (EM*ET1)+TD2M*(-EMPS+POI*GMS/PHIS)*DCOSH(GM*ET1))*DCOS(EMP*PSI)

WXY(I,L,J)=WXY(I,L,J)-EM(II,M)*TD2M*((BMS-POI*PHIS*EMPS)*DCOSH(EM
1 *ETA)+TD2M*(GMS-POI*PHIS*EMPS)*DCOSH(GM*ETA))*DCOS(EMP*PSI)
WXY(I,L,J)=WXY(I,L,J)-EM(II+1,M)*TD2M*((BMS-POI*PHIS*EMPS)*DCOSH(
1 EM*ET1)+TD2M*(GMS-POI*PHIS*EMPS)*DCOSH(GM*ET1))*DCOS(EMP*PSI)

3690 CONTINUE
540 CONTINUE
ZZ20
DO 740 N=1,K
ENP=(N-1)*PI
ENPS=ENP*ENP
ALMDS=ALMDS
PHI=1./PHIST(1)
PHIS=PHI*PHI
EM=PHI*DSQRT(ALMDS+ENPS)
BMS=EM*EM
ZZ=ALMDS-ENPS
IF(ZZ.LT.0.) GO TO 2000
GM=PHI*DSQRT(ZZ)
GMS=GM*GM
TD1M=-DCOSH(EM)/DCOS(GM)
C TD1M=1./(BMS*DCOSH(EM)-TD1M*GMS*DCOS(GM))
TD1M=1./(EM*DSINH(EM)-TD1M*GM*DSIN(GM))
TD1MP=EM*(BMS-POIS*PHIS*EMPS)*DCOSH(EM)/(GM*(GMS+POIS*PHIS*EMPS)
1 *DCOS(GM))
C TD1MP=1./((BMS-POI*PHIS*EMPS)*DSINH(EM)-TD1MP*(GMS+POI*PHIS*
C 1 ENPS)*DSIN(GM))
C TD1MP=1./(EM*DCOSH(EM)+TD1MP*GM*DCOS(GM))
C TD1MV=(BMS-POI*PHIS*EMPS)*DSINH(EM)/((GMS+POI*PHIS*ENPS)*
C 1 DSIN(GM))
TD1MV=-EM*DCOSH(EM)/(GM*DCOS(GM))
TD11MV=1./(EM*(BMS-POIS*PHIS*EMPS)*DCOSH(EM)-TD1MV*GM*(GMS+POIS*
1 PHIS*EMPS)*DCOS(GM))
W(1,L,J)=W(1,L,J)+EM(1,M)*TD1M*(DCOSH(EM*PSI)+TD1M*DCOS(GM*PSI))*
1 DCOS(EMP*ETA)
W(1,L,J)=W(1,L,J)+EM(2,M)*TD1MP*(DSINH(EM*PSI)+TD1MP*DSIN(GM*PSI
1 ))*DCOS(EMP*ETA)

```

```

W(1,L,J)=W(1,L,J)+EN(3,M)*TD11NV*(DSINE(BN*PSI)+TD1NV*DSIN(GN*PSI
1))*DCOS(ENP*ETA)

WS(1,L,J)=WS(1,L,J)-EN(1,N)*TD11N*(BN*DSINE(BN*PSI)-TD1N*GN*DSIN(
1 GN*PSI))*DCOS(ENP*ETA)*PHIST(1)
WS(1,L,J)=WS(1,L,J)+EN(2,M)*TD11NP*(BN*DCOSH(BN*PSI)+TD1NP*GN*
1 DCOS(GN*PSI))*DCOS(ENP*ETA)*PHIST(1)
WS(1,L,J)=WS(1,L,J)+EN(3,N)*TD11NV*(BN*DCOSH(BN*PSI)+TD1NV*GN*DCOS
1(GN*PSI))*DCOS(ENP*ETA)*PHIST(1)

WXY(1,L,J)=WXY(1,L,J)-EN(1,N)*TD11N*((-ENPS+POI*BNS/PHIS)*DCOSH(
1 BN*PSI)+TD1N*(-ENPS-POI*GNS/PHIS)*DCOS(GN*PSI))*DCOS(ENP*ETA)*
1 PHIST(1)
WXY(1,L,J)=WXY(1,L,J)-EN(2,N)*TD11NP*((-ENPS+POI*BNS/PHIS)*DSINH(
1 BN*PSI)+TD1NP*(-ENPS-POI*GNS/PHIS)*DSIN(GN*PSI))*DCOS(ENP*ETA)*
1 PHIST(1)
WXY(1,L,J)=WXY(1,L,J)-EN(3,N)*TD11NV*((-ENPS+POI*BNS/PHIS)*DSINH(
1 BN*PSI)+TD1NV*(-ENPS-POI*GNS/PHIS)*DSIN(GN*PSI))*DCOS(ENP*ETA)*
1 PHIST(1)

WGX(1,L,J)=WGX(1,L,J)-EN(1,N)*TD11N*((BNS-POI*PHIS*ENPS)*DCOSH(
1 BN*PSI)-TD1N*(GNS+POI*PHIS*ENPS)*DCOS(GN*PSI))*DCOS(ENP*ETA)*
1 PHIST(1)

WGX(1,L,J)=WGX(1,L,J)-EN(2,N)*TD11NP*((BNS-POI*PHIS*ENPS)*DSINH(
1 BN*PSI)-TD1NP*(GNS+POI*PHIS*ENPS)*DSIN(GN*PSI))*DCOS(ENP*ETA)*
1 PHIST(1)

WGX(1,L,J)=WGX(1,L,J)-EN(3,N)*TD11NV*((BNS-POI*PHIS*ENPS)*DSINH(
1 BN*PSI)-TD1NV*(GNS+POI*PHIS*ENPS)*DSIN(GN*PSI))*DCOS(ENP*ETA)*
1 PHIST(1)

WV(1,L,J)=WV(1,L,J)-EN(3,N)*TD11NV*(BN*(BNS-POIS*PHIS*ENPS)*DCOSH
1(BN*PSI)-TD1NV*GN*(GNS+POIS*PHIS*ENPS)*DCOS(GN*PSI))*DCOS(ENP*
1 ETA)*PHIST(1)

2000 GO TO 2600
ZZ=-ZZ
GN=FHI*DSQRT(ZZ)
GNS=GN*GN

C TD2N=-DCOSH(BN)/DCOSH(GN)
TD22N=-1./(BNS*DCOSH(BN)+TD2N*GNS*DCOSH(GN))
TD22N=1./(BN*DSINH(BN)+TD2N*GN*DSINH(GN))
TD2NP=-BN*(BNS-POIS*PHIS*ENPS)*DCOSH(BN)/(GN*(GNS-POIS*PHIS*ENPS)
1*DCOSH(GN))
C TD22NP=-1./((BNS-POI*PHIS*ENPS)*DSINH(BN)+TD2NP*(GNS-POI*PHIS*
*DCOSH(GN))
C 1 ENPS)*DSINH(GN)
TD22NP=1./(BN*DCOSH(BN)+TD2NP*GN*DCOSH(GN))

C TD2NV=- (BNS-POI*PHIS*ENPS)*DSINH(BN)/((GNS-POI*PHIS*ENPS)*
C 1 DSINH(GN))
TD2NV=-BN*DCOSH(BN)/(GN*DCOSH(GN))
TD22NV=-1./(BN*(BNS-POIS*PHIS*ENPS)*DCOSH(BN)+TD2NV*GN*(GNS-POIS*
1 PHIS*ENPS)*DCOSH(GN))

W(1,L,J)=W(1,L,J)+EN(1,N)*TD22N*(DCOSH(BN*PSI)+TD2N*DCOSH(GN*PSI))
1*DCOS(ENP*ETA)
W(1,L,J)=W(1,L,J)+EN(2,N)*TD22NP*(DSINE(BN*PSI)+TD2NP*DSINE(GN*PSI
1))*DCOS(ENP*ETA)
W(1,L,J)=W(1,L,J)+EN(3,N)*TD22NV*(DSINE(BN*PSI)+TD2NV*DSINE(GN*PSI
1))*DCOS(ENP*ETA)

WS(1,L,J)=WS(1,L,J)-EN(1,N)*TD22N*(BN*DSINE(BN*PSI)+TD2N*GN*DSINE(
1 GN*PSI))*DCOS(ENP*ETA)*PHIST(1)
WS(1,L,J)=WS(1,L,J)+EN(2,N)*TD22NP*(BN*DCOSH(BN*PSI)+TD2NP*GN*
1 DCOSH(GN*PSI))*DCOS(ENP*ETA)*PHIST(1)
WS(1,L,J)=WS(1,L,J)+EN(3,N)*TD22NV*(BN*DCOSH(BN*PSI)+TD2NV*GN*
1 DCOSH(GN*PSI))*DCOS(ENP*ETA)*PHIST(1)

WXY(1,L,J)=WXY(1,L,J)-EN(1,N)*TD22N*((-ENPS+POI*BNS/PHIS)*DCOSH(
1 BN*PSI)+TD2N*(-ENPS+POI*GNS/PHIS)*DCOSH(GN*PSI))*DCOS(ENP*ETA)*
1 PHIST(1)
WXY(1,L,J)=WXY(1,L,J)-EN(2,N)*TD22NP*((-ENPS+POI*BNS/PHIS)*DSINH(
1 BN*PSI)+TD2NP*(-ENPS+POI*GNS/PHIS)*DSINE(GN*PSI))*DCOS(ENP*ETA)*
1 PHIST(1)
WXY(1,L,J)=WXY(1,L,J)-EN(3,N)*TD22NV*((-ENPS+POI*BNS/PHIS)*DSINH(
1 BN*PSI)+TD2NV*(-ENPS+POI*GNS/PHIS)*DSINE(GN*PSI))*DCOS(ENP*ETA)*
1 PHIST(1)

WGX(1,L,J)=WGX(1,L,J)-EN(1,N)*TD22N*((BNS-POI*PHIS*ENPS)*DCOSH(
1 BN*PSI)+TD2N*(GNS-POI*PHIS*ENPS)*DCOSH(GN*PSI))*DCOS(ENP*ETA)*
1 PHIST(1)
WGX(1,L,J)=WGX(1,L,J)-EN(2,N)*TD22NP*((BNS-POI*PHIS*ENPS)*DSINE(
1 BN*PSI)+TD2NP*(GNS-POI*PHIS*ENPS)*DSINE(GN*PSI))*DCOS(ENP*ETA)*
1 PHIST(1)

```

```

WGX(1,L,J)=WGX(1,L,J)-EN(3,M)*TD22NV*( (BNS-POI*PHIS*ENPS)*DSINE(
1 EN*PSI)+TD2NV*(GNS-POI*PHIS*ENPS)*DSINE(GN*PSI))*DCOS(ENP*ETA)*
1 PHIST(1)

WV(1,L,J)=WV(1,L,J)-EN(3,N)*TD22NV*(EN*(BNS-POIS*PHIS*ENPS)*DCOSH
1 (EN*PSI)+TD2NV*GN*(GNS-POIS*PHIS*ENPS)*DCOSH(GN*PSI))*DCOS(ENP*
1 ETA)*PHIST(1)

2600 CONTINUE

DO 2630 I=2,NST-1

RAT12S=PHIST(I-1)*PHIST(I-1)/(PHIST(I)*PHIST(I))
RAT12C=RAT12S*PHIST(I-1)/PHIST(I)
RAT12C=RAT12C*(DE(I-1)/DE(I))
RAT12S=PHIST(I-1)/PHIST(I)
X=RATIO(I)
ALMS=ALMS*DSQRT(X)
II=(I-1)*2+1
PHI=1./PHIST(I)
PHIS=PHI*PHI
EN=PHI*DSQRT(ALMS+ENPS)
ENS=EN*EN
ZZ=ALMS-ENPS
IF(ZZ.LT.0.) GO TO 4000
GN=PHI*DSQRT(ZZ)
GNS=GN*GN

C
TD1NV=(BNS-POI*PHIS*ENPS)*DCOSH(EN)/((GNS+POI*PHIS*ENPS)*DCOS(GN))
TD1NV=EN*DSINE(EN)/(GN*DSIN(GN))
TD11NV=1./ (EN*(BNS-POIS*PHIS*ENPS)*DSINE(EN)+TD1NV*GN*(GNS+POIS*
1 PHIS*ENPS)*DSIN(GN))

TD1NP=-EN*(BNS-POIS*PHIS*ENPS)*DSINE(EN)/(GN*(GNS+POIS*PHIS*ENPS)*
1 DSIN(GN))
TD11NP=1./ (EN*DSINE(EN)-TD1NP*GN*DSIN(GN))

W(I,L,J)=W(I,L,J)+EN(I,N)*TD11NP*(DCOSH(EN*PSI)+TD1NP*DCOS(GN*
1 PSI))*DCOS(ENP*ETA)*RAT12S
W(I,L,J)=W(I,L,J)+EN(I+1,N)*TD11NV*(DCOSH(EN*PSI)+TD1NV*DCOS(GN*
1 W2S(L,J)=W2S(L,J)+EN21(N)*TD11N*(EN*DCOSH(EN*PSI)+TD1N*
1 PSI))*DCOS(ENP*ETA)*RAT12C
GN*DCOS(GN*PSI))*DCOS(ENP*ETA)

W(I,L,J)=W(I,L,J)+EN(I+2,N)*TD11NP*(DCOSH(EN*PSI)+TD1NP*DCOS(GN
1 *PSI))*DCOS(ENP*ETA)
W(I,L,J)=W(I,L,J)+EN(I+3,N)*TD11NV*(DCOSH(EN*PSI)+TD1NV*DCOS(GN*
1 PSI))*DCOS(ENP*ETA)

WS(I,L,J)=WS(I,L,J)-EN(I,N)*TD11NP*(EN*DSINE(EN*PSI)-TD1NP*GN*
1 DSIN(GN*PSI))*DCOS(ENP*ETA)*PHIST(I)*RAT12S
WS(I,L,J)=WS(I,L,J)-EN(I+1,N)*TD11NV*(EN*DSINE(EN*PSI)-TD1NV*GN*
1 DSIN(GN*PSI))*DCOS(ENP*ETA)*RAT12C*PHIST(I)

WS(I,L,J)=WS(I,L,J)+EN(I+2,N)*TD11NP*(EN*DSINE(EN*PSI)-TD1NP*GN*
1 DSIN(GN*PSI))*DCOS(ENP*ETA)*PHIST(I)
WS(I,L,J)=WS(I,L,J)+EN(I+3,N)*TD11NV*(EN*DSINE(EN*PSI)-TD1NV*GN*
1 DSIN(GN*PSI))*DCOS(ENP*ETA)*PHIST(I)

WXY(I,L,J)=WXY(I,L,J)-EN(I,N)*TD11NP*((-ENPS+POI*ENS/PHIS)*DCOSH
1 (EN*PSI)+TD1NP*(-ENPS-POI*GNS/PHIS)*DCOS(GN*PSI))*DCOS(ENP*ETA)*
1 PHIST(I)*RAT12S
WXY(I,L,J)=WXY(I,L,J)-EN(I+1,N)*TD11NV*((-ENPS+POI*ENS/PHIS)*DCOSH
1 (EN*PSI)+TD1NV*(-ENPS-POI*GNS/PHIS)*DCOS(GN*PSI))*DCOS(ENP*ETA)*
1 PHIST(I)*RAT12C
WXY(I,L,J)=WXY(I,L,J)-EN(I+2,N)*TD11NP*((-ENPS+POI*ENS/PHIS)*DCOSH
1 (EN*PSI)+TD1NP*(-ENPS-POI*GNS/PHIS)*DCOS(GN*PSI))*DCOS(ENP*ETA)*
1 PHIST(I)
WXY(I,L,J)=WXY(I,L,J)-EN(I+3,N)*TD11NV*((-ENPS+POI*ENS/PHIS)*DCOSH
1 (EN*PSI)+TD1NV*(-ENPS-POI*GNS/PHIS)*DCOS(GN*PSI))*DCOS(ENP*ETA)*
1 PHIST(I)

WGX(I,L,J)=WGX(I,L,J)-EN(I,N)*TD11NP*((BNS-POI*PHIS*ENPS)*DCOSH(
1 EN*PSI)-TD1NP*(GNS+POI*PHIS*ENPS)*DCOS(GN*PSI))*DCOS(ENP*ETA)*
1 PHIST(I)*RAT12S

WGX(I,L,J)=WGX(I,L,J)-EN(I+1,N)*TD11NV*((BNS-POI*PHIS*ENPS)*DCOSH(
1 EN*PSI)-TD1NP*(GNS+POI*PHIS*ENPS)*DCOS(GN*PSI))*DCOS(ENP*ETA)*
1 PHIST(I)*RAT12C

WGX(I,L,J)=WGX(I,L,J)-EN(I+2,N)*TD11NP*((BNS-POI*PHIS*ENPS)*DCOSH(
1 EN*PSI)-TD1NP*(GNS+POI*PHIS*ENPS)*DCOS(GN*PSI))*DCOS(ENP*
1 ETA)*PHIST(I)

WGX(I,L,J)=WGX(I,L,J)-EN(I+3,N)*TD11NV*((BNS-POI*PHIS*ENPS)*DCOSH(
1 EN*PSI)-TD1NP*(GNS+POI*PHIS*ENPS)*DCOS(GN*PSI))*DCOS(ENP*

```

1

```

1 ETA)*PHIST(I)

WV(I,L,J)=WV(I,L,J)+EN(I+1,N)*TD11NV*(BN*(BNS-POIS*PHIS*ENPS)*
1 DSINE(BN*PSI)+TD1NV*GN*(GNS+POIS*PHIS*ENPS)*DSIN(GN*PSI))*DCOS(
1 ENP*ETA)*PHIST(I)*RAT12C

WV(I,L,J)=WV(I,L,J)-EN(I+3,N)*TD11NV*(BN*(BNS-POIS*PHIS*ENPS)*
1 DSINE(BN*PSI)+TD1NV*GN*(GNS+POIS*PHIS*ENPS)*DSIN(GN*PSI))*DCOS(
1 ENP*ETA)*PHIST(I)
GO TO 4600
4000 ZZ=ZZ
GN=PHI*DSQRT(ZZ)
GNS=GN*GN

C TD2NV=- (BNS-POI*PHIS*ENPS)*DCOSH(BN)/((GNS-POI*PHIS*ENPS)*
C 1 DCOSH(GN))
TD2NV=-BN*DSINE(BN)/(GN*DSINE(GN))
TD22NV=-1./ (BN*(BNS-POIS*PHIS*ENPS)*DSINE(BN)+TD2NV*GN*(GNS-POIS*
1 PHIS*ENPS)*DSINE(GN))

TD2NP=-BN*(BNS-POIS*PHIS*ENPS)*DSINE(BN)/(GN*(GNS-POIS*PHIS*ENPS)*
1 DSINE(GN))
C TD22NP=-1./((BNS-POI*PHIS*ENPS)*DCOSH(BN)+TD2NP*(GNS-POI*PHIS*
C 1 ENPS)*DCOSH(GN))
C TD22NP=-1./ (BN*DSINE(BN)+TD2NP*GN*DSINE(GN))

W(I,L,J)=W(I,L,J)+EN(I,N)*TD22NP*(DCOSH(BN*PSI)+TD2NP*DCOSH(GN*
1 PS1))*DCOS(ENP*ETA)*RAT12S
W(I,L,J)=W(I,L,J)+EN(I+1,N)*TD22NV*(DCOSH(BN*PSI)+TD2NV*DCOSH(GN*
1 PS1))*DCOS(ENP*ETA)*RAT12C

W(I,L,J)=W(I,L,J)+EN(I+2,N)*TD22NP*(DCOSH(BN*PSI)+TD2NP*DCOSH(GN
1 *PSI))*DCOS(ENP*ETA)
W(I,L,J)=W(I,L,J)+EN(I+3,N)*TD22NV*(DCOSH(BN*PSI)+TD2NV*DCOSH(GN*
1 PS1))*DCOS(ENP*ETA)

WS(I,L,J)=WS(I,L,J)-EN(I,N)*TD22NP*(BN*DSINE(BN*PSI)+TD2NP*GN*
1 DSINE(GN*PS1))*DCOS(ENP*ETA)*PHIST(I)*RAT12S
WS(I,L,J)=WS(I,L,J)-EN(I+1,N)*TD22NV*(BN*DSINE(BN*PSI)+TD2NV*GN*
1 DSINE(GN*PS1))*DCOS(ENP*ETA)*RAT12C*PHIST(I)

WS(I,L,J)=WS(I,L,J)+EN(I+2,N)*TD22NP*(BN*DSINE(BN*PSI)+TD2NP*GN*
1 DSINE(GN*PS1))*DCOS(ENP*ETA)*PHIST(I)
WS(I,L,J)=WS(I,L,J)+EN(I+3,N)*TD22NV*(BN*DSINE(BN*PSI)+TD2NV*GN*
1 DSINE(GN*PS1))*DCOS(ENP*ETA)*PHIST(I)

WXY(I,L,J)=WXY(I,L,J)-EN(I,N)*TD22NP*((-ENPS+POI*BNS/PHIS)*DCOSH
1 (BN*PSI)+TD2NP*(-ENPS+POI*GNS/PHIS)*DCOSH(GN*PS1))*DCOS(ENP*ETA)*
1 PHIST(I)*RAT12S
WXY(I,L,J)=WXY(I,L,J)-EN(I+1,N)*TD22NV*((-ENPS+POI*BNS/PHIS)*DCOSH
1 (BN*PSI)+TD2NV*(-ENPS+POI*GNS/PHIS)*DCOSH(GN*PS1))*DCOS(ENP*ETA)*
1 PHIST(I)*RAT12C
WXY(I,L,J)=WXY(I,L,J)-EN(I+2,N)*TD22NP*((-ENPS+POI*BNS/PHIS)*DCOSH
1 (BN*PSI)+TD2NP*(-ENPS+POI*GNS/PHIS)*DCOSH(GN*PSI))*DCOS(ENP*ETA)*
1 PHIST(I)
WXY(I,L,J)=WXY(I,L,J)-EN(I+3,N)*TD22NV*((-ENPS+POI*BNS/PHIS)*DCOSH
1 (BN*PSI)+TD2NV*(-ENPS+POI*GNS/PHIS)*DCOSH(GN*PSI))*DCOS(ENP*ETA)*
1 PHIST(I)

WGX(I,L,J)=WGX(I,L,J)-EN(I,N)*TD22NP*((BNS-POI*PHIS*ENPS)*DCOSH(
1 BN*PSI)+TD2NP*(GNS-POI*PHIS*ENPS)*DCOSH(GN*PS1))*DCOS(ENP*ETA)*
1 PHIST(I)*RAT12S

WGX(I,L,J)=WGX(I,L,J)-EN(I+1,N)*TD22NV*((BNS-POI*PHIS*ENPS)*DCOSH(
1 BN*PSI)+TD2NV*(GNS-POI*PHIS*ENPS)*DCOSH(GN*PS1))*DCOS(ENP*ETA)*
1 PHIST(I)*RAT12C

ZZZ= TD22NV*((BNS-POI*PHIS*ENPS)*DCOSH(
1 BN*PSI)+TD2NV*(GNS-POI*PHIS*ENPS)*DCOSH(GN*PS1))*DCOS(ENP*ETA)*
1 PHIST(I)*RAT12C

WGX(I,L,J)=WGX(I,L,J)-EN(I+2,N)*TD22NP*((BNS-POI*PHIS*ENPS)*DCOSH(
1 BN*PSI)+TD2NP*(GNS-POI*PHIS*ENPS)*DCOSH(GN*PSI))*DCOS(ENP*
1 ETA)*PHIST(I)

WGX(I,L,J)=WGX(I,L,J)-EN(I+3,N)*TD22NV*((BNS-POI*PHIS*ENPS)*DCOSH(
1 BN*PSI)+TD2NV*(GNS-POI*PHIS*ENPS)*DCOSH(GN*PSI))*DCOS(ENP*
1 ETA)*PHIST(I)

WV(I,L,J)=WV(I,L,J)+EN(I+1,N)*TD22NV*(BN*(BNS-POIS*PHIS*ENPS)*
1 DSINE(BN*PSI)+TD2NV*GN*(GNS-POIS*PHIS*ENPS)*DSINE(GN*PSI))*DCOS(
1 ENP*ETA)*PHIST(I)*RAT12C

WV(I,L,J)=WV(I,L,J)-EN(I+3,N)*TD22NV*(BN*(BNS-POIS*PHIS*ENPS)*
1 DSINE(BN*PSI)+TD2NV*GN*(GNS-POIS*PHIS*ENPS)*DSINE(GN*PSI))*DCOS(
1 ENP*ETA)*PHIST(I)

```

4600 CONTINUE
2630 CONTINUE

```
RAT12B=PHIST(MST-1)*PHIST(MST-1)/(PHIST(MST)*PHIST(MST))
RAT12C=RAT12B*PHIST(MST-1)/PHIST(MST)
RAT12C=RAT12C*(DE(MST-1)/DE(MST))
RAT12B=PHIST(MST-1)/PHIST(MST)
II=2*MST
I=MST
X=RATIO(MST)
ALMDS=ALMDSB*DSQRT(X)
PHI=1./PHIST(MST)
PHIS=PHI*PHI

EN=PHI*DSQRT(ALMDS+ENPS)
ENS=EN*EN
ZZ=ALMDS-ENPS
IF(ZZ.LT.0.) GO TO 8000
GN=PHI*DSQRT(ZZ)
GNS=GN*GN

C   TD1NV=(ENS-POI*PHIS*ENPS)*DCOSH(EN)/((GNS+POI*PHIS*ENPS)*DCOS(GN))
   TD1NV=EN*DSINH(EN)/(GN*DSIN(GN))
   TD11NV=-1./(EN*(ENS-POIS*PHIS*ENPS)*DSINH(EN)+TD1NV*GN*(GNS+POIS*
1  PHIS*ENPS)*DSIN(GN))

   TD1NP=-EN*(ENS-POIS*PHIS*ENPS)*DSINH(EN)/(GN*(GNS+POIS*PHIS*ENPS)*
1  DSIN(GN))
   TD11NP=1./(EN*DSINH(EN)-TD1NP*GN*DSIN(GN))

   TD11NPP=-1./((ENS-POI*PHIS*ENPS)*DCOSH(EN)-TD1NP*(GNS+POI*PHIS*
1  ENPS)*DCOS(GN))

   W(I,L,J)=W(I,L,J)+EN(I+1,N)*TD11NP*(DCOSH(EN*PSI)+TD1NP*DCOS(GN*
1  PSI))*DCOS(ENP*ETA)*RAT12S

   W(I,L,J)=W(I,L,J)+EN(I+2,N)*TD11NV*(DCOSH(EN*PSI)+TD1NV*DCOS(GN*
1  PSI))*DCOS(ENP*ETA)*RAT12C
   W(I,L,J)=W(I,L,J)+EN(I+3,N)*TD11NPP*(DCOSH(EN*PSI)+TD1NP*DCOS(GN*
1  PSI))*DCOS(ENP*ETA)

   WS(I,L,J)=WS(I,L,J)-EN(I+1,N)*TD11NP*(EN*DSINH(EN*PSI)-TD1NP*GN*
1  DSIN(GN*PSI))*DCOS(ENP*ETA)*PHIST(I)*RAT12S
   WS(I,L,J)=WS(I,L,J)-EN(I+2,N)*TD11NV*(EN*DSINH(EN*PSI)-TD1NP*GN*
1  DSIN(GN*PSI))*DCOS(ENP*ETA)*RAT12C*PHIST(I)
   WS(I,L,J)=WS(I,L,J)+EN(I+3,N)*TD11NPP*(EN*DSINH(EN*PSI)-TD1NP*GN*
1  DSIN(GN*PSI))*DCOS(ENP*ETA)*PHIST(I)

   WCK(I,L,J)=WCK(I,L,J)-EN(I+1,N)*TD11NP*((ENS-POI*PHIS*ENPS)*DCOSH(
1  EN*PSI)-TD1NP*(GNS+POI*PHIS*ENPS)*DCOS(GN*PSI))*RAT12S*DCOS(ENP*
1  ETA)*PHIST(I)

   WCK(I,L,J)=WCK(I,L,J)-EN(I+2,N)*TD11NV*((ENS-POI*PHIS*ENPS)*DCOSH(
1  EN*PSI)-TD1NP*(GNS+POI*PHIS*ENPS)*DCOS(GN*PSI))*RAT12C*DCOS(ENP*
1  ETA)*PHIST(I)
   WCK(I,L,J)=WCK(I,L,J)-EN(I+3,N)*TD11NPP*((ENS-POI*PHIS*ENPS)*DCOSH
1  (EN*PSI)-TD1NP*(GNS+POI*PHIS*ENPS)*DCOS(GN*PSI))*DCOS(ENP*
1  ETA)*PHIST(I)

   WMY(I,L,J)=WMY(I,L,J)-EN(I+1,N)*TD11NP*((-ENPS+POI*ENS/PHIS)*DCOSH
1  (EN*PSI)+TD1NP*(-ENPS-POI*GNS/PHIS)*DCOS(GN*PSI))*DCOS(ENP*ETA)*
1  PHIST(I)*RAT12S

   WMY(I,L,J)=WMY(I,L,J)-EN(I+2,N)*TD11NV*((-ENPS+POI*ENS/PHIS)*DCOSH
1  (EN*PSI)+TD1NP*(-ENPS-POI*GNS/PHIS)*DCOS(GN*PSI))*DCOS(ENP*ETA)*
1  PHIST(I)*RAT12C
   WMY(I,L,J)=WMY(I,L,J)-EN(I+3,N)*TD11NPP*((-ENPS+POI*ENS/PHIS)*
1  DCOSH(EN*PSI)+TD1NP*(-ENPS-POI*GNS/PHIS)*DCOS(GN*PSI))*DCOS(ENP*
1  ETA)*PHIST(I)

   WV(I,L,J)=WV(I,L,J)+EN(I+2,N)*TD11NV*(EN*(ENS-POIS*PHIS*ENPS)*
1  DSINH(EN*PSI)+TD1NV*GN*(GNS+POIS*PHIS*ENPS)*DSIN(GN*PSI))*DCOS(
1  ENP*ETA)*PHIST(I)*RAT12C
   GO TO 5600
8000 ZZ=ZZ
   GN=PHI*DSQRT(ZZ)
   GNS=GN*GN

C   TD2NV=(ENS-POI*PHIS*ENPS)*DCOSH(EN)/((GNS-POI*PHIS*ENPS)*
C   1 DCOSH(EN))
   TD2NV=-EN*DSINH(EN)/(GN*DSINH(GN))
   TD22NV=-1./(EN*(ENS-POIS*PHIS*ENPS)*DSINH(EN)+TD2NV*GN*(GNS-POIS*
1  PHIS*ENPS)*DSINH(GN))

   TD2NP=-EN*(ENS-POIS*PHIS*ENPS)*DSINH(EN)/(GN*(GNS-POIS*PHIS*ENPS)*
1  DSINH(GN))
C   TD22NP=-1./((ENS-POI*PHIS*ENPS)*DCOSH(EN)+TD2NP*(GNS-POI*PHIS*
```

```

C      1 ENPS)*DCOSH(GM)
      TD22NP=1./(BN*DSINE(BN)+TD2NP*GM*DSINE(GM))

      TD22NPP=-1./((BNS-POI*PHIS*ENPS)*DCOSH(BN)+TD2NP*(GNS-POI*PHIS*
1 ENPS)*DCOSH(GM))

      W(I,L,J)=W(I,L,J)+EN(I+1,N)*TD22NP*(DCOSH(BN*PSI)+TD2NP*DCOSH(GM*
1 PSI))*DCOS(ENP*ETA)*RAT12S
      W(I,L,J)=W(I,L,J)+EN(I+2,N)*TD22NV*(DCOSH(BN*PSI)+TD2NP*DCOSH(GM*
1 PSI))*DCOS(ENP*ETA)*RAT12C
      W(I,L,J)=W(I,L,J)+EN(I+3,N)*TD22NPP*(DCOSH(BN*PSI)+TD2NP*DCOSH(GM*
1 PSI))*DCOS(ENP*ETA)

      WS(I,L,J)=WS(I,L,J)-EN(I+1,N)*TD22NP*(BN*DSINE(BN*PSI)+TD2NP*GM*
1 DSINE(GM*PSI))*DCOS(ENP*ETA)*PHIST(I)*RAT12S
      WS(I,L,J)=WS(I,L,J)-EN(I+2,N)*TD22NV*(BN*DSINE(BN*PSI)+TD2NP*GM*
1 DSINE(GM*PSI))*DCOS(ENP*ETA)*RAT12C*PHIST(I)
      WS(I,L,J)=WS(I,L,J)+EN(I+3,N)*TD22NPP*(BN*DSINE(BN*PSI)+TD2NP*GM*
1 DSINE(GM*PSI))*DCOS(ENP*ETA)*PHIST(I)

      WMX(I,L,J)=WMX(I,L,J)-EN(I+1,N)*TD22NP*((BNS-POI*PHIS*ENPS)*DCOSH(
1 BN*PSI)+TD2NP*(GNS-POI*PHIS*ENPS)*DCOSH(GM*PSI))*RAT12S*DCOS(ENP*
1 ETA)*PHIST(I)

      WMX(I,L,J)=WMX(I,L,J)-EN(I+2,N)*TD22NV*((BNS-POI*PHIS*ENPS)*DCOSH(
1 BN*PSI)+TD2NP*(GNS-POI*PHIS*ENPS)*DCOSH(GM*PSI))*RAT12C*DCOS(ENP*
1 ETA)*PHIST(I)

      WMX(I,L,J)=WMX(I,L,J)-EN(I+3,N)*TD22NPP*((BNS-POI*PHIS*ENPS)*DCOSH
1 (BN*PSI)+TD2NP*(GNS-POI*PHIS*ENPS)*DCOSH(GM*PSI))*DCOS(ENP*
1 ETA)*PHIST(I)

      WMY(I,L,J)=WMY(I,L,J)-EN(I+1,N)*TD22NP*((-ENPS+POI*BNS/PHIS)*DCOSH
1 (BN*PSI)+TD2NP*(-ENPS+POI*GNS/PHIS)*DCOSH(GM*PSI))*DCOS(ENP*ETA)*
1 PHIST(I)*RAT12S
      WMY(I,L,J)=WMY(I,L,J)-EN(I+2,N)*TD22NV*((-ENPS+POI*BNS/PHIS)*DCOSH
1 (BN*PSI)+TD2NP*(-ENPS+POI*GNS/PHIS)*DCOSH(GM*PSI))*DCOS(ENP*ETA)*
1 PHIST(I)*RAT12C
      WMY(I,L,J)=WMY(I,L,J)-EN(I+3,N)*TD22NPP*((-ENPS+POI*BNS/PHIS)*
1 DCOSH(BN*PSI)+TD2NP*(-ENPS+POI*GNS/PHIS)*DCOSH(GM*PSI))*DCOS(ENP*
1 ETA)*PHIST(I)

      WV(I,L,J)=WV(I,L,J)+EN(I+2,N)*TD22NV*(BN*(BNS-POIS*PHIS*ENPS)*
1 DSINE(BN*PSI)+TD2NP*GM*(GNS-POIS*PHIS*ENPS)*DSINE(GM*PSI))*DCOS(
1 ENP*ETA)*PHIST(I)*RAT12C
5600 CONTINUE

740 CONTINUE
47 CONTINUE

      RETURN
      END

      SUBROUTINE SBAPRT
      IMPLICIT DOUBLE PRECISION (A-H,O-Z)

      DIMENSION PHIST(25),AMMS(150),ANNS(150),ANNSS(150),EM(30,30),
C EN(30,30),W(4,61,61)

      COMMON          POI,POIS,PI,K,K2,K3,K4,NST,
C K5,K6,K7,K8,K9,K10,K11,K12,ALMS,ALM1S,ALM2S,
C ALM3S,          PHIST,AMMS,ANNS,ANNSS,EM,EN,ALMDBS,W

1 FORMAT(7(E13.6,3X))

      NKK=61
      DO 47 L= 1, 1,3
      ETA=(L-1)/ FLOAT(NKK-1)
      ET1=1.-ETA
      LL=62-L
      DO 47 J= 1,61,3
      PSI=(J-1)/ FLOAT(NKK-1)
      PS1=1.-PSI

      DO 540 M=1,K                                          ZZ20

      PHI=PHIST(1)                                          ZZ
      PHIS=PHI*PHI
      ALMS=ALMDBS/PHIS
      ENP=PI*PI                                          ZZ20
      ENPS=ENP*ENP                                          ZZ20
      ENP=(N-1)*PI                                          ZZ
      EM=PHI*DSQRT(ALMS+ENPS)                               ZZ20
      EN=EM*EM
      ES=ALMS-ENPS

```

```

IF(ZZ.LT.0.) GO TO 1000
GM=PHI*DSQRT(ZZ)
GMS=GM*GM
TD1M=-EM*(BMS-POIS*PHIS*EMPS)*DSINE(BM)/(GM*(GMS+POIS*PHIS*EMPS)
1 *DSIN(GM)
C TD1M=-1./((BMS-POI*PHIS*EMPS)*DCOSH(BM)-TD1M*(GMS+POI*PHIS*EMPS)
C 1 *DCOS(GM)
TD1M=1./(BM*DSINE(BM)-TD1M*GM*DSIN(GM))

W(1,L,J)=W(1,L,J)+EM(M,1)*TD1M*(DCOSH(BM*ETA)+TD1M*DCOS(GM*ETA))*
1 DSIN(EMP*PSI)
W(1,L,J)=W(1,L,J)+EM(M,2)*TD1M*(DCOSH(BM*ET1)+TD1M*DCOS(GM*ET1))*
1 DSIN(EMP*PSI)

GO TO 1610
1000 ZZ=-ZZ
GM=PHI*DSQRT(ZZ)
GMS=GM*GM
TD2M=-EM*(BMS-POIS*PHIS*EMPS)*DSINE(BM)/(GM*(GMS-POIS*PHIS*EMPS)
1 *DSINE(GM)
C TD2M=-1./((BMS-POI*PHIS*EMPS)*DCOSH(BM)+TD2M*(GMS-POI*PHIS*EMPS)
C 1 *DCOSH(GM)
TD2M=1./(BM*DSINE(BM)+TD2M*GM*DSINE(GM))

W(1,L,J)=W(1,L,J)+EM(M,1)*TD2M*(DCOSH(BM*ETA)+TD2M*DCOSH(GM*ETA))
1 *DSIN(EMP*PSI)
W(1,L,J)=W(1,L,J)+EM(M,2)*TD2M*(DCOSH(BM*ET1)+TD2M*DCOSH(GM*ET1))
1 *DSIN(EMP*PSI)
1610 CONTINUE

DO 2620 I=2,NST-1
II=(I-1)*2+1
C II=I
PHI=PHIST(I) ZZ
PHIS=PHI*PHI
ALMS=ALMDS/PHIS
EMP=M*PI ZZ
EMPS=EMP*EMP ZZ
ENP=(N-1)*PI Z
EM=PHI*DSQRT(ALMS+EMPS) ZZ
BMS=EM*EM
ZZ=ALMS-EMPS
IF(ZZ.LT.0.) GO TO 3000
GM=PHI*DSQRT(ZZ)
GMS=GM*GM
TD1M=-EM*(BMS-POIS*PHIS*EMPS)*DSINE(BM)/(GM*(GMS+POIS*PHIS*EMPS)
1 *DSIN(GM)
C TD1M=-1./((BMS-POI*PHIS*EMPS)*DCOSH(BM)-TD1M*(GMS+POI*PHIS*EMPS)
C 1 *DCOS(GM)
TD1M=1./(BM*DSINE(BM)-TD1M*GM*DSIN(GM))

W(I,L,J)=W(I,L,J)+EM(M,II)*TD1M*(DCOSH(BM*ETA)+TD1M*DCOS(GM*ETA)
1 ) *DSIN(EMP*PSI)
W(I,L,J)=W(I,L,J)+EM(M,II+1)*TD1M*(DCOSH(BM*ET1)+TD1M*DCOS(GM*ET1)
1 ) *DSIN(EMP*PSI)

GO TO 3600
3000 ZZ=-ZZ
GM=PHI*DSQRT(ZZ)
GMS=GM*GM
TD2M=-EM*(BMS-POIS*PHIS*EMPS)*DSINE(BM)/(GM*(GMS-POIS*PHIS*EMPS)
1 *DSINE(GM)
C TD2M=-1./((BMS-POI*PHIS*EMPS)*DCOSH(BM)+TD2M*(GMS-POI*PHIS*EMPS)
C 1 *DCOSH(GM)
TD2M=1./(BM*DSINE(BM)+TD2M*GM*DSINE(GM))

W(I,L,J)=W(I,L,J)+EM(M,II)*TD2M*(DCOSH(BM*ETA)+TD2M*DCOSH(GM*
1 ETA)) *DSIN(EMP*PSI)
W(I,L,J)=W(I,L,J)+EM(M,II+1)*TD2M*(DCOSH(BM*ET1)+TD2M*DCOSH(GM*
1 ET1)) *DSIN(EMP*PSI)
3600 CONTINUE
2620 CONTINUE

I=NST
II=2*NST-1
PHI=PHIST(NST) ZZ
PHIS=PHI*PHI
ALMS=ALMDS/PHIS
EMP=M*PI ZZ
EMPS=EMP*EMP ZZ
ENP=(N-1)*PI Z
EM=PHI*DSQRT(ALMS+EMPS) ZZ
BMS=EM*EM
ZZ=ALMS-EMPS
IF(ZZ.LT.0.) GO TO 6400
GM=PHI*DSQRT(ZZ)
GMS=GM*GM

```

```

      TD1M=-EM*(BMS-POIS*PHIS*EMPS)*DSINE(BM)/(GM*(GMS+POIS*PHIS*EMPS)
      1 *DSIN(GM))
C      TD11M=-1./((BMS-POI*PHIS*EMPS)*DCOSH(BM)-TD1M*(GMS+POI*PHIS*EMPS)
C      1 *DCOS(GM))
      TD11M=1./(BM*DSINE(BM)-TD1M*GM*DSIN(GM))

      W(I,L,J)=W(I,L,J)+EM(M,II)*TD11M*(DCOSH(BM*ETA)+TD1M*DCOS(GM*ETA
      1 ))*DSIN(EMP*PSI)
      W(I,L,J)=W(I,L,J)+EM(M,II+1)*TD11M*(DCOSH(BM*ET1)+TD1M*DCOS(GM*ET1
      1 ))*DSIN(EMP*PSI)

      GO TO 3690
6400 ZZ=-ZZ
      GM=PHI*DSQRT(ZZ)
      GMS=GM*GM
      TD2M=-EM*(BMS-POIS*PHIS*EMPS)*DSINE(BM)/(GM*(GMS-POIS*PHIS*EMPS)
      1 *DSINE(GM))
C      TD22M=-1./((BMS-POI*PHIS*EMPS)*DCOSH(BM)+TD2M*(GMS-POI*PHIS*EMPS)
C      1 *DCOSH(GM))
      TD22M=1./(BM*DSINE(BM)+TD2M*GM*DSINE(GM))

      W(I,L,J)=W(I,L,J)+EM(M,II)*TD22M*(DCOSH(BM*ETA)+TD2M*DCOSH(GM*ETA
      1 ))*DSIN(EMP*PSI)
      W(I,L,J)=W(I,L,J)+EM(M,II+1)*TD22M*(DCOSH(BM*ET1)+TD2M*DCOSH(GM*
      1 ET1))*DSIN(EMP*PSI)

3690 CONTINUE

540 CONTINUE
ZZ20

      DO 740 N=1,K
ZZ20
      EMP=M*PI
ZZ20
      ENP=(N-1)*PI
ZZ20
      ENPS=ENP*ENP
ZZ20
      ALMDS=ALMDS
      PHI=1./PHIST(1)
      PHIS=PHI*PHI
      BN=PHI*DSQRT(ALMDS+ENPS)
      BNS=BN*BN
      ZZ=ALMDS-ENPS
      IF(ZZ.LT.0.) GO TO 2000
      GN=PHI*DSQRT(ZZ)
      GNS=GN*GN
      TD1N=-DSINE(BN)/DSIN(GN)
      TD11N=-1./(BNS*DSINE(BN)-TD1N*GNS*DSIN(GN))

      W(1,L,J)=W(1,L,J)+EN(N,1)*TD11N*(DSINE(BN*PSI)+TD1N*DSIN(GN*PSI))*
      1 DCOS(ENP*ETA)
      GO TO 2600
2000 ZZ=-ZZ
      GN=PHI*DSQRT(ZZ)
      GNS=GN*GN
      TD2N=-DSINE(BN)/DSINE(GN)
      TD22N=-1./(BNS*DSINE(BN)+TD2N*GNS*DSINE(GN))

      W(1,L,J)=W(1,L,J)+EN(N,1)*TD22N*(DSINE(BN*PSI)+TD2N*DSINE(GN*PSI))
      1 *DCOS(ENP*ETA)
2600 CONTINUE

      DO 2630 I=2,NST-1
      II=(I-1)*2+1
      PHI=1./PHIST(I)
      PHIS=PHI*PHI
      BN=PHI*DSQRT(ALMDS+ENPS)
      BNS=BN*BN
      ZZ=ALMDS-ENPS
      IF(ZZ.LT.0.) GO TO 4000
      GN=PHI*DSQRT(ZZ)
      GNS=GN*GN
      TD1N=-DSINE(BN)/DSIN(GN)
      TD11N=-1./(BNS*DSINE(BN)-TD1N*GNS*DSIN(GN))

      W(I,L,J)=W(I,L,J)+EN(N,II+1)*TD11N*(DSINE(BN*PSI)+TD1N*DSIN(GN*PSI
      1 ))*DCOS(ENP*ETA)
      W(I,L,J)=W(I,L,J)+EN(N,II)*TD11N*(DSINE(BN*PSI)+TD1N*DSIN(GN*PSI))
      W2S(L,J)=W2S(L,J)+EN21(N)*TD11M*(BM*DCOSH(BM*PSI)+TD1M*
      1 *DCOS(EMP*ETA)
      GN*DCOS(GN*PSI))*DCOS(EMP*ETA)

      GO TO 4600
4000 ZZ=-ZZ
      GN=PHI*DSQRT(ZZ)
      GNS=GN*GN
      TD2N=-DSINE(BN)/DSINE(GN)
      TD22N=-1./(BNS*DSINE(BN)+TD2N*GNS*DSINE(GN))

      W(I,L,J)=W(I,L,J)+EN(N,II+1)*TD22N*(DSINE(BN*PSI)+TD2N*DSINE(GN*

```

1

```

1 PS1) ) *DCOS (ENP*ETA)
W(I,L,J) =W(I,L,J) +EN(N,II) *TD22N* (DSINH (BN*PS1) +TD2N*DSINH (GN*PS1
1) ) *DCOS (ENP*ETA)

4600 CONTINUE
2630 CONTINUE
II=2*NST
I=NST
PHI=1./PHIST(NST)
PHIS=PHI*PHI
BN=PHI*DSQRT(ALMS+ENPS)
ENS=BN*BN
ZZ=ALMS-ENPS
IF(ZZ.LT.0.) GO TO 8000
GN=PHI*DSQRT(ZZ)
GNS=GN*GN
TD1N=-DSINH (BN) /DSIN (GN)
TD11N=-1./ (ENS*DSINH (BN) -TD1N*GNS*DSIN (GN) )

W(I,L,J) =W(I,L,J) +EN(N,II) *TD11N* (DSINH (BN*PS1) +TD1N*DSIN (GN*PS1) )
1 *DCOS (ENP*ETA)
GO TO 5600
8000 ZZ=-ZZ
GN=PHI*DSQRT(ZZ)
GNS=GN*GN
TD2N=-DSINH (BN) /DSINH (GN)
TD22N=-1./ (ENS*DSINH (BN) +TD2N*GNS*DSINH (GN) )

W(I,L,J) =W(I,L,J) +EN(N,II) *TD22N* (DSINH (BN*PS1) +TD2N*DSINH (GN*PS1) )
1) *DCOS (ENP*ETA)
5600 CONTINUE

740 CONTINUE
47 CONTINUE

RETURN
END

SUBROUTINE DETERM1(A,N,DET)
C
C THIS IS A STANDARD SUBPROGRAM FOR FINDING THE DETERMINANT OF A
C SQUARE N BY N MATRIX.THE DETERMINANT IS STORED AS DET.
C
C IMPLICIT DOUBLE PRECISION(A-H,O-Z)
C DIMENSION A(250,250)
C SIGN=1.
C LAST=N-1
C
C START OVERALL LOOP FOR(N-1) PIVOTS
C
C DO 200 I=1, LAST
C
C FIND THE LARGEST REMAINING TERM IN I-TH COLUMN FOR PIVOT
C
C BIG=0.
C DO 50 K=I,N
C TERM=DABS(A(K,I))
C IF (TERM-BIG) 50,50,30
30 BIG=TERM
L=K
50 CONTINUE
C
C CHECK WHETHER A NON-ZERO TERM HAS BEEN FOUND
C
C IF (BIG) 80,60,80
C
C L-TH ROW HAS THE BIGGEST TERM----IS I=L
C
80 IF (I=L) 90,120,90
C
C I IS NOT EQUAL TO L,SWITCH ROWS I AND L
90 SIGN=-SIGN
DO 100 J=1,N
TEMP=A(I,J)
A(I,J)=A(L,J)
100 A(L,J)=TEMP
C
C NOW START PIVOTAL REDUCTION
C
120 PIVOT=A(I,I)
NEXTI=I+1
C
C FOR EACH OF THE ROWS AFTER THE I-TH
C DO 200 J=NEXTI,N
C
C MULTIPLYING CONSTANT FOR THE J-TH ROW IS
C

```

ZZ207270

ZZ207280

ZZ207290

ZZ207300

ZZ207310

ZZ207320

ZZ207330

ZZ207340

ZZ207350

ZZ207360

ZZ207370

ZZ207380

ZZ207390

ZZ207400

ZZ207410

ZZ207420

ZZ207430

ZZ207440

ZZ207450

ZZ207460

ZZ207470

ZZ207480

ZZ207490

ZZ207500

ZZ207510

ZZ207520

ZZ207530

ZZ207540

ZZ207550

ZZ207560

ZZ207570

ZZ207580

ZZ207590

ZZ207600

ZZ207610

ZZ207620

ZZ207630

ZZ207640

ZZ207650

ZZ207660

ZZ207670

ZZ207680

ZZ207690

ZZ207700

ZZ207710

```

      CONST=A(J,I)/PIVOT
C
C      NOW REDUCE EACH TERM OF THE J-TH ROW
C
      DO 200 K=I,M
200 A(J,K)=A(J,K)-CONST*A(I,K)
C
C      END OF PIVOTAL REDUCTION---NOW COMPUTE DETERMINANT
      DET=SIGN
      DO 300 I=1,M
300 DET=DET*A(I,I)*10 .
      GO TO 61
60 DET=0.
61 RETURN
      END

      SUBROUTINE EXP1(A,N)
      IMPLICIT DOUBLE PRECISION (A-H,O-Z)
      IFLAG=1
C
C      CHECK IF NUMBER IS NEGATIVE
C
      IF(A.LT.0.0) IFLAG=-1
      A=ABS(A)
C
C      CHECK IF NUMBER IS LESS OR GREATER THAN 1.0
C
      IF(A.EQ.1.) GO TO 100
      IF(A.LT.1.0) GO TO 101
      N=0
20  A=A/10.
      N=N+1
      IF(A.LT.1.) THEN
      A=A*FLOAT(IFLAG)
      A=A
      N=N
      RETURN
      ELSE
      GO TO 20
      ENDIF
101 N=0
30  A=A*10.
      N=N-1
      IF(A.GT.1.) THEN
      A=A*FLOAT(IFLAG)/10.
      N=N+1
      RETURN
      ELSE
      GO TO 30
      ENDIF
100 N=1
      A=A*FLOAT(IFLAG)/10.
      RETURN
      END

      SUBROUTINE SIMQ(A,M,N,X)
      IMPLICIT DOUBLE PRECISION(A-H,O-Z)
      DIMENSION A(M,N) ,X(N)
99  FORMAT (7(E13.6,3X))
      SIGN=1.
      M=N-1
      LAST=M-1
C
C
C      START OVERALL LOOP FOR(N-1) PIVOTS
C
      DO 7 I=1,LAST
C
C      FIND THE LARGEST REMAINING TERM IN I-TH COLUMN FOR PIVOT
C
      BIG=0.
      DO 2 K=I,M
      TERM=ABS(A(K,I))
      IF(TERM-BIG)2,2,1
1  BIG=TERM
      L=K
2  CONTINUE
C
C      CHECK WHETHER A NON-ZERO TERM HAS BEEN FOUND
C
      IF(BIG)3,11,3
C
C      L-TH ROW HAS THE BIGGEST TERM-----IS I=L
C
3  IF(I=L)4,6,4
C
C      I IS NOT EQUAL TO L, SWITCH ROWS I AND L

```

```

ZZ207720
ZZ207730
ZZ207740
ZZ207750
ZZ207760
ZZ207770
ZZ207780
ZZ207790
ZZ207800
ZZ207810
ZZ207820
ZZ207830
ZZ207840
ZZ207850
ZZ207860

```

```

C
4 DO 5 J=1,M
  TEMP=A(I,J)
  A(I,J)=A(L,J)
5 A(L,J)=TEMP
C
C   NOW START PIVOTAL REDUCTION
C
6 PIVOT=A(I,I)
  NEXTR=I+1
C
C   FOR EACH OF THE ROWS AFTER THE I-TH
C
  DO 7 J=NEXTR,M
C
C   MULTIPLYING CONSTANT FOR THE J-TH ROW IS:
C
  CONST=A(J,I)/PIVOT
C
C   NOW REDUCE EACH TERM OF THE J-TH ROW
C
  DO 7 K=I,N
7 A(J,K)=A(J,K)-CONST*A(I,K)
C
C   END OF PIVOTAL REDUCTION-- PERFORM BACK SUBSTITUTION
C
  M=N-1
  DO 10 I=1,M
C
C   IREV IS THE BACKWARD INDEX, GOING FROM M BACK TO 1
C
  IREV=M+1-I
C
  GET Y(IREV) IN PREPARATION
  Y=A(IREV,N)
  IF(IREV-M)8,10,8
C
  NOT WORKING ON LAST ROW, I IS 2 OR GREATER
  DO 9 J=2,I
C
  WORK BACKWARD FOR X(N), X(N-1)-----SUBSTITUTING PREVIOUSLY
  FOUND VALUES
  K=N+1-J
  9 Y=Y-A(IREV,K)*X(K)
C
C   FINALLY, COMPUTE X(IREV)
C
10 X(IREV)=Y/A(IREV,IREV)
  X(N)=-1
11 RETURN
  END
  SUBROUTINE RATO(BM, BX, GM, GX, X1, X2, Y1, Y2)
  IMPLICIT DOUBLE PRECISION(A-H, O-Z)
  QLIM=30.
  X1=0.
  X2=0.
  Y1=0.
  Y2=0.
  IF(BM.GT.QLIM) GO TO 10
  X1=DCOSH(BX)/DSINH(BM)
  X2=DSINH(BX)/DSINH(BM)
  GO TO 11
10 ZZ=BM-BX
  IF(ZZ.GT.QLIM) GO TO 11
  ZZ=-ZZ
  X1=DEXP(ZZ)
  X2=X1
11 CONTINUE
  IF(GM.GT.QLIM) GO TO 15
  Y1=DCOSH(GX)/DSINH(GM)
  Y2=DSINH(GX)/DSINH(GM)
  GO TO 16
15 ZZ=GM-GX
  IF(ZZ.GT.QLIM) GO TO 16
  ZZ=-ZZ
  Y1=DEXP(ZZ)
  Y2=Y1
16 CONTINUE
  RETURN
  END

  SUBROUTINE SS1A(BM, EMP, ALFA, X1, X2)
  IMPLICIT DOUBLE PRECISION(A-H, O-Z)
  X1=(BM*DSIN(EMP*ALFA)*DCOSH(BM*ALFA)-EMP*DCOS(EMP*ALFA)*DSINH(BM*
1 ALFA))/(BM*EM+EMP*EMP)
  X2=(BM*DSIN(EMP*ALFA)*DSINH(BM*ALFA)-EMP*DCOS(EMP*ALFA)*DCOSH(BM*
1 ALFA)+EMP)/(BM*EM+EMP*EMP)
  RETURN
  END

```

```

SUBROUTINE SS2AL (GM,EMP,ALFA,X1,X2)
  IMPLICIT DOUBLE PRECISION (A-H,O-Z)
  X1=(DSIN((GM-EMP)*ALFA)/(GM-EMP)-DSIN((GM+EMP)*ALFA)/(EMP+GM))/2.
  X2=-((DCOS((EMP-GM)*ALFA)-1.)/(EMP-GM)+(DCOS((EMP+GM)*ALFA)-1.)/(
1 EMP+GM))/2.
  RETURN
  END

SUBROUTINE SCC2 (GM,A0,EMP,ENP,X1,X2)
  IMPLICIT DOUBLE PRECISION (A-H,O-Z)
  IF(A0.EQ.0.) GO TO 10
  CALL CCC(GM,EMP,ENP,X)
  CALL CCS(EMP,ENP,GM,Y)
  X1=(DSIN(GM)*X-DCOS(GM)*Y)
  X2=(DCOS(GM)*X+DSIN(GM)*Y)
  GO TO 20
10 CALL CCS(EMP,ENP,GM,X1)
  CALL CCC(GM,EMP,ENP,X2)
  X1=X1
  X2=X2
20 CONTINUE
  RETURN
  END

SUBROUTINE SSS(A,B,C,X)
  IMPLICIT DOUBLE PRECISION (A-H,O-Z)
  A1=A-B+C
  A2=B+C-A
  A3=A+B-C
  A4=A+B+C
  X1=0.
  X2=0.
  X3=0.
  X4=0.
  IF(A1.EQ.0.)GOTO 1
  X1=(DCOS(A1)-1.)/A1
1 IF(A2.EQ.0.)GOTO 2
  X2=(DCOS(A2)-1.)/A2
2 IF(A3.EQ.0.)GOTO 3
  X3=(DCOS(A3)-1.)/A3
3 IF(A4.EQ.0.)GOTO 4
  X4=(DCOS(A4)-1.)/A4
4 X=- (X1+X2+X3-X4)/4.
  RETURN
  END

SUBROUTINE CSS(A,B,C,X)
  IMPLICIT DOUBLE PRECISION (A-H,O-Z)
  A1=A+B-C
  A2=A+C-B
  A3=A+B+C
  A4=B+C-A
  X1=1.
  X2=1.
  X3=1.
  X4=1.
  IF(A1.EQ.0.)GOTO 1
  X1=DSIN(A1)/A1
1 IF(A2.EQ.0.)GOTO 2
  X2=DSIN(A2)/A2
2 IF(A3.EQ.0.)GOTO 3
  X3=DSIN(A3)/A3
3 IF(A4.EQ.0.)GOTO 4
  X4=DSIN(A4)/A4
4 X=(X1+X2-X3-X4)/4.
  RETURN
  END

SUBROUTINE CCS(B,C,A,X)
  IMPLICIT DOUBLE PRECISION (A-H,O-Z)
  A1=A+B+C
  A2=B+C-A
  A3=A+B-C
  A4=A+C-B
  X1=0.
  X2=0.
  X3=0.
  X4=0.
  IF(A1.EQ.0.)GOTO 1
  X1=(DCOS(A1)-1.)/A1
1 IF(A2.EQ.0.)GOTO 2
  X2=(DCOS(A2)-1.)/A2
2 IF(A3.EQ.0.)GOTO 3
  X3=(DCOS(A3)-1.)/A3
3 IF(A4.EQ.0.)GOTO 4
  X4=(DCOS(A4)-1.)/A4
4 X=- (X1-X2+X3+X4)/4.
  RETURN
  END

```

```

SUBROUTINE CCC(A,B,C,X)
  IMPLICIT DOUBLE PRECISION (A-H,O-Z)
  A1=A+B+C
  A2=B+C-A
  A3=A+C-B
  A4=A+B-C
  X1=1.
  X2=1.
  X3=1.
  X4=1.
  IF(A1.EQ.0.)GOTO 1
  X1=DSIN(A1)/A1
1 IF(A2.EQ.0.)GOTO 2
  X2=DSIN(A2)/A2
2 IF(A3.EQ.0.)GOTO 3
  X3=DSIN(A3)/A3
3 IF(A4.EQ.0.)GOTO 4
  X4=DSIN(A4)/A4
4 X=(X1+X2+X3+X4)/4.
  RETURN
  END

SUBROUTINE DETR(A,N,X)
  IMPLICIT DOUBLE PRECISION (A-H,O-Z)
  DIMENSION A(250,250),X(251)
  SIGN=1.
  M=N-1
  LAST=M-1
C
C
C   START OVERALL LOOP FOR(N-1) PIVOTS
C
C   DO 7 I=1,LAST
C
C   FIND THE LARGEST REMAINING TERM IN I-TH COLUMN FOR PIVOT
C
C   BIG=0.
C   DO 2 K=I,M
C     TERM=DABS(A(K,I))
C     IF(TERM-BIG)2,2,1
1   BIG=TERM
   L=K
2 CONTINUE
C
C   CHECK WHETHER A NON-ZERO TERM HAS BEEN FOUND
C
C   IF(BIG)3,11,3
C
C   L-TH ROW HAS THE BIGGEST TERM-----IS I=L
C
3 IF(I-L)4,6,4
C
C   I IS NOT EQUAL TO L, SWITCH ROWS I AND L
C
4 DO 5 J=1,N
  TEMP=A(I,J)
  A(I,J)=A(L,J)
5 A(L,J)=TEMP
C
C   NOW START PIVOTAL REDUCTION
C
6 PIVOT=A(I,I)
  NEXTR=I+1
C
C   FOR EACH OF THE ROWS AFTER THE I-TH
C
C   DO 7 J=NEXTR,M
C
C   MULTIPLYING CONSTANT FOR THE J-TH ROW IS:
C
  CONST=A(J,I)/PIVOT
C
C   NOW REDUCE EACH TERM OF THE J-TH ROW
C
  DO 7 K=I,N
7 A(J,K)=A(J,K)-CONST*A(I,K)
C
C   END OF PIVOTAL REDUCTION-- PERFORM BACK SUBSTITUTION
C
  M=N-1
  DO 10 I=1,M
C
C   IREV IS THE BACKWARD INDEX,GOING FROM M BACK TO 1
C
  IREV=M+1-I
C
C   GET Y(IREV) IN PREPARATION
C

```

```

      Y=A(IREV,N)
      IF(IREV-M)8,10,8
C
C      NOT WORKING ON LAST ROW,I IS 2 OR GREATER
C
      8 DO 9 J=2,I
C
C      WORK BACKWARD FOR X(N),X(N-1)-----SUBSTITUTING PREVIOUSLY
C      FOUND VALUES
C
      K=N+1-J
      9 Y=Y-A(IREV,K)*X(K)
C
C      FINALLY, COMPUTE X(IREV)
C
      10 X(IREV)=Y/A(IREV,IREV)
      X(N)=-1
      11 RETURN
      END

      SUBROUTINE SSS11(BM,A0,EMP,ENP,X1,X2)
      IMPLICIT DOUBLE PRECISION (A-H,O-Z)
      QLIM=240.
      BMS=BM*BM
      BM0=BM*A0
      EMPF=EMP-ENP
      ENPF=ENP+EMP
      EMPFS=EMP*EMP
      ENPFS=ENP*ENP
      IF(BM.GT.QLIM) GO TO 8
      IF(A0.NE.0.) GO TO 2
      X11=(BM*DCOS(EMP)*DSINE(BM)+EMP*DSIN(EMP)*DCOSH(BM))/(BMS+EMPFS)
      X22=(BM*DCOS(ENP)*DSINE(BM)+ENP*DSIN(ENP)*DCOSH(BM))/(BMS+ENPFS)
      X11=(BM*DCOS(EMP)*DSINE(BM)+EMP*DSIN(EMP)*DCOSH(BM))/(BMS+EMPFS)
      X22=(BM*(DCOS(EMP)*DCOSH(BM)-1.)+EMP*DSIN(EMP)*DSINE(BM))/(BMS+
      EMPFS)-(BM*(DCOS(ENP)*DCOSH(BM)-1.)+ENP*DSIN(ENP)*DSINE(BM))/(B
      MS+ENPFS)
      X1=-X22/(2. )
      X2=X11/(2. )
      GO TO 3
      2 X1=- (BM*DCOS(EMP)-BM*DCOSH(BM))/(BMS+EMPFS)+(BM*DCOS(ENP)-BM*
      1 DCOSH(BM))/(BMS+ENPFS)
      X1=X1/(2. )
      X2=(EMP*DSIN(EMP)+BM*DSINE(BM))/(BMS+EMPFS)-(ENP*DSIN(ENP)+BM*
      1 DSINE(BM))/(BMS+ENPFS)
      X2=X2/(2. )
      GO TO 3
      8 CONTINUE
      IF(A0.NE.0.) GO TO 9
      X2=- (BM*DCOS(EMP)+EMP*DSIN(EMP))/(2.*(BMS+EMPFS))+(BM*
      1 DCOS(ENP)+ENP*DSIN(ENP))/(2.*(BMS+ENPFS))
      X2=X2*DSINE(BM)
      X1=X2
      X2=-X2
      GO TO 3
      9 CONTINUE
      X1=(BM/2.)*(1./(BMS+EMPFS)-1./(BMS+ENPFS))
      X1=X1*DSINE(BM)
      X2=X1
      3 IF(A0.NE.0.)GOTO 1
      X1=-X1
      1 CONTINUE
      RETURN
      END

      SUBROUTINE SSS2(GM,A0,EMP,ENP,X1,X2)
      IMPLICIT DOUBLE PRECISION (A-H,O-Z)
      GM0=GM*A0
      CALL CSS(GM,EMP,ENP,X11)
      CALL SSS(GM,EMP,ENP,X22)
      X1=DSIN(GM0)*X11-DCOS(GM0)*X22
      X2=DCOS(GM0)*X11+DSIN(GM0)*X22
      IF(A0.NE.0.)GOTO 1
      X1=-X1
      1 CONTINUE
      X1=X1/DSIN(GM)
      X2=X2/DSIN(GM)
      RETURN
      END

      SUBROUTINE SCS11(BM,A0,EMP,ENP,X1,X2)
      IMPLICIT DOUBLE PRECISION (A-H,O-Z)
      QLIM=240.
      BMS=BM*BM
      BM0=BM*A0
      EMPF=EMP-ENP
      ENPF=ENP+EMP
      EMPFS=EMP*EMP
      ENPFS=ENP*ENP

```

```

      IF (M.GT.QLIM) GO TO 8
      IF (A0.NE.0.) GO TO 2
      X11=(EM*DSIN(EMP)*DCOS(EM)-EMP*(DCOS(EMP)*DCOS(EM)-1.))/(EMS+
      EMP)*DSIN(EMP)*DCOS(EM)-EMP*(DCOS(EMP)*DCOS(EM)-1.)/(EMS+
      EMP)
      X22=(EM*DSIN(EMP)*DCOS(EM)-EMP*(DCOS(EMP)*DCOS(EM)-1.))/(EMS+EMP)
      X1=-X22/(2.)
      X2=X11/(2.)
      GO TO 3
2  X1=(EM*DSIN(EMP)-EMP*DSIN(EM))/(EMS+EMP)+(EM*DSIN(EMP)-EMP
1 *DSIN(EM))/(EMS+EMP)
      X1=X1/(2.)
      X2=(EMP*DCOS(EMP)-EMP*DCOS(EM))/(EMS+EMP)+(EMP*DCOS(EMP)-
1 EMP*DCOS(EM))/(EMS+EMP)
      X2=X2/(2.)
      GO TO 3
8  IF (A0.NE.0.) GO TO 9
      X1=(EM*DSIN(EMP)-EMP*DCOS(EMP))/(2.*(EMS+EMP))+(EM*
1 DSIN(EMP)-EMP*DCOS(EMP))/(2.*(EMS+EMP))
      X1=X1*DSIN(EM)
      X2=-X1
      GO TO 3
9  X1=EMP/(2.*(EMS+EMP))-EMP/(2.*(EMS+EMP))
      X1=X1*DSIN(EM)
      X2=X1
3  IF (A0.NE.0.) GOTO 1
      X1=-X1
1  CONTINUE
      RETURN
      END
      SUBROUTINE SCS2(GM,A0,EMP,ENP,X1,X2)
      IMPLICIT DOUBLE PRECISION (A-H,O-Z)
      GM0=GM*A0
      CALL CCS(GM,EMP,ENP,X11)
      CALL CSS(EMP,GM,ENP,X22)
      X1=OSIN(GM0)*X11-DCOS(GM0)*X22
      X2=DCOS(GM0)*X11+DSIN(GM0)*X22
      X1=X1
      X2=X2
      IF (A0.NE.0.) GOTO 1
      X1=-X1
1  CONTINUE
      RETURN
      END
      SUBROUTINE SCC11(EM,A0,EMP,ENP,X1,X2)
      IMPLICIT DOUBLE PRECISION (A-H,O-Z)
      QLIM=240.
      EMS=EM*EM
      EM0=EM*A0
      EMP=EMP-ENP
      ENP=EMP+ENP
      EMP0=EMP*EMP
      ENP0=ENP*ENP
      IF (M.GT.QLIM) GO TO 8
      IF (A0.EQ.0.) GO TO 2
      X1=(EM*DCOS(EMP)-EM*DCOS(EM))/(EMS+EMP)+(EM*DCOS(EM)-EM*
1 DCOS(EMP))/(EMS+EMP)
      X2=(EM*DSIN(EM)+EMP*DSIN(EMP))/(EMS+EMP)+(EM*DSIN(EM)+EMP*
1 DSIN(EMP))/(EMS+EMP)
      X1=X1/(2.)
      X2=X2/(2.)
      GO TO 3
2  X1=(EM*(DCOS(EMP)*DCOS(EM)-1.)+EMP*DSIN(EMP)*DSIN(EM))/(EMS
1 +EMP)-(EM*(DCOS(EMP)*DCOS(EM)-1.)+EMP*DSIN(EMP)*DSIN(EM))/
1 (EMS+EMP)
      X1=X1/(2.)
      X2=(EM*DCOS(EMP)*DSIN(EM)+EMP*DSIN(EMP)*DCOS(EM))/(EMS+EMP)
1 +(EM*DCOS(EMP)*DSIN(EM)+EMP*DSIN(EMP)*DCOS(EM))/(EMS+EMP)
      X2=X2/(2.)
      GO TO 3
8  CONTINUE
      IF (A0.NE.0.) GO TO 9
      X1=(EM*DCOS(EMP)+EMP*DSIN(EMP))/(2.*(EMS+EMP))-(EM*
1 DCOS(EMP)+EMP*DSIN(EMP))/(2.*(EMS+EMP))
      X1=X1*DSIN(EM)
      X2=-X1
      GO TO 3
9  CONTINUE
      X1=(EM/2.)*(1./(EMS+EMP)+1./(EMS+EMP))
      X2=X1*DSIN(EM)
3  IF (A0.NE.0.) GOTO 1
      X1=-X1
1  CONTINUE
      RETURN
      END

```